Erythrocyte aging and disease

A tale of membranes and microparticles

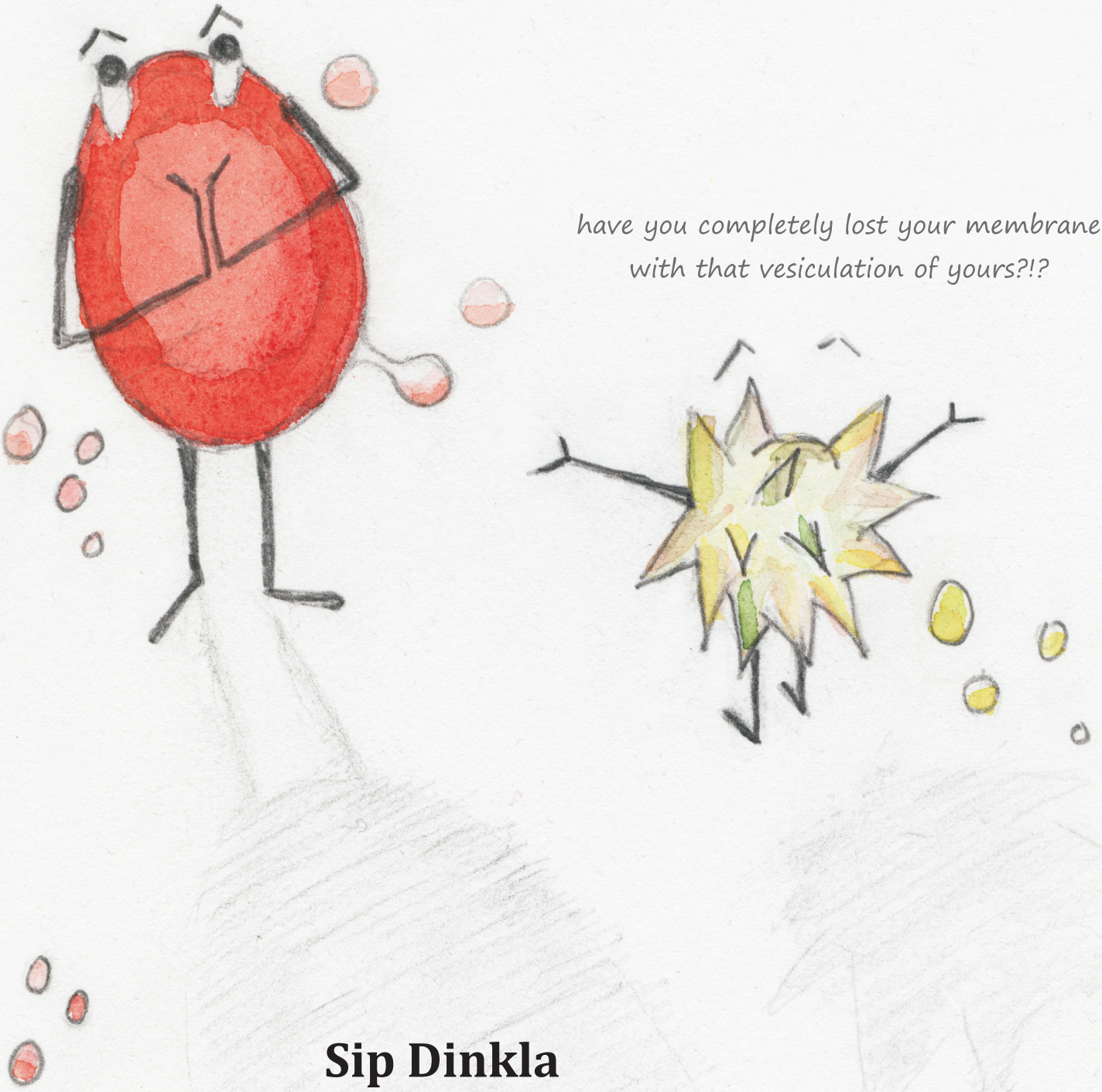

Sip Dinkla

Erythrocyte aging and disease

A tale of membranes and microparticles

Proefschrift

ter verkrijging van de graad van doctor
aan de Radboud Universiteit Nijmegen
op gezag van de rector magnificus prof. mr. S.C.J.J. Kortmann,
volgens besluit van het college van decanen
in het openbaar te verdedigen op maandag 13 oktober 2014
om 14.30 uur precies

door

Sip Dinkla
geboren op 4 april 1984
te Eindhoven

Promotoren

Prof. dr. I. Joosten

Prof. dr. R. Brock

Copromotoren

Dr. G.J.C.G.M. Bosman

Dr. V.M.J. Novotný

Manuscriptcommissie

Prof. dr. G.J. Adema

Prof. dr. F.G.M. Russel

Prof. dr. A. Sturk (Academisch Medisch Centrum, Amsterdam)

Table of contents

Cover illustration: “De pot verwijt de ketel dat hij zwart ziet”

An erythrocyte and a platelet engaged in a heated debate whilst vesiculating

by Ria Dinkla

1

General Introduction

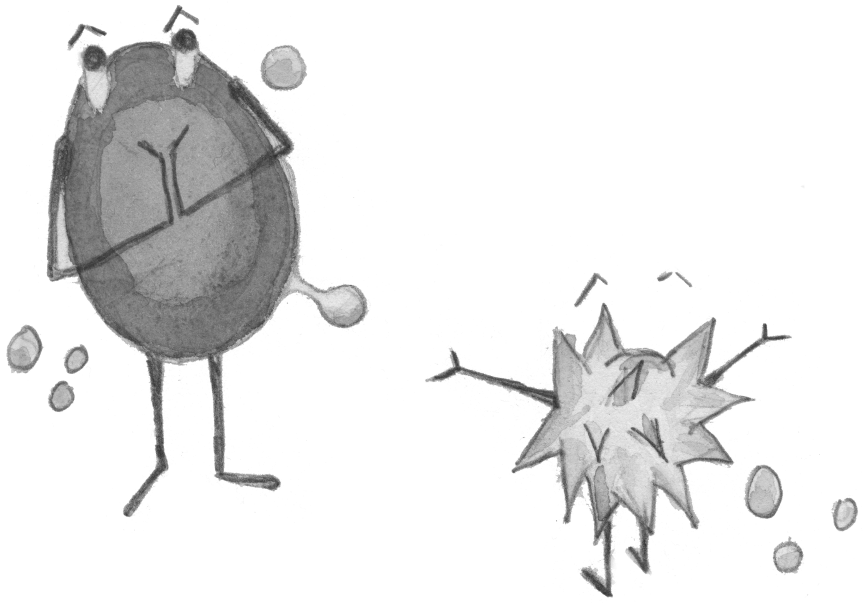

General Introduction

This chapter is an introduction to the research on erythrocytes, microparticles and regulatory T cells that is presented in the subsequent chapters. The first part of this chapter briefly discusses the main functions and characteristics of the erythrocyte. The second part focusses on erythrocyte aging and removal, transfusion side effects, and anemia of inflammation. The third part discusses the functions of erythrocyte-derived and platelet-derived microparticles in the context of health, disease and transfusion medicine. In the fourth part, a brief overview of the immune system and its role in tissue homeostasis is given. In the final part, the scope of this thesis is presented.

I - The erythrocyte

Erythrocytes, commonly known as red blood cells, are the most abundant cells in the circulation, and are the principal means of oxygen delivery to and CO_2 removal from the peripheral tissues. The erythrocyte owes its ability to transport oxygen to its high hemoglobin content. In the human lung, the erythrocytes take up oxygen at the alveolar-capillary interface, which they release whilst traversing the capillary network in the peripheral tissues. This oxygen release is stimulated by the CO_2 that is produced by metabolically active tissues. Upon entering the erythrocyte, CO_2 is converted into $HCO3^-$ and H^+ by the enzyme carbonic anhydrase. The subsequent decrease in intracellular pH serves as a signal for hemoglobin to release oxygen.

Erythrocytes are biconcave disks with an approximate diameter of 7 μm and maximum thickness of 2.5 μm. Unlike almost all the other cells of the body, erythrocytes do not contain intracellular organelles such as a nucleus, endoplasmic reticulum, Golgi apparatus, and mitochondria, which enables a maximal hemoglobin content and plasma membrane deformability. Erythrocytes must be able to undergo large passive deformations in order to pass through the narrow capillaries of the microvasculature and the fenestrae in the spleen. The shear stress that erythrocytes experience when traversing the vessels and the deoxygenation of their hemoglobin trigger the release of potent vasodilators in the form of S-nitrosothiol and ATP, which promote the passage of the erythrocyte. ATP promotes the release of NO by the vascular endothelium, which is further enhanced by the shear stress that the passing erythrocytes exert on the endothelium. This physiological activity is exemplary for the complex interactions between the erythrocyte and its environment.

II - Erythrocyte aging and removal

In the red bone marrow, multipotent hematopoietic stem cells proliferate and differentiate to form erythroblasts [1], which produce large quantities of hemoglobin and ultimately expel their nuclei to form reticulocytes. The reticulocytes mature into erythrocytes in the bone marrow, a process which is completed after their release into the circulation. This maturation process is characterized by loss of intracellular organelles such as mitochondria and ribosomes [2,3], and by extensive membrane remodeling [4,5]. In the circulation, the average lifespan of the human erythrocyte is approximately 120 days [6], which means that 200 billion erythrocytes have to be removed and replaced every day.

Physiological autoantigens

During their stay in the circulation, erythrocyte aging results in an increase in autologous IgG binding, which ultimately leads to the phagocytosis of old erythrocytes by Kupffer cells in the liver (Figure 1) [7]. The work of Marguerite Kay has uncovered that the binding of physiological autoantibodies to senescent erythrocytes is associated with changes in band 3. These changes are thought to be triggered by the binding of denatured hemoglobin to the cytoplasmic domain of band 3 (Figure 1) [7]. It has been suggested that selective tyrosine phosphorylation of oxidized band 3 by Syk may play a role in the recruitment of hemoglobin-bound band 3 molecules in large membrane aggregates that show a high affinity to physiological autoantibodies [8].

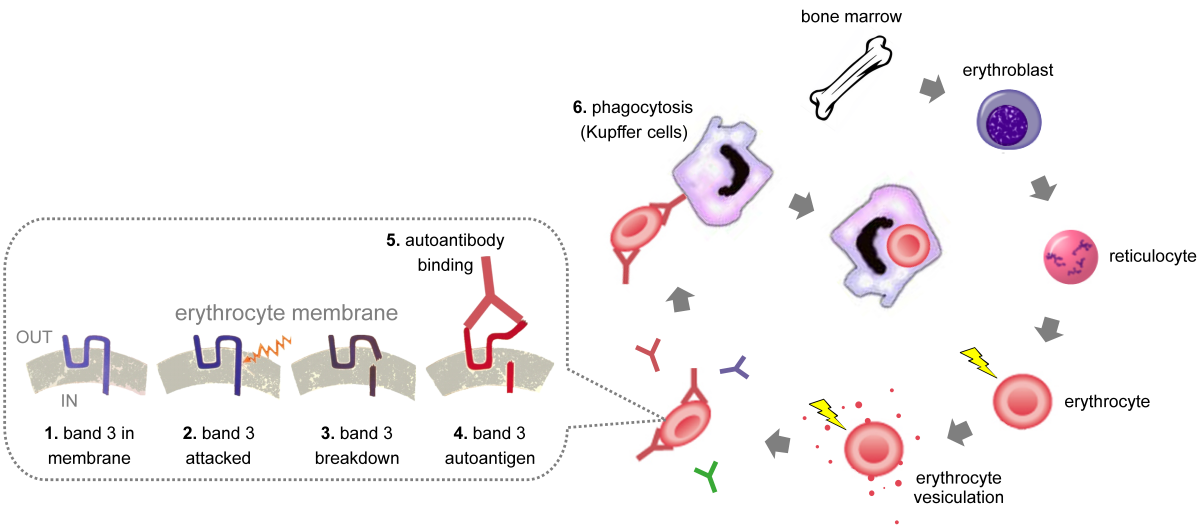

FIGURE 1. Erythrocyte birth, aging and removal.

Band 3

The Cl^-/HCO_3^- exchange protein band 3, or anion exchanger 1, is the most abundant protein in the erythrocyte membrane, facilitates the transport of CO_2 through the body [9], and controls the rate of glycolysis in the erythrocyte by reversible binding of key enzymes such as glyceraldehyde 3-phosphate dehydrogenase [10]. Band 3 is present in three distinct protein complexes within the erythrocyte membrane: as an ankyrin-bound, tetrameric band 3 complex, as a dimeric band 3 complex bound to the protein 4.1–GPC junctional complex, and as freely diffusing dimeric band 3 complexes (Figure 2) [11]. The cytoplasmic domain of band 3 functions as the main anchorage site of the plasma membrane for the cytoskeleton by binding ankyrin, protein 4.1, protein 4.2 and adducin [12-14], and thereby plays a crucial role in the mechanical integrity and the deformability of the erythrocyte. Band 3 also interacts with various integral membrane proteins including glycophorin A, RhAG and/or Rh from the rhesus complex (Figure 2) [15,16].

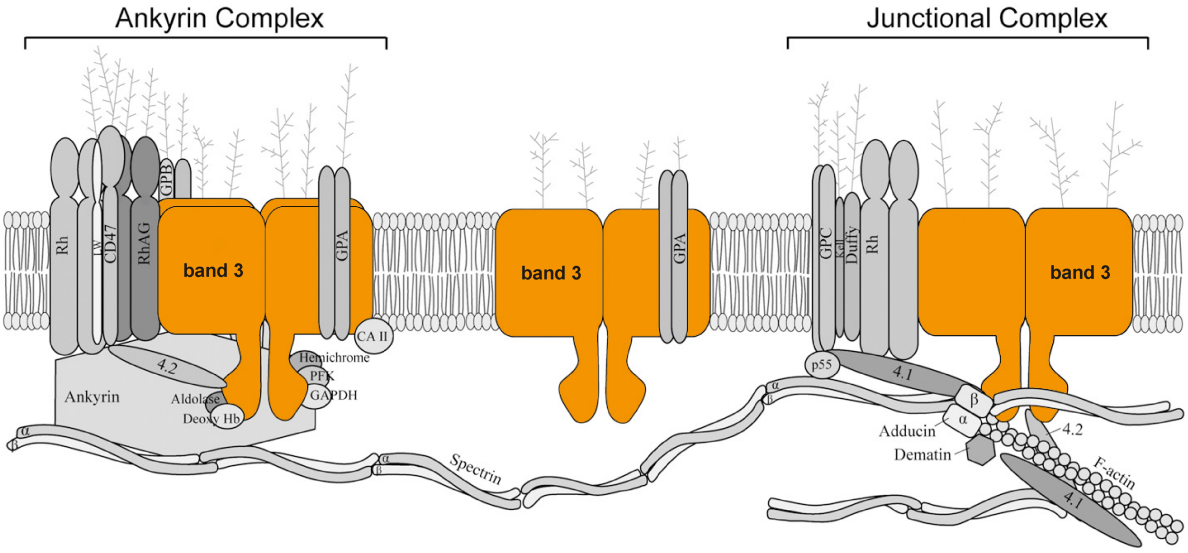

FIGURE 2. Band 3 multiprotein complexes in the human erythrocyte membrane. CA II – carbonic anhydrase II, GAPDH – glyceraldehyde 3-phosphate dehydrogenase, GPA – glycophorin A, GPB – glycophorin B, GPC – glycophorin C, Hb – hemoglobin, LW – Lewis blood group system, PFK – phosphofructokinase, Rh – rhesus blood group system, RhAG – Rh-associated glycoprotein blood group system (van den Akker et al.[11], adapted from Salomao et al.[17])

Erythrocyte deformability

Another mechanism of removal centers on the reduced deformability of aged erythrocytes [18-20]. Erythrocyte deformability is governed by the viscosity of the cytoplasm - largely determined by its hemoglobin concentration -, the surface area-to-volume ratio (S/V), and the mechanical properties of the plasma membrane - primarily determined by its protein and lipid constituent organization - including the interaction between plasma membrane

constituents with the cytoskeleton [19,21,22]. As previously mentioned, the erythrocyte has to undergo large deformations in order to pass through the narrow capillaries of the microvasculature and the fenestrae in the spleen. Poorly deformable erythrocytes tend to get stuck in the spleen, which may trigger phagocytosis [23-25]. Indeed, enhanced splenic sequestration of abnormal erythrocytes with reduced deformability is associated with a decreased life span and anemia in several erythrocyte membranopathies [26]. During its time in the circulation, the erythrocyte loses membrane surface due to continuous membrane vesiculation [27-29]. This vesicle shedding is thought to constitute a mechanism for the removal of damaged/aged membrane patches, postponing the untimely recognition and elimination of functional erythrocytes [29-33]. In addition, vesiculation also contributes to the gradual loss in deformability observed during physiological erythrocyte aging [34], as it leads to a reduced S/V ratio and increased mean cellular hemoglobin concentration [34,35]. This might induce their eventual removal by splenic sequestration.

Phosphatidylserine exposure

The lipid part of the plasma membrane of the erythrocyte is composed of equal proportions of cholesterol and phospholipids [26]. While cholesterol is evenly distributed between the outer and inner leaflet of the membrane, the four dominant phospholipids are asymmetrically distributed. Phosphatidylcholine and sphingomyelin (SM) are primarily located in the outer leaflet, while phosphatidylethanolamine and phosphatidylserine (PS) are predominantly found in the inner leaflet (Figure 3) [36,37]. Various phospholipid transport proteins have been implicated in membrane phospholipid asymmetry. “Flippases” transport phospholipids from the extracellular to the cytoplasmic membrane leaflet, while “floppases” do the opposite, both in an energy-dependent manner (Figure 3). In contrast, “scramblases” move phospholipids bi-directionally down their concentration gradients by an energy-independent mechanism that is triggered by a rise in cytoplasmic calcium (Figure 3) [38]. A novel calcium-activated cation channel (TMEM16F) required for calcium-induced membrane phospholipid scrambling was recently identified, and was found to be mutated in patients with Scott syndrome, a disease characterized by defective calcium-induced phospholipid scrambling activity [39-41]. The plasma membrane lipid composition is involved in erythrocyte homeostasis [42,43], as exemplified by the altered erythrocyte morphology and survival in patients with hemoglobinopathies and severe liver diseases, due to a disturbed membrane lipid asymmetry and lipid metabolism, respectively [43,44]. The maintenance of phospholipid asymmetry, in particular the exclusive localization of PS in the inner plasma membrane leaflet, has several functional implications. One such implication is the association between an increase in PS exposure and vesiculation [45].

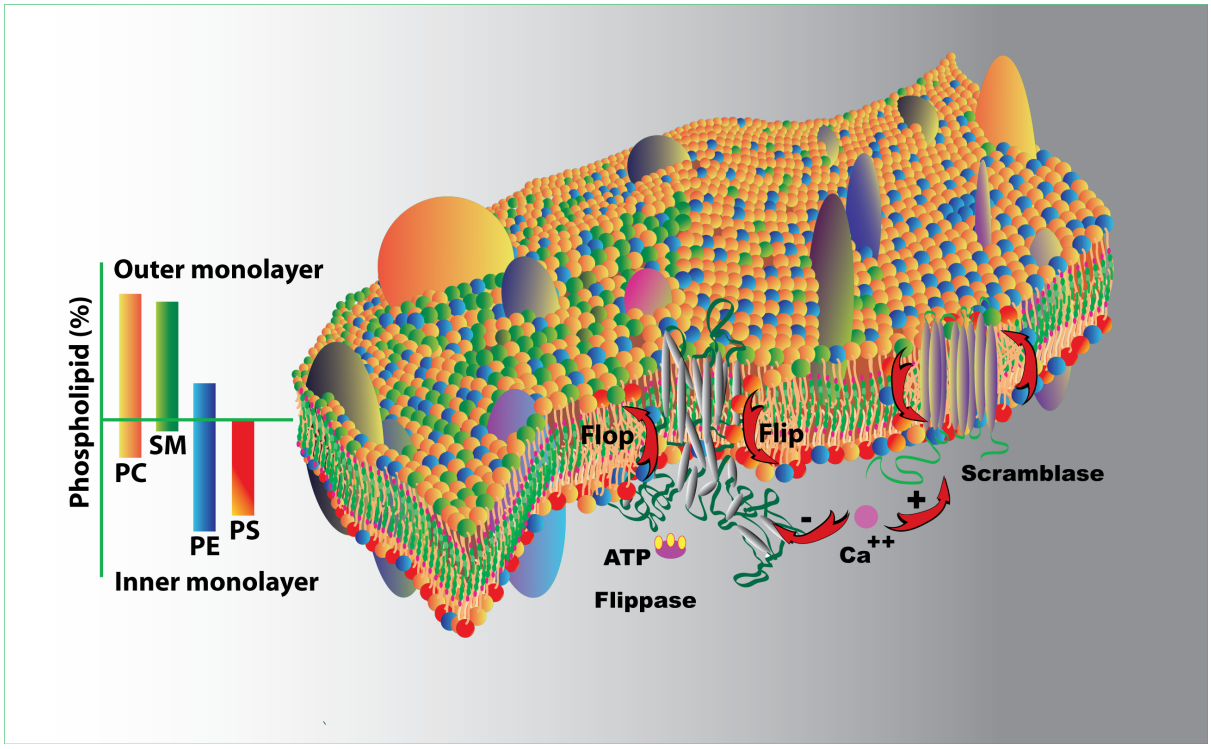

FIGURE 3. Phospholipid distribution and its regulation in the erythrocyte membrane. ATP – adenosine triphosphate, PC – phosphatidylcholine, PE – phosphatidylethanolamine, PS – phosphatidylserine, SM – sphingomyelin (© Frans Kuypers 2011)

Externalization of PS to the outer leaflet of the plasma membrane is a hallmark of apoptotic cell death for many cell types [46-49]. Once exposed, PS is recognized by macrophages which in turn phagocytoze the targeted cell, either directly via PS receptors [50-52], or through PS-mediated opsonisation of cells with lactadherin [53,54]. This has led to the broadly supported postulate that PS exposure by erythrocytes promotes their removal from the circulation. PS exposure on erythrocytes indeed leads to their phagocytosis by Kupffer cells of the liver and macrophages of the spleen in mice [55]. A recent study has shown that stress-induced PS exposure by erythrocytes leads to their recognition by PS receptors TIM-1 and TIM-4, and triggers their removal by TIM-1 and TIM-4-positive phagocytes [50]. Another study demonstrated that endothelial cells bind PS-positive erythrocytes via stabillin-1 and 2, greatly enhancing phagocytosis of these erythrocytes [56]. These findings suggest that liver, splenic, and/or vascular endothelium cooperate with resident macrophages in the removal of PS-positive erythrocytes. Interestingly, few erythrocytes (<1%) in the human circulation expose PS regardless of their age [57], suggesting that PS exposure either does not occur during physiological erythrocyte aging, or leads to the rapid removal of the PS-exposing erythrocyte. In erythrocyte pathologies such as sickle cell anemia, thalassemia and spherocytosis, erythrocyte survival inversely correlated with phosphatidylserine exposure [58].

Another mechanism involved in erythrocyte removal involves the membrane protein CD47. CD47 is generally known as a marker of "self", as it has been shown to inhibit erythrocyte phagocytosis by macrophages of the reticulo-endothelial system [59-61]. A recent study adds another dimension to the CD47 story, by showing that a conformational change in CD47 induced by experimental erythrocyte aging enables thrombospondin binding and subsequent phagocytosis by splenic macrophages *in vitro* [62]. It is reasonable to assume that several of the above-mentioned clearance mechanisms act simultaneously in an effort to efficiently remove old and/or damaged erythrocytes *in vivo*.

Side effects of erythrocyte transfusion

Erythrocyte transfusions are given to raise the hemoglobin concentration in patients with severe anemia, or after acute blood loss due to surgery and trauma. Erythrocytes as well as platelets and plasma are isolated from whole blood of healthy donors by centrifugation. The collected erythrocytes are stored in specially designed plastic bags containing a preservative solution at 4°C. In the Netherlands, the leukocyte numbers in the product are strongly reduced by centrifugation and subsequent filtration prior to storage in SAG-M preservation solution. Dutch legislation dictates that erythrocyte concentrates can only be used for transfusion within 35 days after their collection, in order to meet the international quality standards of 75% erythrocyte survival at 24 hours after transfusion and 0.8% hemolysis in the concentrate [63,64].

Although the more than 100 million annual voluntary blood donations help save millions of lives worldwide [65], erythrocyte transfusions can also have serious side effects, such as acute lung injury, iron deposition resulting in severe organ damage, vasoconstriction, and formation of alloantibodies and autoantibodies [66]. There are a number of changes that occur during erythrocyte storage that may cause the observed side effects after transfusion. These "storage lesions" include vesiculation [30,67], decreased deformability [68,69], decreased 2,3-bisphosphoglycerate [70], ATP and glutathione [71] concentrations, potassium leakage [72], and hemolysis [73].

Immune-mediated side effects

The erythrocyte contains a complex set of regulatory systems that may induce erythrocyte removal after physiological or pathological injury such as osmotic shock, oxidative stress and/or energy depletion [74]. Modulation of these pathways is progressively lost during storage [75,76], and this may result in accelerated aging and the removal of up to 30% of the transfused erythrocytes within 24 hours after transfusion [77]. Disruption of these systems likely include a reduction of the threshold for activation of the pathways governing PS

exposure [78], and may trigger aberrant expression of pathogenic epitopes on stored erythrocytes and their vesicles [79].

Frequent erythrocyte transfusions may induce the formation of alloantibodies. This is especially problematic in the steadily increasing number of transfusion-dependent patients. Almost half of these patients acquire alloantibodies at some point in time, and in approximately 10% of the patients erythrocyte autoantibodies are detected. Some patients that produce these autoantibodies develop autoimmune hemolytic anemia, which can be life-threatening [80,81]. Observations such as these suggest that erythrocyte antigenicity changes during storage, potentially leading to autoantibody production after transfusion against these neoantigens. Murine studies suggest that erythrocyte transfusions can augment inflammation [82,83], that may enhance the risk of immune responses towards erythrocyte autoantigens.

Storage duration versus clinical outcome

The wealth of data available on the gradual changes observed in the erythrocyte during storage [84] has long since sparked the discussion that longer storage time increases the risk of transfusion side effects. Multiple studies have reported that increased storage age of transfused erythrocytes is an independent risk factor for a number of adverse endpoints [85-91]. In contrast, several other studies did not find any difference between short and long stored erythrocytes on clinical outcome [92-95]. The use of either leukocyte-reduced or non-leukocyte-reduced erythrocyte products in these studies may explain the observed discrepancies [96]. Thus far, there are no completed prospective randomized controlled studies examining the effect of storage duration of transfused erythrocytes on morbidity and mortality [96-98]. To definitively answer this question two large clinical trials are currently underway: The US-based initiative Red Cell Storage Duration Study (RECESS), and the complementary UK and Canadian co-initiative Age of Blood Evaluation (ABLE) [98].

Anemia of inflammation

Inflammation arising from various etiologies, including autoimmune disorders, infection and in particular sepsis, promote anemia [99-101]. The preferred treatment is directed at the underlying disease. However, when inflammation persists there are only a few options for treatment of “anemia of inflammation” [99]. Approximately 40% of critically ill individuals, including those with severe sepsis, receive at least one erythrocyte concentrate in the intensive care unit, with a mean of five concentrates per patient, equaling half of the total human blood volume. In these patients, erythrocyte transfusions are associated with increased morbidity and mortality [101]. Because anemia is a comorbid condition that is

associated with poor outcomes in various chronic disease states, understanding its pathogenesis is essential for the development of new remedies [99].

Next to changes in systemic iron homeostasis and defective erythropoiesis [99,100], also a reduced erythrocyte lifespan contributes to anemia of inflammation [102-104]. While iron homeostasis and defective erythropoiesis have been extensively studied in these conditions, erythrocyte survival has received little attention so far [99]. Phagocytic capacity is enhanced during inflammation [105], providing a possible explanation for enhanced erythrocyte clearance. Alternatively, the wide range of changes occurring in the circulation during systemic inflammation might impact erythrocyte characteristics directly. Indeed, alterations in erythrocyte shape, deformability, and aggregability were observed in patients with severe sepsis [106,107]. To date no mechanistic explanation has been provided for these changes.

Erythrocyte membrane lipid remodeling in anemia of inflammation

Membrane protein modification could not be causally linked to the altered erythrocyte rheology observed in patients with severe sepsis [108]. However, lipid metabolism is markedly altered during inflammation, as exemplified by enhanced lipase activity and by changes in lipid constituents in the plasma [109], and could thus affect erythrocyte membrane lipid composition. This hypothesis is supported by the finding that the incubation of erythrocytes from healthy volunteers with plasma of septic patients resulted in enhanced PS exposure and ceramide content [110]. Ceramide is a bioactive lipid involved in many cellular processes including apoptosis, senescence and inflammation [111,112], possibly associated with the tendency of signaling receptors to cluster in ceramide-enriched platforms. In addition, the formation of these platforms alters membrane curvature and decreases plasma membrane integrity [113,114]. Sphingomyelinases (SMases) are the principal enzymes for the generation of ceramide [115]. Since in a variety of diseases, including sepsis, inflammation triggers the secretion of acid SMase in the blood, this SMase is likely responsible for the ceramide formation in erythrocytes [110].

III - Microparticles

Microparticles (MPs) were first described by Peter Wolf in 1967, when he observed a halo of debris surrounding activated platelets which he termed “platelet dust” [116]. They are defined as plasma membrane-derived vesicles with a diameter of 100 to 1000 nm that expose molecules specific to the parental cell [117-119]. The majority of the blood-borne MPs are generated by erythrocytes and platelets [119-121]. Depending on their origin, MPs may contain an array of signaling molecules, including receptors, cytokines and bioactive lipids, but also mRNA and microRNA. This molecular composition renders MPs vectors of

biological information. As such they play an active role in homeostasis and pathogenesis, the latter including atherosclerosis, various malignancies, autoimmune disorders, and infection [118,122].

Erythrocyte-derived microparticles

During aging, the erythrocyte produces numerous vesicles, often termed red cell microparticles (RMPs), that expose PS and autoantigens, which are probably responsible for their rapid removal from the circulation [30,31,121,123]. Data from *in vitro* studies suggest that RMPs are likely to be actively involved in pathophysiology as well. For example, RMPs from erythrocyte storage units were found to modulate platelet function [124], and to be highly procoagulant [125,126]. RMPs can transfer biologically active molecules, exemplified by the transfer of CD59 from control erythrocytes to CD59-lacking erythrocytes of patients with paroxysmal nocturnal hemoglobinuria [127]. Furthermore, RMPs may contribute to the procoagulant state and vaso-occlusions in sickle cell disease [120,128]. RMPs from malaria-infected erythrocytes were found to be major inducers of systemic inflammation during malaria infection [129,130].

Platelet-derived microparticles

In contrast to what the name implies, the majority of the 'platelet-derived microparticles' (PMPs) in the circulation are not derived from platelets, but from megakaryocytes [131,132]. PMPs are likely to be important mediators of coagulation, not only by exposing procoagulant factors [119,126,133], but also by providing a platform for the binding of additional platelets to the subendothelial matrix [119,134]. PMPs may be involved in various other processes, such as hemostasis, maintenance of vascular health, and immunity [135]. Prominent examples are the involvement of PMPs in vasoregeneration [136,137], and their assistance in leukocyte-leukocyte interaction via P-selectin binding to PSGL-1 [138]. A recent study showed that enhanced glycoprotein VI-mediated PMP generation leads to a PMP build-up in the joint fluid of patients suffering from inflammatory arthritis (but not osteoarthritis), inducing an inflammatory response via interleukin-1 signaling [139].

Microparticles in transfusion medicine

Not only *in vivo*, but also *in vitro* during blood bank storage, erythrocytes and platelets shed MPs [30,140]. These MPs may be responsible for some of the side-effects commonly observed after transfusion [141-145]. RMPs from storage products are enriched in removal signals such as PS, immunoglobulins, and complement [30,145]. The supernatant of erythrocyte transfusion units, which contains many RMPs that were shed during storage, was found to have the ability to modulate the functions of T cells [142], neutrophils [146], macrophages [141], and monocytes [147] *in vitro*. Transfusion unit supernatants also caused

lung inflammation and coagulopathy in a rat model [148]. These findings strengthen the view that a high dose of RMPs may induce or augment the inflammatory and/or immunological side-effects of transfusion, including autoantibody formation [149].

Next to coagulation, platelets also have an important role as immune mediators [150,151], making PMPs likely candidates for immune regulation as well [144,152-154]. Side-effects of platelet transfusion include fever and acute lung injury [153], and enhanced PMP levels in platelet units correlated with various allergic transfusion reactions [152]. The ability of PMPs to interact with leukocytes [138,152], as well as their potential to induce CD40L-mediated B cell activation [155], underscore their ability to affect the immune system. The plethora of signaling molecules on PMPs makes it even more likely that they contribute to the transfusion burden [135,156]. While most circulating PMPs originate from megakaryocytes [131,132], P-selectin-positive PMPs from platelet transfusion units constitute an important part of the storage PMP burden, and likely have distinct biological activities [152,157].

IV - The immune system

Our immune system has evolved to defend the body against harmful pathogens. Immune responses are strictly regulated to allow rapid initiation of immune activity upon infection, and quick resolution of the response after elimination of the pathogen, in order to prevent tissue damage. In addition, the immune system must be kept in a resting state in normal situations to prevent harmful responses against the body's own tissues and the commensal microorganisms. Parallel to immune surveillance, immune cells also provide essential support for tissue homeostasis and function [158].

The immune response

Tissue injury caused by pathogens and/or trauma triggers the local release of various soluble pro-inflammatory mediators, including chemokines and the cytokines IL-1 and TNF-α by specialized cells such as resident macrophages. IL-1 and TNF-α promote the expression of selectins and integrins by the local vascular endothelium, enabling the adhesion, arrest, and extravasation of leukocytes, which subsequently migrate along the chemokine gradient towards the inflamed tissue [159]. Platelets adhere to the exposed extracellular matrix and the inflamed endothelial cells, further activating the endothelium and adhering monocytes, and release additional pro-inflammatory factors including IL-1 [160,161]. At the site of tissue injury, neutrophils engulf pathogens and compromised cells, and subsequently release proteolytic enzymes and oxygen metabolites which digest the phagocytozed material [159]. Monocytes recruited to the inflamed tissue differentiate into different types of pro-inflammatory macrophages. Next to their function in phagocytozing pathogens, dead cells

and cell debris, these macrophages are the primary orchestrators of tissue inflammation [162].

Within days, a specific response is mustered due to antigen presentation to T and B cells by antigen-presenting cells like macrophages and dendritic cells. $CD4^+$ helper T (T_H) cells support the further activation of other effector cells of the adaptive immune system including B cells and $CD8^+$ cytotoxic T cells, through cell-cell interactions and the release of cytokines. The activated and differentiated B cells secrete antibodies that bind the antigen-exposing pathogen, assisting in their recognition by other effector cells. Activated cytotoxic T cells search for infected cells in the body that expose the antigen they are primed against, and kill these cells by disrupting their membrane and releasing an array of cytotoxins [156].

Immune cells regulate tissue homeostasis

Initially, inflamed tissue is dominated by M1-polarized macrophages which promote further leukocyte influx and T_H1-mediated and T_H17-mediated inflammatory responses by producing IL-1, TNF-α, IL-12 and IL-23. Inflammation must be resolved in a timely manner to avoid unnecessary tissue damage. M2-polarized macrophages that do not secrete IL-12 , but instead produce anti-inflammatory factors such as IL-10, TGF-β, IL-1 decoy receptor and IL1-RA, gradually appear in the inflamed tissue to dampen the inflammatory process [162,163]. They further consolidate the resolution of inflammation by inducing regulatory T cell (Treg) differentiation [164], and by actively recruiting Tregs through the release of CCL22 [165].

Tregs that express the transcription factor Foxp3 play a critical role in maintaining immune homeostasis and dominant self-tolerance through a combination of cell-cell interactions, the release of soluble factors including the anti-inflammatory cytokines IL-10, TGF-β and IL-35, and the scavenging of the T cell survival factor IL-2 (Figure 4). The majority of the $Foxp3^+$ Tregs are produced in the thymus as an antigen-primed and functionally mature T cell subpopulation (naturally-occurring Tregs), while some Tregs differentiate from naïve conventional T cells in the periphery (induced Tregs) [166,167]. Aside from their ability to suppress effector cell priming in lymphoid tissues [168-171], Tregs are also able to suppress myeloid populations and effector cells in other tissues [172]. Tregs have been shown to drive monocyte differentiation towards a M2-like macrophage phenotype, suggesting they consolidate the anti-inflammatory macrophage phenotype [173].

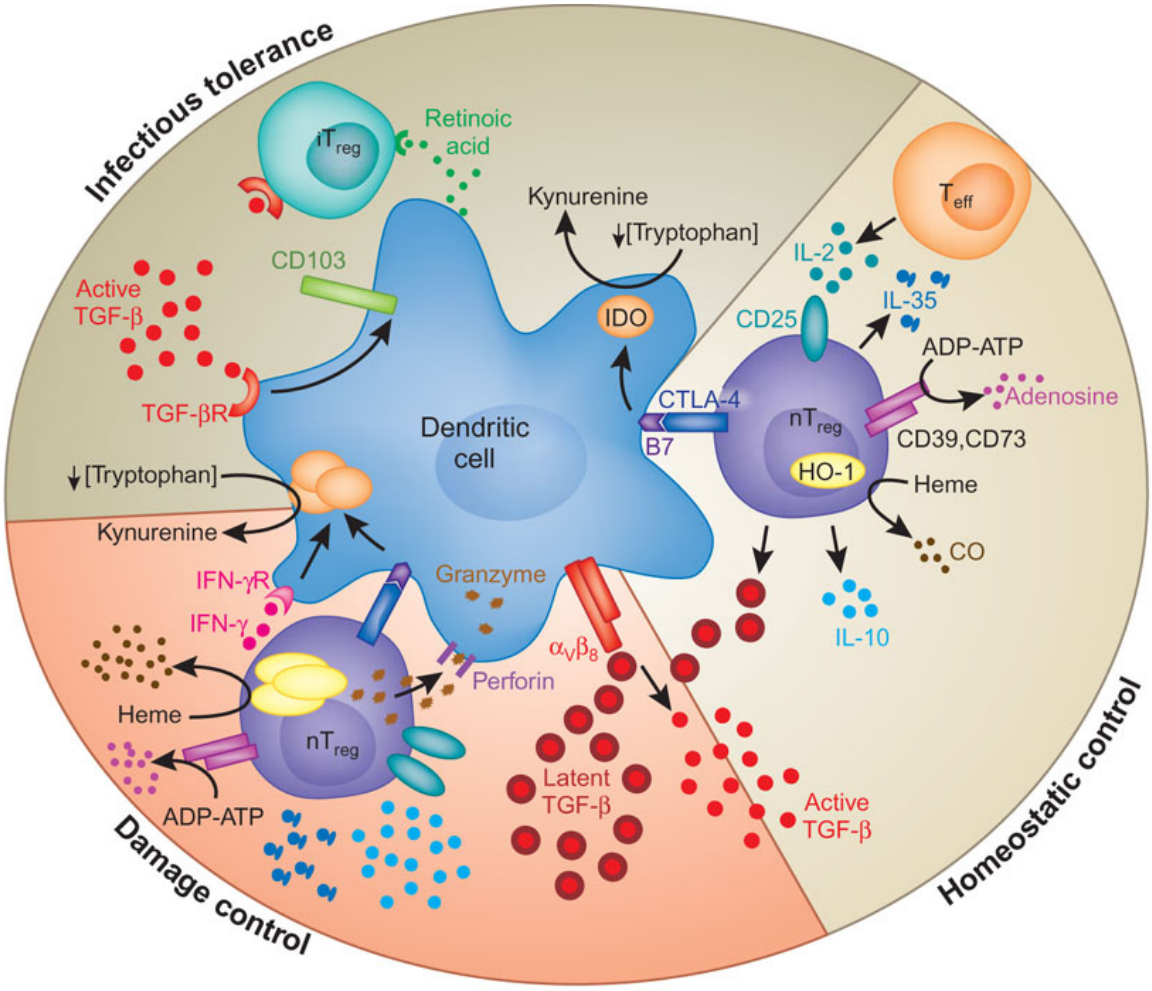

FIGURE 4. Mechanisms potentially used by Tregs to assert tissue homeostasis in the steady state, during 'damage control' in inflamed tissue, and for infectious tolerance after resolution of inflammation. iTreg – induced Treg cell, TGF-βR – TGF-β receptor, nTreg – natural Treg cell, CO – carbon monoxide, IFN-γR – IFN-γ receptor (Tang et al. [174])

During the resolution of inflammation, TGF-β and other growth factors such as VEGF, FGF and PDGF, that are released by macrophages, platelets [175], Tregs [172,176] and various other cell types [175], promote angiogenesis, tissue regeneration and wound repair. Macrophages further regulate wound healing by phagocytozing debris, apoptotic neutrophils, and extracellular matrix (ECM) components that promote inflammation [177,178], and by releasing factors that control ECM turnover [179]. This macrophage-governed healing process is tightly regulated in order to restore homeostatic tissue architecture and function, while preventing fibrosis and scarring.

In summary, the immune system sustains tissue homeostasis by disposing of invading pathogens and by supporting tissue repair and maintenance.

V - Scope of the thesis

Physiological erythrocyte aging leads to membrane alterations ultimately responsible for their removal from the circulation. Similar membrane changes occur during erythrocyte blood banking, and could explain the high removal rate of part of the erythrocytes shortly after transfusion and the transfusion side effects. Furthermore, the changes in the erythrocyte membrane that occur during systemic inflammation might explain a reduced erythrocyte lifespan contributing to the development of anemia. In recent years, increased awareness of the importance of microparticles in homeostasis, various diseases and transfusion medicine, has stimulated research on their exact nature and function. The aim of this thesis is to provide more insight into the erythrocyte membrane changes that occur during storage and systemic inflammation, including vesiculation. In addition, we studied the potential impact of platelet-derived microparticles on the immune system.

The potential formation of pathological antigens during erythrocyte storage was investigated in **Chapter 2**. Using patient plasma containing anti-erythrocyte autoantibodies, immunoprecipitations were performed with erythrocytes and MPs from concentrates of increasing storage periods. Antigen recognition by patient plasma autoantibodies was associated with storage time, and several membrane proteins could be identified as candidate antigens. The composition of the immune complexes recognized on the MPs was markedly different from those on the erythrocytes, indicating that their immunization potential differs from that of their parental cells. These data corroborate the theory that deregulation of the mechanisms governing erythrocyte aging contributes to transfusion-induced alloantibody and autoantibody formation.

In **Chapter 3**, we assessed the potential of PS exposure as a parameter for donor-dependent variation in product quality. PS exposure was determined just prior to, and during a 35-day storage period, and was found to correlate with common blood bank quality parameters and some donor characteristics. PS exposure increased with storage time, and correlated with hemolysis and MP concentration in the concentrate, and with the plasma hemoglobin concentration of the donor. Furthermore, the initial level of PS exposure was found to be predictive for PS exposure after osmotic stress. These findings support the use of PS exposure as a donor-dependent, biologically relevant parameter for erythrocyte transfusion unit quality.

During systemic inflammation, as occurs in patients with severe sepsis, the lipid metabolism in the circulation is markedly altered, involving an enhanced activity of several lipases such as SMases. The functional consequences of these enzymes on erythrocyte structure and function were studied in detail in **Chapter 4**. We found erythrocytes to be very sensitive to

SMase-induced ceramide formation in the membrane. Ceramide build-up led to the loss of the discoid shape, followed by PS exposure and loss of cell integrity. In this process, markedly enhanced vesiculation and reduced deformability were also observed. Erythrocytes aged *in vivo* and *in vitro* were more sensitive to SMase-induced changes than younger erythrocytes. This study indicates that SMase has the potential to alter pathophysiologically relevant erythrocyte parameters, which is especially important in the context of erythrocyte transfusion in patients with prolonged systemic inflammation.

Based on the results described in Chapter 4, we investigated sepsis-associated changes in the erythrocyte membrane lipid composition. In **Chapter 5**, we analyzed the plasma membrane lipid content of freshly isolated erythrocytes from healthy volunteers after incubation with the plasma of patients with septic shock. While ceramide could not be detected, we found markedly increased levels of lysophosphatidylcholine (LPC), which is produced by phospholipase A2. Although secretory phospholipase A2 IIA was greatly enhanced in the septic patient plasmas, its concentration did not correlate with the LPC levels. Enhanced LPC levels were not detected when erythrocytes were incubated with the plasma of healthy volunteers, in whom sepsis was simulated using a low dose of lipopolysaccharide. Interestingly, erythrocyte PS exposure increased in these subjects after lipopolysaccharide infusion. These data provide evidence for active remodeling, during sepsis, of the lipid compartment of the erythrocyte membrane, which is likely to affect erythrocyte survival.

During the course of our studies we extensively studied cell-derived MPs from various sources. The isolation, analysis and quantification of these MPs is challenging due to their small and heterogeneous size. Based on our experience, we present our perspective on the do's and don'ts regarding RMP and PMP isolation and characterization in **Chapter 6**. A novel regulatory function of PMPs on regulatory T cell stability is presented in **Chapter 7**. In this chapter we show that PMPs selectively bind to a specialized subset of $Foxp3^+$ regulatory T cells, and that PMPs inhibit their differentiation into potentially pathogenic effector cells in a pro-inflammatory microenvironment. Our data indicate the direct involvement of the adhesion molecule P-selectin and thus suggest a role for PMPs in vascular healing by regulating the regulators at the sites of vascular insult.

In **Chapter 8**, the findings reported in this manuscript are summarized and discussed, and future perspectives are outlined.

References

1 Gregory CJ, Eaves AC. Three stages of erythropoietic progenitor cell differentiation distinguished by a number of physical and biologic properties. *Blood* 51(3), 527-537 (1978).

2 Kundu M, Lindsten T, Yang CY *et al*. Ulk1 plays a critical role in the autophagic clearance of mitochondria and ribosomes during reticulocyte maturation. *Blood* 112(4), 1493-1502 (2008).

3 Zhang J, Randall MS, Loyd MR *et al*. Mitochondrial clearance is regulated by Atg7-dependent and -independent mechanisms during reticulocyte maturation. *Blood* 114(1), 157-164 (2009).

4 Chasis JA, Prenant M, Leung A, Mohandas N. Membrane assembly and remodeling during reticulocyte maturation. *Blood* 74(3), 1112-1120 (1989).

5 Waugh RE, Mantalaris A, Bauserman RG, Hwang WC, Wu JH. Membrane instability in late-stage erythropoiesis. *Blood* 97(6), 1869-1875 (2001).

6 Dornhorst AC. The interpretation of red cell survival curves. *Blood* 6(12), 1284-1292 (1951).

7 Kay M. Immunoregulation of cellular life span. *Ann. N. Y. Acad. Sci.* 1057 85-111 (2005).

8 Pantaleo A, Ferru E, Giribaldi G *et al*. Oxidized and poorly glycosylated band 3 is selectively phosphorylated by Syk kinase to form large membrane clusters in normal and G6PD-deficient red blood cells. *Biochem. J.* 418(2), 359-367 (2009).

9 Alper SL. Molecular physiology of SLC4 anion exchangers. *Exp. Physiol* 91(1), 153-161 (2006).

10 Campanella ME, Chu H, Low PS. Assembly and regulation of a glycolytic enzyme complex on the human erythrocyte membrane. *Proc. Natl. Acad. Sci. U. S. A* 102(7), 2402-2407 (2005).

11 van den Akker E, Satchwell TJ, Williamson RC, Toye AM. Band 3 multiprotein complexes in the red cell membrane; of mice and men. *Blood Cells Mol. Dis.* 45(1), 1-8 (2010).

12 Anong WA, Franco T, Chu H *et al*. Adducin forms a bridge between the erythrocyte membrane and its cytoskeleton and regulates membrane cohesion. *Blood* 114(9), 1904-1912 (2009).

13 Toye AM, Ghosh S, Young MT *et al*. Protein-4.2 association with band 3 (AE1, SLCA4) in Xenopus oocytes: effects of three natural protein-4.2 mutations associated with hemolytic anemia. *Blood* 105(10), 4088-4095 (2005).

14 Zhang D, Kiyatkin A, Bolin JT, Low PS. Crystallographic structure and functional interpretation of the cytoplasmic domain of erythrocyte membrane band 3. *Blood* 96(9), 2925-2933 (2000).

15 Beckmann R, Smythe JS, Anstee DJ, Tanner MJ. Coexpression of band 3 mutants and Rh polypeptides: differential effects of band 3 on the expression of the Rh complex containing D polypeptide and the Rh complex containing CcEe polypeptide. *Blood* 97(8), 2496-2505 (2001).

16 Bruce LJ, Beckmann R, Ribeiro ML *et al*. A band 3-based macrocomplex of integral and peripheral proteins in the RBC membrane. *Blood* 101(10), 4180-4188 (2003).

17 Salomao M, Zhang X, Yang Y *et al*. Protein 4.1R-dependent multiprotein complex: new insights into the structural organization of the red blood cell membrane. *Proc. Natl. Acad. Sci. U. S. A* 105(23), 8026-8031 (2008).

18 Mchedlishvili G. Disturbed blood flow structuring as critical factor of hemorheological disorders in microcirculation. *Clin. Hemorheol. Microcirc.* 19(4), 315-325 (1998).

19 Mohandas N, Chasis JA. Red blood cell deformability, membrane material properties and shape: regulation by transmembrane, skeletal and cytosolic proteins and lipids. *Semin. Hematol.* 30(3), 171-192 (1993).

20 Parthasarathi K, Lipowsky HH. Capillary recruitment in response to tissue hypoxia and its dependence on red blood cell deformability. *Am. J. Physiol* 277(6 Pt 2), H2145-H2157 (1999).

21 Mohandas N, Evans E. Mechanical properties of the red cell membrane in relation to molecular structure and genetic defects. *Annu. Rev. Biophys. Biomol. Struct.* 23 787-818 (1994).

22 Mokken FC, Kedaria M, Henny CP, Hardeman MR, Gelb AW. The clinical importance of erythrocyte deformability, a hemorrheological parameter. *Ann. Hematol.* 64(3), 113-122 (1992).

23 Mebius RE, Kraal G. Structure and function of the spleen. *Nat. Rev. Immunol.* 5(8), 606-616 (2005).

24 Deplaine G, Safeukui I, Jeddi F *et al*. The sensing of poorly deformable red blood cells by the human spleen can be mimicked in vitro. *Blood* 117(8), e88-e95 (2011).

25 Safeukui I, Buffet PA, Deplaine G *et al*. Quantitative assessment of sensing and sequestration of spherocytic erythrocytes by the human spleen. *Blood* 120(2), 424-430 (2012).

26 Mohandas N, Gallagher PG. Red cell membrane: past, present, and future. *Blood* 112(10), 3939-3948 (2008).

27 Willekens FL, Roerdinkholder-Stoelwinder B, Groenen-Dopp YA *et al*. Hemoglobin loss from erythrocytes in vivo results from spleen-facilitated vesiculation. *Blood* 101(2), 747-751 (2003).

28 Willekens FL, Werre JM, Kruijt JK *et al*. Liver Kupffer cells rapidly remove red blood cell-derived vesicles from the circulation by scavenger receptors. *Blood* 105(5), 2141-2145 (2005).

29 Willekens FL, Werre JM, Groenen-Dopp YA, Roerdinkholder-Stoelwinder B, de Pauw B, Bosman GJ. Erythrocyte vesiculation: a self-protective mechanism? *Br. J. Haematol.* 141(4), 549-556 (2008).

30 Bosman GJ, Lasonder E, Luten M *et al*. The proteome of red cell membranes and vesicles during storage in blood bank conditions. *Transfusion* 48(5), 827-835 (2008).

31 Bosman GJ, Lasonder E, Groenen-Dopp YA, Willekens FL, Werre JM. The proteome of erythrocyte-derived microparticles from plasma: new clues for erythrocyte aging and vesiculation. *J. Proteomics.* (2012).

33 Ferru E, Giger K, Pantaleo A *et al*. Regulation of membrane-cytoskeletal interactions by tyrosine phosphorylation of erythrocyte band 3. *Blood* 117(22), 5998-6006 (2011).

34 Bosch FH, Werre JM, Schipper L *et al*. Determinants of red blood cell deformability in relation to cell age. *Eur. J. Haematol.* 52(1), 35-41 (1994).

35 Bosch FH, Werre JM, Roerdinkholder-Stoelwinder B, Huls TH, Willekens FL, Halie MR. Characteristics of red blood cell populations fractionated with a combination of counterflow centrifugation and Percoll separation. *Blood* 79(1), 254-260 (1992).

36 Verkleij AJ, Zwaal RF, Roelofsen B, Comfurius P, Kastelijn D, van Deenen LL. The asymmetric distribution of phospholipids in the human red cell membrane. A combined study using phospholipases and freeze-etch electron microscopy. *Biochim. Biophys. Acta* 323(2), 178-193 (1973).

37 Zwaal RF, Schroit AJ. Pathophysiologic implications of membrane phospholipid asymmetry in blood cells. *Blood* 89(4), 1121-1132 (1997).

38 Daleke DL. Regulation of phospholipid asymmetry in the erythrocyte membrane. *Curr. Opin. Hematol.* 15(3), 191-195 (2008).

39 Castoldi E, Collins PW, Williamson PL, Bevers EM. Compound heterozygosity for 2 novel TMEM16F mutations in a patient with Scott syndrome. *Blood* 117(16), 4399-4400 (2011).

40 Suzuki J, Umeda M, Sims PJ, Nagata S. Calcium-dependent phospholipid scrambling by TMEM16F. *Nature* 468(7325), 834-838 (2010).

41 Yang H, Kim A, David T *et al*. TMEM16F forms a Ca2+-activated cation channel required for lipid scrambling in platelets during blood coagulation. *Cell* 151(1), 111-122 (2012).

42 Daleke DL. Regulation of phospholipid asymmetry in the erythrocyte membrane. *Curr. Opin. Hematol.* 15(3), 191-195 (2008).

43 Kuypers FA. Red cell membrane lipids in hemoglobinopathies. *Curr. Mol. Med.* 8(7), 633-638 (2008).

44 Morse EE. Mechanisms of hemolysis in liver disease. *Ann. Clin. Lab Sci.* 20(3), 169-174 (1990).

45 Bucki R, Bachelot-Loza C, Zachowski A, Giraud F, Sulpice JC. Calcium induces phospholipid redistribution and microvesicle release in human erythrocyte membranes by independent pathways. *Biochemistry* 37(44), 15383-15391 (1998).

46 Fadok VA, Voelker DR, Campbell PA, Cohen JJ, Bratton DL, Henson PM. Exposure of phosphatidylserine on the surface of apoptotic lymphocytes triggers specific recognition and removal by macrophages. *J. Immunol.* 148(7), 2207-2216 (1992).

47 Bratton DL, Fadok VA, Richter DA, Kailey JM, Guthrie LA, Henson PM. Appearance of phosphatidylserine on apoptotic cells requires calcium-mediated nonspecific flip-flop and is enhanced by loss of the aminophospholipid translocase. *J. Biol. Chem.* 272(42), 26159-26165 (1997).

48 Brown SB, Clarke MC, Magowan L, Sanderson H, Savill J. Constitutive death of platelets leading to scavenger receptor-mediated phagocytosis. A caspase-independent cell clearance program. *J. Biol. Chem.* 275(8), 5987-5996 (2000).

49 Kamp D, Sieberg T, Haest CW. Inhibition and stimulation of phospholipid scrambling activity. Consequences for lipid asymmetry, echinocytosis, and microvesiculation of erythrocytes. *Biochemistry* 40(31), 9438-9446 (2001).

50 Kobayashi N, Karisola P, Pena-Cruz V *et al*. TIM-1 and TIM-4 glycoproteins bind phosphatidylserine and mediate uptake of apoptotic cells. *Immunity.* 27(6), 927-940 (2007).

51 Oka K, Sawamura T, Kikuta K *et al*. Lectin-like oxidized low-density lipoprotein receptor 1 mediates phagocytosis of aged/apoptotic cells in endothelial cells. *Proc. Natl. Acad. Sci. U. S. A* 95(16), 9535-9540 (1998).

52 Park SY, Jung MY, Kim HJ *et al*. Rapid cell corpse clearance by stabilin-2, a membrane phosphatidylserine receptor. *Cell Death. Differ.* 15(1), 192-201 (2008).

53 Fens MH, Mastrobattista E, de Graaff AM *et al*. Angiogenic endothelium shows lactadherin-dependent phagocytosis of aged erythrocytes and apoptotic cells. *Blood* 111(9), 4542-4550 (2008).

54 Hanayama R, Tanaka M, Miwa K, Shinohara A, Iwamatsu A, Nagata S. Identification of a factor that links apoptotic cells to phagocytes. *Nature* 417(6885), 182-187 (2002).

55 Schroit AJ, Madsen JW, Tanaka Y. In vivo recognition and clearance of red blood cells containing phosphatidylserine in their plasma membranes. *J. Biol. Chem.* 260(8), 5131-5138 (1985).

56 Lee SJ, Park SY, Jung MY, Bae SM, Kim IS. Mechanism for phosphatidylserine-dependent erythrophagocytosis in mouse liver. *Blood* 117(19), 5215-5223 (2011).

57 Bosman GJ, Willekens FL, Werre JM. Erythrocyte aging: a more than superficial resemblance to apoptosis? *Cell Physiol Biochem.* 16(1-3), 1-8 (2005).

58 Kuypers FA, de Jong K. The role of phosphatidylserine in recognition and removal of erythrocytes. *Cell Mol. Biol. (Noisy. -le-grand)* 50(2), 147-158 (2004).

59 Oldenborg PA, Zheleznyak A, Fang YF, Lagenaur CF, Gresham HD, Lindberg FP. Role of CD47 as a marker of self on red blood cells. *Science* 288(5473), 2051-2054 (2000).

60 Oldenborg PA, Gresham HD, Lindberg FP. CD47-signal regulatory protein alpha (SIRPalpha) regulates Fcgamma and complement receptor-mediated phagocytosis. *J. Exp. Med.* 193(7), 855-862 (2001).

61 Olsson M, Oldenborg PA. CD47 on experimentally senescent murine RBCs inhibits phagocytosis following Fcgamma receptor-mediated but not scavenger receptor-mediated recognition by macrophages. *Blood* 112(10), 4259-4267 (2008).

62 Burger P, Hilarius-Stokman P, de Korte D, van den Berg TK, van Bruggen R. CD47 functions as a molecular switch for erythrocyte phagocytosis. *Blood* 119(23), 5512-5521 (2012).

63 Dumont LJ, AuBuchon JP. Evaluation of proposed FDA criteria for the evaluation of radiolabeled red cell recovery trials. *Transfusion* 48(6), 1053-1060 (2008).

64 European Directorate for the Quality of Medicines & HealthCare. Guide to the Preparation, Use, and Quality Assurance of Blood Components. 17 ed. Council of Europe publishing; 2013.

65 World Health Organization. Blood safety and availability - Fact sheet N°279. http://www.who.int/mediacentre/factsheets/fs279/en/; 2013 Jul. Report No.: Fact sheet N°279.

66 Perrotta PL, Snyder EL. Non-infectious complications of transfusion therapy. *Blood Rev.* 15(2), 69-83 (2001).

67 Donadee C, Raat NJ, Kanias T *et al*. Nitric oxide scavenging by red blood cell microparticles and cell-free hemoglobin as a mechanism for the red cell storage lesion. *Circulation* 124(4), 465-476 (2011).

68 Bahrstein G, Manny N, Yedgar S. Circulatory risk in the transfusion of red blood cells with impaired flow properties induced by storage. *Transfus. Med. Rev.* 25(1), 24-35 (2011).

69 Berezina TL, Zaets SB, Morgan C *et al*. Influence of storage on red blood cell rheological properties. *J. Surg. Res.* 102(1), 6-12 (2002).

70 Bennett-Guerrero E, Veldman TH, Doctor A *et al*. Evolution of adverse changes in stored RBCs. *Proc. Natl. Acad. Sci. U. S. A* 104(43), 17063-17068 (2007).

71 Whillier S, Raftos JE, Sparrow RL, Kuchel PW. The effects of long-term storage of human red blood cells on the glutathione synthesis rate and steady-state concentration. *Transfusion* 51(7), 1450-1459 (2011).

72 de Korte D, Verhoeven AJ. Quality determinants of erythrocyte destined for transfusion. *Cell Mol. Biol. (Noisy-le-grand)* 50(2), 187-195 (2004).

73 Sowemimo-Coker SO. Red blood cell hemolysis during processing. *Transfus. Med. Rev.* 16(1), 46-60 (2002).

74 Lang KS, Lang PA, Bauer C *et al*. Mechanisms of suicidal erythrocyte death. *Cell Physiol Biochem.* 15(5), 195-202 (2005).

75 Antonelou MH, Kriebardis AG, Stamoulis KE, Economou-Petersen E, Margaritis LH, Papassideri IS. Red blood cell aging markers during storage in citrate-phosphate-dextrose-saline-adenine-glucose-mannitol. *Transfusion* 50(2), 376-389 (2010).

76 Messana I, Ferroni L, Misiti F *et al*. Blood bank conditions and RBCs: the progressive loss of metabolic modulation. *Transfusion* 40(3), 353-360 (2000).

77 Luten M, Roerdinkholder-Stoelwinder B, Schaap NP, de Grip WJ, Bos HJ, Bosman GJ. Survival of red blood cells after transfusion: a comparison between red cells concentrates of different storage periods. *Transfusion* 48(7), 1478-1485 (2008).

78 Bosman GJ, Cluitmans JC, Groenen YA, Werre JM, Willekens FL, Novotny VM. Susceptibility to hyperosmotic stress-induced phosphatidylserine exposure increases during red blood cell storage. *Transfusion* 51(5), 1072-1078 (2011).

79 Fossati-Jimack L, Azeredo da SS, Moll T *et al*. Selective increase of autoimmune epitope expression on aged erythrocytes in mice: implications in anti-erythrocyte autoimmune responses. *J. Autoimmun.* 18(1), 17-25 (2002).

80 Garratty G. Immune hemolytic anemia associated with negative routine serology. *Semin. Hematol.* 42(3), 156-164 (2005).

81 Young PP, Uzieblo A, Trulock E, Lublin DM, Goodnough LT. Autoantibody formation after alloimmunization: are blood transfusions a risk factor for autoimmune hemolytic anemia? *Transfusion* 44(1), 67-72 (2004).

82 Hod EA, Zhang N, Sokol SA *et al*. Transfusion of red blood cells after prolonged storage produces harmful effects that are mediated by iron and inflammation. *Blood* 115(21), 4284-4292 (2010).

83 Mangalmurti NS, Xiong Z, Hulver M *et al*. Loss of red cell chemokine scavenging promotes transfusion-related lung inflammation. *Blood* 113(5), 1158-1166 (2009).

84 Bosman GJ, Werre JM, Willekens FL, Novotny VM. Erythrocyte ageing in vivo and in vitro: structural aspects and implications for transfusion. *Transfus. Med.* 18(6), 335-347 (2008).

85 Baek JH, D'Agnillo F, Vallelian F *et al*. Hemoglobin-driven pathophysiology is an in vivo consequence of the red blood cell storage lesion that can be attenuated in guinea pigs by haptoglobin therapy. *J. Clin. Invest* 122(4), 1444-1458 (2012).

86 Edgren G, Kamper-Jorgensen M, Eloranta S *et al*. Duration of red blood cell storage and survival of transfused patients (CME). *Transfusion* 50(6), 1185-1195 (2010).

87 Eikelboom JW, Cook RJ, Liu Y, Heddle NM. Duration of red cell storage before transfusion and in-hospital mortality. *Am. Heart J.* 159(5), 737-743 (2010).

88 Gauvin F, Spinella PC, Lacroix J *et al*. Association between length of storage of transfused red blood cells and multiple organ dysfunction syndrome in pediatric intensive care patients. *Transfusion* 50(9), 1902-1913 (2010).

89 Koch CG, Li L, Sessler DI *et al*. Duration of red-cell storage and complications after cardiac surgery. *N. Engl. J. Med.* 358(12), 1229-1239 (2008).

90 Sanders J, Patel S, Cooper J *et al*. Red blood cell storage is associated with length of stay and renal complications after cardiac surgery. *Transfusion* 51(11), 2286-2294 (2011).

91 Zallen G, Offner PJ, Moore EE *et al*. Age of transfused blood is an independent risk factor for postinjury multiple organ failure. *Am. J. Surg.* 178(6), 570-572 (1999).

92 Kor DJ, Kashyap R, Weiskopf RB *et al*. Fresh red blood cell transfusion and short-term pulmonary, immunologic, and coagulation status: a randomized clinical trial. *Am. J. Respir. Crit Care Med.* 185(8), 842-850 (2012).

93 Phelan HA, Eastman AL, Aldy K *et al*. Prestorage leukoreduction abrogates the detrimental effect of aging on packed red cells transfused after trauma: a prospective cohort study. *Am. J. Surg.* 203(2), 198-204 (2012).

94 Vamvakas EC, Carven JH. Length of storage of transfused red cells and postoperative morbidity in patients undergoing coronary artery bypass graft surgery. *Transfusion* 40(1), 101-109 (2000).

95 van de Watering L, Lorinser J, Versteegh M, Westendord R, Brand A. Effects of storage time of red blood cell transfusions on the prognosis of coronary artery bypass graft patients. *Transfusion* 46(10), 1712-1718 (2006).

96 van de Watering L. Pitfalls in the current published observational literature on the effects of red blood cell storage. *Transfusion* 51(8), 1847-1854 (2011).

97 Lee JS, Gladwin MT. Bad blood: the risks of red cell storage. *Nat. Med.* 16(4), 381-382 (2010).

98 Edelstein SB. Blood product storage: does age really matter? *Semin. Cardiothorac. Vasc. Anesth.* 16(3), 160-165 (2012).

99 Roy CN. Anemia of inflammation. *Hematology. Am. Soc. Hematol. Educ. Program.* 2010 276-280 (2010).

100 Weiss G, Goodnough LT. Anemia of chronic disease. *N. Engl. J. Med.* 352(10), 1011-1023 (2005).

101 Napolitano LM, Kurek S, Luchette FA *et al*. Clinical practice guideline: red blood cell transfusion in adult trauma and critical care. *Crit Care Med.* 37(12), 3124-3157 (2009).

102 Manodori AB, Kuypers FA. Altered red cell turnover in diabetic mice. *J. Lab Clin. Med.* 140(3), 161-165 (2002).

103 Mitlyng BL, Singh JA, Furne JK, Ruddy J, Levitt MD. Use of breath carbon monoxide measurements to assess erythrocyte survival in subjects with chronic diseases. *Am. J. Hematol.* 81(6), 432-438 (2006).

104 Moldawer LL, Marano MA, Wei H *et al*. Cachectin/tumor necrosis factor-alpha alters red blood cell kinetics and induces anemia in vivo. *FASEB J.* 3(5), 1637-1643 (1989).

105 Brown GC, Neher JJ. Eaten alive! Cell death by primary phagocytosis: 'phagoptosis'. *Trends Biochem. Sci.* 37(8), 325-332 (2012).

106 Piagnerelli M, Boudjeltia KZ, Brohee D *et al*. Alterations of red blood cell shape and sialic acid membrane content in septic patients. *Crit Care Med.* 31(8), 2156-2162 (2003).

107 Reggiori G, Occhipinti G, De Gasperi A, Vincent JL, Piagnerelli M. Early alterations of red blood cell rheology in critically ill patients. *Crit Care Med.* 37(12), 3041-3046 (2009).

108 Piagnerelli M, Cotton F, van Nuffelen M, Vincent JL, Gulbis B. Modifications in erythrocyte membrane protein content are not responsible for the alterations in rheology seen in sepsis. *Shock* 37(1), 17-21 (2012).

109 Khovidhunkit W, Kim MS, Memon RA *et al*. Effects of infection and inflammation on lipid and lipoprotein metabolism: mechanisms and consequences to the host. *J. Lipid Res.* 45(7), 1169-1196 (2004).

110 Kempe DS, Akel A, Lang PA *et al*. Suicidal erythrocyte death in sepsis. *J. Mol. Med. (Berl)* 85(3), 273-281 (2007).

111 Grassme H, Riethmuller J, Gulbins E. Biological aspects of ceramide-enriched membrane domains. *Prog. Lipid Res.* 46(3-4), 161-170 (2007).

112 Hannun YA, Obeid LM. Principles of bioactive lipid signalling: lessons from sphingolipids. *Nat. Rev. Mol. Cell Biol.* 9(2), 139-150 (2008).

113 Goni FM, Alonso A. Sphingomyelinases: enzymology and membrane activity. *FEBS Lett.* 531(1), 38-46 (2002).

114 Lopez-Montero I, Monroy F, Velez M, Devaux PF. Ceramide: from lateral segregation to mechanical stress. *Biochim. Biophys. Acta* 1798(7), 1348-1356 (2010).

115 Goni FM, Alonso A. Sphingomyelinases: enzymology and membrane activity. *FEBS Lett.* 531(1), 38-46 (2002).

116 Wolf P. The nature and significance of platelet products in human plasma. *Br. J. Haematol.* 13(3), 269-288 (1967).

117 Gyorgy B, Szabo TG, Pasztoi M *et al*. Membrane vesicles, current state-of-the-art: emerging role of extracellular vesicles. *Cell Mol. Life Sci.* 68(16), 2667-2688 (2011).

118 Thery C, Ostrowski M, Segura E. Membrane vesicles as conveyors of immune responses. *Nat. Rev. Immunol.* 9(8), 581-593 (2009).

119 Owens AP, III, Mackman N. Microparticles in hemostasis and thrombosis. *Circ. Res.* 108(10), 1284-1297 (2011).

120 van Beers EJ, Schaap MC, Berckmans RJ *et al*. Circulating erythrocyte-derived microparticles are associated with coagulation activation in sickle cell disease. *Haematologica* 94(11), 1513-1519 (2009).

121 Willekens FL, Roerdinkholder-Stoelwinder B, Groenen-Dopp YA *et al*. Hemoglobin loss from erythrocytes in vivo results from spleen-facilitated vesiculation. *Blood* 101(2), 747-751 (2003).

122 Mause SF, Weber C. Microparticles: protagonists of a novel communication network for intercellular information exchange. *Circ. Res.* 107(9), 1047-1057 (2010).

123 Willekens FL, Werre JM, Kruijt JK *et al*. Liver Kupffer cells rapidly remove red blood cell-derived vesicles from the circulation by scavenger receptors. *Blood* 105(5), 2141-2145 (2005).

124 Xiong Z, Cavaretta J, Qu L, Stolz DB, Triulzi D, Lee JS. Red blood cell microparticles show altered inflammatory chemokine binding and release ligand upon interaction with platelets. *Transfusion* 51(3), 610-621 (2011).

125 Gao Y, Lv L, Liu S, Ma G, Su Y. Elevated levels of thrombin-generating microparticles in stored red blood cells. *Vox Sang.* (2013).

126 van der Meijden PE, van Schilfgaarde M, van Oerle R, Renne T, ten Cate H, Spronk HM. Platelet- and erythrocyte-derived microparticles trigger thrombin generation via factor XIIa. *J. Thromb. Haemost.* 10(7), 1355-1362 (2012).

127 Sloand EM, Mainwaring L, Keyvanfar K *et al*. Transfer of glycosylphosphatidylinositol-anchored proteins to deficient cells after erythrocyte transfusion in paroxysmal nocturnal hemoglobinuria. *Blood* 104(12), 3782-3788 (2004).

128 Camus SM, Gausseres B, Bonnin P *et al*. Erythrocyte microparticles can induce kidney vaso-occlusions in a murine model of sickle cell disease. *Blood* 120(25), 5050-5058 (2012).

129 Couper KN, Barnes T, Hafalla JC *et al*. Parasite-derived plasma microparticles contribute significantly to malaria infection-induced inflammation through potent macrophage stimulation. *PLoS. Pathog.* 6(1), e1000744 (2010).

130 Mantel PY, Hoang AN, Goldowitz I *et al*. Malaria-infected erythrocyte-derived microvesicles mediate cellular communication within the parasite population and with the host immune system. *Cell Host. Microbe* 13(5), 521-534 (2013).

131 Rank A, Nieuwland R, Delker R *et al*. Cellular origin of platelet-derived microparticles in vivo. *Thromb. Res.* 126(4), e255-e259 (2010).

132 Flaumenhaft R, Dilks JR, Richardson J *et al*. Megakaryocyte-derived microparticles: direct visualization and distinction from platelet-derived microparticles. *Blood* 113(5), 1112-1121 (2009).

133 Sinauridze EI, Kireev DA, Popenko NY *et al*. Platelet microparticle membranes have 50- to 100-fold higher specific procoagulant activity than activated platelets. *Thromb. Haemost.* 97(3), 425-434 (2007).

134 Merten M, Pakala R, Thiagarajan P, Benedict CR. Platelet microparticles promote platelet interaction with subendothelial matrix in a glycoprotein IIb/IIIa-dependent mechanism. *Circulation* 99(19), 2577-2582 (1999).

135 Aatonen M, Gronholm M, Siljander PR. Platelet-derived microvesicles: multitalented participants in intercellular communication. *Semin. Thromb. Hemost.* 38(1), 102-113 (2012).

136 Mause SF, Ritzel E, Liehn EA *et al*. Platelet microparticles enhance the vasoregenerative potential of angiogenic early outgrowth cells after vascular injury. *Circulation* 122(5), 495-506 (2010).

137 Prokopi M, Pula G, Mayr U *et al*. Proteomic analysis reveals presence of platelet microparticles in endothelial progenitor cell cultures. *Blood* 114(3), 723-732 (2009).

138 Forlow SB, McEver RP, Nollert MU. Leukocyte-leukocyte interactions mediated by platelet microparticles under flow. *Blood* 95(4), 1317-1323 (2000).

139 Boilard E, Nigrovic PA, Larabee K *et al*. Platelets amplify inflammation in arthritis via collagen-dependent microparticle production. *Science* 327(5965), 580-583 (2010).

140 Cauwenberghs S, Feijge MA, Harper AG, Sage SO, Curvers J, Heemskerk JW. Shedding of procoagulant microparticles from unstimulated platelets by integrin-mediated destabilization of actin cytoskeleton. *FEBS Lett.* 580(22), 5313-5320 (2006).

141 Sadallah S, Eken C, Schifferli JA. Erythrocyte-derived ectosomes have immunosuppressive properties. *J. Leukoc. Biol.* 84(5), 1316-1325 (2008).

142 Baumgartner JM, Silliman CC, Moore EE, Banerjee A, McCarter MD. Stored red blood cell transfusion induces regulatory T cells. *J. Am. Coll. Surg.* 208(1), 110-119 (2009).

143 Donadee C, Raat NJ, Kanias T *et al*. Nitric oxide scavenging by red blood cell microparticles and cell-free hemoglobin as a mechanism for the red cell storage lesion. *Circulation* 124(4), 465-476 (2011).

144 Morrell CN. Immunomodulatory mediators in platelet transfusion reactions. *Hematology. Am. Soc. Hematol. Educ. Program.* 2011 470-474 (2011).

145 Dinkla S, Novotny VM, Joosten I, Bosman GJ. Storage-induced changes in erythrocyte membrane proteins promote recognition by autoantibodies. *PLoS. One.* 7(8), e42250 (2012).

146 Belizaire RM, Prakash PS, Richter JR *et al*. Microparticles from stored red blood cells activate neutrophils and cause lung injury after hemorrhage and resuscitation. *J. Am. Coll. Surg.* 214(4), 648-655 (2012).

147 Muszynski J, Nateri J, Nicol K, Greathouse K, Hanson L, Hall M. Immunosuppressive effects of red blood cells on monocytes are related to both storage time and storage solution. *Transfusion* 52(4), 794-802 (2012).

148 Vlaar AP, Hofstra JJ, Levi M *et al*. Supernatant of aged erythrocytes causes lung inflammation and coagulopathy in a "two-hit" in vivo syngeneic transfusion model. *Anesthesiology* 113(1), 92-103 (2010).

149 Young PP, Uzieblo A, Trulock E, Lublin DM, Goodnough LT. Autoantibody formation after alloimmunization: are blood transfusions a risk factor for autoimmune hemolytic anemia? *Transfusion* 44(1), 67-72 (2004).

150 Flad HD, Brandt E. Platelet-derived chemokines: pathophysiology and therapeutic aspects. *Cell Mol. Life Sci.* 67(14), 2363-2386 (2010).

151 Li N. Platelet-lymphocyte cross-talk. *J. Leukoc. Biol.* 83(5), 1069-1078 (2008).

152 Nomura S, Okamae F, Abe M *et al*. Platelets expressing P-selectin and platelet-derived microparticles in stored platelet concentrates bind to PSGL-1 on filtrated leukocytes. *Clin. Appl. Thromb. Hemost.* 6(4), 213-221 (2000).

153 Refaai MA, Phipps RP, Spinelli SL, Blumberg N. Platelet transfusions: impact on hemostasis, thrombosis, inflammation and clinical outcomes. *Thromb. Res.* 127(4), 287-291 (2011).

154 Vlaar AP, Hofstra JJ, Kulik W *et al*. Supernatant of stored platelets causes lung inflammation and coagulopathy in a novel in vivo transfusion model. *Blood* 116(8), 1360-1368 (2010).

155 Sprague DL, Elzey BD, Crist SA, Waldschmidt TJ, Jensen RJ, Ratliff TL. Platelet-mediated modulation of adaptive immunity: unique delivery of CD154 signal by platelet-derived membrane vesicles. *Blood* 111(10), 5028-5036 (2008).

156 Garcia BA, Smalley DM, Cho H, Shabanowitz J, Ley K, Hunt DF. The platelet microparticle proteome. *J. Proteome. Res.* 4(5), 1516-1521 (2005).

157 Rank A, Nieuwland R, Liebhardt S *et al*. Apheresis platelet concentrates contain platelet-derived and endothelial cell-derived microparticles. *Vox Sang.* 100(2), 179-186 (2011).

158 Parham P. The Immune System. 3rd ed. Garland Science; 2009.

159 Kumar V, Abbas AK, Aster J. Inflammation and Repair. In: *Robbins Basic Pathology (Volume 9th)*. Elsevier, (2013).

160 Gawaz M, Langer H, May AE. Platelets in inflammation and atherogenesis. *J. Clin. Invest* 115(12), 3378-3384 (2005).

161 Semple JW, Italiano JE, Jr., Freedman J. Platelets and the immune continuum. *Nat. Rev. Immunol.* 11(4), 264-274 (2011).

162 Murray PJ, Wynn TA. Protective and pathogenic functions of macrophage subsets. *Nat. Rev. Immunol.* 11(11), 723-737 (2011).

163 Biswas SK, Mantovani A. Macrophage plasticity and interaction with lymphocyte subsets: cancer as a paradigm. *Nat. Immunol.* 11(10), 889-896 (2010).

164 Savage ND, de Boer T, Walburg KV *et al*. Human anti-inflammatory macrophages induce Foxp3+ GITR+ CD25+ regulatory T cells, which suppress via membrane-bound TGFbeta-1. *J. Immunol.* 181(3), 2220-2226 (2008).

165 Curiel TJ, Coukos G, Zou L *et al*. Specific recruitment of regulatory T cells in ovarian carcinoma fosters immune privilege and predicts reduced survival. *Nat. Med.* 10(9), 942-949 (2004).

166 Sakaguchi S, Miyara M, Costantino CM, Hafler DA. FOXP3+ regulatory T cells in the human immune system. *Nat. Rev. Immunol.* 10(7), 490-500 (2010).

167 Josefowicz SZ, Lu LF, Rudensky AY. Regulatory T cells: mechanisms of differentiation and function. *Annu. Rev. Immunol.* 30 531-564 (2012).

168 Chaudhry A, Rudra D, Treuting P *et al*. CD4+ regulatory T cells control TH17 responses in a Stat3-dependent manner. *Science* 326(5955), 986-991 (2009).

169 Chung Y, Tanaka S, Chu F *et al*. Follicular regulatory T cells expressing Foxp3 and Bcl-6 suppress germinal center reactions. *Nat. Med.* 17(8), 983-988 (2011).

170 Koch MA, Tucker-Heard G, Perdue NR, Killebrew JR, Urdahl KB, Campbell DJ. The transcription factor T-bet controls regulatory T cell homeostasis and function during type 1 inflammation. *Nat. Immunol.* 10(6), 595-602 (2009).

171 Linterman MA, Pierson W, Lee SK *et al*. Foxp3+ follicular regulatory T cells control the germinal center response. *Nat. Med.* 17(8), 975-982 (2011).

172 Burzyn D, Benoist C, Mathis D. Regulatory T cells in nonlymphoid tissues. *Nat. Immunol.* 14(10), 1007-1013 (2013).

173 Tiemessen MM, Jagger AL, Evans HG, van Herwijnen MJ, John S, Taams LS. CD4+CD25+Foxp3+ regulatory T cells induce alternative activation of human monocytes/macrophages. *Proc. Natl. Acad. Sci. U. S. A* 104(49), 19446-19451 (2007).

174 Tang Q, Bluestone JA. The Foxp3+ regulatory T cell: a jack of all trades, master of regulation. *Nat. Immunol.* 9(3), 239-244 (2008).

175 Barrientos S, Stojadinovic O, Golinko MS, Brem H, Tomic-Canic M. Growth factors and cytokines in wound healing. *Wound. Repair Regen.* 16(5), 585-601 (2008).

176 Burzyn D, Kuswanto W, Kolodin D *et al*. A special population of regulatory T cells potentiates muscle repair. *Cell* 155(6), 1282-1295 (2013).

177 Barron L, Wynn TA. Fibrosis is regulated by Th2 and Th17 responses and by dynamic interactions between fibroblasts and macrophages. *Am. J. Physiol Gastrointest. Liver Physiol* 300(5), G723-G728 (2011).

178 Atabai K, Jame S, Azhar N *et al*. Mfge8 diminishes the severity of tissue fibrosis in mice by binding and targeting collagen for uptake by macrophages. *J. Clin. Invest* 119(12), 3713-3722 (2009).

179 Wynn TA. Cellular and molecular mechanisms of fibrosis. *J. Pathol.* 214(2), 199-210 (2008).

2

Storage-induced changes in erythrocyte membrane proteins promote recognition by autoantibodies

Sip Dinkla[1], Věra M. J. Novotný[2], Irma Joosten[1] and Giel J.C.G.M. Bosman[3]

[1]Department of Laboratory Medicine – Laboratory of Medical Immunology, [2]Department of Hematology, [3]Department of Biochemistry, Radboud University Medical Centre

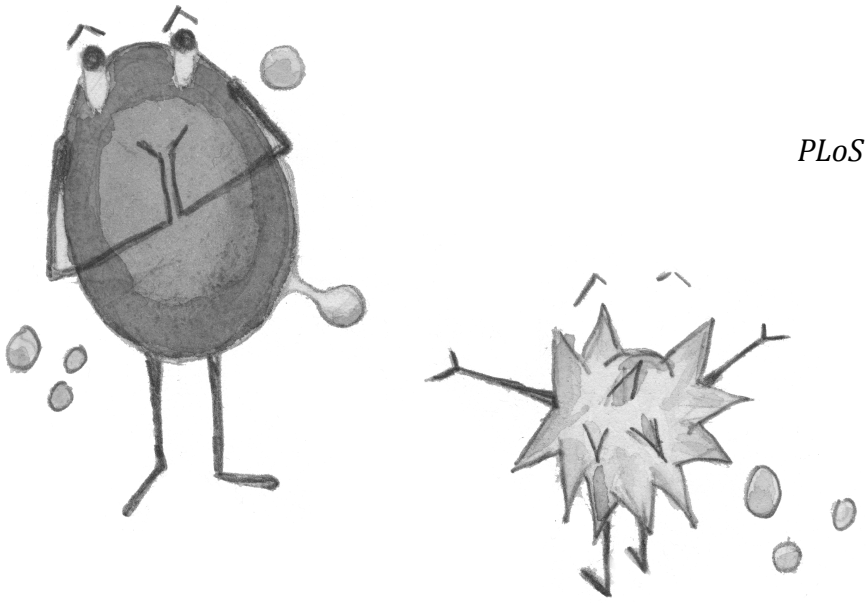

PLoS One. 2012;**7**(**8**):e42250

Abstract

Physiological erythrocyte removal is associated with a selective increase in expression of neoantigens on erythrocytes and their vesicles, and subsequent autologous antibody binding and phagocytosis. Chronic erythrocyte transfusion often leads to immunization and the formation of alloantibodies and autoantibodies. We investigated whether erythrocyte storage leads to the increased expression of non-physiological antigens. Immunoprecipitations were performed with erythrocytes and vesicles from blood bank erythrocyte concentrates of increasing storage periods, using patient plasma containing erythrocyte autoantibodies. Immunoprecipitate composition was identified using proteomics. Patient plasma antibody binding increased with erythrocyte storage time, while the opposite was observed for healthy volunteer plasma, showing that pathology-associated antigenicity changes during erythrocyte storage. Several membrane proteins were identified as candidate antigens. The protein complexes that were precipitated by the patient antibodies in erythrocytes were different from the ones in the vesicles formed during erythrocyte storage, indicating that the storage-associated vesicles have a different immunization potential. Soluble immune mediators including complement factors were present in the patient plasma immunoprecipitates, but not in the allogeneic control immunoprecipitates. The results support the theory that disturbed erythrocyte aging during storage of erythrocyte concentrates contributes to transfusion-induced alloantibody and autoantibody formation.

Introduction

Physiological, age-dependent removal of erythrocytes is an efficient and well-regulated process, consisting of controlled exposure of molecules that induce recognition of old erythrocytes by the immune system. This process includes senescent cell antigen formation on band 3, possibly in combination with phosphatidylserine (PS) exposure on the outer leaflet of the membrane and/or decreased CD47 expression, ultimately resulting in binding of autologous IgG and subsequent phagocytosis by macrophages of the reticulo-endothelial system [1]. During aging, the erythrocyte produces numerous vesicles, most of which expose PS, and that are enriched for IgG and age-related band 3 breakdown products. These vesicles are rapidly removed from the circulation, probably by the same mechanism that is responsible for erythrocyte removal. Vesiculation may constitute a protective mechanism to prevent untimely erythrocyte removal [2].

A clear picture of the molecular mechanisms involved in this age-dependent increase in removal signals is gradually emerging, and involves oxidative damage-induced, high-affinity binding of hemoglobin to band 3, activation of Ca^{2+}-permeable channels, phosphorylation-controlled loss of metabolism and structure, and degradation and/or aggregation of band 3 fragments. However, the molecular details, triggers and cross-talk between these pathways are largely unknown [1].

Also, the erythrocyte contains a complex set of regulatory systems that may induce erythrocyte removal after physiological or pathological injury such as osmotic shock, oxidative stress and/or energy depletion [3]. Modulation of these pathways becomes progressively lost during storage [4,5], and this may result in accelerated aging and the removal of up to 30% of the transfused erythrocytes within 24 hours after transfusion [6]. Disruption of these systems may trigger aberrant expression of pathogenic epitopes on stored erythrocytes and their vesicles [7].

Frequent erythrocyte transfusions can lead to immunization and the formation of alloantibodies. This is especially problematic in the steadily increasing number of transfusion-dependent patients. Almost half of these patients acquire alloantibodies at some point in time, and in approximately 10% of the patients erythrocyte autoantibodies are detected. Part of the patients that produce these autoantibodies develop autoimmune hemolytic anemia (AIHA), which can be life-threatening [8].

We postulated that accelerated and/or altered erythrocyte aging during blood bank storage leads to the formation of non-physiological neoantigens that trigger the formation of autoantibodies. In order to test this hypothesis, we performed immunoprecipitations with

erythrocytes and vesicles from blood bank concentrates of increasing storage periods, using plasma from patients containing erythrocyte autoantibodies. Subsequently, immunochemical and proteomic techniques were applied to identify the captured immune complexes. Our findings strengthen and deepen the view that disturbed erythrocyte aging during storage is related to transfusion-induced, anti-erythrocyte antibody formation.

Materials and Methods

Ethics

The study has been approved by the Committee on Research involving Human Subjects (CMO) of the Radboud University Medical Center ("Instituut Waarborging kwaliteit en veiligheid/ Commissie Mensgebonden onderzoek regio- Arnhem-Nijmegen") and in accordance with the declaration of Helsinki. Written informed consent was obtained from all blood donors participating in this study.

Patients and healthy volunteers

Plasma samples from nine patients with a positive direct antiglobulin test (DAT) and confirmed erythrocyte autoantibodies were included in this study. Four patients were diagnosed with AIHA. One of these patients presented with AIHA after which a relapse acute myeloid leukemia was observed, while another was diagnosed with having both AIHA and anti-phospholipid syndrome. Two additional patients were diagnosed with immune thrombocytopenia and AIHA (Evans syndrome). Three patients with detectable erythrocyte autoantibodies without any clinical consequences were included as well (Table 1). The antibodies of one patient reacted with the erythrocyte Rhesus e-antigen on the patient's autologous erythrocytes. In five patients anti-Wright^a (Wr^a) antibodies were detected, and in one patient additional anti-C^w antibodies were present. Cold reactive autoantibodies were not detected in any of the samples. Allogeneic plasma from healthy volunteer blood donors was used as a control. All plasma samples used in this study had been stored at -20°C before use.

Isolation and storage of erythrocytes

An erythrocyte concentrate was obtained using standard blood bank procedures, from a single eligible donor who was AB0, Rhesus, Wr^a and C^w compatible for the detected antibodies in the patient plasmas. Whole blood (500 ml) was collected in a Composelect quadruple CPD-SAGM top-and-bottom bag system (Fresenius Kabi, Bad Homburg, Germany), containing 70 ml CPD as an anticoagulant. After cooling and centrifugation, erythrocytes were isolated using a Compomat G4 (Fresenius Kabi, Bad Homburg,

Germany), after which 110 ml SAG-M was added to the erythrocytes. The erythrocyte suspension was leukocyte-depleted by in-line filtration, and subsequently stored at 2 to 6°C.

Sampling of erythrocyte concentrates

During a storage period of 35 days, this erythrocyte concentrate was sampled at regular intervals. After sampling, erythrocytes were isolated by 10 min centrifugation at 1500 g. At the time of blood collection, an additional EDTA tube of whole blood was collected for isolation of plasma and fresh erythrocytes using a Ficoll gradient.

Isolation of erythrocyte vesicles

Erythrocyte-derived vesicles were obtained from 35 day-old erythrocyte concentrates of two donors who were AB0, Rhesus and Wr^a compatible for the detected antibodies in the patient plasmas. The concentrates were centrifuged for 10 min at 1500 g to remove all cells. Membrane debris was then removed from the supernatant by centrifugation for 20 min at 1500 g. Vesicles were isolated by centrifuging 1.4 ml aliquots of supernatant for 20 min at 21,000 g. All but 25 µl of the supernatant was then removed, and the vesicle pellet was resuspended and stored at -80°C.

Indirect immunoprecipitation of erythrocyte autoantigens

Immunoprecipitation was performed using a modified version of the procedure described by Barker and colleagues [9]. Erythrocytes (1.5×10^9) were washed three times using incomplete Ringer (IR) solution (32 mM HEPES, 125 mM NaCl, 5 mM glucose, 5 mM KCl, 1 mM $MgSO_4$, pH 7.4), before incubation for 1 h at 37°C with 500 µl plasma diluted 1/1 in IR. The sensitized erythrocytes were then washed three times with IR, and lysed by adding lysis buffer (10 mM HEPES, 1 mM EDTA, 1 mM EGTA, 1 mM benzamidin, 5 µM leupeptin, pH 8.0). The erythrocyte membranes were pelleted by centrifugation at 21,000 g for 10 min and washed multiple times with lysis buffer to remove hemoglobin. The membranes were dissolved in 200 µl 1% TX-100 buffer (25 mM HEPES, 150 mM NaCl, 1 mM EDTA, 1 mM EGTA, 1 mM benzamidin, 5 µM leupeptin, pH 7.4) or RIPA buffer (1% NP-40, 1% deoxycholate, 0.1% SDS, 25 mM HEPES, 150 mM NaCl, 1 mM EDTA, 1 mM EGTA, 1 mM benzamidin, 5 µM leupeptin, pH 7.4) for 30 min on ice with regular vortexing. Unless mentioned otherwise, the TX100 buffer was applied. Insoluble cytoskeletal components were removed by 15 min centrifugation at 21,000 g. The protein content of the supernatant was determined using the Bradford assay [10]. Supernatant (250 µl) containing 0.35 mg protein was incubated with 50 µl protein G Dynabeads (Invitrogen, Carlsbad, USA) for 16 h at 4°C to capture immune complexes. The beads were washed three times with 1% TX-100 buffer or RIPA buffer prior to, and directly after the incubation with the supernatant. Then the captured proteins were dissociated in 15 µl Laemmli sample buffer (BioRad, Hercules, USA)

containing 5% 2-mercaptoethanol for 30 min at 37°C. When non-denaturing conditions were applied, proteins were eluted using 50 mM glycine pH 2.8 for 5 min at room temperature, after which sample buffer was added (1/4 ratio) without 2-mercaptoethanol. Samples were stored at -80°C, and thawed on ice on the day of analysis. Immunoprecipitation of erythrocyte vesicles was performed using the same protocol without the lysis step, using a single vesicle aliquot per sample. Smaller (100 µl) incubation volumes were used for vesicle opsonisation, membrane dissolution and immune complex capture. Plasma was depleted of vesicles by centrifugation for 60 min at 21,000 g before being used to opsonize erythrocyte vesicles. Subsequent erythrocyte vesicle isolation and washing was performed by centrifugation for 20 min at 21,000 g. Direct anti-band 3 immunoprecipitation in vesicles was performed using protein G Dynabeads, opsonized with a mouse monoclonal antibody that recognizes an N-terminal epitope of band 3 (BIII-136, Sigma-Aldrich, St. Louis, USA), diluted 1:20 in 200 µl phosphate-buffered saline (PBS), pH 7.4. In the immunoprecipitation experiments we observed 25-30 and 50-60 kDa bands, representing the light and heavy chains of the bound antibodies, respectively.

SDS-PAGE

SDS-PAGE was performed using TGX 4-15% gels in the Mini Protean 3 system (both BioRad, Hercules, USA) [11]. Approximate molecular masses were calculated based on the Precision Plus Protein Standard (BioRad, Hercules, USA). Following SDS-PAGE (12.5 µl sample per lane), the gels were either used for immunoblotting, or developed using a silver stain [12]. Optical densities (OD) of the protein bands were determined using the GS 690 imaging densitometer (Bio-Rad, Hercules, USA) in combination with Molecular Analyst version 1.5 software. Total erythrocyte membrane fractions were loaded as positive controls and for normalization purposes.

Erythrocyte vesicle membrane protein biotinylation

For immunoblotting, vesicle membrane proteins were biotinylated prior to IP. Vesicles were washed once with PBS pH 7.4, and labeled with 1 mM sulfo-NHS-biotin (Thermo Fisher, Waltham, USA) in PBS pH 8.0 for 30 min at 4°C. Residual sulfo-NHS-biotin was removed by two consecutive washing steps with PBS pH 7.4 containing 100 mM glycine.

Immunoblotting

After SDS-PAGE, the proteins were transferred to PVDF membranes using the iBlot system (Invitrogen, Carlsbad, USA). The membranes were then blocked with Odyssey Blocking Buffer (OBB, LI-COR, Lincoln, USA), and incubated for 16 h at 4°C in OBB containing 0.1% Tween-20 and 1/1000 rabbit polyclonal antiserum against the membrane domain of human band 3 (K2N6B/PMB3 [13]). After three washing steps with PBS containing 0.1% Tween-20,

the blots were incubated for 1 h at room temperature in OBB, 0.1% Tween-20, 0.01% SDS, 1/10,000 streptavidin-Alexa Fluor 680 (Invitrogen, Carlsbad, USA), and 1/10,000 goat anti-rabbit IgG-IRDye 800 (LI-COR, Lincoln, USA). This final incubation was followed by a single washing step using PBS containing 0.1% Tween-20, and three subsequent washes with PBS. Immunoblots were scanned using the Odyssey Infrared Imaging System (LI-COR, Lincoln, USA), and analyzed using Odyssey Software version 2.1.

Proteomics

After one-dimensional gel electrophoresis and blue silver staining [14], protein bands of interest were excised and submitted to in-slice tryptic digestion. In case of total protein identification, the sample was run briefly into the gel, after which the entire product was excised and digested. Peptide sequencing of tryptic digests was performed by nano-liquid chromatography tandem mass spectrometry using the LTQ-FT ICR (Thermo Fisher, Waltham, USA) mass spectrometer essentially as described previously [15]. Peptide and protein identifications were extracted with the Mascot search engine version 2.2, using the Reference Sequence (RefSeq) database at the National Center for Biotechnical Information (NCBI) with Homo sapiens taxonomy and added sequence-tags. Carbamidomethylation of cysteines (fixed), oxidation of methionine (variable) and acetylation of the N-terminus (variable) were the modifications allowed in the search. Protein identification validation was performed by an in-house developed script [15]. The software classifies protein identifications based on the number of uniquely identified peptide sequences, clusters proteins sharing the same set of peptides, and validates the proteins with the following criteria: proteins with a single peptide must have a peptide score of >49, proteins with multiple peptides must have a score of >29.

Statistical analysis

Differences between the patient and allogeneic control group were determined using a two-way ANOVA followed by a Bonferroni post-test. Differences within a single group were determined using a one-way ANOVA followed by a Tukey's post-test. A confidence level of $p<0.05$ was considered to be significant.

Results

Altered epitope expression of erythrocytes during blood bank storage

Storage lesions, possibly resulting in accelerated aging, are responsible for the fast removal of a considerable portion of the erythrocytes after transfusion. Both non-physiological aging and enhanced removal are likely to contribute to the antibody responses against

erythrocytes frequently observed in chronically transfused patients. In order to test the hypothesis that storage of erythrocytes under blood bank conditions leads to the formation of non-physiological neoantigens, a modified indirect immunoprecipitation was performed using plasma of six patients with erythrocyte autoantibodies (Table 1) or of healthy donors (see Materials and Methods), in combination with erythrocytes sampled at different time points from a stored erythrocyte unit. Immunoprecipitations were performed at regular intervals during blood bank storage.

Table 1. Summary of patient information.

Patient	Clinical diagnosis	Blood group	DAT	IAT	Alloantibody	Autoantibody
1	AIHA (AML)	0 cc d ee	IgG, C3	1:4	anti-Wr^a	NS
2	Evans syndrome	0 cc d ee	IgG	1:8	-	NS
3	AIHA (APLS)	AB CC D ee	IgG, C3	1:1	anti-Wr^a	NS
4	-	A CC D ee	IgG	1:1	anti-Wr^a, -C^w	NS, anti-e
5	AIHA	A Cc D Ee	IgG, C3	1:1	anti-Wr^a	NS
6	AIHA	A Cc D ee	IgG	1:4	anti-Wr^a	NS
7	Evans syndrome	0 Cc D ee	IgG	1:1	-	NS
8	-	0 Cc D ee	IgG	1:1	-	NS
9	-	0 cc d ee	IgG, C3	1:1	-	NS

DAT = direct antiglobulin test, IAT = indirect antiglobulin test (bovine) titer, AIHA = autoimmune hemolytic anemia, AML = acute myeloid leukemia, NS = non-specific, APLS = anti-phospholipid syndrome. All patients had a positive DAT and IAT.

All plasmas tested precipitated proteins in the 90 to 100 kDa range (Figure 1). Immunoprecipitation using Ringer buffer instead of plasma did not result in any detectable protein precipitation (Figure 1A). Our data show that, although protein quantification of complex protein mixtures using silver staining can be problematic due to a limited dynamic range of the technique [16], silver staining proved to work well with the highly purified immunoprecipitates we obtained (Figure 1A). Both the patient and the allogeneic control plasmas showed a decrease in signal after the first week of erythrocyte storage. In contrast to the control samples that revealed a further significant decrease in signal with time, the signals derived from patient plasma significantly increased again with storage time (Figure 1B). Immunoblot analysis of membrane fractions from erythrocytes of various storage

periods using patient and allogeneic control plasma resulted in high background signals and/or non-specific binding, probably due to the denaturing conditions of SDS-PAGE and blotting (data not shown).

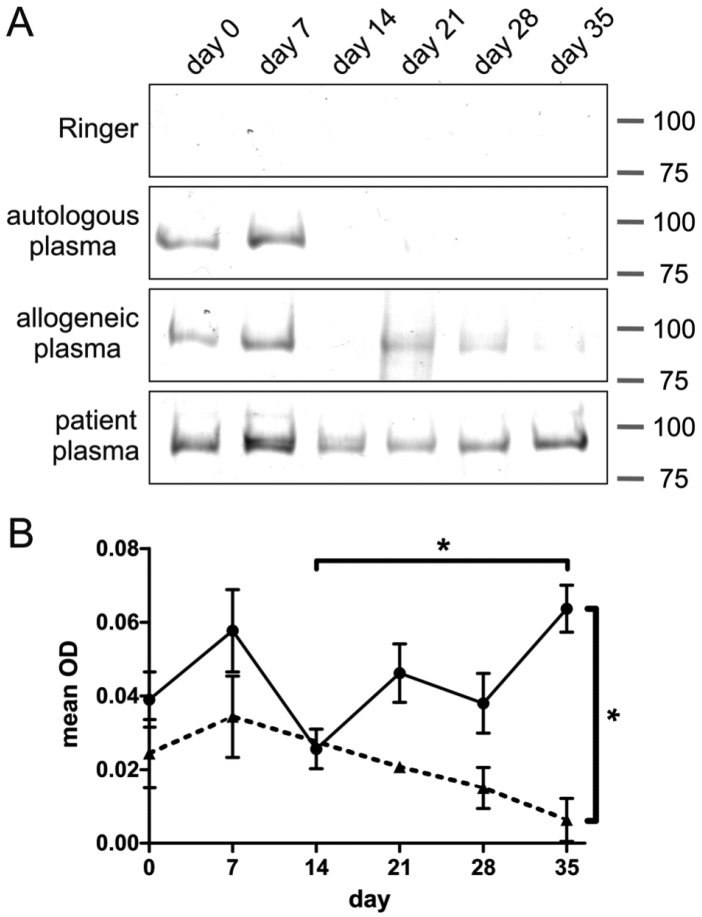

Figure 1. Erythrocyte autoantibody immunoprecipitation of erythrocytes sampled at regular time intervals during storage. Analysis was performed by SDS-PAGE, followed by silver staining. (A) Protein patterns of precipitates obtained using Ringer, autologous plasma, and a representative example from one out of three allogeneic plasmas, and one out of six autoantibody-containing plasmas (patient No. 2). For the allogeneic controls, day 14 is missing. (B) Mean optical density (OD) of patient (●, solid line, N=6 patients) and allogeneic control plasma (▲, dotted line, N=3 volunteers) precipitations. Numbers indicate approximate molecular weight (kDa). Error bars represent standard error, *p<0.05.

Freshly stored erythrocytes are recognized by naturally occurring antibodies [1]. At the later stages of storage, only autoantibodies present in the patient plasmas show enhanced binding to erythrocytes, suggesting a change in erythrocyte make-up upon storage that is only detectable with patient plasma. This change may be a trigger for pathological events. In order to determine the identity of the protein(s) involved, we proceeded to analyze the precipitated proteins by proteomics.

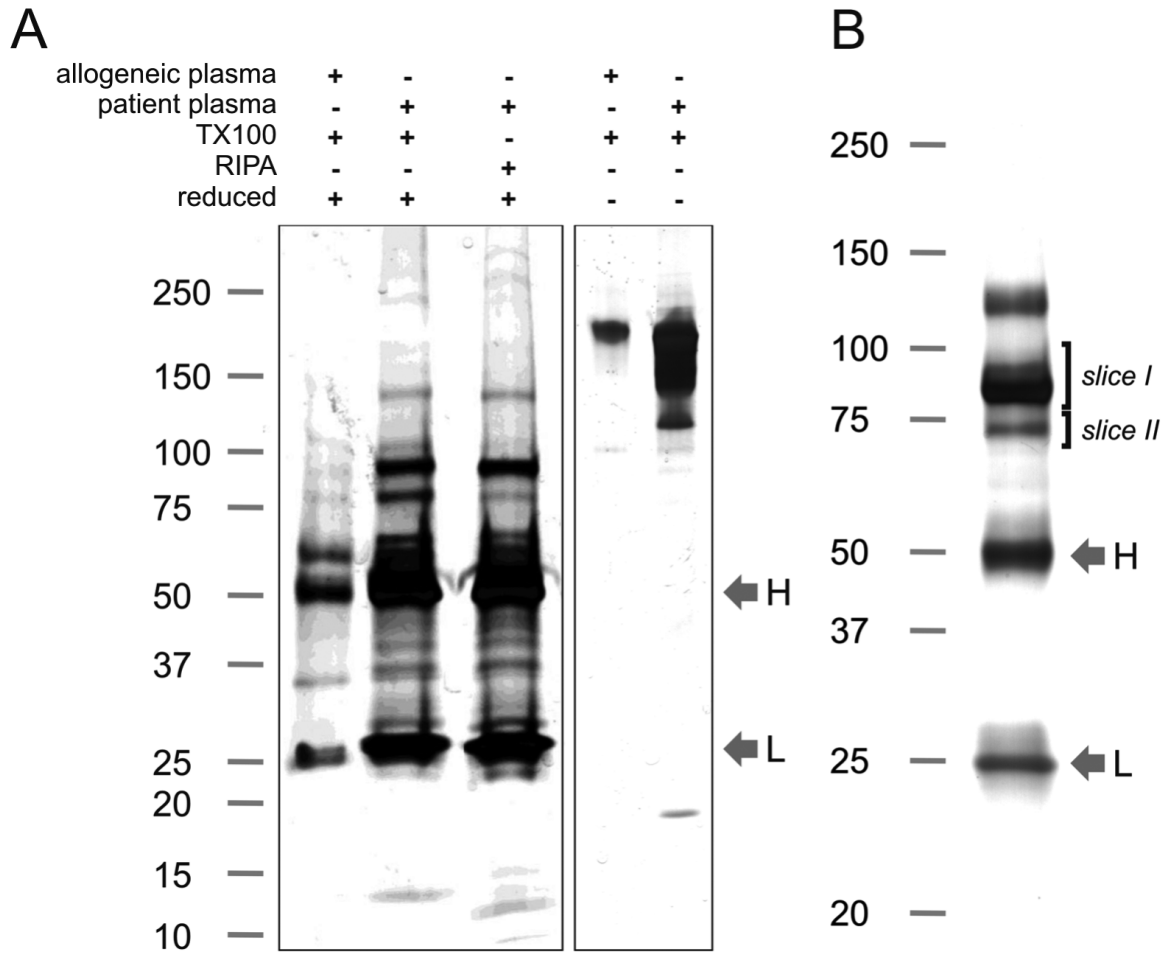

Figure 2. Erythrocyte autoantibody immunoprecipitation of stored erythrocytes. (A) Immunoprecipitation of 35 day-old erythrocytes with erythrocyte autoantibody-containing patient plasma and allogeneic control plasma, using TX100 or RIPA extraction buffer and analyzed by SDS-PAGE under reducing or non-reducing conditions, followed by silver staining. A representative result (patient No. 2) from one out of three patient plasmas is shown. (B) Example of a silver stained gel of an immunoprecipitation of 35 day stored erythrocytes with plasma of patient No. 1. The same sample was used for Coomassie blue gel staining and subsequent proteomics analysis (Table 2). Gel slices which were excised for proteomic analyses are indicated as slices I and II (see also Table S1). Numbers indicate molecular weight (kDa). Heavy [H] and light [L] antibody chains are indicated by arrows.

Identity of the precipitated proteins

In addition to the proteins in the 90 to 100 kDa range, immunoprecipitation of erythrocyte membrane fractions using patient plasmas revealed multiple other protein bands (Figure 2A). Differential extraction experiments showed that the proteins in the 90 to 100 kDa range were directly targeted by the patient plasma, instead of being co-precipitated as was the case for several other proteins, such as the 80 kDa protein band, which dissociated from the immune complex under the more stringent conditions of the RIPA buffer (Figure 2A). Furthermore, SDS-PAGE under non-reducing conditions indicated that the precipitated

proteins mostly reside in one or more large complexes (Figure 2A). Heavy and light antibody chains (H and L in Figure 2A) are clearly visible due to the nature of the technique used.

For proteomics analysis, an immunoprecipitation using patient plasma (patients 1, 8 and 9) and allogeneic plasma (control) was performed in triplicate on erythrocytes stored for 35 days. A representative silver stained gel of one of these immunoprecipitations is depicted in Figure 2B. The total products of these immunoprecipitations were analyzed by mass spectrometry (Table 2). In addition, gel slices in the 80-100 and 70-80 kDa ranges (Figure 2B, slices I and II, respectively) were excised from the immunoprecipitation product of the erythrocytes incubated with the plasma of patient 1 and analyzed by proteomics.

In summary, the proteomic analysis revealed that erythrocyte autoantibodies from the patient plasma precipitate multiple proteins. The samples consisted of membrane as well as cytosolic proteins, all of which have been described in previous proteomic inventories of the erythrocyte membrane (Table 2) [17]. Furthermore they contained various plasma proteins, such as immunoglobulins, complement components, lipoproteins, and several immunoglobulins, and complement and coagulation-associated proteins. The protein composition of the samples from the different patient samples revealed significant overlap, although fewer proteins were detected in the samples of patients 8 and 9. This could be due to the lower titer of these plasmas (Table 1). Proteomic analysis of the allogeneic plasma control precipitation did not reveal any erythrocyte-related proteins. A complete list of all the proteins detected in the proteomics analysis is provided in Table S1.

Finally, we attempted to elucidate the nature of the most dominant antigens. The proteomic analysis of gel slice I (Figure 2B) identified several proteins, including band 3 as the only membrane protein detected (Table S1).

Erythrocyte autoantibodies recognize erythrocyte vesicles formed during blood banking

During their stay in the circulation, erythrocytes form vesicles that are rapidly removed once they appear in the bloodstream. Vesiculation also occurs during blood banking, especially during the later stages of storage [18]. Since erythrocyte vesiculation *in vivo* may constitute a mechanism for the removal of damaged membrane patches, and these vesicles are efficiently opsonized [2,15], we investigated whether vesicles formed during blood bank storage were also recognized by patient anti-erythrocyte antibodies.

Table 2. Summary of proteins identified by proteomics analyses of erythrocyte/vesicle immunoprecipitations using erythrocyte autoantibody-containing plasma of patients 1, 8 and 9, and allogeneic plasma (control).

Protein	***MW*** (kDa)	***Erythrocyte*** Control	Patient 1	Patient 8	Patient 9	***Vesicle*** Patient 1
Structural						
Band 3	95		+	+		+
Band 4.1	66		+		+	+
Band 4.2	80			+	+	
Adducin	81		+		+	
Ankyrin	206					+
Actin	42		+	+	+	+
Spectrin	246					+
Metabolism						
GAPDH	36		+			+
Glucose transporter 1	54		+			+
Glutathione S-transferase	26		+			
Phosphofructokinase	85					
Type II PIP kinase	46					+
Various						
α globin	15		+			+
β globin	16		+	+	+	+
Annexin II	39					+
Carbonic anhydrase I	29		+			
Carbonic anhydrase II	29		+			+
HSP 70	70		+			
Stomatin	32		+			+
Thioredoxin	12		+			
Thrombospondin 1	129					+
Transglutaminase 3	77					
Ig heavy chain	50-60		+			+
Ig light chain	25-30		+			+
Complement						
CC 1	26			+	+	+
CC 3	187		+	+	+	+
CC 4	193	+	+	+	+	+
CC 5	188		+	+	+	+
CC 6	105				+	
CC 8	22				+	+
CC 9	63					+
Factor B	90			+	+	
Complement inhibitors						
C1 inhibitor				+	+	
Clusterin	58		+	+	+	+
Factor H	155			+	+	
Inter-α inhibitor	101-107		+	+	+	+
Vitronectin	54					+
Lipoproteins						
Apolipoprotein A	31		+	+	+	+
Apolipoprotein B	516	+	+	+	+	+
Apolipoprotein D	21					+
Apolipoprotein E	36		+		+	+
Apolipoprotein L1	44					+

We performed immunoprecipitations using patient plasma and biotinylated erythrocyte vesicles isolated from 35 day-old erythrocyte concentrates (see Materials and Methods). These precipitates were then visualized by immunoblotting for biotinylated membrane proteins. In stored erythrocyte vesicles, multiple proteins were targeted by the patient anti-erythrocyte antibodies, including the proteins in the 90 to 100 kDa range also observed in the erythrocyte precipitates (Figure 3A).

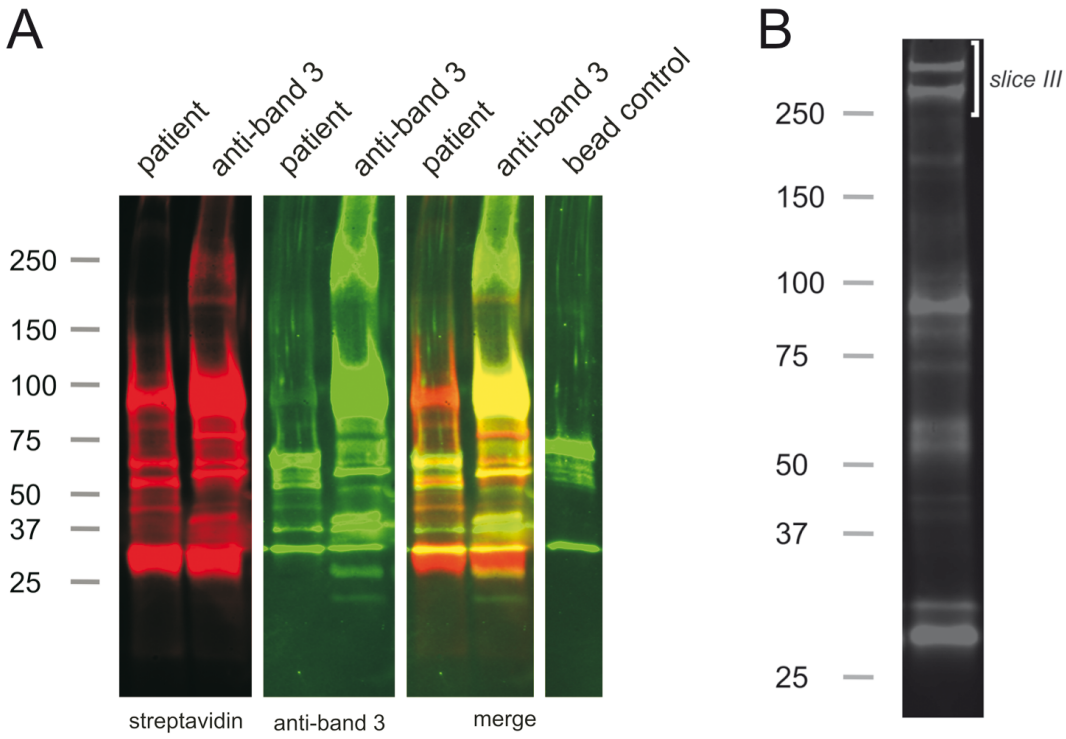

Figure 3. Erythrocyte autoantibody immunoprecipitation of biotinylated erythrocyte vesicles from a 35 day-old transfusion unit. (A) Immunoprecipitation with either plasma from patient No. 2, or a monoclonal antibody against band 3 (see Materials and Methods). Analysis was performed by SDS-PAGE, followed by detection of biotinylated membrane proteins (red, streptavidin) and band 3 (green, polyclonal rabbit antibody). A protein G bead control was included. (B) Example immunoprecipitation of biotinylated erythrocyte vesicles from a 35 day-old transfusion unit using plasma from patient No. 1. Analysis was performed by SDS-PAGE, followed by detection of biotinylated membrane proteins using fluorochrome conjugated streptavidin. The same sample was used for Coomassie blue gel staining and subsequent proteomics analysis (Table 2). The gel slice which was excised for proteomic analysis is indicated as slice III (see also Table S1). Numbers indicate approximate molecular weight (kDa). Blots were analyzed using the Odyssey Infrared Imaging System.

In order to identify the protein content of the targeted complex in these vesicles, an immunoprecipitation was performed in triplicate on vesicles obtained from a 35 day-old transfusion unit and analyzed by mass spectrometry (Table 2). An immunoblot of the immunoprecipitate is depicted in Figure 3B. In addition, we identified the proteins in a 240-320 kDa gel slice from the immunoprecipitation (Figure 3B, slice III and Table S1). A

comparison of the erythrocyte to the vesicle precipitate shows a large overlap in their protein contents, including the presence of band 3. However, some clear differences were observed as well. Most notable are the absence of ankyrin and spectrin in the erythrocyte complex, and the absence of adducin in the vesicle complex (Table 2). In the vesicle immunoprecipitation, complement and lipoprotein peptides were much more abundant than in the erythrocyte immunoprecipitations (Table 2 and Table S1).

Since band 3 was found to be part of the vesicle-derived precipitates, immunoprecipitations using either patient plasma or a monoclonal anti-band 3 antibody and biotinylated erythrocyte vesicles were performed as well (Figure 3A). These precipitates were then visualized by immunoblotting for biotinylated membrane proteins and band 3. The latter immunoprecipitation revealed a biotinylated protein pattern that is different from that obtained with the patient plasma, indicating that different proteins were targeted (Figure 3A). Although band 3 staining of the patient sample immunoblot using a polyclonal anti-band 3 antiserum did not detect full-length band 3 (Figure 3A), several band 3 breakdown products that form during erythrocyte aging and storage were observed [1,15].

Discussion

During storage under blood bank conditions, erythrocytes undergo a number of functional and structural alterations, known as storage lesions. An accelerated and/or disturbed cellular aging process is likely to trigger aberrant expression of removal signals, thereby contributing to the removal of up to 30% of the erythrocytes within the first 24 hours after transfusion. This may contribute to the immunologic responses associated especially with chronic transfusions [1,8].

Here we show that the main targets of the erythrocyte autoantibody-containing patient plasmas tested in this study are proteins in the 90 to 100 kDa range, which proteomic analysis revealed to include the membrane protein band 3. Band 3 is known to form three distinct complexes with other membrane and cytosolic proteins, and is the membrane anchorage site for the erythrocyte cytoskeleton [19]. Proteomic analysis showed that the band 3 binding partners adducin, ankyrin, band 4.1, band 4.2, GAPDH, hemoglobin and carbonic anhydrase were part of the precipitated immune complex, which suggests that band 3 complexes were indeed recognized. Although other candidate antigens cannot be completely ruled out, the observation that band 3 is the only membrane protein detected in the immunoprecipitates, makes it the most likely candidate antigen. Band 3 likely contains epitopes that trigger the harmful immune response leading to the formation of these erythrocyte autoantibodies [20]. This is underscored by the ability of a band 3 peptide to

prime T cells for a band 3 response and accelerates the development of erythrocyte autoantibodies and anemia in a mouse model for AIHA [21].

Our data reveal that autologous and allogeneic plasma predominantly reacted with fresh and short stored erythrocytes, possibly by the binding of naturally occurring anti-band 3 antibodies [1]. In contrast, patient plasma autoantibody binding increased during erythrocyte storage, which suggests that non-physiological antigens become expressed during blood bank storage. One explanation for the enhanced autoantibody binding could be storage lesion-induced expression of erythrocyte aging-associated antigens [1,4,5].

Notably, previous work on erythrocyte autoantibodies, showed these antibodies to be specific for either band 3 or Rhesus protein [9,20]. The apparent absence of Rhesus proteins in our analyses is probably due to the exclusion of patient plasma that showed (partial) specificity toward Rhesus antigens. The presence of alloantibodies against Wr^a, an epitope located on band 3 [22], in five of the nine patients also hints at specificity for band 3 rather than Rhesus protein.

A remarkable observation was the precipitation of adaptor protein 2 (AP2) complex by the patient plasma (Table S1), as this protein is responsible for membrane attachment of, and membrane protein recruitment to clathrin-coated vesicles [23]. AP2 might be a remnant from the reticulocyte stage that binds to one or more proteins in the precipitated complex. Band 3 has been shown to interact with clathrin-coated vesicle machinery in kidney cells, which supports this possibility [24].

Although erythrocyte-derived vesicles formed during storage are known to be enriched in immunoglobulins [15,25], we here show that anti-erythrocyte autoantibodies readily recognized the vesicles as well. The vesicle precipitates contained spectrin and ankyrin, while the erythrocyte precipitates did not. The opposite was observed for adducin, which was present only in the erythrocyte precipitates. Ankyrin and adducin are known to reside in two functionally different complexes in the erythrocyte membrane, the ankyrin complex and the junctional complex [19]. An explanation for our observations may be the selective erythrocyte autoantibody binding of the band 3 - ankyrin complex in vesicles, compared to the selective targeting of the junctional complex in erythrocytes. The differences in protein composition between erythrocytes and their vesicles could also account for the absence of adducin in the vesicle precipitates [2,15,18]. The strikingly high complement content and apparent presence of autoantigens in the patient plasma vesicle precipitates indicate that these vesicles may be involved in clinically relevant immune responses.

The possibility of selective recognition of damaged or degraded band 3 in the vesicles was also investigated by comparing the patient plasma immunoprecipitation to that of a monoclonal anti-band 3 antibody. Patient erythrocyte autoantibodies appear to recognize a subset of the band 3 complexes in the vesicles, as there was only a partial overlap in the membrane proteins that were precipitated. This fits with the known selective binding of physiological autoantibodies to damaged band 3 [1,4]. The presence of damage-associated proteins (e.g. HSP70, 26S proteasome and transglutaminases) and band 3 degradation products in the complex precipitated using patient plasma supports this view (Table S1, and Figure 3, respectively) [26,27].

Intriguingly, vesicle-associated spectrin was biotinylated using the membrane-impermeable sulfo-NHS-biotin (Table S1, and Figure 3C). One possible explanation is the diffusion of the sulfo-NHS-biotin into damaged vesicles via membrane pores [25]. Alternatively, the presence of inside-out oriented membrane vesicles could explain the presence of biotinylated spectrin [28]. The latter implies that, after erythrocyte transfusion, intracellular epitopes become accessible to the immune system [29], a process generally known to be involved in the onset of autoimmune disorders [30].

The alternative erythrocyte autoantibody targeting in these vesicles, combined with the enhanced complement binding, support the notion that erythrocyte-derived vesicles might be important players in the inflammatory side-effects encountered during and after chronic erythrocyte transfusion [8,31]. This is in line with the increasing amount of evidence showing that vesicles of different cellular origins are actively involved in inflammation [32-34]. Also, vesicle-containing supernatants from erythrocyte concentrates were found to have immune regulatory functions [35,36].

Taken together, we have demonstrated a change in pathology-associated erythrocyte antigenicity during blood bank storage, which is accompanied with enhanced patient erythrocyte autoantibody binding. These changes probably include storage-related band 3 breakdown, as described in previous studies [1,4]. The composition of the immune complex targeted in the vesicles was different from that of stored erythrocytes, implying that the vesicles might have a different capacity to modulate the immune system.

These findings corroborate the hypothesis that prolonged storage increases the transfusion-associated risks [37], in particular the formation of anti-erythrocyte alloantibodies and autoantibodies by transfusion-dependent patients. We aim to elucidate the molecular identity of the involved epitopes, the mechanism(s) underlying these changes, and their pathophysiological implications.

Acknowledgements

The authors thank Hetty Peters-van den Bovenkamp, Gani Bahar, and Tom Verhoeven from the Laboratory of Medical Immunology, RUMC for technical support.

References

1 Bosman GJ, Werre JM, Willekens FL, Novotny VM. Erythrocyte ageing in vivo and in vitro: structural aspects and implications for transfusion. *Transfus. Med.* 18(6), 335-347 (2008).

2 Willekens FL, Werre JM, Groenen-Dopp YA, Roerdinkholder-Stoelwinder B, de Pauw B, Bosman GJ. Erythrocyte vesiculation: a self-protective mechanism? *Br. J. Haematol.* 141(4), 549-556 (2008).

3 Lang KS, Lang PA, Bauer C *et al*. Mechanisms of suicidal erythrocyte death. *Cell Physiol Biochem.* 15(5), 195-202 (2005).

4 Antonelou MH, Kriebardis AG, Stamoulis KE, Economou-Petersen E, Margaritis LH, Papassideri IS. Red blood cell aging markers during storage in citrate-phosphate-dextrose-saline-adenine-glucose-mannitol. *Transfusion* 50(2), 376-389 (2010).

5 Messana I, Ferroni L, Misiti F *et al*. Blood bank conditions and RBCs: the progressive loss of metabolic modulation. *Transfusion* 40(3), 353-360 (2000).

6 Luten M, Roerdinkholder-Stoelwinder B, Schaap NP, de Grip WJ, Bos HJ, Bosman GJ. Survival of red blood cells after transfusion: a comparison between red cells concentrates of different storage periods. *Transfusion* 48(7), 1478-1485 (2008).

7 Fossati-Jimack L, Azeredo da SS, Moll T *et al*. Selective increase of autoimmune epitope expression on aged erythrocytes in mice: implications in anti-erythrocyte autoimmune responses. *J. Autoimmun.* 18(1), 17-25 (2002).

8 Young PP, Uzieblo A, Trulock E, Lublin DM, Goodnough LT. Autoantibody formation after alloimmunization: are blood transfusions a risk factor for autoimmune hemolytic anemia? *Transfusion* 44(1), 67-72 (2004).

9 Barker RN, Casswell KM, Reid ME, Sokol RJ, Elson CJ. Identification of autoantigens in autoimmune haemolytic anaemia by a non-radioisotope immunoprecipitation method. *Br. J. Haematol.* 82(1), 126-132 (1992).

10 Bradford MM. A rapid and sensitive method for the quantitation of microgram quantities of protein utilizing the principle of protein-dye binding. *Anal. Biochem.* 72 248-254 (1976).

11 Laemmli UK. Cleavage of structural proteins during the assembly of the head of bacteriophage T4. *Nature* 227(5259), 680-685 (1970).

12 Blum H, Beier H, Gross HJ. Improved silver staining of plant proteins, RNA and DNA in polyacrylamide gels. Electrophoresis 8(2), 93-99 (1987).

13 Bosman GJ, Visser FE, de Man AJ, Bartholomeus IG, de Grip WJ. Erythrocyte membrane changes of individuals with Down's syndrome in various stages of Alzheimer-type dementia. *Neurobiol. Aging* 14(3), 223-228 (1993).

14 Candiano G, Bruschi M, Musante L *et al*. Blue silver: a very sensitive colloidal Coomassie G-250 staining for proteome analysis. *Electrophoresis* 25(9), 1327-1333 (2004).

15 Bosman GJ, Lasonder E, Luten M *et al*. The proteome of red cell membranes and vesicles during storage in blood bank conditions. *Transfusion* 48(5), 827-835 (2008).

16 Grove H, Faergestad EM, Hollung K, Martens H. Improved dynamic range of protein quantification in silver-stained gels by modelling gel images over time. *Electrophoresis* 30(11), 1856-1862 (2009).

17 D'Alessandro A, Righetti PG, Zolla L. The red blood cell proteome and interactome: an update. *J. Proteome. Res.* 9(1), 144-163 (2010).

18 Salzer U, Zhu R, Luten M *et al*. Vesicles generated during storage of red cells are rich in the lipid raft marker stomatin. *Transfusion* 48(3), 451-462 (2008).

19 van den Akker E, Satchwell TJ, Williamson RC, Toye AM. Band 3 multiprotein complexes in the red cell membrane; of mice and men. *Blood Cells Mol. Dis.* 45(1), 1-8 (2010).

20 Leddy JP, Falany JL, Kissel GE, Passador ST, Rosenfeld SI. Erythrocyte membrane proteins reactive with human (warm-reacting) anti-red cell autoantibodies. *J. Clin. Invest* 91(4), 1672-1680 (1993).

21 Shen CR, Youssef AR, Devine A *et al*. Peptides containing a dominant T-cell epitope from red cell band 3 have in vivo immunomodulatory properties in NZB mice with autoimmune hemolytic anemia. *Blood* 102(10), 3800-3806 (2003).

22 Bruce LJ, Ring SM, Anstee DJ, Reid ME, Wilkinson S, Tanner MJ. Changes in the blood group Wright antigens are associated with a mutation at amino acid 658 in human erythrocyte band 3: a site of interaction between band 3 and glycophorin A under certain conditions. *Blood* 85(2), 541-547 (1995).

23 Lundmark R, Carlsson SR. Sorting nexin 9 participates in clathrin-mediated endocytosis through interactions with the core components. *J. Biol. Chem.* 278(47), 46772-46781 (2003).

24 Sawasdee N, Junking M, Ngaojanlar P *et al*. Human kidney anion exchanger 1 interacts with adaptor-related protein complex 1 mu1A (AP-1 mu1A). *Biochem. Biophys. Res. Commun.* 401(1), 85-91 (2010).

25 Kriebardis AG, Antonelou MH, Stamoulis KE, Economou-Petersen E, Margaritis LH, Papassideri IS. RBC-derived vesicles during storage: ultrastructure, protein composition, oxidation, and signaling components. *Transfusion* 48(9), 1943-1953 (2008).

26 Facchiano A, Facchiano F. Transglutaminases and their substrates in biology and human diseases: 50 years of growing. *Amino. Acids* 36(4), 599-614 (2009).

27 Stolz A, Wolf DH. Endoplasmic reticulum associated protein degradation: a chaperone assisted journey to hell. *Biochim. Biophys. Acta* 1803(6), 694-705 (2010).

28 Willekens FL, Roerdinkholder-Stoelwinder B, Groenen-Dopp YA *et al*. Hemoglobin loss from erythrocytes in vivo results from spleen-facilitated vesiculation. *Blood* 101(2), 747-751 (2003).

29 Galletti J, Canones C, Morande P *et al*. Chronic lymphocytic leukemia cells bind and present the erythrocyte protein band 3: possible role as initiators of autoimmune hemolytic anemia. *J. Immunol.* 181(5), 3674-3683 (2008).

30 Racanelli V, Prete M, Musaraj G, Dammacco F, Perosa F. Autoantibodies to intracellular antigens: Generation and pathogenetic role. *Autoimmun. Rev.* 10(8), 503-508 (2011).

31 Hod EA, Zhang N, Sokol SA *et al*. Transfusion of red blood cells after prolonged storage produces harmful effects that are mediated by iron and inflammation. *Blood* 115(21), 4284-4292 (2010).

32 Boilard E, Nigrovic PA, Larabee K *et al*. Platelets amplify inflammation in arthritis via collagen-dependent microparticle production. *Science* 327(5965), 580-583 (2010).

33 Couper KN, Barnes T, Hafalla JC *et al*. Parasite-derived plasma microparticles contribute significantly to malaria infection-induced inflammation through potent macrophage stimulation. *PLoS. Pathog.* 6(1), e1000744 (2010).

34 Mause SF, Weber C. Microparticles: protagonists of a novel communication network for intercellular information exchange. *Circ. Res.* 107(9), 1047-1057 (2010).

35 Vlaar AP, Hofstra JJ, Levi M *et al*. Supernatant of aged erythrocytes causes lung inflammation and coagulopathy in a "two-hit" in vivo syngeneic transfusion model. *Anesthesiology* 113(1), 92-103 (2010).

36 Xiong Z, Cavaretta J, Qu L, Stolz DB, Triulzi D, Lee JS. Red blood cell microparticles show altered inflammatory chemokine binding and release ligand upon interaction with platelets. *Transfusion* 51(3), 610-621 (2011).

37 Koch CG, Li L, Sessler DI *et al*. Duration of red-cell storage and complications after cardiac surgery. *N. Engl. J. Med.* 358(12), 1229-1239 (2008).

Table S1. Proteins identified by proteomics analyses of erythrocyte/vesicle immunoprecipitations using erythrocyte autoantibody-containing plasma of patients 1, 8 and 9, and allogeneic plasma (control). Numbers represent the identified peptide sequences per protein. Either total products or gel slices containing proteins of a certain MW (kDa) were analyzed. Proteins in specific gel slices were also identified (slices I and II: Figure 2B, slice III: Figure 3B). Skin and trypsin contaminants were excluded from this overview. Immunoprecipitations and proteomics analyses were performed as mentioned in Materials and Methods.

Protein	***Erythrocyte***						***Vesicle***	
	Control	Patient 1	Patient 8	Patient 9	Slice I	Slice II	Patient 1	Slice III
Actin	0	1	3	3	2	0	1	0
Adaptor-related protein complex 2, alpha 1 subunit	0	0	0	0	6	1	0	0
Adaptor-related protein complex 2, beta 1 subunit	0	0	0	0	7	1	0	0
Adducin 2	0	5	0	2	1	0	0	0
Afamin	0	0	2	0	0	0	0	0
Aldehyde dehydrogenase 16 family, member A1	0	0	0	0	0	2	0	0
Alpha globin	0	5	0	0	0	1	2	3
Alpha-1-antichymotrypsin	0	0	7	7	0	0	0	0
Alpha-1-microglobulin/bikunin	0	0	0	2	0	0	0	0
Alpha-2-HS-glycoprotein	0	0	2	2	0	0	0	0
Alpha-2-macroglobulin	0	0	13	15	0	0	1	0
Angiotensinogen	1	0	2	3	0	0	0	0
Ankyrin 1	0	0	0	0	0	0	1	0
Annexin A2 isoform 2	0	0	0	0	0	0	1	0
Antithrombin III	0	0	5	5	0	0	0	0
Apolipoprotein A	0	2	7	6	0	0	1	0
Apolipoprotein B	2	35	22	33	0	0	63	2
Apolipoprotein D	0	0	0	0	0	0	1	0
Apolipoprotein E	0	3	0	4	0	0	8	0
Apolipoprotein H	0	0	3	2	0	0	0	0
Apolipoprotein L1	0	0	0	0	0	0	2	0
Arginase, type I	0	0	0	0	0	0	0	0
Band 3 (solute carrier family 4, anion exchanger,	0	6	3	0	5	3	2	0
Beta globin	0	9	3	1	4	3	6	4
Biliverdin reductase B (flavin reductase (NADPH))	0	1	0	0	0	0	0	0
Carbonic anhydrase I	0	2	0	0	0	1	0	0
Carbonic anhydrase II	0	1	0	0	0	0	1	0
Ceruloplasmin	2	0	8	9	0	0	2	0
Clusterin	0	4	3	3	0	0	4	0
Complement C1s subcomponent	0	0	2	2	0	0	0	0
Complement C6	0	0	0	1	0	0	0	0
Complement component 1, q subcomponent, B chain	0	0	1	2	0	0	2	0
Complement component 1, q subcomponent, C chain	0	0	2	2	0	0	3	2
Complement component 3	0	12	3	2	0	2	20	0
Complement component 4	5	1	16	17	0	0	4	0
Complement component 5	0	4	3	4	0	0	24	0
Complement component 8, gamma polypeptide	0	0	0	1	0	0	1	0
Complement component 9	0	0	2	2	0	0	6	0
Complement factor B	0	0	3	2	0	0	0	0
Complement factor H isoform a	0	0	5	4	0	0	0	0
Corticotropin releasing hormone	0	3	0	0	2	1	2	2
Cyclin M2	0	1	0	0	2	2	2	3
Erythrocyte membrane protein band 4.1	0	1	0	4	1	11	5	0
Erythrocyte membrane protein band 4.2	0	0	1	1	0	0	0	0
Eukaryotic translation initiation factor 2C, 2	0	0	0	0	7	4	0	0
Eukaryotic translation initiation factor 4A	0	0	0	0	0	1	0	0
Fibrinogen alpha chain	0	0	2	4	0	0	0	0
Fibrinogen beta chain	0	0	4	2	0	0	0	0
Fibrinogen gamma chain	0	0	5	4	0	0	0	0
Fibronectin 1	0	0	1	1	0	0	2	3
Glutathione S-transferase	0	1	0	0	0	0	0	1
Glyceraldehyde-3-phosphate dehydrogenase	0	1	0	0	1	0	1	0
Heat shock 70kDa protein	0	1	0	0	0	0	0	0
Hemopexin	0	0	6	4	0	0	0	0
Heparin cofactor II	0	0	2	2	0	0	3	0
Histidine-rich glycoprotein	0	0	3	2	0	0	2	0
Ig heavy chain	0	3	0	0	3	3	2	0
Ig heavy chain	0	3	0	0	3	2	1	0
Ig heavy chain	0	1	0	0	2	2	0	0
Ig heavy chain	0	1	0	0	1	1	1	0
Ig heavy chain	0	0	0	0	1	1	0	0
Ig light chain	0	1	0	0	0	1	1	0
Ig light chain	0	1	0	0	0	1	1	0
Ig light chain	0	1	0	0	1	1	1	0
Ig light chain	0	1	0	0	1	1	1	0
Insulin-like growth factor-binding protein complex acid	0	0	0	2	0	0	0	0
Inter-alpha (globulin) inhibitor H1	0	0	5	4	0	0	4	2
Inter-alpha (globulin) inhibitor H2	0	2	4	3	0	0	5	1

Inter-alpha (globulin) inhibitor H4	0	1	7	6	0	0	4	0
Kininogen-1 isoform 2	0	0	6	4	0	0	0	0
Leucine-rich alpha-2-glycoprotein	0	0	0	3	0	0	0	0
Lipocalin 1	0	0	0	0	0	0	1	0
Lipopolysaccharide-binding protein	0	0	0	0	0	0	2	0
Liver phosphofructokinase	0	0	0	0	0	5	0	0
Lysozyme	0	0	2	0	0	0	1	0
Neuroblastoma RAS viral (v-ras) oncogene homolog	0	0	0	0	0	0	1	0
Peptidylprolyl isomerase B	0	0	0	0	0	0	0	0
Phosphatidylinositol-5-phosphate 4-kinase, type II, alpha	0	0	0	0	0	0	1	0
Plasma protease C1 inhibitor	0	0	3	2	0	0	0	0
Plasminogen	0	0	2	0	0	0	0	0
Prolactin-induced protein	0	0	0	0	0	0	1	0
Proteasome 26S non-ATPase subunit 2	0	0	0	0	2	0	0	0
Prothrombin	0	0	5	3	0	0	0	0
Serine (or cysteine) proteinase inhibitor, clade A, member	0	0	0	0	0	0	1	0
Serine (or cysteine) proteinase inhibitor, clade A, member	0	0	0	0	0	0	1	0
Serine (or cysteine) proteinase inhibitor, clade B, member	0	0	0	0	0	0	0	0
Serine (or cysteine) proteinase inhibitor, clade B, member	0	0	0	0	1	0	0	0
Serotransferrin	0	0	4	3	0	0	0	0
Serpin peptidase inhibitor, clade A, member 3	0	0	0	0	0	0	1	0
Serum albumin	0	0	4	0	0	0	0	0
Serum amyloid P-component	0	0	2	3	0	0	0	0
Solute carrier family 2 (facilitated glucose transporter),	0	1	0	0	1	2	1	0
Sorting nexin 9	0	0	0	0	0	1	0	0
Spectrin beta	0	0	0	0	0	0	1	2
Stomatin isoform a	0	2	0	0	0	0	10	0
Thioredoxin	0	1	0	0	0	0	0	0
Thrombospondin 1	0	0	0	0	0	0	2	0
Thyroxine-binding globulin	0	0	2	1	0	0	0	0
Transglutaminase 2 isoform a	0	0	0	0	0	2	0	0
Transglutaminase 3	0	0	0	0	0	0	0	0
Transmembrane protein 24	0	1	0	0	1	0	0	0
Ubiquitin and ribosomal protein	0	1	0	0	1	1	1	1
Urocortin	0	0	0	0	0	0	1	2
Vitronectin	0	0	0	0	0	0	2	0
Von Willebrand factor	0	0	0	0	0	0	4	0

3

Phosphatidylserine exposure on stored red blood cells as a parameter for donor-dependent variation in product quality

Sip Dinkla[1], Malou Peppelman[1], Jori van der Raadt[1], Femke Atsma[2], Věra M.J. Novotný[3], Marian G.J. van Kraaij[4], Irma Joosten[1] and Giel J.C.G.M. Bosman[5]

[1]Department of Laboratory Medicine – Laboratory of Medical Immunology, Radboud University Medical Centre, [2]Department of Donor Studies, Sanquin Research, [3]Department of Hematology, Radboud University Medical Centre, [4]Unit Medical Affairs, Sanquin Blood Bank Southeast Region, [5]Department of Biochemistry, Radboud University Medical Centre

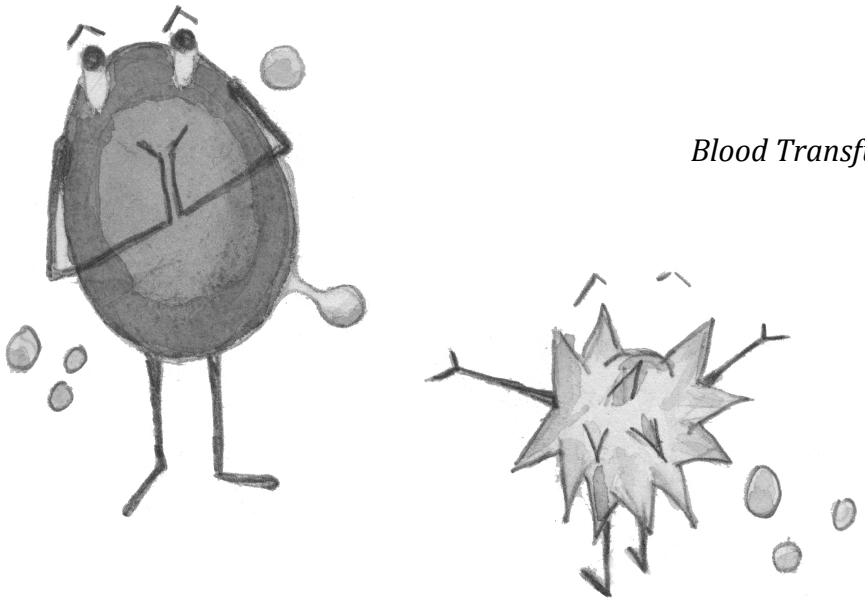

Blood Transfus. 2014;**12**(**2**):204-209

Abstract

Background. Exposure of phosphatidylserine (PS) on the outside of the red blood cell (RBC) contributes to recognition and removal of old and damaged cells. The fraction of PS-exposing RBCs varies between donors, and increases in RBC concentrates during storage. Also, the susceptibility of RBCs to stress-induced PS exposure increases with storage. Therefore, PS exposure may constitute a link between donor variation and the quality of RBC concentrates.

Materials and methods. In order to examine the relationship between storage parameters and donor characteristics, the percentage of PS-exposing RBCs was measured in RBC concentrates during storage and in fresh RBCs from blood bank donors. The percentage of PS-exposing RBCs was compared with RBC susceptibility to osmotic stress-induced PS exposure *in vitro*, with the regular RBC concentrate quality parameters, and with the donor characteristics age, BMI, haemoglobin level, gender and blood group.

Results. PS exposure varies between donors, both on RBCs freshly isolated from the blood, and on RBCs in RBC concentrates. PS exposure increases with storage time, and is correlated with stress-induced PS exposure. Increased PS exposure during storage was found to be associated with haemolysis and vesicle concentration in RBC concentrates. The percentage of PS-exposing RBCs showed a positive correlation with the plasma haemoglobin concentration of the donor.

Discussion. The fraction of PS-exposing RBCs is a parameter of RBC integrity in RBC concentrates and may be an indicator of RBC survival after transfusion. Measurement of PS exposure may be useful in the selection of donors and RBC concentrates for specific patient groups.

Introduction

During storage in the blood bank, RBCs undergo a number of structural and biochemical changes, the storage lesions [1]. Some of these changes, such as a decrease in intracellular adenosine-5'-triphosphate (ATP), are parameters of the current RBC concentrate quality control system. This control system includes a 24 hour-survival of at least 75% of the transfused RBCs [2]. The decrease in ATP concentration is readily reversible [2], but the effects of the storage lesions on the capacity to deform - and thereby to deliver oxygen to the tissues - are hardly known [3,4]. Also, the relationship between the storage lesions and the development of side effects such as inflammatory immune reactions and iron accumulation is not clear.

Externalized PS is a sensitive marker for fast recognition and removal of RBCs by the reticulo-endothelial system, as suggested by the currently available data on RBC aging *in vivo* and *in vitro,* on the response of RBCs to various stress treatments *in vitro*, and on RBCs in pathological conditions [5-8]. The number of PS-exposing RBCs increases with storage in the blood bank [6,7]. We have shown that storage is also accompanied by an increase in PS exposure upon hyperosmotic stress [7]. These data suggest a storage-associated lowering of the threshold for activation of the pathways that induce PS exposure. Various pathways have been proposed [6-8], but their activity and especially their response to extracellular stimuli after transfusion *in vivo* remain to be elucidated. The fraction of PS-exposing RBCs after near-physiological stress of stored RBCs is similar to the fraction of RBCs that disappears shortly after transfusion [7,9]. This suggests that control of PS exposure may be a determinant of RBC survival in the first 24 hours after transfusion.

Therefore, we examined whether the degree of initial PS exposure in the donor blood is associated with PS exposure in the RBC concentrate and/or predictive for its susceptibility to stress-induced PS exposure. Our findings indicate that RBC concentrate production itself affects PS exposure, that initial PS exposure is correlated with RBC susceptibility to osmotic stress-induced PS exposure, and that PS exposure is associated with some quality control parameters of RBC concentrates.

Materials and methods

Donor characteristics

A population of 97 frequent blood bank whole blood donors participated in this study (Table 1). RBCs from an initial group of 37 donors were used to examine PS exposure before processing and after 6 days of storage. Fresh RBCs from an additional 37 donors were

included to examine PS exposure with and without the application of osmotic stress (N=74). Fresh RBCs from an additional 23 donors were used to determine whether the donor characteristics correlated with PS exposure (N=97). Fresh RBCs and RBC concentrates from 12 donors were used to examine PS exposure during blood bank storage. The study was performed following the guidelines of the local medical ethical committee and in accordance with the declaration of Helsinki. Written informed consent was obtained from all blood donors participating in this study.

Table 1. Summary of donor characteristics.

parameter	characteristics
gender	66% male, 34% female
rhesus D	80% positive, 20% negative
AB0	46% O, 41% A, 13% B
age (years)	48.9 ± 12.9
length (cm)	176.8 ± 7.9
weight (kg)	82.2 ± 15.1
body mass index	26.2 ± 4.1
haemoglobin (mmol/L)	9.2 ± 0.8

Mean and standard deviation are given for age, length, weight, body mass index and haemoglobin (normal haemoglobin ranges are 8.6-11.2 for men, and 7.5-9.4 mmol/L for women).

RBC isolation

Fresh RBCs were isolated from five ml whole blood (EDTA) as described before [7]. RBC concentrates were collected and processed according to standard Dutch blood bank protocols in the regional blood bank Sanquin Blood Bank South East Region, Nijmegen, The Netherlands [7,9,10]. Samples of two to five ml were taken aseptically from the concentrates, and RBCs were washed to remove medium, plasma and vesicles using Ringer's solution (NaCl 125 mM, KCl 5 mM, $MgSO_4$ 1 mM, $CaCl_2$ 2.5 mM, glucose 5 mM, HEPES/NaOH 32 mM, pH 7.4) by repeated centrifugation (5 min, 1500g, 4^oC). All experiments were performed in Ringer's solution. Where indicated, osmotic stress was induced by adding 400 mM sucrose aseptically and incubation overnight at 37^oC and 5% CO_2 [7].

PS measurement

The percentage of PS-exposing RBCs was determined as described previously [7]. RBCs were incubated for one hour at room temperature in the dark with Ringer containing 0.2% bovine serum albumin (BSA), annexin V FLUOS (1:25, Roche, Basel, Switzerland) to detect PS, and with PE-conjugated anti-CD235a antibody (1:100, mouse IgG1, clone KC16, Beckman Coulter, Brea CA, USA). Flow cytometry was performed using an Epics XL-CML flow cytometer (Beckman Coulter, Brea CA, USA), and the data were analysed with CXP Analysis software version 2.2 (Beckman Coulter, Brea CA, USA). Only CD235a-positive events (100,000) in the RBC size range were gated for further analysis. The intra-assay variation in the number of Annexin V-positive RBC was ≤0.05% before and ≤0.1% after stress treatment. A combined anti-CD41-PC5 (1:10, BioLegend, San Diego, CA, USA) and anti-CD235a-PE (1:100, Beckman Coulter, Fullerton, CA, USA) antibody staining revealed the virtual absence of platelets and high RBC purity (>99.9%) of the samples that were tested.

Vesicle isolation and quantification

All buffers used for vesicle isolation and analysis were complemented with 0.2% BSA and filtered (0.22 µm) before use. Samples from RBC concentrates were centrifuged (20 min at 1500g) twice to remove cells and cell debris. Vesicles were pelleted from the supernatant (1 ml) by centrifugation at 21,000g for 20 minutes. The vesicle pellet was resuspended in 10 µl supernatant and stored at -80^{o}C until analysis. Frozen vesicles were thawed on ice and washed with Ringer without calcium. Vesicles were labelled for flow cytometry analysis by incubation in Ringer with annexin V FLUOS (1:50, Roche, Basel, Switzerland) to detect PS, and with PE-conjugated anti-CD235a antibody (1:200, mouse IgG1, clone KC16, Beckman Coulter, Brea CA, USA) for 30 min at 4^{o}C in the dark. After this incubation, vesicles were washed once by centrifugation, resuspended in Ringer, and washed Flow-Count Fluorospheres (Beckman Coulter, Brea CA, USA) were added (1×10^{4}) for quantification. Annexin V/CD235a-double-positive vesicles were quantitated using a FACsCalibur flow cytometer (BD Biosciences, Franklin Lakes NJ, USA) in combination with CXP Analysis software version 2.2 (Beckman Coulter, Brea CA, USA). Sulphate latex microspheres (Invitrogen, Carlsbad CA, USA; 0.9 µm) were used to determine the maximum upper boundary allowed for forward and sideward scatter gating. All staining solutions were centrifuged at 21,000g and 4ºC for 20 min prior to use to remove fluorescent aggregates. PE-conjugated IgG1 isotype control (Dako, Glostrup, Denmark) did not show any aspecific binding.

Quality parameters

The blood bank quality parameters extracellular haemoglobin, pH, mean corpuscular volume (MCV), mean corpuscular haemoglobin (MCH), mean corpuscular haemoglobin concentration (MCHC), ATP and 2,3-DPG were measured as described before [7,11,12].

Statistical analysis

Differences before and after whole blood processing and stress were tested with a Mann-Whitney U test. Differences between multiple groups were assessed with a one-way ANOVA in combination with Tukey's post-test. Pearson's correlation coefficients were computed to measure bivariate correlations. The reported *p* values are two-sided, and a *p* value of < 0.05 was used to assess statistical significance.

Results

Donor variation in PS exposure before and after RBC concentrate production

As a first step to examine a putative correlation between donor characteristics and RBC concentrate quality, we determined whether there is donor variation in the percentage of PS-exposing RBCs, both in freshly drawn blood before RBC concentrate production and during the first week of storage. A large donor variation in the amount of PS-exposing RBC was observed in both fresh and short stored RBC concentrates (Figure 1A). There was a small but statistically significant increase in the number of PS-exposing RBCs during blood bank processing and/or occurring within the first week of storage (Figure 1A). Osmotic stress induced a strong increase in the number of PS-exposing RBCs, with similar donor variation (Figure 1B) in the fresh RBCs and in RBCs that had been stored for one week under blood bank conditions. After a short storage period, RBCs were more susceptible to osmotic stress than fresh RBCs (Figure 1B). The latter data are in accordance with previous observations showing an increase in susceptibility with storage time [7].

PS exposure in the RBC concentrates predicts susceptibility to stress

Since PS exposure increases with RBC storage [6,7], and is involved in the recognition and removal of damaged cells [5,13], stress-induced PS exposure might be involved in the removal of up to 30% of the transfused RBCs that is known to occur within the first hours after transfusion [9]. Therefore, we examined whether there is a relationship between initial PS exposure of RBCs and their susceptibility to osmotic stress-induced PS exposure. We observed a strong positive correlation between PS exposure before and after stress (Figure 1C), showing that the percentage of PS-exposing RBCs may serve as a marker for the susceptibility of the entire RBC population.

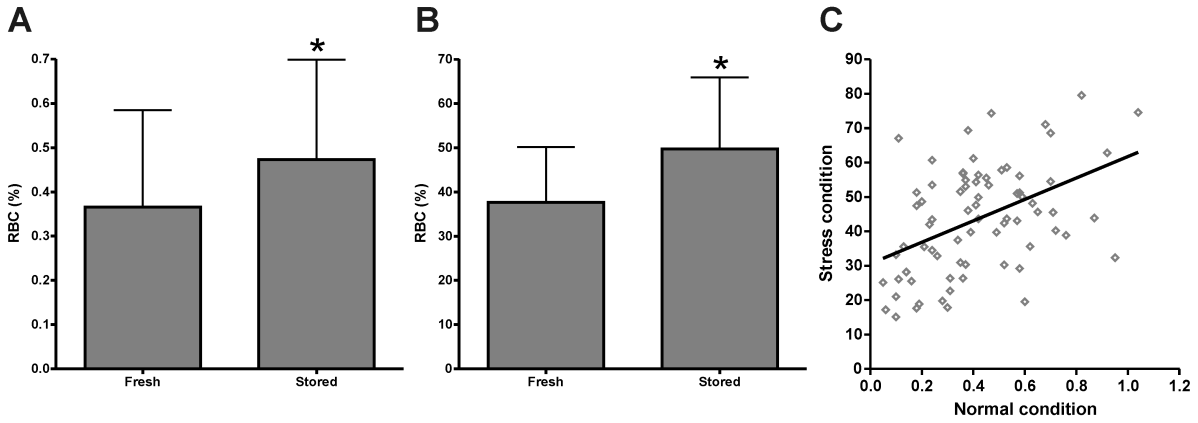

Figure 1. Exposure of PS by RBCs before and after the first week of storage in the presence or absence of osmotic stress. RBCs were collected from freshly drawn blood (fresh) and from six day-old RBC concentrates (stored) obtained from the same donor. Using flow cytometry, the percentage of PS-exposing RBCs (RBC (%)) was determined before (**A**, **P* = 0.04) and after (**B**, **P* = 0.001) osmotic stress. Results are expressed as the mean ± SD (N=37). The correlation between PS exposure of fresh RBCs before and after osmotic stress (**C**) had a Pearson coefficient of 0.64 (N=74).

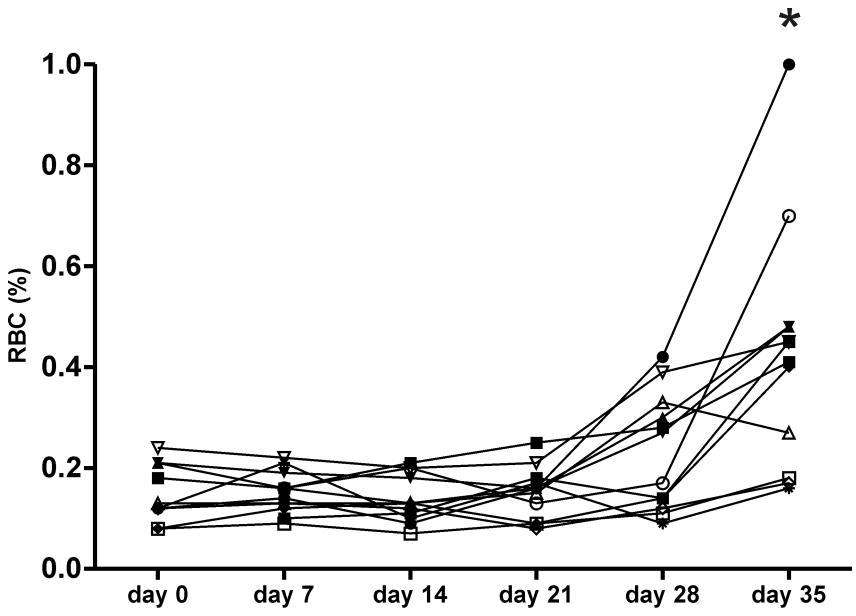

Figure 2. PS exposure during storage of RBCs under blood bank conditions. Blood was drawn from twelve donors, RBCs were collected from the RBC concentrates at the indicated times, and analysed for the percentage of PS-exposing RBCs (RBC (%)) by flow cytometry. **P* = <0.0001.

Relation of PS exposure with RBC concentrate quality parameters and vesiculation

The variation in PS exposure between donors, together with the correlation with stress-induced PS exposure, raised the question if PS exposure is related to any of the regular quality parameters of RBC concentrates. Therefore, the percentage of PS-exposing RBCs, as well as extracellular haemoglobin, pH, MCV, MCH, MCHC, ATP and 2,3-DPG of twelve

RBC concentrates were followed in time. In six of the twelve units tested, the percentage of PS-exposing RBCs started to increase in the fourth week of storage (Figure 2). In the fifth week, an additional three RBC concentrates showed an increased percentage of PS-exposing RBCs. Variation in PS exposure between donors became more apparent from week four onwards (Figure 2). The rise in the percentage of PS-exposing RBCs ran parallel with a decrease in ATP, 2,3-DPG, and pH, and increases in MCV and haemolysis, confirming previous data [11,12]. However, only the degree of haemolysis showed a positive correlation with the percentage of PS-exposing RBCs at multiple time points during storage (data not shown). Furthermore, both the percentage of PS-exposing RBCs and the degree of haemolysis showed a positive correlation with the number of RBC vesicles in the 35 day-old concentrate (Figure 3).

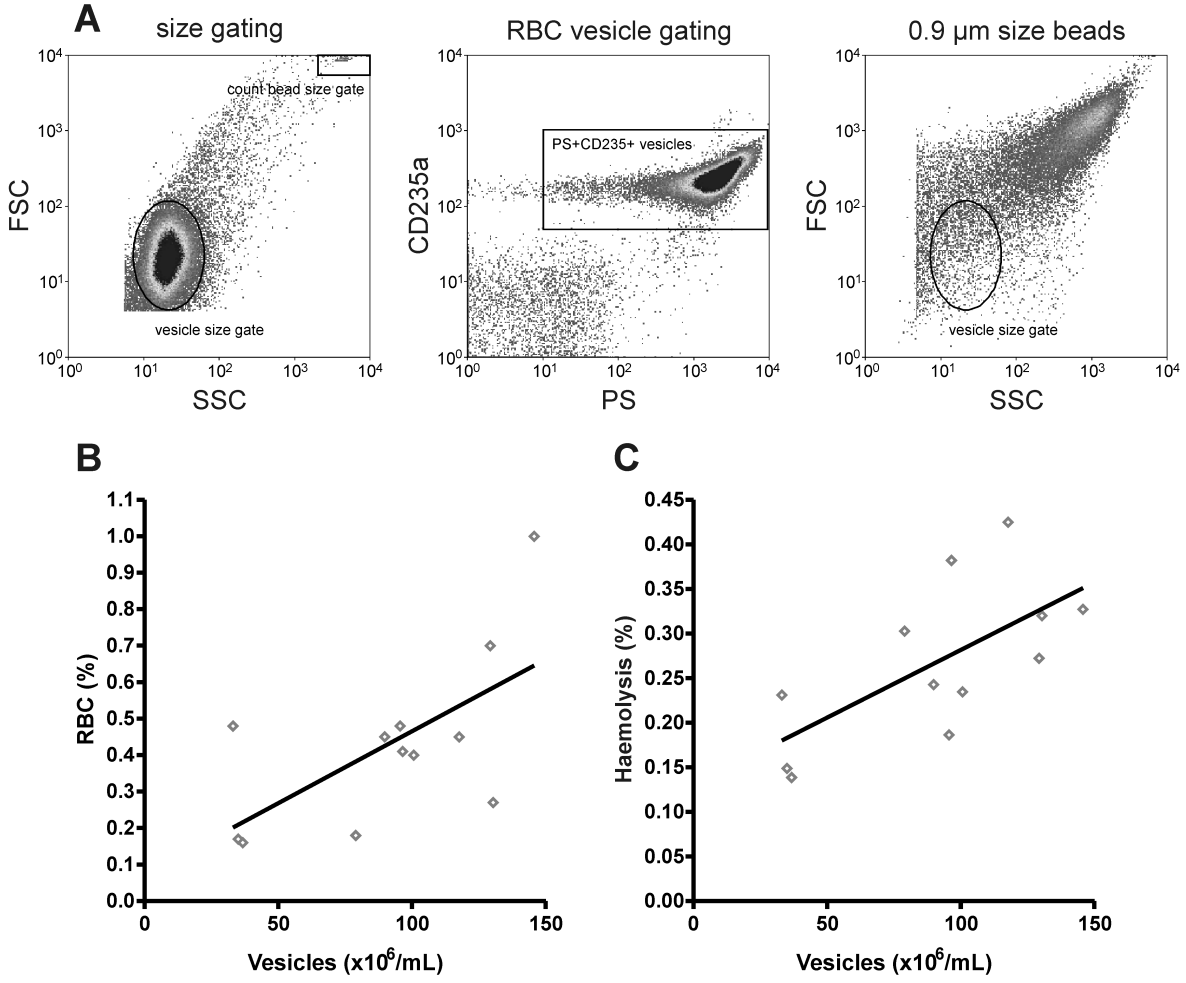

Figure 3. Correlation of RBC PS exposure and haemolysis with vesicle content in transfusion concentrates. After 35 days of storage, haemolysis was measured, and the percentage of PS-exposing RBCs was determined by flow cytometry detection of annexin V binding. The number of $PS^{+}CD235a^{+}$ vesicles was determined per mL transfusion concentrate supernatant as described in Materials and Methods. (**A**) Vesicle characteristics and quantification. (**B**) The correlation between vesicle number and PS exposure (RBC (%); Pearson coefficient of 0.64, N=12). (**C**) The correlation between vesicle number and haemolysis (Pearson coefficient of 0.67, N=12).

Relation of PS exposure with donor parameters

Since the percentage of PS-exposing RBCs varies between RBC concentrates from various donors (Figure 1), we investigated whether it would be possible to identify donors with high or low PS exposure by readily available donor parameters (Table 1). In the 97 donors examined, the numbers of PS-exposing RBCs in freshly drawn donor blood, i.e. before blood bank processing, did not differ significantly between gender, age, BMI, and ABO or Rhesus D blood groups. There was a weak positive correlation between PS exposure with the haemoglobin concentration of the donor plasma (Pearson coefficient 0.21), but not with the other parameters (data not shown).

Discussion

Stored RBCs are less resistant to hypo-osmotic and mechanical stress-induced haemolysis than fresh RBCs [14]. The positive correlation we observed between PS exposure and haemolysis suggests that PS exposure is an indicator for RBC integrity during storage in blood bank conditions. Indeed, time lapse microscopy data show that PS exposure precedes lysis when exposed to various stressors [15]. The small, but significant difference we observed in PS exposure between freshly isolated RBCs and RBCs sampled from the RBC concentrates within the first week after processing the RBCs, suggests that processing of the blood before storage induces membrane restructuring. In addition, the correlation between the percentage of PS-exposing RBCs and vesicle concentration in RBC concentrates is compatible with the hypothesis that the changes in membrane organization that lead to the appearance of PS in the outer layer of the cell membrane, also lead to the generation of vesicles [12]. Our data suggest that concentrates from donors with higher initial numbers of PS-exposing RBCs may be less effective upon transfusion, due to enhanced susceptibility to physiological stress in the circulation and subsequent removal. We propose to test PS exposure as a novel quality parameter of RBC concentrates, since the conventional parameters do not accurately predict RBC survival after transfusion [16].

Of the donor parameters that we examined, only the haemoglobin concentration showed a correlation with RBC PS exposure. Therefore, it might be worth investigating whether other donor parameters might be predictive for PS exposure. Recent findings indicate that donor differences in PS exposure may reflect variation in iron status and hormonal factors [17,18]. Accumulation of HbA1c and other modified haemoglobin species in RBC-derived vesicles [19] suggests a functional relationship between haemoglobin composition and RBC structure in healthy donors. Thus, the recently described donor variation in the rate of haemoglobin glycation [20] may contribute to the variation from concentrate to concentrate. This leads to

our prediction that in donors, HbA1c content is positively correlated to both a decrease in RBC life span and PS-exposure. Indeed, the percentage of PS-exposing RBCs in individuals with type 2 diabetes mellitus is twice that of control subjects [21]. Similarly, the increased susceptibility to mechanical stress of RBC in post-menopausal women [18] may very well correlate with the number of PS-exposing RBCs.

In conclusion, the correlations between PS exposure, donor characteristics and RBC concentrate quality parameters indicate that PS exposure may be a biologically relevant parameter of RBC quality. These results emphasize the need for the elucidation of the mechanisms that stimulate PS exposure on RBCs *in vivo*. Such knowledge could lead to the development of methods to improve RBC survival during storage and after transfusion, and could enable the selection of RBC concentrates - and even donors - for specific patient groups. It has been suggested that RBC concentrates with high haemoglobin content may be selected for patients with the largest blood volume [22]. Similarly, it may be feasible to select concentrates with the lowest PS exposure for chronically transfused and/or critically ill patients, or remove the RBCs that are susceptible to stress-induced PS exposure from the RBC concentrate. This would be of benefit especially for chronically transfused patients, as a reduction in the number of rapidly removed RBCs will lead to enhanced transfusion efficacy and a significant reduction in the rate of iron accumulation and pathological activation of the immune system.

Acknowledgements

We thank Sanquin Blood Supply Foundation, Amsterdam, The Netherlands for performing the ATP and 2,3-DPG measurements. This study was financed by the Radboud University Medical Centre.

References

1 Hess JR. Red cell changes during storage. *Transfus. Apher. Sci.* 43(1), 51-59 (2010).

2 Hogman CF, Meryman HT. Red blood cells intended for transfusion: quality criteria revisited. *Transfusion* 46(1), 137-142 (2006).

3 Raat NJ, Hilarius PM, Johannes T, de Korte D, Ince C, Verhoeven AJ. Rejuvenation of stored human red blood cells reverses the renal microvascular oxygenation deficit in an isovolemic transfusion model in rats. *Transfusion* 49(3), 424-427 (2009).

4 Raat NJ, Ince C. Oxygenating the microcirculation: the perspective from blood transfusion and blood storage. *Vox Sang.* 93(1), 12-18 (2007).

5 Kuypers FA, de Jong K. The role of phosphatidylserine in recognition and removal of erythrocytes. *Cell Mol. Biol. (Noisy-le-grand)* 50(2), 147-158 (2004).

6 Verhoeven AJ, Hilarius PM, Dekkers DW, Lagerberg JW, de Korte D. Prolonged storage of red blood cells affects aminophospholipid translocase activity. *Vox Sang.* 91(3), 244-251 (2006).

7 Bosman GJ, Cluitmans JC, Groenen YA, Werre JM, Willekens FL, Novotny VM. Susceptibility to hyperosmotic stress-induced phosphatidylserine exposure increases during red blood cell storage. *Transfusion* 51(5), 1072-1078 (2011).

8 Lang F, Lang KS, Lang PA, Huber SM, Wieder T. Mechanisms and significance of eryptosis. *Antioxid. Redox. Signal.* 8(7-8), 1183-1192 (2006).

9 Luten M, Roerdinkholder-Stoelwinder B, Schaap NP, de Grip WJ, Bos HJ, Bosman GJ. Survival of red blood cells after transfusion: a comparison between red cells concentrates of different storage periods. *Transfusion* 48(7), 1478-1485 (2008).

10 Pistorius AM, Luten M, Bosman GJ, de Grip WJ. A single assay for multiple storage-sensitive red blood cell characteristics by means of infrared spectroscopy. *Transfusion* 50(2), 366-375 (2010).

11 Luten M, Roerdinkholder-Stoelwinder B, Bost HJ, Bosman GJ. Survival of the fittest?--survival of stored red blood cells after transfusion. *Cell Mol. Biol. (Noisy-le-grand)* 50(2), 197-203 (2004).

12 Salzer U, Zhu R, Luten M *et al*. Vesicles generated during storage of red cells are rich in the lipid raft marker stomatin. *Transfusion* 48(3), 451-462 (2008).

13 Lee SJ, Park SY, Jung MY, Bae SM, Kim IS. Mechanism for phosphatidylserine-dependent erythrophagocytosis in mouse liver. *Blood* 117(19), 5215-5223 (2011).

14 Gelderman MP, Vostal JG. Rejuvenation improves roller pump-induced physical stress resistance of fresh and stored red blood cells. *Transfusion* 51(5), 1096-1104 (2011).

15 Dinkla S, Wessels K, Verdurmen WP *et al*. Functional consequences of sphingomyelinase-induced changes in erythrocyte membrane structure. *Cell Death. Dis.* 3 e410 (2012).

16 Hogman CF, Meryman HT. Storage parameters affecting red blood cell survival and function after transfusion. *Transfus. Med. Rev.* 13(4), 275-296 (1999).

17 Cable RG, Glynn SA, Kiss JE *et al*. Iron deficiency in blood donors: analysis of enrollment data from the REDS-II Donor Iron Status Evaluation (RISE) study. *Transfusion* 51(3), 511-522 (2011).

18 Raval JS, Waters JH, Seltsam A *et al*. Menopausal status affects the susceptibility of stored RBCs to mechanical stress. *Vox Sang.* 100(4), 418-421 (2011).

19 Bosman GJ, Lasonder E, Groenen-Dopp YA, Willekens FL, Werre JM, Novotny VM. Comparative proteomics of erythrocyte aging in vivo and in vitro. *J. Proteomics.* 73(3), 396-402 (2010).

20 Wenk RE, McGann H, Gibble J. Haemoglobin A1c in donor erythrocytes. *Transfus. Med.* 21(5), 349-350 (2011).

21 Calderon-Salinas JV, Munoz-Reyes EG, Guerrero-Romero JF *et al*. Eryptosis and oxidative damage in type 2 diabetic mellitus patients with chronic kidney disease. *Mol. Cell Biochem.* 357(1-2), 171-179 (2011).

22 Reikvam H, van de Watering L, Prowse C, Devine D, Heddle NM, Hervig T. Evaluation of noninvasive methods for the estimation of haemoglobin content in red blood cell concentrates. *Transfus. Med.* 21(3), 145-149 (2011).

4

Functional consequences of sphingomyelinase-induced changes in erythrocyte membrane structure

Sip Dinkla[1,2*], Katharina Wessels[1*], Wouter P. R. Verdurmen[1], Carlo Tomelleri[3], Judith C. A. Cluitmans[1], Jack Fransen[4], Beate Fuchs[5], Jürgen Schiller[5], Irma Joosten[2], Roland Brock[1] and Giel J.C.G.M. Bosman[1]

*These authors contributed equally to this work

[1]Department of Biochemistry, [2]Department of Laboratory Medicine – Laboratory of Medical Immunology, Radboud University Medical Centre, [3]Department of Medicine, University of Verona, [4]Department of Cell Biology, Radboud University Medical Centre, [5]Medical Department, University of Leipzig

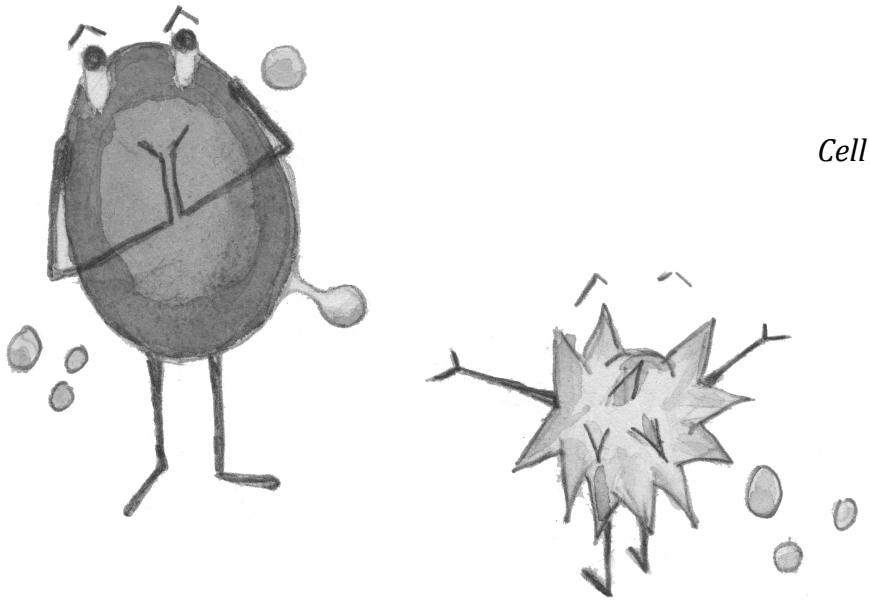

Cell Death Dis. 2012;**3**:e410

Abstract

Inflammation enhances the secretion of sphingomyelinases. Sphingomyelinases catalyze the hydrolysis of sphingomyelin into phosphocholine and ceramide. In erythrocytes, ceramide formation leads to exposure of the removal signal phosphatidylserine, creating a potential link between sphingomyelinase activity and anemia of inflammation. Therefore, we studied the effects of sphingomyelinase on various pathophysiologically relevant parameters of erythrocyte homeostasis. Time-lapse confocal microscopy revealed a sphingomyelinase-induced transition from the discoid to a spherical shape, followed by phosphatidylserine exposure, and finally loss of cytoplasmic content. Also, sphingomyelinase treatment resulted in ceramide-associated alterations in membrane-cytoskeleton interactions and membrane organization, including microdomain formation. Furthermore, we observed increases in membrane fragility, vesiculation and invagination, and large protein clusters. These changes were associated with enhanced erythrocyte retention in a spleen-mimicking model. Erythrocyte storage under blood bank conditions and during physiological aging increased the sensitivity to sphingomyelinase. A low sphingomyelinase activity already induced morphological and structural changes, demonstrating the potential of sphingomyelinase to disturb erythrocyte homeostasis. Our analyses provide a comprehensive picture in which ceramide-induced changes in membrane microdomain organization disrupt the membrane-cytoskeleton interaction and membrane integrity, leading to vesiculation, reduced deformability, and finally loss of erythrocyte content. Understanding these processes is highly relevant for understanding anemia during chronic inflammation, especially in critically ill patients receiving blood transfusions.

Introduction

During their stay in the circulation for approximately 120 days, erythrocytes undergo age-related changes involving senescent cell antigen formation, cell shrinkage, vesiculation, and loss of deformability. The binding of autologous IgG and exposure of recognition molecules, possibly including phosphatidylserine (PS), ultimately lead to recognition of senescent erythrocytes by macrophages of the reticulo-endothelial system [1]. Also, the deformability of the erythrocyte constitutes an important survival parameter, as splenic sequestration of abnormal erythrocytes with reduced deformability leads to a decreased erythrocyte lifespan and anemia in several erythrocyte membranopathies [2].

Chronic inflammation as occurring in various pathological conditions is associated with anemia and poor disease outcome [3]. This inflammation-driven anemia is especially troublesome in patients with severe sepsis. Furthermore, blood transfusions to counter sepsis-induced anemia only have a limited beneficial effect, and may lead to severe complications [4]. Reduced erythrocyte production can only partly explain the low erythrocyte count. Enhanced erythrocyte clearance is likely to contribute to the anemia, but its causes are largely unknown [5]. Therefore, understanding the underlying mechanisms of anemia of inflammation is of critical importance.

Inflammation triggers the secretion of acid sphingomyelinase (SMase), which is involved in various pathologies, including diabetes, sepsis, cardiovascular and pulmonary diseases [6]. SMases catalyze the hydrolysis of sphingomyelin (SM), a major lipid component of cell membranes, into phosphocholine and ceramide [7]. Ceramide functions as a lipid second messenger in many cellular processes including apoptosis, senescence and inflammation, which is partially explained by the tendency of signaling receptors to cluster in ceramide-enriched platforms [8,9]. Also, the formation of these rigid platforms alters membrane curvature and decreases plasma membrane integrity [7,10].

Although erythrocytes do not possess SMase activity of their own [11], and SMases have not been reported as part of the erythrocyte proteome [12], erythrocytes can be exposed to SMase secreted by vascular endothelium, leukocytes and platelets [6]. SMase treatment of, and direct ceramide incorporation into erythrocytes induces PS exposure [13-15]. Also, erythrocytes expose PS and ceramide after incubation with SMase-containing plasma of patients suffering from sepsis or Wilson's disease [16,17]. So far however, only PS exposure and size have been studied. Pathophysiologically relevant molecular processes on the membrane and protein level and their association with functionally relevant parameters have not been addressed as yet.

In the current study we comprehensively addressed the changes that erythrocytes undergo with respect to morphology, deformability, membrane lipid organization and protein-protein interactions upon exposure to SMase. Time-lapse microscopy revealed that SMase-driven PS exposure precedes loss of membrane integrity. We also demonstrate a clear erythrocyte age-related increase in sensitivity to SMase, both in erythrocytes from freshly drawn blood and from blood bank units. Next to PS exposure as a critical removal signal, enhanced vesiculation, that is associated with several erythrocyte-associated pathologies [18], was observed. These findings reveal SMase-induced ceramide formation as a critical event in erythrocyte membrane reorganization on both the lipid and protein level, and provide a possible explanation for the reduced effectiveness and harmful side-effects of erythrocyte transfusion in patients with sepsis.

Results

SMase alters erythrocyte morphology and increases PS exposure

Secretion of SMase is enhanced during inflammation and involved in the pathophysiology of various diseases [6]. Since SMase-induced ceramide formation changes membrane lipid organization, enhanced SMase activity could also affect erythrocyte physiology including deformability and exposure of removal signals such as PS, thereby explaining excessive erythrocyte clearance in anemia of inflammation. This hypothesis is supported by the observation that plasma of septic patients induced ceramide formation and PS exposure on the erythrocyte membrane [16].

In order to determine the sensitivity of erythrocytes to SMase, erythrocytes were incubated with ascending activities of SMase and analyzed by flow cytometry. Bacterial SMase was used as a valid surrogate for acid and neutral SMase encountered by erythrocytes *in vivo* [19]. Cytoplasmic proteins were labeled by incubation with membrane-permeable carboxyfluorescein diacetate succinimidyl ester (CFSE diacetate). In this way, a potential loss of membrane integrity was detectable through loss of fluorescence from the cytoplasm.
Erythrocyte size, as reflected by forward scatter, significantly decreased already at 1 mU/mL, with a further reduction in size and a high increase in PS exposure at activities of 10 mU/mL and higher (Figure 1 A-C). Also, the asymmetric shape of the forward-versus-sideward scatter plot of the erythrocyte population was lost upon treatment, suggesting that the cell shape was affected (Figure 1A). The sideward scatter increased, which is indicative of the degree of cell granularity. In the absence of extracellular calcium during 10 and 100 mU/mL SMase treatment PS exposure was not induced (0.92% and 0.72% respectively), suggesting the involvement of a calcium-activated scramblase in this process [20].

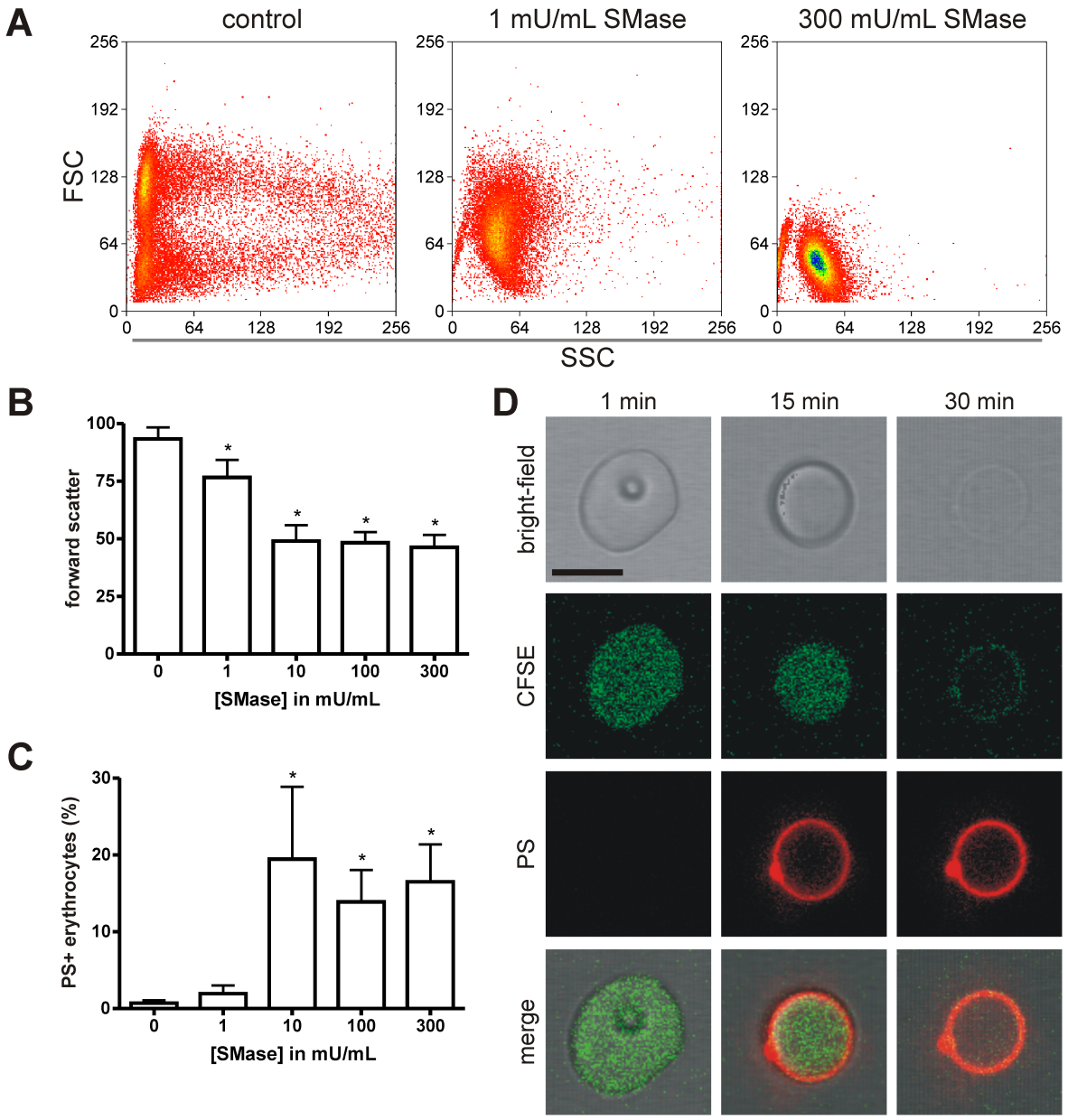

Figure 1 – Erythrocyte shape and PS exposure during SMase treatment. (A-C), Flow cytometry of erythrocytes treated with increasing activities of SMase for 15 min at 37ºC. Annexin V-FLUOS staining was performed to determine the percentage of phosphatidylserine (PS)-exposing erythrocytes. (A), Forward and sideward scatter (FSC and SSC, respectively) density plots are presented. (B and C) The graphs represent mean values of three healthy volunteers; error bars represent standard deviation; * $p < 0.05$. (D), Time-lapse confocal laser scanning microscopy of CFSE-labeled erythrocytes treated with 10 mU/mL SMase at 37ºC in the presence of Annexin V-Alexa 647. Confocal laser scanning microscopy was used to image fluorescence as described in Materials and Methods. Scale bar = 5 µm. A typical result from one of three experiments is presented.

While the flow cytometry analyses provided information on the erythrocyte population at a fixed time point, time-lapse confocal laser scanning microscopy revealed a characteristic sequence of events upon SMase treatment: first, erythrocytes lost their discoid shape, which was followed by a gradual increase in the percentage of PS-exposing cells (Figure 1D and supplemental Movie S1). Subsequently, some erythrocytes lost their cellular content, as indicated by the loss of the CFSE-signal. After 45 min of SMase treatment, a considerable part of the cells had an irregular membrane surface, as observed by bright-field microscopy (supplemental Figure S1). Intriguingly, most of these cells showed high-intensity CFSE spots which co-localized with the membrane irregularities (supplemental Figure S1). These clusters are most likely large protein clusters, since CFSE covalently binds to proteins. Furthermore, only a few of the irregularly shaped cells exposed PS, as compared to the spherical cells with a smooth surface and high PS exposure (supplemental Figure S1 and Movie S1).

SMase specifically hydrolyzes SM in erythrocytes

In order to confirm enzyme specificity and to estimate the extent of SM breakdown and ceramide formation, lipid analyses were performed on the membrane fractions of erythrocytes treated with various SMase activities.

Consistent with the expected activity of SMase, positive-ion matrix-assisted laser desorption and ionization time-of-flight (MALDI-TOF) mass spectrometry (MS) revealed the presence of ceramide and absence of SM in membrane lipid fractions of 10 and 100 mU/mL SMase-treated erythrocytes (Figure 2A). In controls and 1 mU/mL-treated cells, no ceramide was detected. Apparently, at 1 mU/mL the extent of ceramide formation was below the detection limit of this method. Alternatively, the small amount of ceramide might have been suppressed by more abundant lipids, such as phosphatidylcholines [21]. We were not able to detect ceramide subsequent to analysis by combined thin-layer chromatography/MALDI as previously described [22]. However, after 1 and 5 mU/mL SMase treatment the percentage of cells with ceramide-enriched platforms was increased, as detected by immunofluorescence (see below). This is a strong indication that the amount of the generated ceramide at 1 mU/mL SMase is beyond the detection limit of mass spectrometry. ^{31}P nuclear magnetic resonance (NMR) spectroscopy confirmed the nearly complete disappearance of SM after 100 mU/mL SMase treatment of erythrocytes, while the major membrane phospholipids phosphatidylethanolamine (PE), phosphatidylcholine (PC) and phosphatidylserine (PS) were not affected (Figure 2B). Thus, the used enzyme preparation specifically hydrolyzed SM in the erythrocyte plasma membrane.

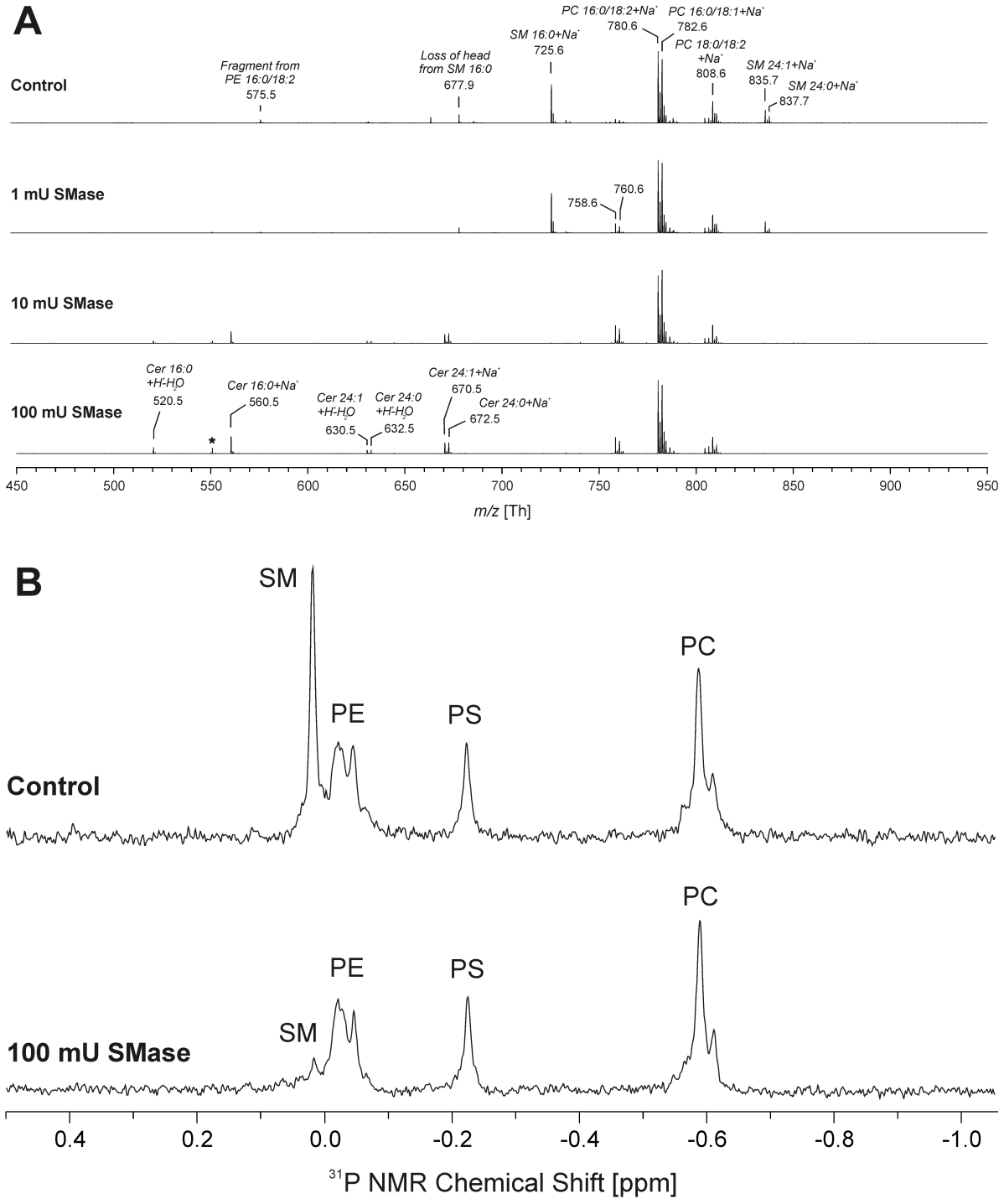

Figure 2 – Erythrocyte membrane lipid analyses after SMase treatment. Erythrocytes were treated with SMase for 1 h at 37ºC. (A), Positive-ion MALDI-TOF MS of isolated membrane lipids. All samples were 1:1 (*v*/*v*) diluted with the matrix (0.5 M 2,5-dihydroxybenzoic acid in methanol). All peaks are labeled based on their *m/z* ratios and matrix cluster ions are marked by an asterisk. (B), ^{31}P NMR spectra of membrane lipid extracts. All samples were investigated in the presence of 200 mM sodium cholate in order to suppress the aggregation of phospholipids. Abbreviations – Cer, ceramide; SM, sphingomyelin; PE, phosphatidylethanolamine, PC, phosphatidylcholine; PS, phosphatidylserine.

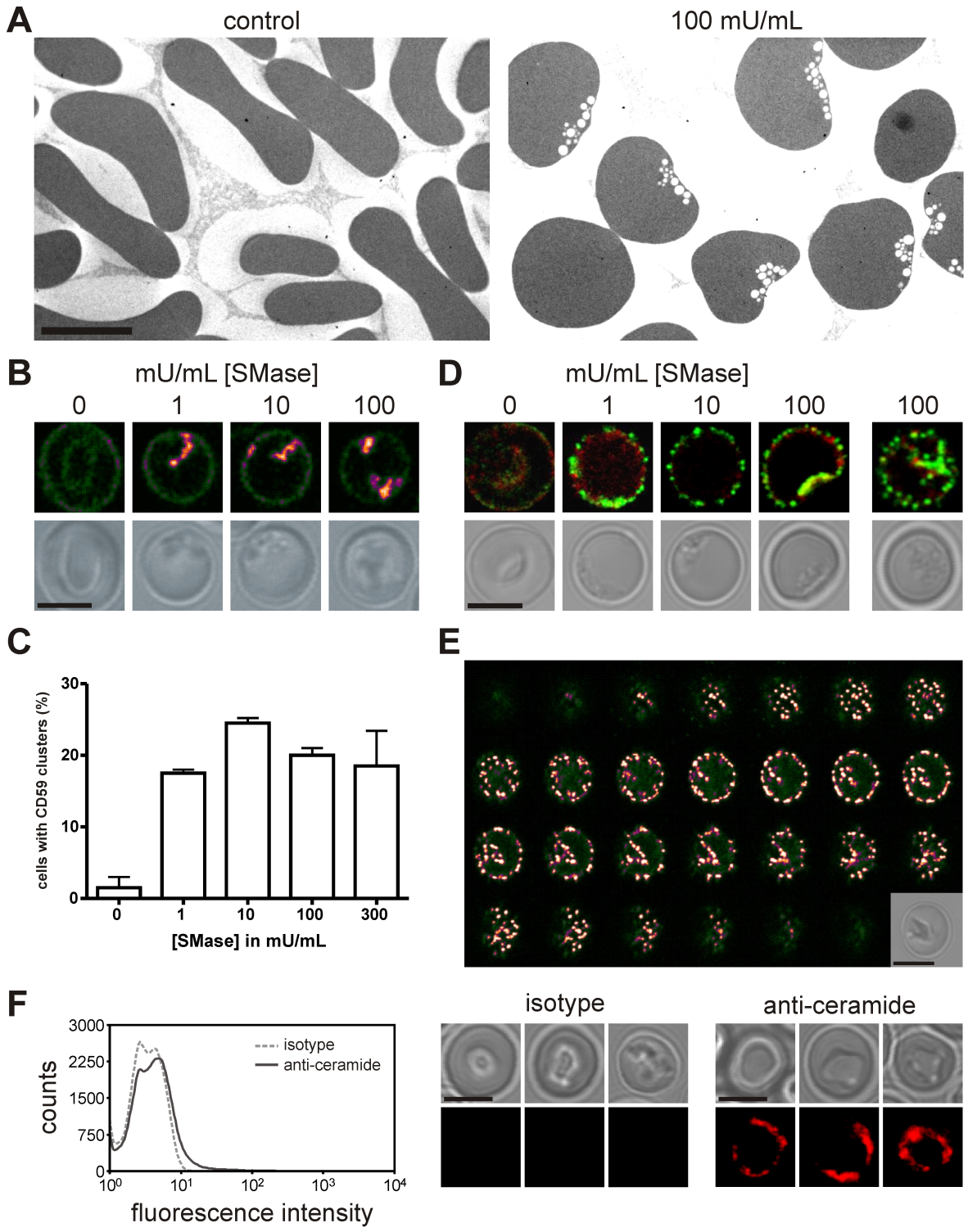

Figure 3 – SMase-induced erythrocyte morphology, membrane lipid rafts and intracellular invaginations. SMase treatment of erythrocytes was performed for 15 min at 37ºC. (A), Electron microscopy of control and SMase-treated erythrocytes as described in Materials and Methods. (B), Erythrocytes stained with an anti-CD59 antibody. (C), Quantification of CD59 cluster-positive erythrocytes. The graph presents mean values (N=2), error bars represent standard deviation. 200 cells were scored by eye per experiment. (D), Acrolein-fixed erythrocytes stained with anti-stomatin (green) and anti-band 3 (red) antibodies. (E), Z-stack of an anti-stomatin-stained, tubulated, erythrocyte after treatment with 10 mU/mL SMase. A Z-slice spacing of 0.25 µm was used. (F), Flow cytometry and confocal microscopy of erythrocytes treated with 5 mU/mL SMase, stained with anti-ceramide or

isotype control antibody. Confocal laser scanning microscopy was used to image fluorescence as described in Materials and Methods. Bright-field images are shown in combination with fluorescence images. Signal intensity in B and E; low = blue, intermediate = red, high = yellow/white. Scale bar = 5 µm. Representative images from one of two experiments are shown in all cases.

SMase-induced erythrocyte membrane reorganization

The changes in erythrocyte morphology, PS externalization, and ceramide formation, suggest that SMase induces major membrane reorganization. This reorganization was studied in more detail using electron microscopy and confocal laser scanning microscopy.

Consistent with our observations by confocal microscopy, electron microscopy also showed a SMase treatment-induced loss of the typical biconcave shape (Figure 3A). A striking finding was the presence of structures resembling intracellular membrane vesicles, or endovesicles, in the SMase-treated erythrocytes. In most cells these structures were confined to one side of the cell in one large cluster.

We also investigated the presence of microdomains in SMase-treated erythrocytes [23]. In untreated erythrocytes, the glycosyl phosphatidylinositol-anchored microdomain marker CD59 [24], was distributed evenly over the erythrocyte membrane (Figure 3B). SMase treatment at activities of 1 mU/mL and higher induced CD59 clusters that co-localized with the membrane irregularities observed in the bright-field images (Figure 3B).

SMase-treated erythrocytes were also stained for stomatin, which is anchored at the cytoplasmic side of the membrane and is associated with lipid rafts in erythrocytes [25]. The findings with stomatin were similar to those obtained with CD59, although many additional small clusters were observed upon SMase treatment (Figure 3D). Moreover, a combined staining for stomatin and band 3, which is an abundant erythrocyte membrane protein involved, among others, in linking the plasma membrane to the cytoskeleton, revealed the presence of tubular plasma membrane invaginations in cross-sections of a subpopulation of the SMase-treated erythrocytes (Figure 3D, right-most images and Figure 3E) [26]. The tubular invaginations also co-localized with membrane irregularities seen in bright-field. A three-dimensional reconstruction and animation showing these invaginations is provided in the supplemental data (supplemental Movies S2 and S3).

Finally, anti-ceramide antibody staining revealed the presence of ceramide-enriched platforms on SMase-treated erythrocytes (Figure 3F). It is worth to note that following acrolein fixation 7 to 8 times more positive events were detected (after correction for isotype control) than following paraformaldehyde fixation.

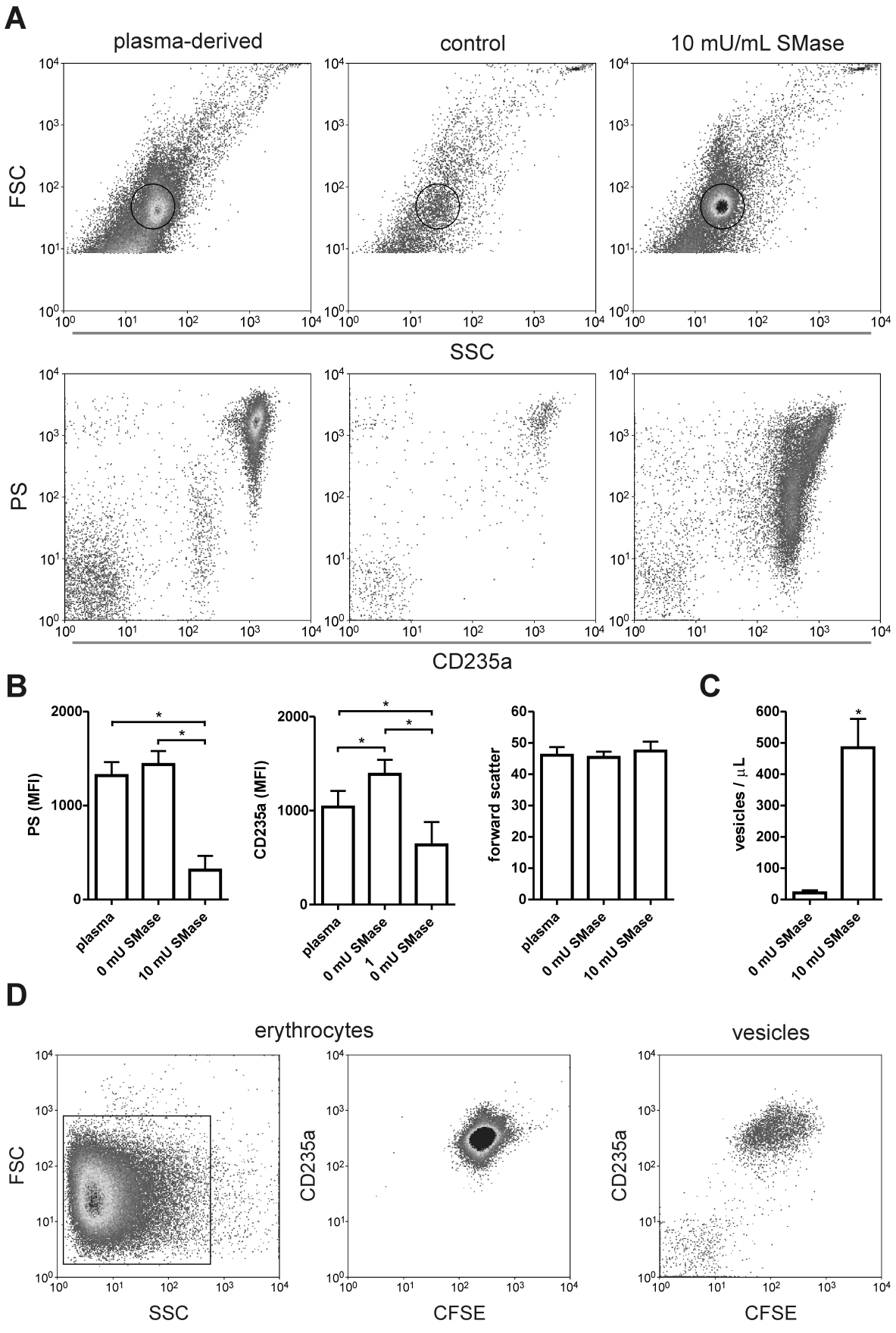
A
plasma-derived
control
10 mU/mL SMase
FSC
SSC
PS
CD235a
B
PS (MFI)
CD235a (MFI)
forward scatter
plasma
0 mU SMase
10 mU SMase
1 mU SMase
C
vesicles / µL
D
erythrocytes
vesicles
FSC
SSC
CD235a
CFSE

Figure 4 – SMase-induced vesiculation of erythrocytes. Erythrocytes were allowed to vesiculate in the presence or absence of 10 mU/mL SMase for 1 h at 37ºC. The vesicles were analyzed by flow cytometry. (A), Density plots of forward/sideward scatter (FSC and SSC, respectively), and Annexin V-FLUOS (phosphatidylserine (PS))/anti-CD235a-PE staining of plasma-derived vesicles and vesicles generated *in vitro*. Vesicles were gated according to FSC/SSC for fluorescence analysis. (B), PS and CD235a mean fluorescence intensity (MFI), and forward scatter of plasma-derived and *in vitro* $CD235a^+$ vesicles. (C), Quantification of $CD235a^+$ vesicles after erythrocyte vesiculation in the absence or presence of SMase. Fluorescent 10 µm counting beads were used as an internal standard. (D), Bottom left and center: Density plots of CFSE-loaded erythrocytes treated with SMase and stained with anti-CD235a-PE. The vesicles generated during the treatment of these cells were stained with anti-CD235a-PE and Annexin V-Alexa 647. Bottom right: Vesicles that were within the standard FSC/SSC vesicle range and that were positive for Annexin V are shown in the CFSE/CD235a density plot. For the assessment of dimensions, only $PS^+CD235a^+$ vesicles were considered. Data from five healthy volunteers are presented. The graphs present mean values, error bars represent standard deviation, and * = $p < 0.05$.

The recognition of ceramide on only a subpopulation of the cells after 5 mU/mL SMase treatment, and the high dependence of antibody binding on the fixative used, suggest that the specificity and activity of this antibody is strongly affected by membrane organization.

Next, we investigated whether SMase-induced membrane reorganization also affected the interaction between the plasma membrane and the cytoskeleton. Differential membrane protein extraction showed that the insoluble fraction of band 3 increased upon SMase treatment (supplemental Figure S2). In contrast, the extractability of β-actin with detergent increased upon SMase treatment. These changes implicate that, in addition to the membrane microdomain organization at the protein and lipid levels, also the cytoskeletal integrity and the interaction between plasma membrane and cytoskeleton are altered by SMase.

SMase enhances erythrocyte vesicle formation

During aging, the erythrocyte produces numerous vesicles that expose removal signals including PS, that are enriched in damaged membrane patches, and that are rapidly removed from the circulation. Physiologically, erythrocyte vesiculation may constitute a protective mechanism to prevent untimely erythrocyte removal [27]. Increased erythrocyte vesicle numbers were observed in several inflammation-associated diseases, including chronic renal failure, sickle cell disease and β-thalassemia [18]. Therefore, we investigated whether erythrocyte vesiculation rate and vesicle composition are affected by SMase treatment.

Erythrocytes were allowed to vesiculate *in vitro* in the presence or absence of SMase. The vesicles generated *in vitro* and the plasma vesicles from the corresponding healthy volunteers were assessed for PS exposure and the presence of the erythrocyte-specific marker glycophorin A (CD235a). Erythrocyte-derived plasma vesicles, control vesicles

generated *in vitro,* and vesicles from SMase-treated erythrocytes all exposed PS and expressed CD235a (Figure 4A). Plasma vesicles and control vesicles formed a single population with a comparable, high PS exposure and CD235a expression. An additional population with clearly reduced PS exposure and CD235a expression was observed in the SMase-induced vesicles (Figure 4A and B). In contrast, glycophorin C expression was found to be identical in all conditions (data not shown). Based on the forward scatter, all $PS^+CD235a^+$ vesicles had similar dimensions (Figure 4B). In addition to these qualitative differences between control and SMase-induced vesicles erythrocyte, vesiculation was enhanced more than 20-fold when the cells were exposed to SMase (Figure 4C). This heterogeneity in PS exposure and CD235a expression indicates that SMase-induced vesiculation differs qualitatively from vesiculation in the absence of SMase. Finally, CFSE-loaded erythrocytes generated CFSE-positive vesicles during SMase treatment (Figure 4D), showing that these vesicles contain cytoplasmic content of the parent cells.

Loss of osmotic responsiveness in erythrocytes treated with SMase

Following the analysis of the impact of SMase treatment on the structural organization of erythrocytes, we were interested in potential functional implications of SMase exposure. In the circulation, erythrocytes are constantly exposed to changing osmolalities, in particular when passing through the kidneys, and osmotic stress is known to induce PS exposure [28]. In order to study the effect of SMase on the osmotic responsiveness and fragility of erythrocytes, SMase-treated erythrocytes were exposed to different osmolalities and analyzed by flow cytometry.

When erythrocytes were treated with SMase activities of 1 mU/mL and higher, a population could be discerned with a low sideward scatter that was not seen in control erythrocytes (Figure 5). These populations had a nearly identical CFSE content and forward scatter, indicating that they had intact membranes and were of comparable size. When exposed to a hypertonic or hypotonic buffer, the SMase-treated erythrocytes with a normal sideward scatter and the control erythrocytes shrank and swelled, respectively (Figure 5). In contrast, the size of the additional population in the SMase-treated erythrocytes did not change upon incubation with these buffers, indicating a loss of osmotic responsiveness. When erythrocytes were treated with higher (≥10 mU/mL) SMase activities and subsequently incubated in hypotonic buffer, nearly all cells, including this additional population, were lysed, showing a SMase-induced increase in membrane fragility (Figure 5).

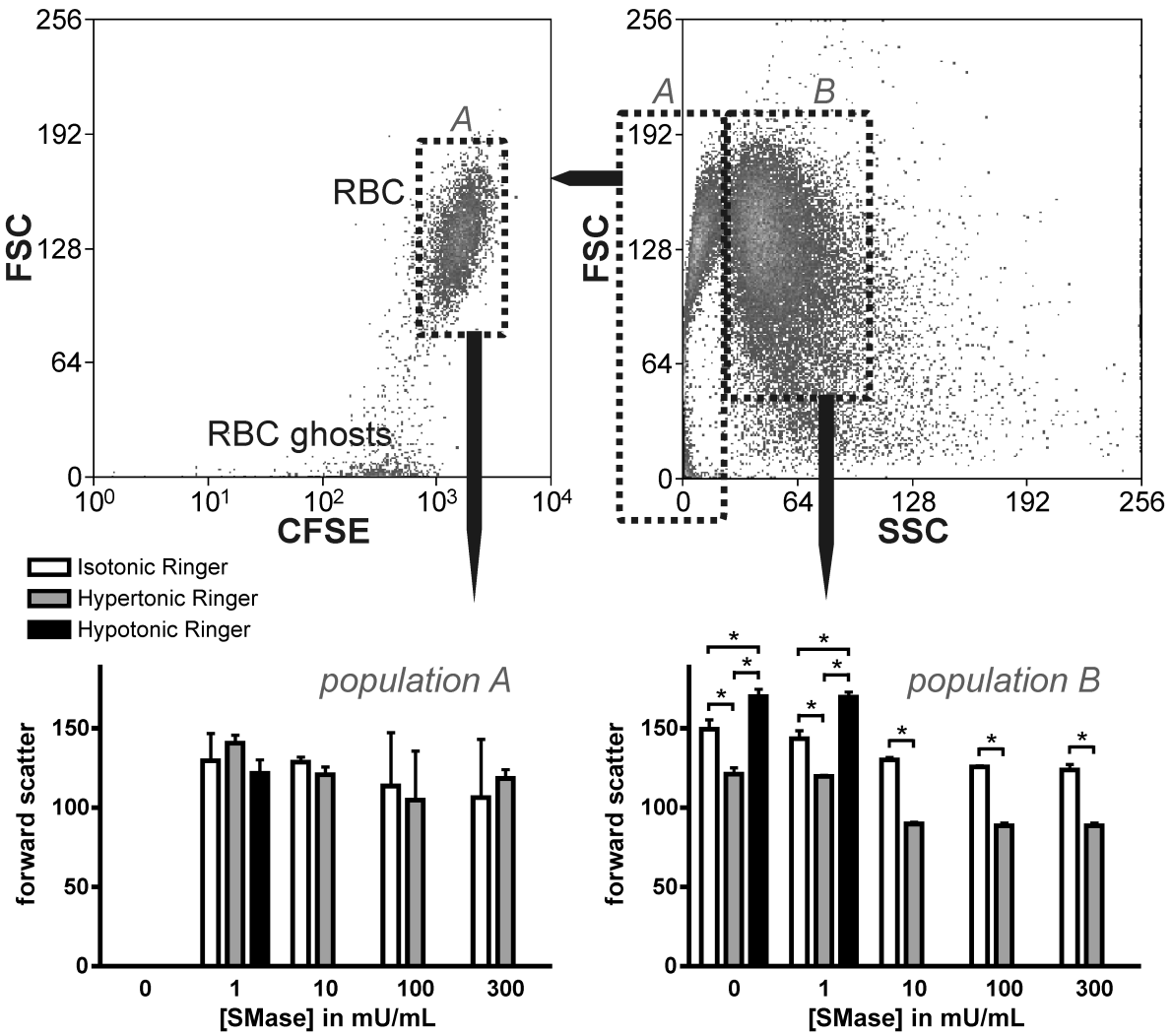

Figure 5 – Osmotic responsiveness and fragility of SMase-treated erythrocytes. CFSE-labeled erythrocytes from three healthy volunteers were treated with increasing activities of SMase for 15 min at 37ºC, and subsequently incubated with hypotonic, isotonic, and hypertonic buffer for 15 min at room temperature. The cells were analyzed by flow cytometry. A forward/sideward scatter (FSC and SSC, respectively) density plot of SMase-treated erythrocytes is shown in the upper-right. A FSC/CFSE density plot of erythrocyte subpopulation A is shown in the upper-left. Forward scatter of subpopulations A and B are depicted in the bottom graphs. Populations of < 2500 cells are not shown in the graphs. The graphs present mean values, error bars represent standard deviation, and * $p < 0.05$.

SMase enhances erythrocyte retention in a spleen-mimicking model

Sequestration of poorly deformable erythrocytes by the spleen is known to be critically involved in the decreased erythrocyte lifespan and anemia in several erythrocyte disorders [2]. The observed changes in erythrocyte morphology, ceramide formation, and membrane organization upon SMase treatment, likely also affect erythrocyte deformability. In order to determine whether SMase treatment affected deformability and splenic retention, we used a bead sorting device that mimics the mechanical deformation that erythrocytes experience in the spleen.

Erythrocytes were treated with SMase for 15 min at 37°C, labeled with CFSE and perfused through the spleen-mimicking model. Treatment with SMase induced a decrease in the permeation of the model spleen, concomitant with an increase in the retention (Figure 6). As before, SMase treatment reduced erythrocyte size, as reflected by forward scatter (Figure 6).

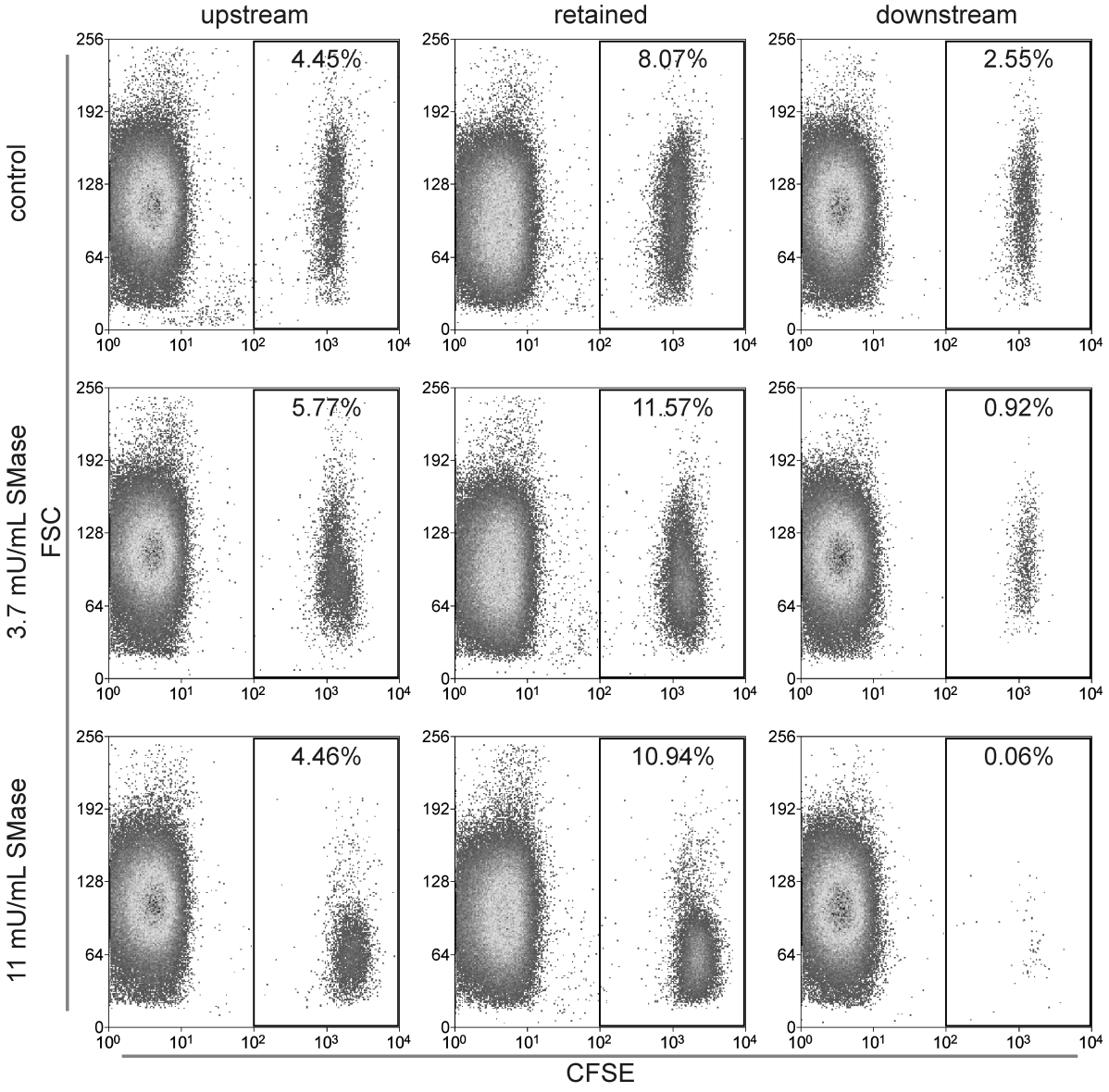

Figure 6 – Perfusion of SMase-treated erythrocytes through a spleen-mimicking device. A suspension consisting of approximately 5% CFSE-labeled erythrocytes treated with SMase for 15 min at 37°C and 95% untreated/unlabeled erythrocytes was passed through a bead sorting device at a flow rate of 60 mL/h (see Materials and Methods). Flow cytometry was used to determine the percentage of labeled cells in the initial upstream compartment, the bead compartment, and the downstream fractions. Forward scatter (FSC) is presented as a measure for erythrocyte diameter. Representative data from one of two experiments are shown.

Age and storage of erythrocytes increase their sensitivity to SMase

Erythrocytes become more sensitive to stressors such as energy depletion and hyperosmotic conditions with age and storage time [28-30]. Since SMase plasma levels increase during inflammation, and critically ill patients often receive erythrocyte transfusions, the sensitivity of stored erythrocytes for SMase-induced changes in cell size and PS exposure were studied by flow cytometry.

Erythrocytes from six healthy donors were obtained immediately after donation, and after 14 and 35 days of storage under blood bank conditions. After incubation with 1 mU/mL SMase for 15 min at 37°C, we observed a much more pronounced size reduction and increase in PS exposure for 35 day stored erythrocytes, compared to fresh and 14 day stored cells (Figure 7A).

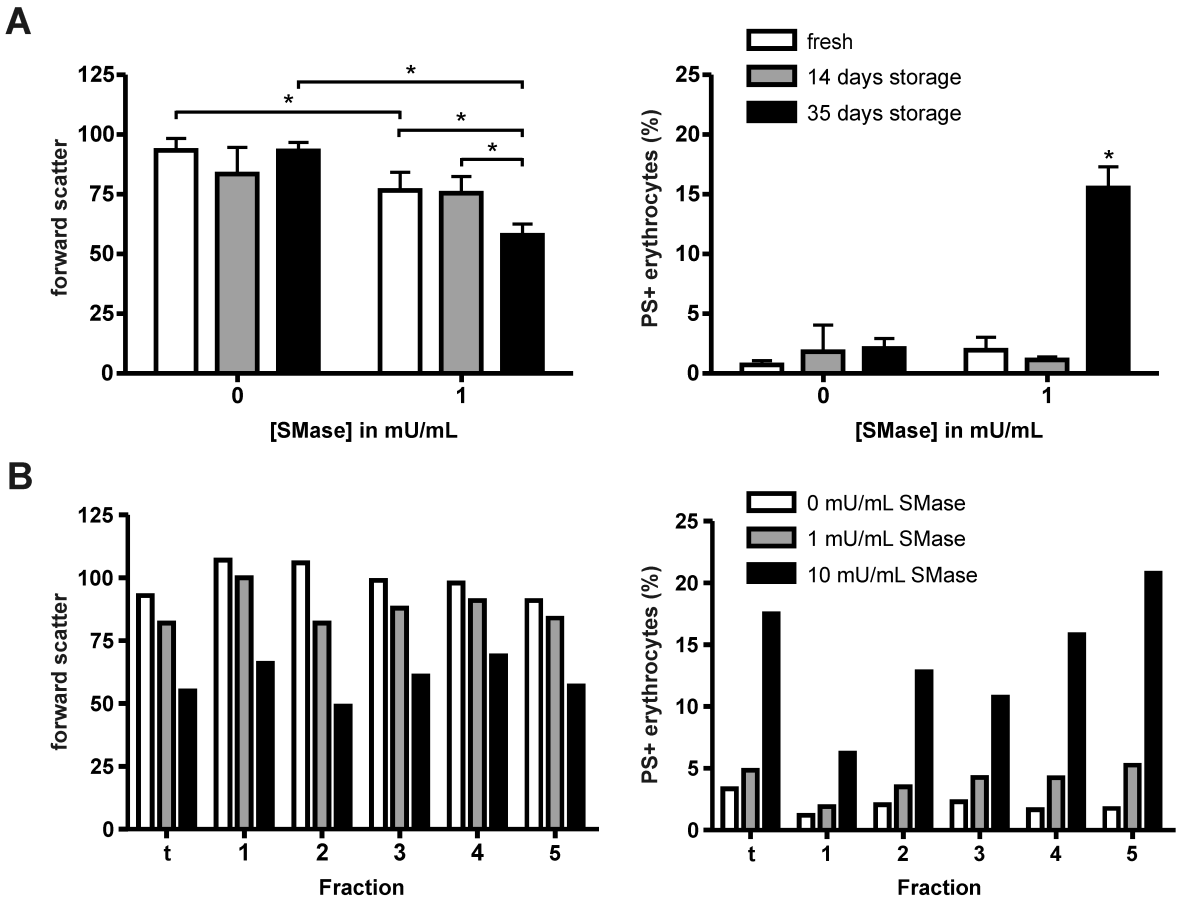

Figure 7 – SMase-induced size change and PS exposure in stored and aged erythrocytes. Flow cytometry of erythrocytes treated with SMase. Annexin V-FLUOS staining was performed to determine the percentage of phosphatidylserine (PS)-exposing erythrocytes. Forward scatter is presented as a measure of erythrocyte diameter. (A), Fresh, 14 and 35 days stored erythrocytes from six healthy donors treated with 1 mU/mL SMase for 15 min at 37ºC. (B), Erythrocytes of various mean age obtained from a 27 year-old male donor by combined density and volumetric separation (see Materials and Methods), treated with 1 and 10 mU/mL SMase for 15 min at 37ºC. t, total erythrocyte product. Erythrocyte fractions 1 and 5 have the lowest and highest mean age, respectively. The graphs present mean values, error bars represent standard deviation, and * = $p < 0.05$.

As erythrocyte age might also affect the response to SMase-induced ceramide formation in the plasma membrane, a combination of volume and density separation was used to obtain well-defined erythrocyte populations of different mean age. These were treated with 1 and 10 mU/mL SMase, and showed an age-dependent increase in the sensitivity for SMase-induced PS exposure (Figure 7B).

Discussion

The chronic inflammation that arises in patients with various diseases, including sepsis, can induce anemia, which is associated with poor disease outcome [3]. Inflammation enhances SMase secretion, and ceramide formation and PS exposure were observed when erythrocytes were incubated with plasma from septic patients *ex vivo* [16]. PS exposure is a marker for cellular stress and contributes to erythrocyte removal [31]. So far, studies concerning SMase activity on erythrocytes focused on membrane lipid rearrangement and shape changes [13,32]. In this study we show that ceramide-induced membrane lipid rearrangement affects multiple processes that are critical for erythrocyte function and removal, including protein-protein interactions, membrane stability and vesiculation. Furthermore, we directly correlated these molecular changes to parameters relating to erythrocyte function *in vivo* by addressing sensitivity to osmotic stress, permeation through a spleen-mimicking device, and dependence on erythrocyte age.

In agreement with earlier findings [13], we observed a reduction in cell size and increase in the percentage of PS-exposing erythrocytes upon SMase treatment of erythrocytes. Our time-lapse confocal microscopy experiments revealed that the transition of their typical discoid to a spherical shape preceded PS exposure, which was followed by disintegration and loss of cytoplasmic content. The combination of shape change and enhanced vesiculation explain the reduction in size observed by flow cytometry and confocal microscopy after SMase treatment.

Anchorage of the plasma membrane to the cytoskeleton maintains the discoid shape and membrane stability of the erythrocyte, as several erythrocyte disorders that affect membrane anchorage to the cytoskeleton induce abnormal cell shape and enhanced hemolysis [2]. Similar to the observations in pathological erythrocytes, our analyses using differential membrane protein extraction demonstrated that this anchorage is also affected by SMase. This may be mediated by protein phosphorylation, which is known to regulate protein-protein interactions in the erythrocyte [33]. Furthermore, membrane lipid interaction with cytoskeletal proteins might be affected by SMase-induced membrane reorganization [34].

An intriguing finding was the presence of large CFSE-positive protein clusters that appeared in conjunction with the detected membrane irregularities. As CFSE aspecifically reacts with the intracellular proteins - of which >95% is hemoglobin - the observed high-intensity CFSE signals are most likely hemoglobin clusters. This hemoglobin clustering is probably the indirect result of the effect of SMase on the conformation of band 3, which has a high affinity binding site for hemoglobin in its cytoplasmic domain [26].

As shown by high-resolution, immunofluorescence microscopy analysis of CD59 and stomatin localization, SMase treatment not only led to morphological changes, but also to a reorganization of membrane microdomains. The resulting larger domains were comparable in size to the endovesicle-like structures observed with electron microscopy. Due to their small head group in comparison to the original phospholipids, ceramides induce negative membrane curvature which promotes both lipid membrane invagination and blebbing [10]. This provides a plausible explanation for the SMase-induced tubular plasma membrane invaginations. Endovesicles could result from membrane fusion in such tubular structures [35]. Membrane blebbing may also further contribute to the large, SMase-induced increase in vesiculation [27].

Also, we observed ceramide-enriched membrane platforms, which are known to originate in plasma membranes with high ceramide content [8]. The increase in membrane fragility can be attributed to the formation of these large ceramide-enriched membrane platforms, as earlier studies revealed them to be very rigid, resulting in a weak interface between the platform and the surrounding plasma membrane [10]. Small pores are known to form at this interface, which may readily explain the loss of osmotic responsiveness of the affected erythrocytes [10]. Splenic sequestration of abnormal erythrocytes with reduced deformability has been observed in several erythrocyte disorders, and is associated with a decreased life span and resulting hemolytic anemia in afflicted patients [2]. The presence of rigid ceramide platforms in SMase-treated erythrocytes may lead to enhanced splenic retention. Indeed, we could link SMase-induced ceramide formation to reduced deformability by showing that SMase treatment enhanced erythrocyte retention in a bead-sorting device that mimics the mechanical deformation that erythrocytes experience in the spleen.

Vesiculation is an integral part of erythrocyte aging and appears to constitute a protective mechanism to enhance erythrocyte survival [27]. Vesicles from erythrocyte concentrates were found to modulate platelet function *in vitro* [36]. Furthermore, increased erythrocyte vesicle numbers were observed in several disease states (e.g. chronic renal failure, sickle cell disease and β-thalassemia) [18]. SMase-induced increase in erythrocyte vesiculation, probably resulting from a weakening of membrane anchorage, may contribute to disease

pathology due to the pro-coagulant nature of the vesicles [37]. The presence of two distinct vesicle populations as observed by annexin V and anti-CD235a double staining indicates that vesiculation occurs in distinct types of microdomains that are present on the erythrocyte membrane during SMase treatment. Furthermore, the high CFSE content of the microparticles generated by treatment of CFSE-loaded erythrocytes with SMase indicates that the microparticles contain a high concentration of cytoplasmic proteins. This suggests that they are sealed vesicles containing hemoglobin, similar to those generated in the circulation [27]. This is supported by the reddish color of the vesicle pellet.

Positive-ion MALDI-TOF MS after chromatographic separation of the total lipid extract is a very sensitive analytical method for the detection of cell membrane ceramide content. The observation that 1 mU/mL SMase affected erythrocyte shape, membrane organization and osmotic responsiveness, even though membrane ceramide content was below the detection limit of the positive-ion MALDI-TOF MS, suggests that erythrocytes are very sensitive to ceramide-induced changes in membrane organization. The absence of other, non-specific breakdown products at higher enzyme activities excludes alternative degradation processes as the basis for these observations.

Critically ill patients, in particular those suffering from severe inflammation and sepsis, frequently receive blood transfusions. We showed that erythrocyte storage under blood bank conditions increased the sensitivity to SMase. This may reduce erythrocyte survival after transfusion, especially in patients with enhanced SMase activity. Also, in healthy individuals, physiological erythrocyte age is associated with enhanced sensitivity. Therefore, cellular age likely underlies the observed heterogeneity in susceptibility to SMase per individual cell, as is particularly apparent in Figure S1 and Movie S1. These findings imply that the use of older erythrocyte concentrates in patients suffering from systemic inflammation might result in reduced transfusion efficacy and a higher risk of harmful side-effects, such as extravascular hemolysis and increased plasma iron concentrations that are associated with a SMase-induced rapid clearance [38].

In summary, we have shown that multiple, pathophysiologically relevant erythrocyte parameters are affected by SMase. These parameters are associated with changes that exceeded mere membrane lipid rearrangement, and included altered protein-protein interaction, membrane stability, deformability, and enhanced erythrocyte vesiculation. Furthermore, our findings suggest that enhanced SMase secretion during chronic inflammation contribute to the enhanced erythrocyte clearance that is often associated with inflammation. In particular, these data suggest that transfusion in patients with increased SMase activity should be restricted to fresh erythrocyte concentrates.

Materials and Methods

Collection, isolation and storage of erythrocytes

Fresh erythrocytes were isolated from whole blood (EDTA) donated by healthy human volunteers, using Ficoll (GE Healthcare, Waukesha WI, USA) density centrifugation. To obtain erythrocyte populations of different age, a combination of volume and density separation was used [27]. Erythrocyte concentrates were obtained using standard blood bank procedures. In short, whole blood (500 mL) was collected in a Composelect quadruple CPD-SAGM top-and-bottom bag system (Fresenius Kabi, Bad Homburg, Germany), containing 70 mL CPD as an anticoagulant. After cooling and centrifugation, erythrocytes were isolated using a Compomat G4 (Fresenius Kabi, Bad Homburg, Germany), after which 110 mL SAG-M was added to the erythrocytes. The erythrocyte suspension was leukocyte-depleted by in-line filtration, and subsequently stored at 2 to 6ºC. The study was performed following the guidelines of the local medical ethical committee and in accordance with the declaration of Helsinki. Written informed consent was obtained from all blood donors participating in this study.

Solutions

Erythrocytes were kept in Ringer solution (125 mM NaCl, 5 mM KCl, 1 mM $MgSO_4$, 32 mM HEPES, 5 mM glucose, 2.5 mM $CaCl_2$, pH 7.4). NaCl concentrations of 162.5 mM and 87.5 mM NaCl were used for hyper- and hypotonic Ringer, respectively. Calcium-free Ringer was used during whole blood erythrocyte and vesicle isolation to prevent clotting.

Erythrocyte lysis was performed using lysis buffer (10 mM HEPES, 1 mM EDTA, 1 mM EGTA, 1 mM benzamidine and 0.005 mM leupeptin, pH 8.0). Protein extractions were performed using extraction buffer (25 mM HEPES, 150 mM NaCl, 1 mM EDTA, 1 mM EGTA, 1 mM benzamidine, 0.005 mM leupeptin, 1% Triton X-100, pH 7.4). When indicated, Triton X-100 was replaced by 10 mM n-Dodecyl-ß-D-Maltoside (DDM).

SMase treatment

Unless mentioned otherwise, 2×10^6 erythrocytes were incubated in 100 µL Ringer containing various concentrations of SMase (Sigma-Aldrich, St. Louis MO, USA; 159 U/mg; one unit of SMase hydrolyzes 1 µM of SM per min at pH 7.4 at 37ºC) for 15 min at 37ºC. After treatment, cells were washed twice with Ringer and centrifuged at 1000g for 3 min. When treated in the absence of extracellular calcium, cells were washed five times with calcium-free Ringer before treatment in this buffer. Subsequent washing and staining of cells in Ringer was performed at 4ºC.

Flow cytometry

To probe PS exposure, cells were washed with Ringer containing 0.2% bovine serum albumin (BSA, Sigma-Aldrich, St. Louis MO, USA) and stained with Annexin V-FLUOS (Roche, Basel, Switzerland; 1/25) for 1 h at room temperature. Alternatively, erythrocytes were stained with 1 µM CFSE diacetate (Invitrogen, Carlsbad CA, USA) in Ringer for 15 min at 37ºC prior to SMase treatment. Excess CFSE diacetate was removed by washing cells three times with Ringer containing 0.2% BSA. Flow cytometry was performed on a FACSCalibur system (BD Biosciences, Franklin Lakes NJ, USA) using Cellquest Pro software version 6.0. Per sample, 25,000 cells were measured and data analysis was performed using Cyan Summit software version 4.3.

Confocal microscopy

For time-lapse confocal laser scanning microscopy experiments, 200 µL Ringer containing 1×10^6 CFSE diacetate-labeled erythrocytes, Annexin V-Alexa 647 (Roche, Basel, Switzerland; 1/20) and 10 mU SMase were added to a Lab-Tek chambered cover glass (Thermo Fisher Scientific, Rochester NY, USA). One min after addition of SMase to the erythrocytes, recording of images was started with 30 sec intervals for a total of 60 min.

Mouse anti-CD59-Alexa 647 monoclonal antibody (clone MEM-43, AbD Serotec, Düsseldorf, Germany; 1/200) staining was performed on erythrocytes in Ringer buffer. Acrolein-fixated erythrocytes were used for combined antibody staining with mouse anti-stomatin (GARP-50, kindly provided by Rainer Prohaska, University of Vienna, Austria; 1/200) and rabbit polyclonal antiserum against the membrane domain of human band 3 (K2N6B/PMB3 [39]); 1/100). Acrolein fixation and subsequent staining were performed as described by Matte et al [40]. BSA (1%) was used instead of fish skin gelatin for blocking purposes. Secondary antibodies were goat anti-mouse-Alexa 488 and goat anti-rabbit-Alexa 633 (Invitrogen, Carlsbad CA, USA; 1/1000). Ceramide staining on acrolein-fixated erythrocytes was performed using anti-ceramide IgM (clone MID 15B4, Enzo life sciences, Farmingdale NY, USA, 1/50) and isotype control IgM (BD Biosciences, Franklin Lakes NJ, USA, 1/50), followed by goat anti-mouse-Alexa 647 staining (Invitrogen, Carlsbad CA, USA; 1/200).

Confocal laser scanning microscopy was performed on a TCS SP5 confocal laser scanning microscope (Leica Microsystems, Mannheim, Germany) equipped with a HCX Plan-Apochromat 63X/N.A. 1.2 water immersion lens. Cells were imaged at a temperature-controlled stage set at 37ºC. The Leica TCS SP5 LAS AF software was used for image acquisition. Image J version 1.45J was used for further image analysis.

Electron microscopy

Erythrocytes were fixated with 1% glutaraldehyde in 0.1 M sodium cacodylate buffer (pH 7.2) for 1 h at room temperature. The cells were then washed twice in cacodylate buffer and post-fixated for 1 h in 1% osmium tetraoxide. After two more washes with cacodylate buffer, samples were pelleted in 2% agarose (ultra-low gelling temperature, Sigma-Aldrich, St. Louis MO, USA) and cells were dehydrated by incubation in an ascending series of aqueous ethanol for 15 min per incubation step. Cells were then incubated overnight in ethanol and Epon at a 1/1 ratio, subsequently incubated for 4 h in pure Epon and embedded at 37ºC overnight in fresh Epon. The samples were then stored at 60ºC overnight, after which 80 nm sections were made using a Reichert Ultracut 6 Microtome. After drying, sections were stained in uranyl acetate for 20 minutes and subsequently in lead citrate for 10 minutes. Sections were examined with a JEOL TEM 1010 (JEOL Ltd., Tokyo, Japan).

Erythrocyte vesiculation

All buffers used for vesicle generation, isolation and analysis were complemented with 0.2% BSA and filtered (0.22 µm) before use. Erythrocytes (1×10^9) were incubated with 5 mL Ringer containing 10 mU/mL SMase for 1 h. The cell suspension was centrifuged for 10 min at 1500g, and the supernatant was centrifuged again for 20 min at 1500g. Vesicles were then pelleted by centrifugation at 21,000g and 4ºC for 20 min. The vesicles were washed once with Ringer and resuspended in 25 µL Ringer. Vesicles from whole blood were isolated from 200 µL plasma as described above, with an additional calcium-free Ringer wash of the vesicle pellet after high speed centrifugation.

Vesicles were stained with Annexin V-FLUOS and anti-CD235a-PE monoclonal antibody (clone KC16, Beckman Coulter, Brea CA, USA; 1/50) in a total volume of 50 µL Ringer for 45 min at room temperature, and washed once with Ringer. Vesicles were resuspended in 150 µL Ringer, and washed Flow-Count Fluorospheres (Beckman Coulter, Brea CA, USA) were added (1×10^4) for quantification. Samples were analyzed by flow cytometry as described for erythrocytes at high speed for 1 min, using a protocol optimized for vesicle analysis. Sulfate latex microspheres (Invitrogen, Carlsbad CA, USA; 0.9 µm) were used to determine the maximum upper boundary allowed for forward and sideward scatter gating. All staining solutions were centrifuged at 21,000g and 4ºC for 20 min prior to use to remove fluorescent aggregates. PE-conjugated IgG1 isotype control (Dako, Glostrup, Denmark) did not show any aspecific binding.

Membrane protein extraction, SDS-PAGE and immunoblot

Erythrocytes (1×10^9) were incubated with 5 mL Ringer containing 10 mU/mL SMase for 1 hour and subsequently lysed in 1 mL lysis buffer. The membrane fraction was washed

repeatedly by centrifugation at 21,000g for 10 min to remove free hemoglobin. Membrane proteins were extracted by adding 200 µL extraction buffer and samples were vortexed for 30 s. The samples were incubated for 30 min with regular vortexing and were subsequently centrifuged at 21,000g for 15 min. Laemmli sample buffer (BioRad, Hercules CA, USA) containing 5% 2-mercaptoethanol was added to the supernatant at a 1/1 ratio (v/v). The remaining pellet was washed once with phosphate-buffered saline (PBS, pH 7.4) and resuspended in 50 µL sample buffer.

SDS-PAGE was performed using 12.5% running gels with in the Mini Protean 3 system (both BioRad, Hercules CA, USA), according to the method of Laemmli Either band 3 protein or actin were used as loading controls. Apparent molecular masses were calculated based on the Precision Plus Protein Standard (BioRad, Hercules CA, USA). After SDS-PAGE, the proteins were transferred to PVDF membranes using the iBlot system (Invitrogen, Carlsbad CA, USA). The membranes were then blocked with Odyssey Blocking Buffer (OBB, LI-COR, Lincoln NE, USA), and incubated for 16 h at 4ºC in OBB containing 0.1% Tween-20, rabbit anti-band 3 serum (K2N6B/PMB3(39); 1/5000) and mouse anti-β actin monoclonal antibody (clone AC-15, Sigma-Aldrich, St. Louis MO, USA; 1/5000). After washing with PBS containing 0.1% Tween-20, the blots were incubated for 1 h at room temperature in OBB, 0.1% Tween-20, 0.01% SDS, goat anti-rabbit IgG-Alexa Fluor 680 (Invitrogen, Carlsbad CA, USA; 1/10,000), and goat anti-mouse IgG-IRDye 800 (LI-COR, Lincoln NE, USA; 1/10,000). This final incubation was followed by a single washing step with PBS containing 0.1% Tween-20, and three subsequent washes with PBS. Immunoblots were scanned using the Odyssey Infrared Imaging System (LI-COR, Lincoln NE, USA), and analyzed using Odyssey Software version 2.1.

Positive-ion MALDI-TOF MS and ^{31}P NMR analyses of membrane lipids

Packed erythrocytes (300 µL) were incubated with 5 mL Ringer containing SMase for 1 hour and subsequently lysed and washed as described for membrane protein extraction. Membrane pellets (200 µL) were transferred to glass tubes and 2 mL methanol and 1 mL dichloromethane were added. After vortexing, another 1 mL dichloromethane and 1.6 mL 0.5% acetic acid were added and vortexed once more. After 10 min centrifugation at 800g, the bottom dichloromethane layer was isolated. Residual lipids were extracted from the aqueous layer by extraction with 1 mL dichloromethane. The two dichloromethane fractions were pooled and the solvent evaporated. The lipid fraction was analyzed by positive-ion MALDI-TOF MS and ^{31}P NMR spectroscopy as described by Dannenberger et al [41]. Shortly, the lipid extract was mixed 1:1 (v/v) with the matrix solution (0.5 M 2,5-dihdyroxybenzoic acid in methanol) and 1 µL of this mixture was directly applied onto the MALDI target. All MALDI-TOF mass spectra were acquired on an Autoflex I mass

spectrometer (Bruker Daltonics, Bremen, Germany) with ion reflector. The system utilizes a pulsed 50 Hz nitrogen laser, emitting at 337 nm. The extraction voltage was 20 kV and gated matrix suppression was applied to prevent the saturation of the detector by matrix ions. All spectra were acquired in the reflector mode using delayed extraction conditions. Peak identities were additionally confirmed by recording post source decay spectra as previously described [42]. As the focus of this study is on SM, no negative-ion spectra were acquired because SM is much more sensitively detectable in the positive-ion mode [43].

Erythrocyte bead sorting device

Erythrocyte retention/deformability was assessed using a bead sorting device that mimics the mechanical deformation that erythrocytes experience in the spleen [44]. After SMase treatment, erythrocytes (1×10^8) were labeled with CFSE diacetate. A 2% hematocrit suspension (600 µL) consisting of 5% treated/labeled and 95% untreated/unlabeled erythrocytes in Ringer with 1% BSA was passed through the bead sorting device at a flow rate of 60 mL/h. The untreated/unlabeled erythrocytes acted as both facilitators of steady perfusion of the cells of interest, and as an internal control for retention/deformability. Flow cytometry measurement (100,000 cells) of the initial upstream compartment, the bead compartment, and downstream fractions was performed to determine the ratio of labeled versus unlabeled erythrocytes in each separate fraction.

Statistical analysis

Differences between two groups of data were determined using a paired T test. Differences between multiple groups were assessed with repeated measures one-way ANOVA in combination with Tukey's post-test. Reported *p* values are two sided, and a *p* value of < 0.05 was used to assess statistical significance.

Acknowledgements

The authors would like to thank Mietske Wijers-Rouw from the Department of Cell Biology, RUMC, NCMLS, for assisting with the electron microscopy. We are grateful to Lucas van Eijk from the Department of Intensive Care Medicine, RUMC, for blood sampling of healthy volunteers. We thank the people who have volunteered to donate blood for this study.

References

1 Bosman GJ, Werre JM, Willekens FL, Novotny VM. Erythrocyte ageing in vivo and in vitro: structural aspects and implications for transfusion. *Transfus. Med.* 18(6), 335-347 (2008).

2 Mohandas N, Gallagher PG. Red cell membrane: past, present, and future. *Blood* 112(10), 3939-3948 (2008).

3 Roy CN. Anemia of inflammation. *Hematology. Am. Soc. Hematol. Educ. Program.* 2010 276-280 (2010).

4 Gould S, Cimino MJ, Gerber DR. Packed red blood cell transfusion in the intensive care unit: limitations and consequences. *Am. J. Crit Care* 16(1), 39-48 (2007).

5 Weiss G, Goodnough LT. Anemia of chronic disease. *N. Engl. J. Med.* 352(10), 1011-1023 (2005).

6 Jenkins RW, Canals D, Hannun YA. Roles and regulation of secretory and lysosomal acid sphingomyelinase. *Cell Signal.* 21(6), 836-846 (2009).

7 Goni FM, Alonso A. Sphingomyelinases: enzymology and membrane activity. *FEBS Lett.* 531(1), 38-46 (2002).

8 Grassme H, Riethmuller J, Gulbins E. Biological aspects of ceramide-enriched membrane domains. *Prog. Lipid Res.* 46(3-4), 161-170 (2007).

9 Hannun YA, Obeid LM. Principles of bioactive lipid signalling: lessons from sphingolipids. *Nat. Rev. Mol. Cell Biol.* 9(2), 139-150 (2008).

10 Lopez-Montero I, Monroy F, Velez M, Devaux PF. Ceramide: from lateral segregation to mechanical stress. *Biochim. Biophys. Acta* 1798(7), 1348-1356 (2010).

11 Hanada K, Mitamura T, Fukasawa M, Magistrado PA, Horii T, Nishijima M. Neutral sphingomyelinase activity dependent on Mg2+ and anionic phospholipids in the intraerythrocytic malaria parasite Plasmodium falciparum. *Biochem. J.* 346 Pt 3 671-677 (2000).

12 D'Alessandro A, Righetti PG, Zolla L. The red blood cell proteome and interactome: an update. *J. Proteome. Res.* 9(1), 144-163 (2010).

13 Lang KS, Myssina S, Brand V *et al*. Involvement of ceramide in hyperosmotic shock-induced death of erythrocytes. *Cell Death. Differ.* 11(2), 231-243 (2004).

14 Lang F, Gulbins E, Lang PA, Zappulla D, Foller M. Ceramide in suicidal death of erythrocytes. *Cell Physiol Biochem.* 26(1), 21-28 (2010).

15 Lang F, Lang KS, Lang PA, Huber SM, Wieder T. Osmotic shock-induced suicidal death of erythrocytes. *Acta Physiol (Oxf)* 187(1-2), 191-198 (2006).

16 Kempe DS, Akel A, Lang PA *et al*. Suicidal erythrocyte death in sepsis. *J. Mol. Med.* 85(3), 273-281 (2007).

17 Lang PA, Schenck M, Nicolay JP *et al*. Liver cell death and anemia in Wilson disease involve acid sphingomyelinase and ceramide. *Nat. Med.* 13(2), 164-170 (2007).

18 Hind E, Heugh S, Ansa-Addo EA, Antwi-Baffour S, Lange S, Inal J. Red cell PMVs, plasma membrane-derived vesicles calling out for standards. *Biochem. Biophys. Res. Commun.* 399(4), 465-469 (2010).

19 Ago H, Oda M, Takahashi M *et al*. Structural basis of the sphingomyelin phosphodiesterase activity in neutral sphingomyelinase from Bacillus cereus. *J. Biol. Chem.* 281(23), 16157-16167 (2006).

20 Daleke DL. Phospholipid flippases. *J. Biol. Chem.* 282(2), 821-825 (2007).

21 Schiller J, Suss R, Fuchs B, Muller M, Zschornig O, Arnold K. MALDI-TOF MS in lipidomics. *Front Biosci.* 12 2568-2579 (2007).

22 Fuchs B, Schiller J, Suss R, Schurenberg M, Suckau D. A direct and simple method of coupling matrix-assisted laser desorption and ionization time-of-flight mass spectrometry (MALDI-TOF MS) to thin-layer chromatography (TLC) for the analysis of phospholipids from egg yolk. *Anal. Bioanal. Chem.* 389(3), 827-834 (2007).

23 Simons K, Gerl MJ. Revitalizing membrane rafts: new tools and insights. *Nat. Rev. Mol. Cell Biol.* 11(10), 688-699 (2010).

24 Civenni G, Test ST, Brodbeck U, Butikofer P. In vitro incorporation of GPI-anchored proteins into human erythrocytes and their fate in the membrane. *Blood* 91(5), 1784-1792 (1998).

25 Salzer U, Prohaska R. Stomatin, flotillin-1, and flotillin-2 are major integral proteins of erythrocyte lipid rafts. *Blood* 97(4), 1141-1143 (2001).

26 van den Akker E, Satchwell TJ, Williamson RC, Toye AM. Band 3 multiprotein complexes in the red cell membrane; of mice and men. *Blood Cells Mol. Dis.* 45(1), 1-8 (2010).

27 Willekens FL, Werre JM, Groenen-Dopp YA, Roerdinkholder-Stoelwinder B, de Pauw B, Bosman GJ. Erythrocyte vesiculation: a self-protective mechanism? *Br. J. Haematol.* 141(4), 549-556 (2008).

28 Bosman GJ, Cluitmans JC, Groenen YA, Werre JM, Willekens FL, Novotny VM. Susceptibility to hyperosmotic stress-induced phosphatidylserine exposure increases during red blood cell storage. *Transfusion* 51(5), 1072-1078 (2011).

29 Bennett-Guerrero E, Veldman TH, Doctor A *et al*. Evolution of adverse changes in stored RBCs. *Proc. Natl. Acad. Sci. U. S. A* 104(43), 17063-17068 (2007).

30 Gevi F, D'Alessandro A, Rinalducci S, Zolla L. Alterations of red blood cell metabolome during cold liquid storage of erythrocyte concentrates in CPD-SAGM. *J. Proteomics.* (2012).

31 Kuypers FA, de Jong K. The role of phosphatidylserine in recognition and removal of erythrocytes. *Cell Mol. Biol. (Noisy-le-grand)* 50(2), 147-158 (2004).

32 Montes LR, Lopez DJ, Sot J *et al*. Ceramide-enriched membrane domains in red blood cells and the mechanism of sphingomyelinase-induced hot-cold hemolysis. *Biochemistry* 47(43), 11222-11230 (2008).

33 Gauthier E, Guo X, Mohandas N, An X. Phosphorylation-dependent perturbations of the 4.1R-associated multiprotein complex of the erythrocyte membrane. *Biochemistry* 50(21), 4561-4567 (2011).

34 An X, Guo X, Sum H, Morrow J, Gratzer W, Mohandas N. Phosphatidylserine binding sites in erythroid spectrin: location and implications for membrane stability. *Biochemistry* 43(2), 310-315 (2004).

35 Hagerstrand H, Kralj-Iglic V, Fosnaric M *et al*. Endovesicle formation and membrane perturbation induced by polyoxyethyleneglycolalkylethers in human erythrocytes. *Biochim. Biophys. Acta* 1665(1-2), 191-200 (2004).

36 Xiong Z, Cavaretta J, Qu L, Stolz DB, Triulzi D, Lee JS. Red blood cell microparticles show altered inflammatory chemokine binding and release ligand upon interaction with platelets. *Transfusion* 51(3), 610-621 (2011).

37 Kozuma Y, Sawahata Y, Takei Y, Chiba S, Ninomiya H. Procoagulant properties of microparticles released from red blood cells in paroxysmal nocturnal haemoglobinuria. *Br. J. Haematol.* 152(5), 631-639 (2011).

38 Hod EA, Zhang N, Sokol SA *et al*. Transfusion of red blood cells after prolonged storage produces harmful effects that are mediated by iron and inflammation. *Blood* 115(21), 4284-4292 (2010).

39 Bosman GJ, Visser FE, de Man AJ, Bartholomeus IG, de Grip WJ. Erythrocyte membrane changes of individuals with Down's syndrome in various stages of Alzheimer-type dementia. *Neurobiol. Aging* 14(3), 223-228 (1993).

40 Matte A, Low PS, Turrini F *et al*. Peroxiredoxin-2 expression is increased in beta-thalassemic mouse red cells but is displaced from the membrane as a marker of oxidative stress. *Free Radic. Biol. Med.* 49(3), 457-466 (2010).

41 Dannenberger D, Suss R, Teuber K, Fuchs B, Nuernberg K, Schiller J. The intact muscle lipid composition of bulls: an investigation by MALDI-TOF MS and 31P NMR. *Chem. Phys. Lipids* 163(2), 157-164 (2010).

42 Fuchs B, Schober C, Richter G, Suss R, Schiller J. MALDI-TOF MS of phosphatidylethanolamines: different adducts cause different post source decay (PSD) fragment ion spectra. *J. Biochem. Biophys. Methods* 70(4), 689-692 (2007).

43 Fuchs B, Suss R, Schiller J. An update of MALDI-TOF mass spectrometry in lipid research. *Prog. Lipid Res.* 49(4), 450-475 (2010).

44 Deplaine G, Safeukui I, Jeddi F *et al*. The sensing of poorly deformable red blood cells by the human spleen can be mimicked in vitro. *Blood* 117(8), e88-e95 (2011).

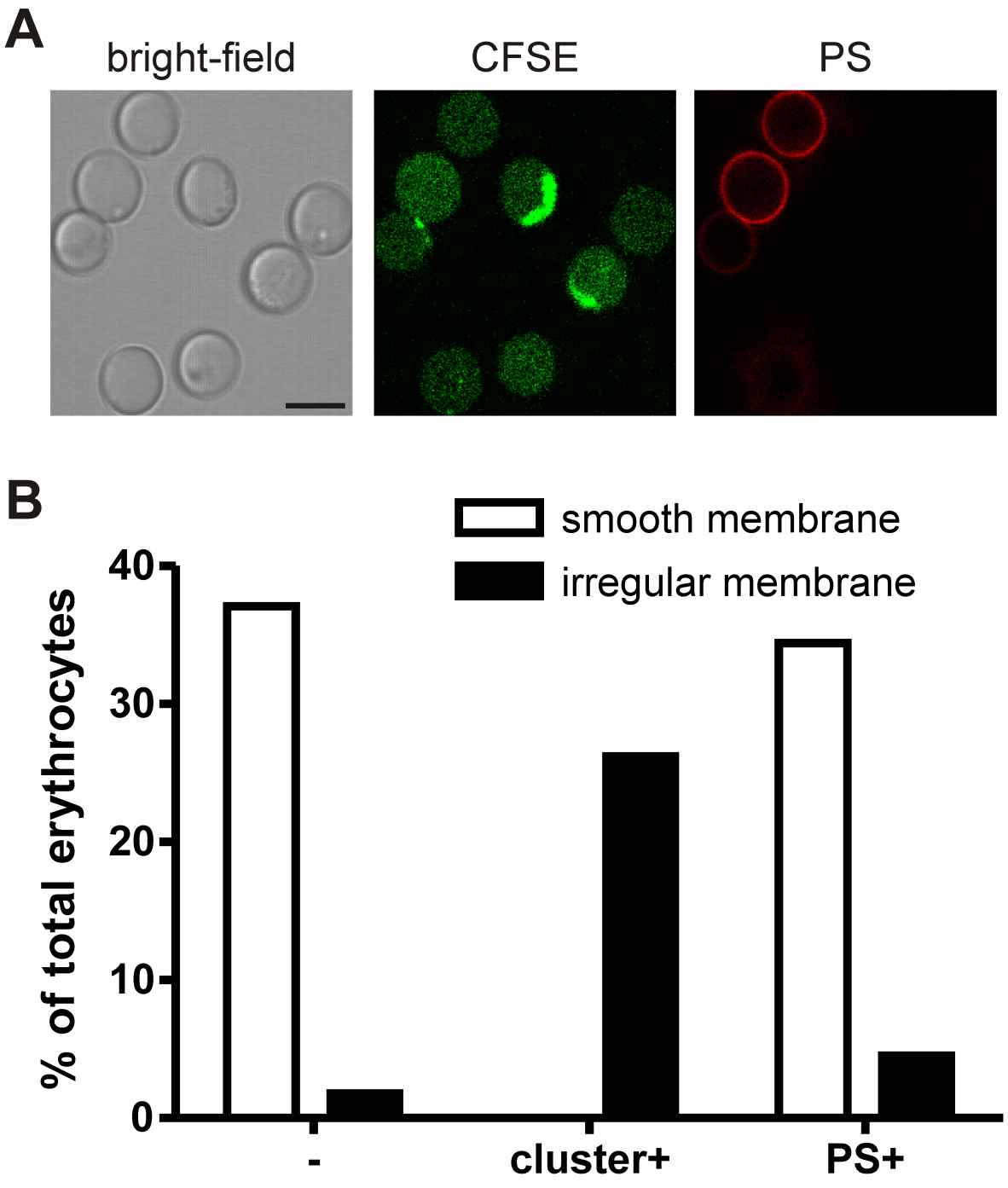

Figure S1 – Erythrocyte membrane irregularities, protein clustering and PS exposure during SMase treatment. Time-lapse confocal laser scanning microscopy of CFSE-labeled erythrocytes treated with 10 mU/mL SMase at 37ºC in the presence of Annexin V-Alexa 647 (also see Figure 1D and supplemental Movie 1). (A), Representative picture of erythrocytes at t = 45 min after the addition of SMase. Scale bar = 5 µm. (B), Quantification of CFSE cluster-positive and PS-exposing erythrocytes with or without observable membrane irregularities in bright-field. 200 cells were assessed in a single experiment (t = 45 min). Confocal laser scanning microscopy was used to image fluorescence as described in Materials and Methods.

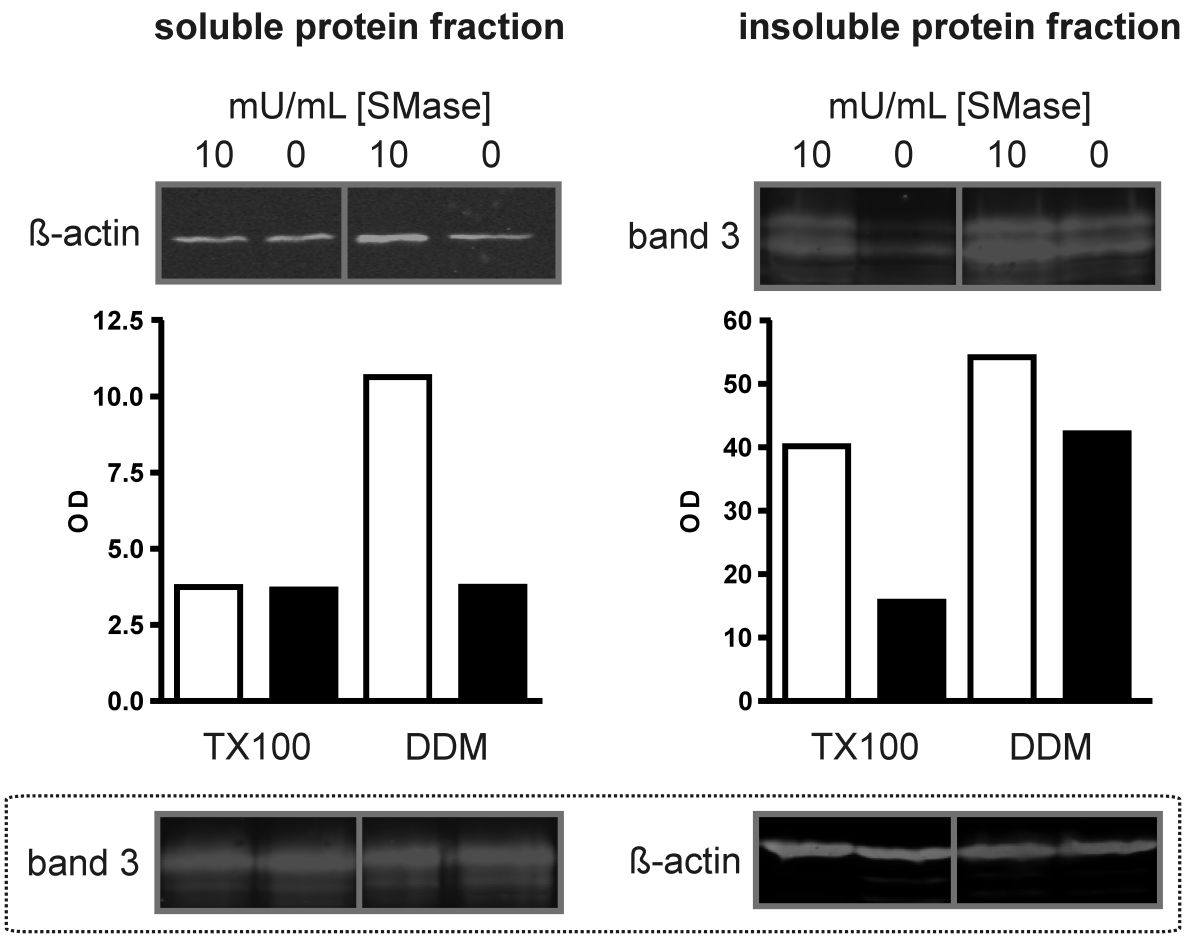

Figure S2 – Differential membrane protein extraction of SMase-treated erythrocyte membrane fractions. Erythrocytes were treated with 10 mU/mL SMase at 37ºC for one hour. Membrane extractions were performed using extraction buffers containing either Triton X-100 or dodecyl maltoside. After SDS-PAGE of the soluble and insoluble protein fractions, immunoblot analysis was performed using monoclonal antibodies against band 3 (red) and β-actin (green). The blots were analyzed and the mean optical density (OD) of the bands was determined using the Odyssey Infrared Imaging System. Band 3 in the soluble protein fraction and β-actin in the insoluble protein fraction acted as loading controls.

Supplemental movies S1, S2 and S3 are available at Cell Death & Disease's website (http://www.nature.com/cddis)

5

Inflammation-associated changes in the erythrocyte membrane lipid composition and organization

Sip Dinkla[1,2*], Lucas T. van Eijk[3*], Beate Fuchs[4], Jürgen Schiller[4], Irma Joosten[2],

Roland Brock[1], Peter Pickkers[3] and Giel J.C.G.M. Bosman[1]

*These authors contributed equally to this work

[1]Department of Biochemistry, [2]Department of Laboratory Medicine – Laboratory of Medical Immunology,

[3]Department of Intensive Care Medicine, Radboud University Medical Centre,

[4]Medical Department, University of Leipzig

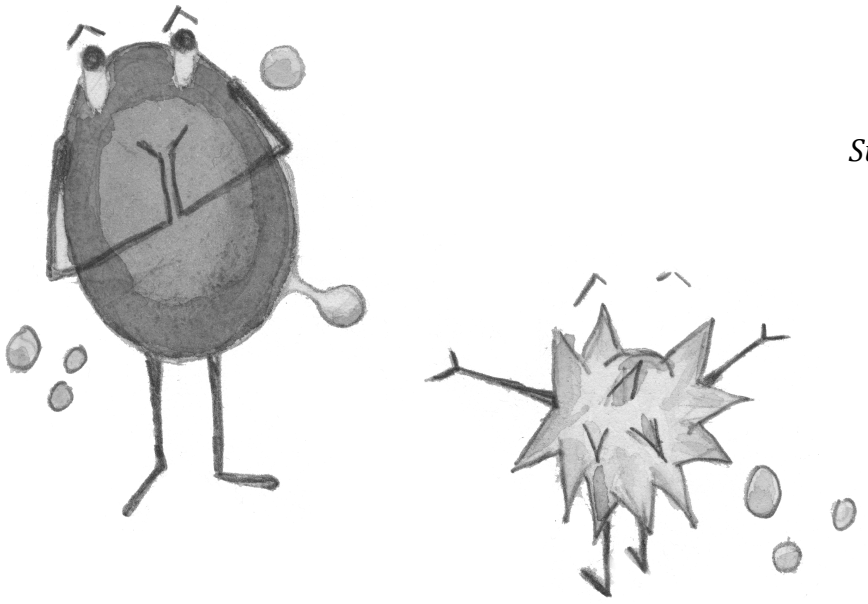

Submitted for publication

Abstract

Objective: Reduced erythrocyte survival and deformability contribute to the "anemia of inflammation" observed in severe sepsis. Erythrocyte structure and function depend on plasma membrane lipid composition and organization. We therefore aimed to determine whether this composition is affected by altered lipid metabolism in the circulation during systemic inflammation.

Design: Case control study.
Setting: Intensive care department of a university hospital.
Patients and Subjects: 10 patients with septic shock, 10 healthy volunteers subjected to experimental endotoxemia, and 10 healthy controls.

Measurements and Main Results: A sensitive matrix-assisted laser desorption and ionization time-of-flight mass spectrometry method was used to investigate erythrocyte membrane lipid content. Incubation of erythrocytes of healthy blood group O, Rhesus-negative donors with plasma from patients with septic shock resulted in membrane phosphatidylcholine hydrolysis into lysophosphatidylcholine (LPC). Ceramide or lysophospholipids other than LPC were not observed in this study. Plasmas taken during experimental human endotoxemia did not induce LPC formation. Secretory phospholipase A_2 IIA was enhanced in all patient plasmas and plasmas from endotoxin-treated subjects, but could not be correlated to its ability to generate LPC in erythrocytes. Erythrocyte phosphatidylserine exposure increased during experimental endotoxemia.

Conclusions: Erythrocyte membrane lipid remodeling reflected by enhanced LPC formation and PS exposure occurs during systemic inflammation in a secretory phospholipase A_2 IIA-independent manner.

Introduction

In patients with inflammation, anemia is associated with a poor disease outcome. Next to changes in systemic iron homeostasis and defective erythropoiesis [1,2], reduced erythrocyte lifespan is a cause of “anemia of inflammation” [3-5]. This condition is common in patients suffering from sepsis [6]. Erythrocyte shape, deformability, and aggregability were shown to be altered in these patients [7,8]. Reduced erythrocyte deformability may contribute to the microcirculatory alterations that are linked with a poor disease outcome in septic patients [8], and to untimely erythrocyte removal by sequestration in the spleen [9].

Erythrocyte structure and function are dependent on plasma membrane lipid composition [10,11], as exemplified by the altered erythrocyte morphology and survival in patients with hemoglobinopathies and various liver diseases, which are caused by a disturbed membrane lipid asymmetry and lipid metabolism, respectively [11,12]. Also in patients with sepsis, membrane lipid composition may contribute to alterations in erythrocyte function. Indeed, incubation of erythrocytes from healthy volunteers with plasma of septic patients was found to induce phosphatidylserine (PS) exposure and membrane ceramide formation [13], both of which have functional consequences for the erythrocyte [10,14].

Phospholipids constitute the majority of the erythrocyte plasma membrane lipids, with the glycerophospholipid (GPL) phosphatidylcholine (PC) and the sphingolipid sphingomyelin (SM) dominating the outer membrane of the lipid bilayer [10,11]. Secretory phospholipase A_2 ($sPLA_2$) and sphingomyelinase (SMase) catalyze the hydrolysis of GPLs into lysophospholipids (LPLs) and fatty acids, and SM into ceramide and choline, respectively. The activity of both lipases is enhanced in the plasma of patients suffering from sepsis [15,16], and the lipids they generate have been shown to play a role in the pathology of various inflammatory diseases [17]. Erythrocyte deformability and survival were shown to be negatively influenced by $sPLA_2$ and SMase or by the direct incorporation of their lipid products *in vitro* [9,14,18,19].

The aim of the current study was to investigate the involvement of lipase activity in the erythrocyte-related pathophysiology during systemic inflammation in patients with sepsis and in experimental human endotoxemia. Using a sensitive matrix-assisted laser desorption and ionization time-of-flight (MALDI-TOF) mass spectrometry (MS) approach, we investigated the lipid composition of erythrocytes after incubation with the plasma of patients suffering from septic shock and with plasma of subjects participating in a human experimental endotoxemia model. A mechanistic explanation for the observed changes was explored by measuring plasma $sPLA_2$ IIA levels and erythrocyte PS exposure.

Methods

Septic Patients

Four mL of lithium–heparin anticoagulated (Vacutainer, BD Biosciences, San Jose, CA, USA) blood was collected from 10 septic shock patients, residing in the department of Intensive Care Medicine of the Radboud University Medical Centre, Nijmegen, the Netherlands. Septic shock was defined as having two or more systemic inflammatory response syndrome (SIRS) criteria [20], in combination with a proven or suspected infection and the need for vasopressor therapy following adequate fluid resuscitation. The study has been carried out in the Netherlands in accordance with the applicable rules concerning the review of research ethics committees and informed consent. Blood from all patients was drawn within the first 24 hours after the start of vasopressor therapy. Plasma was obtained by centrifugation (2000×g, 4°C) under sterile conditions. Erythrocytes were isolated using Ficoll (GE Healthcare, Waukesha WI, USA) density centrifugation and washed with calcium-free Ringer's solution (125 mM NaCl, 5 mM KCl, 1 mM $MgSO_4$, 32 mM HEPES, 5 mM glucose, pH 7.4). Plasma and erythrocyte membranes were snap-frozen and stored at -80°C following isolation.

Healthy volunteers

Ten healthy volunteers donated 4 mL of lithium–heparin anticoagulated blood to serve as control, after having provided written informed consent to the study protocol. Plasma was obtained by centrifugation (2000×g, 4°C) under sterile conditions. Erythrocytes were isolated and processed as described above.

Human Endotoxemia Trial

Subjects: In order to investigate the effects of systemic inflammation in a controlled environment, a model of experimental human endotoxemia was used. This study was part of a larger endotoxemia trial that was designed to investigate the effect of iron administration and iron chelation on the innate immune response in healthy males *(clinicaltrials.gov identifier: NCT01349699)*. In order to prevent confounding by the different pharmacological interventions, our analyses were performed on data of the ten placebo-LPS-treated subjects only. The trial was approved by the local ethics committee, and carried out according to GCP standards and the declaration of Helsinki. All volunteers gave written informed consent and had a normal physical examination, electrocardiography, and routine laboratory values before the start of the experiment. Volunteers did not take any prescription drugs and refrained from caffeine and alcohol intake 24 h prior to endotoxemia. The subjects were admitted to our clinical research unit on the day of the experiment and were kept under observation during 10 h.

Experimental Protocol: A detailed protocol of the human endotoxemia trial was previously described [21]. Briefly, a venous cannula was placed for administration of fluids to ensure an optimal hydration status [22], and an arterial catheter was placed in the radial artery to permit the continuous measurement of blood pressure, as well as blood drawing. Heart rate, intra-arterial blood pressure, and temperature were monitored throughout the experiment and the subjects were supervised at all time. They received 1.5 L 2.5% glucose/0.45% saline solution in 1 h immediately before LPS infusion (pre-hydration), followed by 150 mL/h until 6 h after LPS infusion, and 75 mL/h until the end of the experiment. E. coli endotoxin (Escherichia coli O:113, Clinical Center Reference Endotoxin, National Institute of Health, Bethesda, MD) was reconstituted in 0.9% NaCl for injection and vortex-mixed for at least 10 min. At t=0 hours, 2 ng/kg E. coli endotoxin was injected intravenously. Blood was collected at various time points thereafter. Plasma from lithium–heparin anticoagulated (Vacutainer, BD Biosciences, San Jose, CA, USA) blood was obtained by centrifugation, snap-frozen and stored at -80°C under sterile conditions. Erythrocytes from 4 mL of EDTA anticoagulated (Vacutainer, BD Biosciences, San Jose, CA, USA) blood were isolated using Ficoll (GE Healthcare, Waukesha WI, USA) density centrifugation and washed with calcium-free Ringer for flow cytometry analysis within 4 hours after collection.

$sPLA_2$ IIA and Cytokine Measurements

Plasma $sPLA_2$ IIA concentrations were determined using a $sPLA_2$ ELISA assay ($sPLA_2$ (human Type IIA) EIA Kit, Cayman Chemical, Ann Arbor, MI, USA) according to the manufacturer's instructions. Plasma concentrations of tumour necrosis factor (TNF)-α and interleukin-6 (IL-6) were determined at various time points using a simultaneous Luminex assay (Bio-Plex cytokine assay, Bio-Rad, Hercules, CA, USA) according to the manufacturer's instructions.

Erythrocyte isolation from blood group O, Rhesus negative donors

Healthy volunteer EDTA-anti-coagulated (Vacutainer, BD Biosciences, San Jose, CA, USA) blood was collected from several blood group O, Rhesus-negative donors, and erythrocytes were isolated using Ficoll (GE Healthcare, Waukesha WI, USA) density centrifugation.

Plasma incubation

The allogeneic blood group O, Rhesus-negative erythrocytes were incubated in the plasma of patients or healthy volunteers at 10% hematocrit in a final volume of 500 µL, for 20 h at 37°C with gentle agitation. Incubation of the erythrocytes with calcium-containing (2.5 mM $CaCl_2$) Ringer with or without bee venom $sPLA_2$ type III (Cayman Chemical, Ann Arbor, MI, USA) served as positive and negative controls for ($sPLA_2$-induced) lysophospholipid formation, respectively. The absorption at 415 nm of the supernatant was determined to

assess hemolysis. After incubation, the erythrocytes were washed with calcium-free Ringer prior to flow cytometry and membrane lipid analyses.

Flow cytometry

Erythrocytes were probed for PS exposure by incubation with Annexin V-FLUOS (Roche, Basel, Switzerland; 1/25) for 1 h at room temperature in calcium-containing Ringer. PE conjugated anti-CD235a antibody (clone KC16, Beckman Coulter, Brea CA, USA; 1/100) was included as an erythrocyte marker. Flow cytometry was performed on a FACSCalibur system (BD Biosciences, Franklin Lakes NJ, USA) using Cellquest Pro software version 6.0. Per sample, 100,000 cells were measured and data analysis was performed using Cyan Summit software version 4.3.

MALDI-TOF MS detection of membrane lipids

Erythrocytes (50 µL) were lysed and the lysate membranes were washed repeatedly with lysis buffer (10 mM HEPES, 1 mM EDTA, 1 m EGTA, pH 8.0) by centrifugation at 21,000×g for 10 min to remove free hemoglobin. Membrane pellets were resuspended and transferred to glass tubes and 500 µL methanol and 250 µL dichloromethane were added. After vortexing, another 250 µL dichloromethane and 400 µL 0.5% acetic acid were added and vortexed once more. After 10 min centrifugation at 800×g, the bottom dichloromethane layer was isolated. Residual lipids were extracted from the aqueous layer by extraction with 250 µL dichloromethane. The two dichloromethane fractions were pooled and the solvent was evaporated. For some plasmas, lipids were isolated directly from 100 µL plasma using the method described for membrane pellets above. The lipid fraction was analyzed by positive-ion (and in selected cases also negative-ion) MALDI-TOF MS as described previously [23]. Shortly, the lipid extract was mixed 1:1 (v/v) with the matrix solution (0.5 M 2,5-dihdyroxybenzoic acid in methanol) and 1 µl of this mixture was directly applied onto the MALDI target. For negative ion mass spectra, 9-aminoacridine (9-AA) (Fisher Scientific GmbH, Nidderau, Germany) as 10 mg/mL solution in 60/40 (v/v) isopropanol/acetonitrile [24] was used and mixed 1:1 (v/v) with the samples of the lipid extracts.

All MALDI-TOF mass spectra were acquired on an Autoflex I mass spectrometer (Bruker Daltonics, Bremen, Germany) with ion reflector. The system utilized a pulsed 50 Hz nitrogen laser, emitting at 337 nm. The extraction voltage was 20 kV and gated matrix suppression was applied to prevent the saturation of the detector by matrix ions. All spectra were acquired in the reflector mode using delayed extraction conditions. Peak identities were additionally confirmed by recording post source decay spectra as previously described [25]. Quantitative data can be obtained with a standard deviation of ±10% [26].

Thin layer chromatography (TLC)

Lipid extracts were applied onto high performance TLC silica gel 60 plates (10×10 cm in size, on aluminum backs; Merck, Darmstadt, Germany), using a Linomat 5 device (CAMAG, Berlin, Germany), and developed in vertical TLC chambers with $CHCl_3$, ethanol, water, and triethylamine (30:35:7:35, v/v/v/v) as the solvent system. Lipids were visualized by spraying the plate with primuline (Direct Yellow 59) as previously described [27]. Upon illumination with UV light (366 nm), individual lipid classes were detected as colored spots. These spots were assessed using a digital image system in combination with the program Argus X1 (BioStep, Jahnsdorf, Germany). MALDI mass spectra were recorded directly from the TLC plate as described before [28].

Statistical analysis

Differences in the percentages of total membrane LysoPC (LPC) between two groups were determined using Fisher's exact test. A repeated measures one-way ANOVA in combination with Tukey's post-test was used to assess changes in erythrocyte PS exposure over time for the human endotoxemia model. Differences between two groups of continuous data were determined using the Mann Whitney U test. The relation between two parameters was assessed by performing a Pearson correlation. Reported values are two-sided, and a *p* value of <0.05 was used to assess statistical significance.

Results

Demographic characteristics

Characteristics of the septic patients are provided in Table 1. Characteristics of the healthy subjects who participated in the endotoxemia trial and the healthy volunteers that served as controls for the septic patient group are presented in Table 2.

Enhanced LPC generation in erythrocytes incubated with septic patient plasma

We investigated the changes in membrane lipid composition in detail by positive-ion MALDI-TOF MS analysis of allogeneic blood group O, Rhesus-negative erythrocytes incubated overnight with plasma of healthy volunteers and of patients suffering from septic shock. This *ex vivo* approach allowed us to mimic erythrocyte lipid remodeling as it would occur in the circulation, without losing affected erythrocytes due to hemolysis and clearance. The number of PS-exposing erythrocytes after incubation, assessed using Annexin V staining and flow cytometry, was within the normal range observed *in vivo* [29] for both patient (0.39%±0.11) and healthy volunteer (0.43%±0.07) plasma. A small degree of hemolysis (<1%) was observed after incubation (data not shown). This low degree of PS exposure and hemolysis

for control plasmas indicates that the assay procedure did not cause cellular stress, a feature which might have influenced the LPC formation *ex vivo*. These data also demonstrate that patient plasma hardly induced any PS exposure.

Table 1. Demographic characteristics of septic patients

Pt Nr.	Sex (M/F)	Age (years)	Diagnosis	APACHE II	Hb (mmol/l)	Transfusion history
1	V	54	pneumosepsis	28	4.9	None
2	M	68	abdominal sepsis after intestinal ischemia		5.1	Day before blood drawing : 3 thrombocyte transfusions 3 plasma transfusions Day of blood drawing: 2 thrombocyte transfusions 8 plasma transfusions 9 erythrocyte transfusions
3	V	81	abdominal sepsis in ulcerative colitis	28	6.0	None
4	M	59	infected hip prosthesis		4.9	Day before blood drawing : 1 erythrocyte transfusion Day of blood drawing: 1 erythrocyte transfusion
5	M	75	cholangitis	23	8.6	Day before blood drawing : 2 thrombocyte transfusions 2 plasma transfusions Day of blood drawing: 1 thrombocyte transfusion
6	M	82	abdominal sepsis after intestinal ischemia	23	7.5	Day before blood drawing : 3 erythrocyte transfusions
7	M	34	pneumosepsis	14	7.8	None
8	M	84	urosepsis	16	6.3	None
9	V	51	pneumosepsis	27	5.9	None
10	V	65	toxicodermia	23	6.6	None
Mean ± SD		**66.3 ± 16.1**		**22.8 ± 5.3**	**6.4 ± 1.3**	

Table 2: Characteristics of healthy subjects

	Endotoxemia subjects	Healthy volunteers
N	10	10
Age (years ± SD)	22.7 ± 2.8	34.7 ± 14.8
Sex (M/F)	10 / 0	8 / 2

Using the positive-ion mode, both lysophosphatidylcholine (LPC) and ceramide species can be readily detected in plasma membrane lipid extracts [30]. While no LPC or ceramide could be observed after the incubation of erythrocytes in Ringer's solution, incubation with septic patient plasma, and to a lesser extent with healthy volunteer plasma, caused the formation of LPC, but not of ceramide (Figure 1A). Although reactive oxygen species (ROS) can also generate LPLs, these ROS-produced LPLs were not observed in our study, even though they are readily detectable by means of MS and easily discernible from other LPLs and PLs [31]. The observed LPC percentages were within the same range as observed after incubating the erythrocytes of different blood donors with 20 and 100 ng/mL $sPLA_2$ (Figure 1B). Additionally, the results suggest an erythrocyte donor-dependent variation in the susceptibility to $sPLA_2$-induced LPC generation (Figure 1B).

Compared to that of the healthy volunteers, LPC formation was significantly enhanced in samples treated with plasma from septic patients (Figure 1C). This suggests that the latter possessed enhanced phospholipase activity that might affect erythrocytes in the circulation of patients with sepsis. No LPC could be detected in the healthy volunteer and patient erythrocytes.

The percentage of LPC in the total PC pool in the plasma itself was lower for the septic patients (0.63±0.35, n=3), than for the healthy volunteers (4.91±0.49, n=3), confirming earlier observations [32]. This observation makes incorporation of LPC from the plasma into the erythrocyte membrane an unlikely explanation for the observed increase after incubation with patient plasma.

Enhanced LPC generation does not correlate to the $sPLA_2$ IIA plasma concentration

Phospholipases of the $sPLA_2$ family are the plasma components that generate LPC and other lysophospholipids *in vivo* [33]. Only $sPLA_2$ type IIA is upregulated during sepsis [34], making its lipase activity a primary candidate responsible for the observed LPC formation. Therefore, we determined the $sPLA_2$ IIA concentrations in the patient and control plasmas to assess their sepsis-associated involvement in observed LPC generation in erythrocytes.

All septic patients had enhanced plasma $sPLA_2$ IIA concentrations (50.2-1654.0 ng/mL) as compared to the healthy volunteers (1.3-9.3 ng/mL), corroborating earlier observations (Figure 1D) [15,34]. However, there was no correlation between the observed degree of LPC formation and the $sPLA_2$ IIA concentration in the septic patient plasmas (Figure 1E), indicating other causes for the enhanced generation of LPC. Also, no correlations were observed between percentage LPC and $sPLA_2$ IIA concentration with the following known patient parameters; sex, age, weight, length, focus of infection, APACHE II, temperature,

mean arterial pressure, heart rate, fluid balance, Glasgow coma scale, PaO_2, FiO_2, thrombocytes, bilirubin, creatinine and leukocytes.

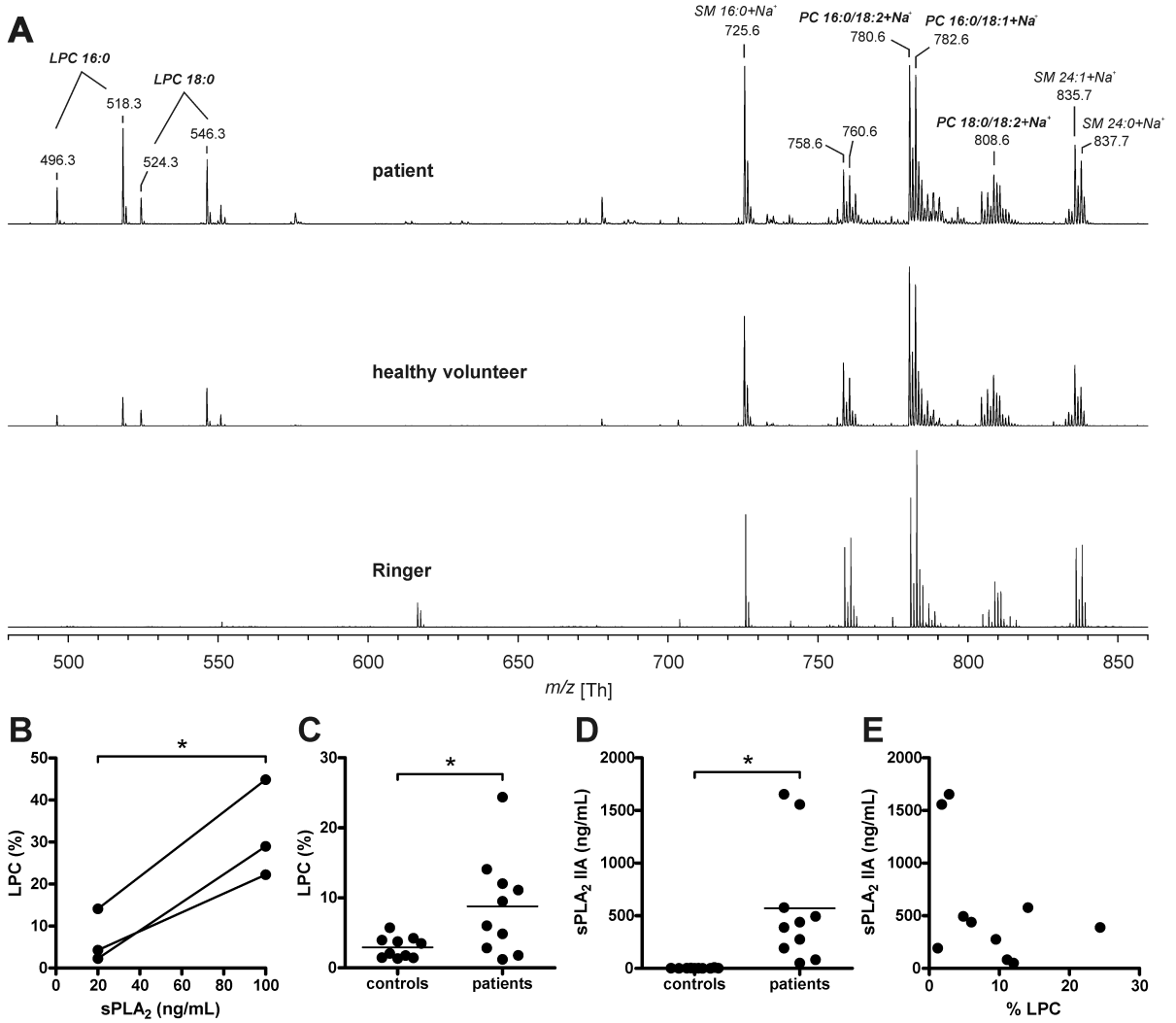

Figure 1. Septic patient plasma-induced LPC formation in the erythrocyte membrane. Three representative examples of positive-ion MALDI-TOF MS spectra of membrane lipid extracts of allogeneic erythrocytes incubated overnight at 37°C with i) plasma from septic patients, ii) plasma from healthy controls, and iii) Ringer solution (A). All peaks are labeled according to their mass-to-charge (*m/z)* ratios and assignments of the most prominent peaks are given directly in the figure. The percentage of hydrolyzed PC (LPC) was determined by comparing the proton and sodium adducts of LPC 16:0 (*m/z* 496.3 and 518.3), to the combined pool of LPC 16:0 and PC 16:0/18:2 (*m/z* 758.6 and 780.6). LPC formation after incubation of erythrocytes of three different donors with Ringer containing 20 and 100 ng/mL $sPLA_2$ (B). LPC formation after overnight incubation with plasma from 10 septic patients and 10 healthy controls (C). The human $sPLA_2$ IIA concentration in all plasmas was determined using an ELISA (D). The $sPLA_2$ IIA concentrations measured in patients did not correlate (r = -0.44, P = 0.22) to the observed LPC percentage (E). Means are shown and *P<0.05. Lipid abbreviations: LPC = lysophosphatidylcholine, PC = phosphatidylcholine, SM = sphingomyelin.

LPC generation and sPLA$_2$ IIA plasma concentration in human endotoxemia

Sepsis is a medical condition that encompasses a highly heterogeneous group of clinical disorders, varying with origin of infection, bacteriology, and progression [35]. In order to overcome this heterogeneity and to address to which extent endotoxemia affects erythrocyte lipid metabolism, we used a human endotoxemia model to study the LPC formation in erythrocytes *ex vivo*. Subjects enrolled in the trial were infused with 2 ng/kg LPS, and blood samples were drawn just prior to, and 8 hours after the administration. Allogeneic blood group O, Rhesus-negative erythrocytes were then incubated with the obtained plasmas, and their membrane lipid content was analyzed by positive-ion MALDI-TOF MS, and plasma sPLA$_2$ IIA concentrations were measured. The 8-hour time point was based on the previous observation that sPLA$_2$ IIA plasma concentration peaked between 4 and 12 hours after LPS infusion in a comparable endotoxemia trial [36]. sPLA$_2$ IIA concentrations increased in almost all subjects after LPS infusion (Figure 2A), albeit not to the extent observed in the septic patients, corroborating earlier results [36].

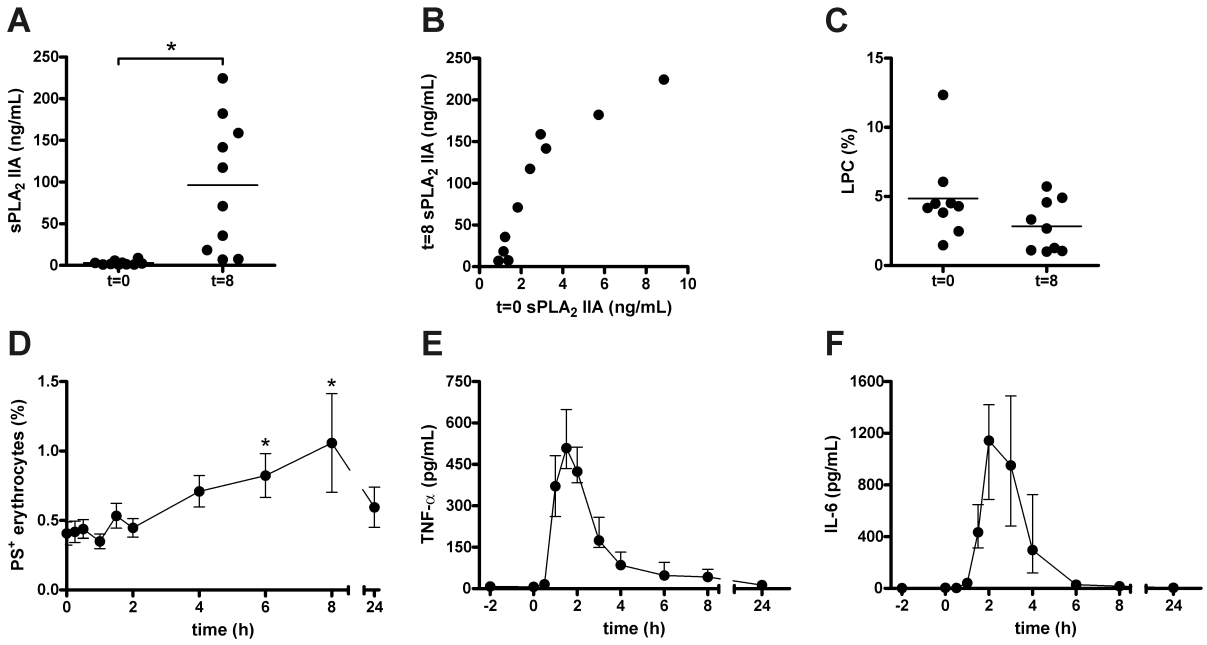

Figure 2. Erythrocyte lipid remodeling during human experimental endotoxemia-induced inflammation. Allogeneic erythrocytes were incubated overnight at 37°C with plasma obtained from 10 endotoxemia trial subjects just prior to (t=0) and eight hours after (t=8) the administration of 2 ng/kg clinical grade LPS. The sPLA$_2$ IIA concentration in all plasma samples was determined using an ELISA (A). The sPLA$_2$ IIA concentrations at t=0 were correlated to the concentrations at t=8 (r = 0.89, P<0.001) (B). The percentage of hydrolyzed PC (LPC) was determined by positive-ion MALDI-TOF MS, by comparing the intensities of the proton and sodium adducts of LPC 16:0 (*m/z* 496.3 and 518.3), with the combined pool of LPC 16:0 and PC 16:0/18:2 (*m/z* 758.6 and 780.6) (C). The percentage of PS-exposing erythrocytes was determined by flow cytometry detection of Annexin V-FLUOS staining (D), and TNF-α (E) and IL-6 (F) plasma concentrations were assessed by Luminex. In panel A, C and D means are shown, *P<0.05, and error bars in panel D represent SEM. In panel E and F median values are shown, and the error bars represent the inter quartile range.

Interestingly, a strong correlation (r = 0.89, P<0.001) was observed between $sPLA_2$ IIA levels before, and 8 hours after LPS infusion (Figure 2B). These data indicate that $sPLA_2$ IIA status at baseline has predictive value for the $sPLA_2$ IIA response upon (LPS-induced) inflammation. Furthermore, $sPLA_2$ IIA concentration at t=0 also correlated (r = 0.68, P=0.032) with the rise in body temperature after LPS infusion.

However, in contrast to that of septic patients, the plasma of the LPS-infused subjects did not induce any additional LPC formation in erythrocytes (Figure 2C). This corroborates our finding that $sPLA_2$ IIA concentration appears not to be related with the observed LPC formation in septic patients (see above).

Erythrocyte PS exposure is induced during the initial phase of human endotoxemia

In vivo, LPC is rapidly converted into lysophosphatidic acid (LPA), a molecule that was found to induce the exposure of the removal signal PS in erythrocytes [37]. The initial observation that septic patient plasmas induce LPC generation in erythrocytes, therefore, led us to investigate erythrocyte PS exposure in the individuals enrolled in the endotoxemia trial.

A significant increase in the number of PS-exposing erythrocytes was observed 6 and 8 hours after LPS infusion, which had returned to baseline level at t=24 hours (Figure 2D). This increase in PS-exposing erythrocytes was observed after the onset of inflammation, as was determined by monitoring TNF-α (Figure 2E) and IL-6 (Figure 2F) plasma levels. These data show that acute systemic inflammation induces plasma membrane lipid remodeling in a subpopulation of erythrocytes, possibly rendering them susceptible to $sPLA_2$ IIA in the circulation *in vivo*. However, it does not explain the LPC formation observed in erythrocytes incubated with plasma from septic patients. A strong positive correlation (r = 0.91, P=0.002) was observed between erythrocyte PS exposure before, and 6 hours after LPS infusion. These data indicate that erythrocyte PS exposure at baseline has predictive value for the tendency of erythrocyte to expose PS during (LPS-induced) inflammation.

The observed lipase activity selectively targets PC in the erythrocyte

$sPLA_2$s do not only hydrolyze PC, but also other glycerophospholipids such as PS and phosphatidylethanolamine (PE), albeit with various affinities depending on the $sPLA_2$ type [33]. Therefore, we evaluated the hydrolysis of other GPLs in the erythrocyte membrane by performing negative-ion MALDI-TOF MS and TLC analysis. Allogeneic erythrocytes were incubated with septic patient plasma selected for its potency to generate LPC. Indeed, high LPC levels were observed again by both positive-ion MALDI-TOF MS (Figure 3A) and TLC (Figure 3B).

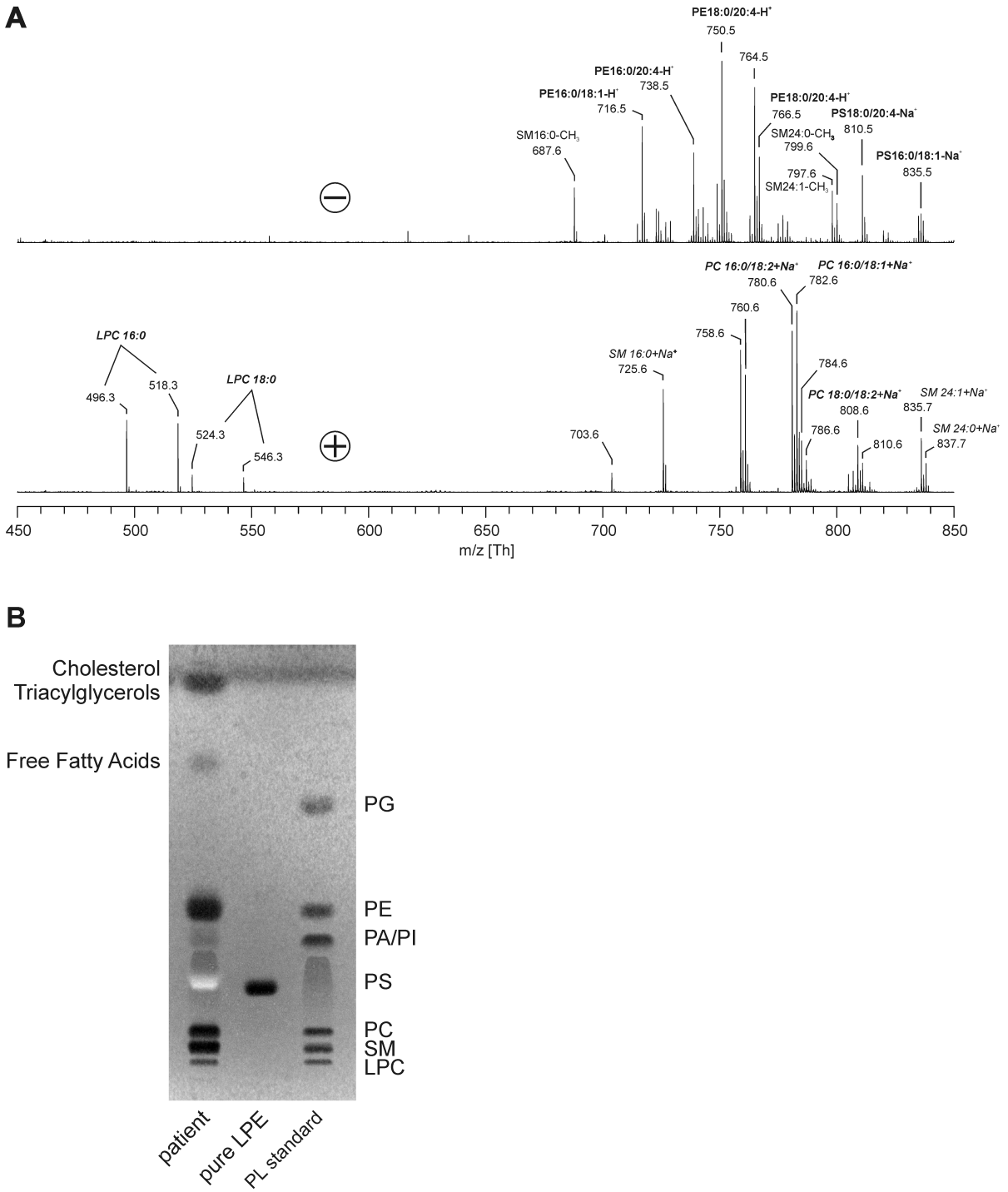

Figure 3. Detection of lysophospholipids. Allogeneic erythrocytes were incubated overnight at 37°C with plasma of a septic patient. Both positive and negative-ion MALDI-TOF MS of isolated membrane lipids were performed (A). All peaks are labeled according to their *m/z* ratios. Note that there are intense signals of LPC, but no signals of other LPL species. A TLC was performed using the identical lipid extract (B) to verify the absence of LPL other than LPC. Lipid standards were included to delineate the different lipid species. The pale white band in the TLC is most probably caused by the presence of small amounts of hemoglobin that could not be completely removed during the extraction process [38]: due to its aromatic character it has a high probability to interfere with the absorption of the primuline dye. Lipid abbreviations: LPC = lysophosphatidylcholine, LPE = lysophosphatidylethanolamine, PA = phosphatidic acid, PC = phosphatidylcholine, PE = phosphatidylethanolamine, PG = phosphatidylglycerol, PI = phosphatidylinositol, PL = phospholipid, PS = phosphatidylserine, SM = sphingomyelin.

However, other LPLs such as LysoPE (LPE), LysoPS, and lysophosphatidylinositol could not be detected (Figure 3B). Incubation in Ringer that had been spiked with recombinant $sPLA_2$ was also unable to generate LPLs other than LPC (data not shown). Most likely the plasma phospholipases are unable to attack these GPLs, as they reside in the inner leaflet of the plasma membrane.

In summary, we here show that plasma of septic patients caused enhanced LPC formation in erythrocytes *ex vivo*. This was not observed for plasma from LPS-infused subjects during an endotoxemia trial. Interestingly, erythrocyte membrane lipid remodeling was present in the form of PS exposure in the LPS-infused subjects. LPC formation could not be correlated to $sPLA_2$ IIA for either the patients or the LPS-infused subjects.

Discussion

Reduced erythrocyte survival and deformability contribute to the “anemia of inflammation” and microcirculatory problems observed in patients suffering from sepsis [8]. Plasma membrane lipid composition is essential for erythrocyte homeostasis [10,11], and changes in lipid composition and/or distribution might explain altered erythrocyte characteristics in sepsis [7,8,13]. In the human body, the $sPLA_2$ family of phospholipases is the principal catalysts for the hydrolysis of GPLs into LPLs and fatty acids, while SMase catalyzes the hydrolysis of SM into ceramide and phosphocholine. The activity of both enzymes is enhanced in patients suffering from severe sepsis [15,16], and LPLs and ceramide have been shown to play a role in the pathology of various inflammatory diseases [17]. $sPLA_2$ has attracted particular attention as a therapeutic target in atherosclerosis due to its direct involvement in the development of this disease by modifying LDL and HDL [33,39]. In the current study we investigated the involvement of $sPLA_2$ lipases in erythrocyte-mediated pathophysiology during systemic inflammation.

In this study we show that the plasma of patients with severe sepsis triggers erythrocyte membrane lipid remodeling illustrated by enhanced LPC formation. $sPLA_2$ IIA is the only $sPLA_2$ family member of which the secretion is significantly promoted in the circulation during sepsis [34], which points towards its involvement in the observed LPC generation in erythrocytes. Indeed, we found $sPLA_2$ IIA to be strongly enhanced in our septic patient plasmas. However, the plasma $sPLA_2$ IIA concentration did not correlate with the amount of LPC generated in the erythrocytes. This might be due to the relatively small group size and the large heterogeneity of the patients studied, as patients with different causes of sepsis

were included, and nearly all patients had different co-morbidities. The heterogeneity in the causes and clinical presentation of sepsis [35] is exemplified by our observation that only five out of ten septic patient plasmas induced enhanced LPC formation. Interestingly, we did not detect an increase in LPC generation using the plasmas obtained during experimentally induced endotoxemia, even though inflammation and a subsequent rise in plasma $sPLA_2$ IIA were observed. Thus, although the experimentally-induced acute endotoxemia is a useful model for several aspects of sepsis, it does not fully mimic sepsis at the erythrocyte level. This could be ascribed to the use of a model that mimics only the initial phase of septic shock. Alternatively, the enhanced lipase activity in the septic patients might be mediated by inflammatory pathways other than the Toll-like receptor-4 pathway that is triggered by LPS.

The absence of enhanced LPC formation in the endotoxemia model also points towards the involvement of other $sPLA_2$s, and/or the requirement of additional plasma factors to direct $sPLA_2$ IIA activity towards erythrocytes. Alternatively, the lack of $sPLA_2$ IIA involvement might be due to the strong binding preference of this enzyme for anionic GPLs such as PS, which in healthy cells primarily reside in the inner leaflet of the plasma membrane. In contrast, $sPLA_2$ type V and X exhibit a much higher preference for PC as a substrate than other members of the $sPLA_2$ family, and are thus able to attack healthy cells [33]. This makes type V and X $sPLA_2$ possible candidates responsible for the observed LPC generation in our study, even though the concentration of these enzymes does not increase in the circulation during sepsis [34]. Transgenic $sPLA_2$ X mice have revealed that the conversion of a secreted inactive $sPLA_2$ X pro-peptide into the catalytically active enzyme is promoted during inflammation [40], effectively enhancing the activity of pre-existing $sPLA_2$ X. Other factors that could play a role are plasma phospholipids, mainly in the form of lipoproteins, which are reduced in patients with severe sepsis [41]. This reduction was also observed during experimentally induced human endotoxemia, but only started appearing 12 hours after infusion of LPS [42]. Since $sPLA_2$s are able to attack PC in lipoproteins [43,44], the readily accessible plasma lipoproteins might compete with PC in erythrocytes for $sPLA_2$ binding.

$sPLA_2$ IIA has been implicated in the activation of the inflammatory processes responsible for multiple organ failure in sepsis [45,46], and its plasma level correlated with the rate of mortality [15,47]. During the human endotoxemia trial, we noticed that $sPLA_2$ IIA status at baseline was predictive for the $sPLA_2$ IIA response upon LPS infusion. This suggests that there is a pre-existing inter-individual variability in the $sPLA_2$ IIA response to systemic inflammation. It remains to be elucidated whether this can be harnessed as a predictive biomarker for lipid remodeling/signaling in response to systemic inflammation.

The induction of LPC formation through plasma of the sepsis patients, as shown in our current study, points towards the involvement of membrane lipid remodeling in this process, and could potentially explain enhanced erythrocyte clearance in patients with severe sepsis. Therefore, we propose to assess erythrocyte clearance, removal markers, and membrane lipid remodeling and hydrolysis in future studies.

In contrast to earlier findings [13], we did not observe the formation of ceramide after erythrocyte incubation with septic patient plasma. This discrepancy is probably caused by the use of different techniques to detect ceramide in the erythrocyte membrane. Kempe et al. combined a monoclonal mouse anti-ceramide IgM (clone 15B4) with flow cytometry to detect ceramide in erythrocytes [13]. Unfortunately, this antibody is aspecific as it does not only detect ceramide, but also recognizes phosphatidylcholine and sphingomyelin [48]. Furthermore, we have previously noticed that the reactivity of this antibody with the erythrocyte also depends on the membrane organization [14]. In contrast, the use of our current MS method enables both specific and sensitive detection of different ceramide species in membrane lipid preparations [30].

The absence of LPLs other than LPC in our study can be explained by the inability of the responsible plasma lipases to attack their substrate GPLs, since they primarily reside in the inner leaflet of the plasma membrane [10,11]. Enhanced LPC formation contributes to inflammatory signaling in sepsis [17], and LPC acts as a substrate for lysophospholipase D and LPC acetyltransferase, to produce the pro-inflammatory lipid mediators (LPA) and platelet-activating factor [49]. Enhanced activity of these enzymes might explain why LPC plasma levels are reduced in septic patients [32]. LPA has been suggested to open a calcium channel in the erythrocyte membrane [50], resulting in exposure of the removal signal PS and subsequent microparticle generation [37].

We observed an increase in the percentage of PS-exposing erythrocytes in healthy subjects after LPS infusion. PS exposure on the outer leaflet of the plasma membrane alters rheologic and hemostatic properties of the erythrocyte [10], and is a recognition signal for their removal [51-53]. Fever is one of the hallmarks of systemic inflammation, which is known to enhance phagocytic activity [54]. The negative correlation between PS exposure and body temperature indicates increased phagocytic activity in our patients. Since PS-exposing erythrocytes are rapidly removed from the circulation, the increase in PS-exposing erythrocytes observed in our endotoxemia trial likely underrepresents the actual number of erythrocytes that expose PS after LPS infusion. In addition, PS exposure makes erythrocytes sensitive to $sPLA_2$ IIA-mediated GPL hydrolysis *in vitro* [19,55], promoting further membrane lipid remodeling. In addition, significant LPC buildup in the erythrocyte

membrane can induce hemolysis [19,56], alter morphology, induce microparticle release, and reduce deformability leading to splenic retention *ex vivo*.[9] However, since LPC is quickly metabolized by lysophospholipases and acyltransferases [57], it is uncertain whether such a build-up will occur *in vivo*. Both the removal and/or metabolism hypotheses fit with our inability to detect LPC in the erythrocytes taken from the patients with septic shock.

PS exposure and PC hydrolysis in the membrane may thus contribute to the reduced erythrocyte lifespan in "anemia of inflammation" [3-5]. This might also impact erythrocyte transfusion in septic patients, as blood bank erythrocytes are already more prone to expose PS [58]. This hypothesis is in line with the association of erythrocyte transfusion with increased morbidity and mortality in these patients [6]. Erythrocyte PS exposure just prior to LPS infusion was found to be predictive for the extent of erythrocyte PS exposure upon LPS-induced inflammation. This is in line with our previous finding that PS exposure on stored erythrocytes predicts their extent of PS exposure after the application of osmotic stress [29]. Determining the PS exposure in erythrocyte concentrates might therefore allow the selection of preferred products for the transfusion of septic patients. Since blood bank erythrocytes were also found to be more susceptible for SMase activity, it would be interesting to assess whether this also applies to $sPLA_2$s [14].

Conclusions

We here provide evidence for erythrocyte membrane lipid remodeling during systemic inflammation, as illustrated by enhanced LPC formation and PS exposure during sepsis and endotoxemia. The enhanced LPC formation in erythrocytes could not be attributed to $sPLA_2$ IIA alone, and was not observed in experimentally induced endotoxemia. As membrane lipid remodeling affects erythrocyte integrity, it is necessary to focus future research on elucidating the identity of the phospholipase(s) involved in erythrocyte membrane LPC generation during sepsis. Comparing the endotoxemia model with actual septic patients would be helpful in short-listing relevant candidates, as the enhanced ability to hydrolyze PC is lacking in the endotoxemia model.

References

1 Roy CN. Anemia of inflammation. *Hematology. Am. Soc. Hematol. Educ. Program.* 2010 276-280 (2010).

2 Weiss G, Goodnough LT. Anemia of chronic disease. *N. Engl. J. Med.* 352(10), 1011-1023 (2005).

3 Manodori AB, Kuypers FA. Altered red cell turnover in diabetic mice. *J. Lab Clin. Med.* 140(3), 161-165 (2002).

4 Mitlyng BL, Singh JA, Furne JK, Ruddy J, Levitt MD. Use of breath carbon monoxide measurements to assess erythrocyte survival in subjects with chronic diseases. *Am. J. Hematol.* 81(6), 432-438 (2006).

5 Moldawer LL, Marano MA, Wei H *et al*. Cachectin/tumor necrosis factor-alpha alters red blood cell kinetics and induces anemia in vivo. *FASEB J.* 3(5), 1637-1643 (1989).

6 Napolitano LM, Kurek S, Luchette FA *et al*. Clinical practice guideline: red blood cell transfusion in adult trauma and critical care. *Crit Care Med.* 37(12), 3124-3157 (2009).

7 Piagnerelli M, Boudjeltia KZ, Brohee D *et al*. Alterations of red blood cell shape and sialic acid membrane content in septic patients. *Crit Care Med.* 31(8), 2156-2162 (2003).

8 Reggiori G, Occhipinti G, De Gasperi A, Vincent JL, Piagnerelli M. Early alterations of red blood cell rheology in critically ill patients. *Crit Care Med.* 37(12), 3041-3046 (2009).

9 Safeukui I, Buffet PA, Deplaine G *et al*. Quantitative assessment of sensing and sequestration of spherocytic erythrocytes by the human spleen. *Blood* 120(2), 424-430 (2012).

10 Daleke DL. Regulation of phospholipid asymmetry in the erythrocyte membrane. *Curr. Opin. Hematol.* 15(3), 191-195 (2008).

11 Kuypers FA. Red cell membrane lipids in hemoglobinopathies. *Curr. Mol. Med.* 8(7), 633-638 (2008).

12 Morse EE. Mechanisms of hemolysis in liver disease. *Ann. Clin. Lab Sci.* 20(3), 169-174 (1990).

13 Kempe DS, Akel A, Lang PA *et al*. Suicidal erythrocyte death in sepsis. *J. Mol. Med. (Berl)* 85(3), 273-281 (2007).

14 Dinkla S, Wessels K, Verdurmen WP *et al*. Functional consequences of sphingomyelinase-induced changes in erythrocyte membrane structure. *Cell Death. Dis.* 3 e410 (2012).

15 Guidet B, Piot O, Masliah J *et al*. Secretory non-pancreatic phopholipase A2 in severe sepsis: relation to endotoxin, cytokines and thromboxane B2. *Infection* 24(2), 103-108 (1996).

16 Claus RA, Bunck AC, Bockmeyer CL *et al*. Role of increased sphingomyelinase activity in apoptosis and organ failure of patients with severe sepsis. *FASEB J.* 19(12), 1719-1721 (2005).

17 Wymann MP, Schneiter R. Lipid signalling in disease. *Nat. Rev. Mol. Cell Biol.* 9(2), 162-176 (2008).

18 Lang KS, Myssina S, Brand V *et al*. Involvement of ceramide in hyperosmotic shock-induced death of erythrocytes. *Cell Death. Differ.* 11(2), 231-243 (2004).

19 Neidlinger NA, Larkin SK, Bhagat A, Victorino GP, Kuypers FA. Hydrolysis of phosphatidylserine-exposing red blood cells by secretory phospholipase A2 generates lysophosphatidic acid and results in vascular dysfunction. *J. Biol. Chem.* 281(2), 775-781 (2006).

20 Bone RC. Toward an epidemiology and natural history of SIRS (systemic inflammatory response syndrome). *JAMA* 268(24), 3452-3455 (1992).

21 Pickkers P, Dorresteijn MJ, Bouw MP, van der Hoeven JG, Smits P. In vivo evidence for nitric oxide-mediated calcium-activated potassium-channel activation during human endotoxemia. *Circulation* 114(5), 414-421 (2006).

22 Dorresteijn MJ, van Eijk LT, Netea MG, Smits P, van der Hoeven JG, Pickkers P. Iso-osmolar prehydration shifts the cytokine response towards a more anti-inflammatory balance in human endotoxemia. *J. Endotoxin. Res.* 11(5), 287-293 (2005).

23 Dannenberger D, Suss R, Teuber K, Fuchs B, Nuernberg K, Schiller J. The intact muscle lipid composition of bulls: an investigation by MALDI-TOF MS and 31P NMR. *Chem. Phys. Lipids* 163(2), 157-164 (2010).

24 Sun G, Yang K, Zhao Z, Guan S, Han X, Gross RW. Matrix-assisted laser desorption/ionization time-of-flight mass spectrometric analysis of cellular glycerophospholipids enabled by multiplexed solvent dependent analyte-matrix interactions. *Anal. Chem.* 80(19), 7576-7585 (2008).

25 Fuchs B, Schober C, Richter G, Suss R, Schiller J. MALDI-TOF MS of phosphatidylethanolamines: different adducts cause different post source decay (PSD) fragment ion spectra. *J. Biochem. Biophys. Methods* 70(4), 689-692 (2007).

26 Bresler K, Pyttel S, Paasch U, Schiller J. Parameters affecting the accuracy of the MALDI-TOF MS determination of the phosphatidylcholine/lysophosphatidylcholine (PC/LPC) ratio as potential marker of spermatozoa quality. *Chem. Phys. Lipids* 164(7), 696-702 (2011).

27 White T, Bursten S, Federighi D, Lewis RA, Nudelman E. High-resolution separation and quantification of neutral lipid and phospholipid species in mammalian cells and sera by multi-one-dimensional thin-layer chromatography. *Anal. Biochem.* 258(1), 109-117 (1998).

28 Fuchs B, Schiller J, Suss R, Schurenberg M, Suckau D. A direct and simple method of coupling matrix-assisted laser desorption and ionization time-of-flight mass spectrometry (MALDI-TOF MS) to thin-layer chromatography (TLC) for the analysis of phospholipids from egg yolk. *Anal. Bioanal. Chem.* 389(3), 827-834 (2007).

29 Dinkla S, Peppelman M, van Der Raadt J *et al*. Phosphatidylserine exposure on stored red blood cells as a parameter for donor-dependent variation in product quality. *Blood Transfus.* 12(2), 204-209 (2014).

30 Fuchs B, Suss R, Schiller J. An update of MALDI-TOF mass spectrometry in lipid research. *Prog. Lipid Res.* 49(4), 450-475 (2010).

31 Schober C, Schiller J, Pinker F, Hengstler JG, Fuchs B. Lysophosphatidylethanolamine is - in contrast to - choline - generated under in vivo conditions exclusively by phospholipase A2 but not by hypochlorous acid. *Bioorg. Chem.* 37(6), 202-210 (2009).

32 Drobnik W, Liebisch G, Audebert FX *et al*. Plasma ceramide and lysophosphatidylcholine inversely correlate with mortality in sepsis patients. *J. Lipid Res.* 44(4), 754-761 (2003).

33 Boyanovsky BB, Webb NR. Biology of secretory phospholipase A2. *Cardiovasc. Drugs Ther.* 23(1), 61-72 (2009).

34 Nevalainen TJ, Eerola LI, Rintala E, Laine VJ, Lambeau G, Gelb MH. Time-resolved fluoroimmunoassays of the complete set of secreted phospholipases A2 in human serum. *Biochim. Biophys. Acta* 1733(2-3), 210-223 (2005).

35 Marshall JC. Sepsis: rethinking the approach to clinical research. *J. Leukoc. Biol.* 83(3), 471-482 (2008).

36 de la Llera MM, McGillicuddy FC, Hinkle CC *et al*. Inflammation modulates human HDL composition and function in vivo. *Atherosclerosis* 222(2), 390-394 (2012).

37 Chung SM, Bae ON, Lim KM *et al*. Lysophosphatidic acid induces thrombogenic activity through phosphatidylserine exposure and procoagulant microvesicle generation in human erythrocytes. *Arterioscler. Thromb. Vasc. Biol.* 27(2), 414-421 (2007).

38 Richter G, Schober C, Suss R, Fuchs B, Muller M, Schiller J. The reaction between phosphatidylethanolamines and HOCl investigated by TLC: fading of the dye primuline is induced by dichloramines. *J. Chromatogr. B Analyt. Technol. Biomed. Life Sci.* 867(2), 233-237 (2008).

39 Rosenson RS, Hislop C, McConnell D *et al*. Effects of 1-H-indole-3-glyoxamide (A-002) on concentration of secretory phospholipase A2 (PLASMA study): a phase II double-blind, randomised, placebo-controlled trial. *Lancet* 373(9664), 649-658 (2009).

40 Ohtsuki M, Taketomi Y, Arata S *et al*. Transgenic expression of group V, but not group X, secreted phospholipase A2 in mice leads to neonatal lethality because of lung dysfunction. *J. Biol. Chem.* 281(47), 36420-36433 (2006).

41 Levels JH, Lemaire LC, van den Ende AE, van Deventer SJ, van Lanschot JJ. Lipid composition and lipopolysaccharide binding capacity of lipoproteins in plasma and lymph of patients with systemic inflammatory response syndrome and multiple organ failure. *Crit Care Med.* 31(6), 1647-1653 (2003).

42 Hudgins LC, Parker TS, Levine DM *et al*. A single intravenous dose of endotoxin rapidly alters serum lipoproteins and lipid transfer proteins in normal volunteers. *J. Lipid Res.* 44(8), 1489-1498 (2003).

43 Pruzanski W, Stefanski E, de Beer FC *et al*. Lipoproteins are substrates for human secretory group IIA phospholipase A2: preferential hydrolysis of acute phase HDL. *J. Lipid Res.* 39(11), 2150-2160 (1998).

44 Sato H, Kato R, Isogai Y *et al*. Analyses of group III secreted phospholipase A2 transgenic mice reveal potential participation of this enzyme in plasma lipoprotein modification, macrophage foam cell formation, and atherosclerosis. *J. Biol. Chem.* 283(48), 33483-33497 (2008).

45 Anderson BO, Moore EE, Banerjee A. Phospholipase A2 regulates critical inflammatory mediators of multiple organ failure. *J. Surg. Res.* 56(2), 199-205 (1994).

46 Liu MS, Liu CH, Wu G, Zhou Y. Antisense inhibition of secretory and cytosolic phospholipase A2 reduces the mortality in rats with sepsis*. *Crit Care Med.* 40(7), 2132-2140 (2012).

47 Endo S, Inada K, Nakae H *et al*. Plasma levels of type II phospholipase A2 and cytokines in patients with sepsis. *Res. Commun. Mol. Pathol. Pharmacol.* 90(3), 413-421 (1995).

48 Cowart LA, Szulc Z, Bielawska A, Hannun YA. Structural determinants of sphingolipid recognition by commercially available anti-ceramide antibodies. *J. Lipid Res.* 43(12), 2042-2048 (2002).

49 Karasawa K. Clinical aspects of plasma platelet-activating factor-acetylhydrolase. *Biochim. Biophys. Acta* 1761(11), 1359-1372 (2006).

50 Yang L, Andrews DA, Low PS. Lysophosphatidic acid opens a Ca(++) channel in human erythrocytes. *Blood* 95(7), 2420-2425 (2000).

51 Schroit AJ, Madsen JW, Tanaka Y. In vivo recognition and clearance of red blood cells containing phosphatidylserine in their plasma membranes. *J. Biol. Chem.* 260(8), 5131-5138 (1985).

52 Lee SJ, Park SY, Jung MY, Bae SM, Kim IS. Mechanism for phosphatidylserine-dependent erythrophagocytosis in mouse liver. *Blood* 117(19), 5215-5223 (2011).

53 Kobayashi N, Karisola P, Pena-Cruz V *et al*. TIM-1 and TIM-4 glycoproteins bind phosphatidylserine and mediate uptake of apoptotic cells. *Immunity.* 27(6), 927-940 (2007).

54 Brown GC, Neher JJ. Eaten alive! Cell death by primary phagocytosis: 'phagoptosis'. *Trends Biochem. Sci.* 37(8), 325-332 (2012).

55 Fourcade O, Simon MF, Viode C *et al*. Secretory phospholipase A2 generates the novel lipid mediator lysophosphatidic acid in membrane microvesicles shed from activated cells. *Cell* 80(6), 919-927 (1995).

56 Tanaka Y, Mashino K, Inoue K, Nojima S. Mechanism of human erythrocyte hemolysis induced by short-chain phosphatidylcholines and lysophosphatidylcholine. *J. Biochem.* 94(3), 833-840 (1983).

57 Jackson SK, Abate W, Tonks AJ. Lysophospholipid acyltransferases: novel potential regulators of the inflammatory response and target for new drug discovery. *Pharmacol. Ther.* 119(1), 104-114 (2008).

58 Bosman GJ, Cluitmans JC, Groenen YA, Werre JM, Willekens FL, Novotny VM. Susceptibility to hyperosmotic stress-induced phosphatidylserine exposure increases during red blood cell storage. *Transfusion* 51(5), 1072-1078 (2011).

6

The gateway to understanding microparticles: Standardized isolation and identification of plasma membrane-derived vesicles

Sip Dinkla[1,2], Roland Brock[1], Irma Joosten[2] and Giel J.C.G.M. Bosman[1]

[1]Department of Biochemistry, [2]Department of Laboratory Medicine –

Laboratory of Medical Immunology, Radboud University Medical Centre

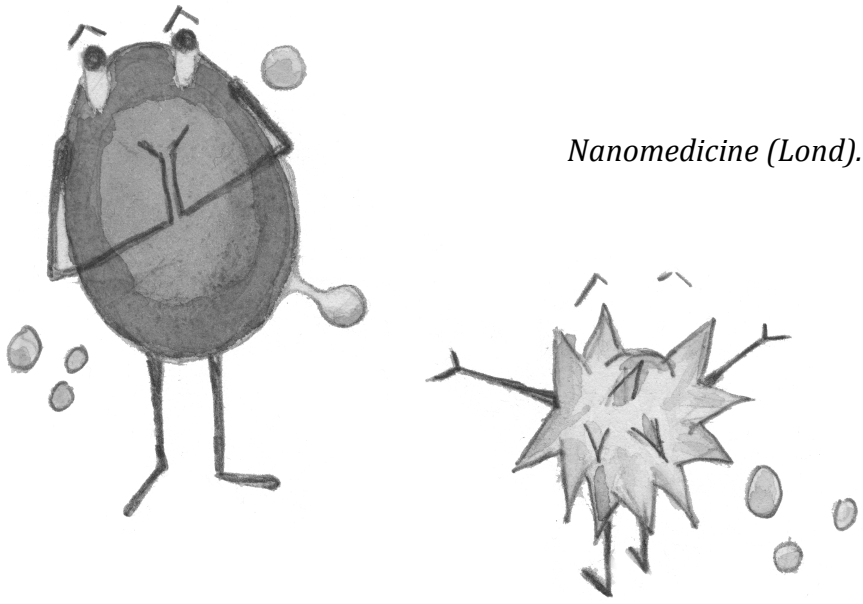

Nanomedicine (Lond). 2013;**8**(**10**):1657-1668

Summary

Microparticles (MPs) are small plasma membrane-derived vesicles that can expose molecules originating from their parental cells. As vectors of biological information they are likely to play an active role in both homeostasis and pathogenesis, making them promising biomarkers and nanomedicine tools. Therefore, there is an urgent need for standardization of MP isolation and analysis protocols to propel our understanding of MP biology to the next level. Based on current methodology and recent insights, this chapter proposes an optimized protocol for the isolation and biochemical characterization of MPs.

Introduction

MPs constitute a promising alternative microparticulated drug delivery system, with significant advantages over liposomes and nanoparticles [1,2]. Since MPs are an integral part of the regular blood transfusion products, their biocompatibility poses a relatively small challenge compared to other delivery vehicles. Especially erythrocyte transfusion units provide a reliable natural source for large quantities of erythrocyte-derived MPs, often termed red cell MPs (RMPs). Their negative surface charge and rapid clearance by the reticulo-endothelial system may be used for efficient targeting to resident and circulating macrophages as well as to the vascular endothelium [3]. This makes them promising agents for use in nanomedicine for the treatment of vascular diseases, as immunosuppressors in inflammatory and autoimmune diseases [4,5], and as delivery platforms for imaging agents [6].

MPs were first described by Peter Wolf in 1967, when he observed a halo of debris surrounding activated platelets which he termed “platelet dust” [7]. Since then the techniques that are available for MP detection have greatly improved and diversified, and now include flow cytometry, dynamic light scattering, nanoparticle tracking analysis, fluorescence correlation spectroscopy, immunoblotting, mass spectrometry, and transmission electron microscopy and atomic force microscopy [8,9].

Unfortunately, MP nomenclature has also diversified with time, replacing “dust” for an array of terms including nanoparticle, microvesicle, exosome-like vesicle, ectosome, oncosome, texosome, prostasome, epididymosome, and dexosome, depending on the sample source or isolation protocol used. To add to the confusion, microparticles are often designated as exosomes, smaller (40-100 nm) particles of endocytic origin, and apoptotic blebs (50-5000 nm) released by dying cells [8,10,11].

Most commonly, MPs are defined as plasma membrane-derived vesicles with a diameter of 100 to 1000 nm that expose molecules specific to the parental cell, with the majority residing in the 100 to 200 nm range [8,10,12]. Depending on their origin MPs may contain an array of signaling molecules, including receptors, cytokines, mRNA, microRNA and bioactive lipids. This molecular composition renders MPs vectors of biological information. As such they play an active role in homeostasis and pathogenesis, the latter including atherosclerosis, various malignancies, autoimmune disorders, and infection [10,13]. Therefore, MPs may be harnessed as diagnostic and/or prognostic biomarkers for disease [14-17].

The majority of the blood-borne MPs are generated by erythrocytes and platelets [12,18,19] RMPs are generated as part of the physiological erythrocyte aging process [20-22], and platelet-derived MPs (PMPs) are involved in coagulation after vascular injury [12]. During storage in the blood bank, erythrocytes and platelets continuously shed MPs, which might be responsible for some of the side-effects observed after transfusion [23,24].

As a consequence, proper identification and quantification of MPs is of great value, but the methods that are currently applied to isolate, characterize, and quantify MPs are far from standardized, and contain several technical hurdles [8,25]. The call for a consensus on both MP nomenclature, and methods for isolation and identification has therefore increased over the last years, and was one of the main topics during the first annual meeting of the International Society for Extracellular Vesicles [26]. A widely supported consensus on these aspects will prove vital for future MP research, as the current lack of methodological clarity obfuscates the identification and the molecular elucidation of their generation and of their biological function.

This review briefly discusses the possibilities of RMPs and PMPs for future science and medicine, while focusing on the technical limitations and challenges in isolation and flow cytometry analysis of MPs from plasma and from transfusion products.

RMPs and PMPs in health and disease

RMPs

During aging, the erythrocyte produces numerous RMPs exposing removal signals such as phosphatidylserine (PS) and autoantigens, which are probably responsible for their rapid removal from the circulation [3,19-21]. Physiologically, erythrocyte MP shedding may constitute a protective mechanism to prevent untimely erythrocyte removal [20-22]. Furthermore, increased or decreased RMP concentrations have been observed in the blood of patients with chronic renal failure, sickle cell disease, β-thalassemia, paroxysmal nocturnal hemoglobinuria, graft-versus-host-disease and Scott syndrome [14,15]. These findings suggest that RMP concentration (and possibly composition) may be employed as a biomarker for disease status.

Data from *in vitro* studies suggest that RMPs are likely to be actively involved in pathophysiology as well. For example, RMPs from erythrocyte storage units were found to modulate platelet function [27], and are highly procoagulant [28,29]. RMPs can transfer biologically active molecules, exemplified by the transfer of CD59 from one erythrocyte to the

other by membrane fusion in cells from patients with paroxysmal nocturnal hemoglobinuria [30]. Furthermore, RMPs may contribute to the procoagulant state and vaso-occlusions in sickle cell disease [18,31], and RMPs from malaria-infected erythrocytes were found to be major inducers of systemic inflammation during malaria infection [32].

PMPs

In contrast to what the name implies, the majority of the PMPs in the circulation are not derived from platelets, but from megakaryocytes [33,34]. PMPs are likely to be important mediators of coagulation, not only by exposing procoagulant factors [12,29,35], but also by providing a platform for binding of additional platelets to the subendothelial matrix [12,36]. PMPs may be involved in various other processes, such as hemostasis, maintenance of vascular health, and immunity [16]. Prominent examples are the involvement of PMPs in vasoregeneration [37,38], the transfer of CD41 integrin and CXCR4 receptors from megakaryocytes to nucleated cells *in vitro* [39], and their assistance in leukocyte-leukocyte interaction via P-selectin binding to PSGL-1 [40]. In addition, PMPs can transfer microRNA to endothelial cells, and thereby reprogram them [41,42].

Like RMPs, PMP levels are altered in various disease states, indicating that they play a role in thrombotic and inflammatory diseases, as well as in cancer progression [16]. A recent example is the pivotal role of PMPs in rheumatoid arthritis, where enhanced glycoprotein VI-mediated PMP generation may lead to PMP build-up in the joint fluid of patients suffering from inflammatory arthritis (but not osteoarthritis), inducing an inflammatory response via interleukin-1 signaling [43]. A related study showed the formation of highly pro-inflammatory PMP-immune complexes in patients with rheumatoid arthritis [44].

MPs in transfusion medicine

During blood bank storage, erythrocytes and platelets shed MPs [20,45]. These MPs might be responsible for some of the side-effects commonly observed after transfusion [4,5,23,24,46]. RMPs from storage products are enriched in removal signals such as PS, immunoglobulins, and complement [20,46]. The supernatant of erythrocyte transfusion units, which contains many RMPs that were shed during storage, was found to have the ability to modulate the functions of T cells [5], neutrophils [47], macrophages [4], and monocytes [48] *in vitro*. Transfusion supernatant also caused lung inflammation and coagulopathy in a rat model [49]. These findings strengthen the view that a high dose of RMPs received upon transfusion, might be responsible for or contribute to the inflammatory and/or immunological side-effects of transfusion, including autoantibody formation [50]. Storage may also prime erythrocytes to shed RMPs after transfusion [51], adding to the already present storage RMP burden.

Next to coagulation, platelets also have an important role as immune mediators [52,53], making PMPs likely candidates for immune regulation as well [24,54-56]. Side-effects of platelet transfusion include fever and transfusion-related acute lung injury [55]. and enhanced PMP levels in platelet units were shown to be correlated with various allergic transfusion reactions [54]. The ability of PMPs to interact with leukocytes via P-selectin binding to PSGL-1 [40,54], as well as their potential to induce CD154 (CD40L)-mediated B cell activation [57], underscore their ability to affect the immune system. The plethora of signaling molecules on PMPs makes it even more likely that they contribute to the transfusion burden [16,58]. While most circulating PMP derive from megakaryocytes [33,34], CD62-positive platelet-derived MPs constitute an important part of the storage PMP burden, and likely have a distinct biological function [54,59].

MP removal

One aspect of MPs that has received little attention thus far is their removal from the circulation. Phagocytosis is believed to be the main mechanism by which MPs are eliminated *in vivo* [3]. RMPs were rapidly removed in a rat model, mainly by the reticulo-endothelial system in the liver and in the bone marrow, and mediated by scavenger receptors [3].

The enrichment of RMPs in removal signals such as PS, immunoglobulins, and complement [20,22,46], likely causes this rapid removal by macrophages [3,22]. Further elucidation of the mechanisms involved in the generation of these signals, including PS exposure [60,61], autoantigen formation, and CD47 as a marker of ‘self’ and ‘non-self’ [62,63], might help to understand RMP removal. Both RMP and PMP removal seem to biphasic [64], but in contrast to RMPs, PMPs appear to have a half-life of hours instead of seconds [65]. PMPs are phagocytized by endothelial cells in a developmental endothelial locus-1-dependent manner [66]. This suggests that different pathways for MP removal exist depending on the cell of origin.

MP analysis using differential centrifugation in combination with flow cytometry

Focusing on RMPs and PMPs, this part of the review provides an overview of the current views on the most commonly used methods for the isolation, identification, quantitation and biochemical characterization of MPs in peripheral blood samples and transfusion products. We also provide new insights based on our own recent observations, which raise additional questions regarding current MP analysis strategies [8,67,68].

The most common protocol for analysis of MPs consists of differential centrifugation followed by fluorescence flow cytometry analysis [69]. Flow cytometry does not allow one to define size distribution and is poor at detecting very small particles (<200 nm), such as exosomes and smaller MPs. This is exacerbated by “swarm” detection of multiple small MPs as a single event using flow cytometry [70]. Consequently, the detected MPs do not represent the entire population. The upside of flow cytometry is that it enables the distinction of MPs of different cellular origin and the analysis of biochemical composition using fluorescently-labeled antibodies and other probes (e.g. Figure 1) [9].

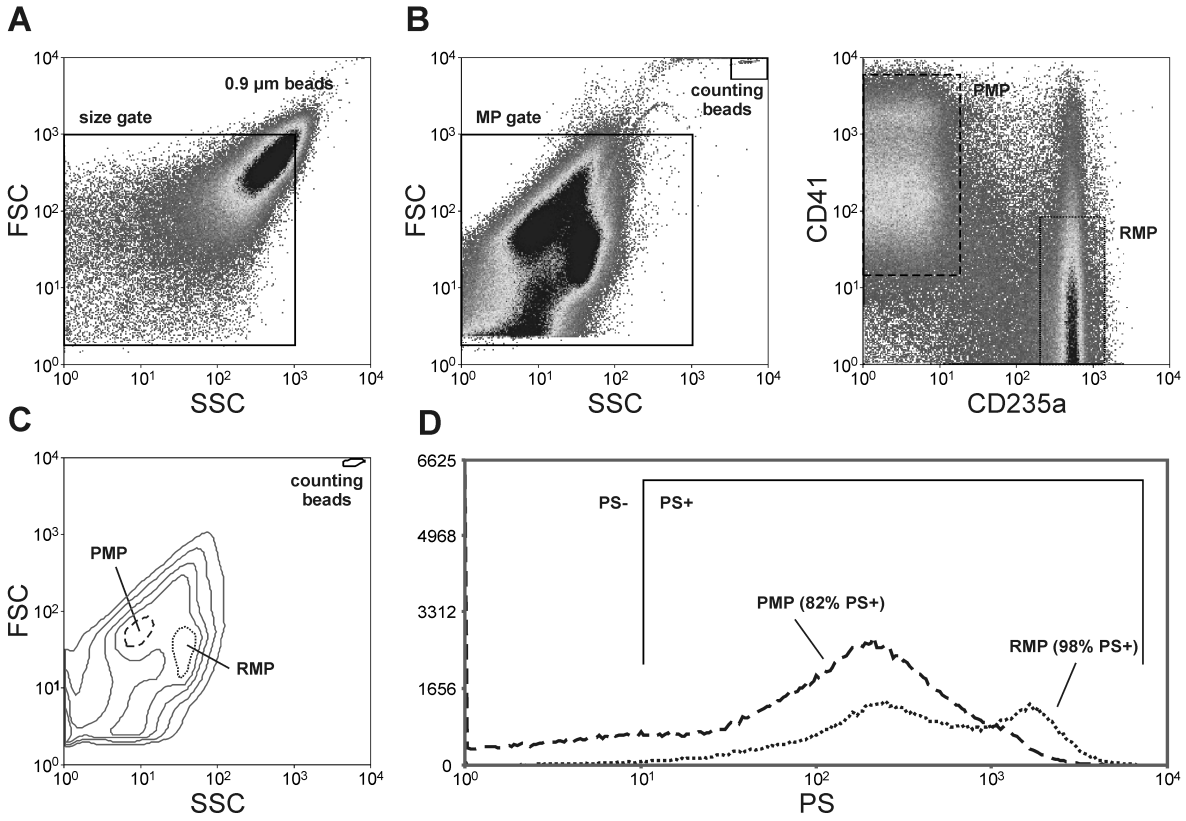

Figure 1. Flow cytometry analysis of PMPs and RMPs from plasma. Whole blood from a healthy volunteer was obtained in an EDTA Vacutainer and centrifuged for 5 min at 1500g. The plasma was depleted of platelets and large membrane fragments by 20 min centrifugation at 1500g. MPs were pelleted by 30 min centrifugation at 20,000g. The MPs were washed with calcium-free Ringer solution, resuspended in regular Ringer solution and probed for PS (Annexin V), the PMP marker CD41 and the RMP marker CD235a. This protocol prevented clot formation. After additional washing, the MPs were resuspended and fluorescent count beads (10 µm diameter) were added for MP quantification. **(A)** Size beads (0.9 µm diameter) were used to delineate the upper boundary for FSC/SSC MP gating. **(B, C)** MPs were analyzed on a flow cytometer, gated according to forward/sideward scatter (FSC and SSC, respectively) for fluorescent probe (α-CD41 and α-CD235a) analysis. **(D)** PS exposure of PMP and RMP populations was also analyzed. All solutions used were complemented with 0.2% BSA and filtered (0.22 µm) before use. A FACSCalibur (BD Biosciences) flow cytometer was used in combination with Annexin V-FLUOS, and anti-CD235a-PE and anti-CD41-PC5 antibodies. Detectors/Amps: FSC – V=E01, Amp=9.99; SSC – V=375, Amp=1.50; FL1 – V=690; FL2 – V=665; FL3 – V=800. Compensation: FL1 – 0.9% FL2; FL2 – 27.0% FL1; FL2 – 2.5% FL3; FL3 – 15.0% FL2.

The options for MP isolation from sample fluids are very limited. They consist of differential centrifugation and/or gradient purification, resulting in impure MP preparations contaminated with exosomes, apoptotic blebs and protein aggregates including immune complexes [8,25,26]. In spite of these limitations, the combination of differential centrifugation and flow cytometry has proven to be invaluable for the detection of changes in the make-up and size of MP populations in various disease states [14-17].

Optimization of the pre-analytical handling of MPs and the analysis itself is still in its early stages, and there is a strong need for standardization of protocols, in order to enable better comparison of data [8,26,69]. There are a multitude of parameters that affect the final composition and biological activity of the isolated MP fraction, many of which will be discussed below.

Blood collection

The method of blood collection, including the needle diameter, application of a tourniquet, and the use of a vacutainer to withdraw blood may all affect the MP concentration in the sample. In addition, the type of anticoagulant used has a profound effect on observed MP numbers, as exemplified by the apparent loss of PMP and endothelial cell-derived MP in chelating anticoagulants [71,72]. For erythrocyte-derived RMP, no such data are available, but in our hands, citrate (Acid Citrate Dextrose, ACD) and heparin are both suboptimal, i.e. detecting less RMP, in comparison with EDTA (Figure 2A). This might be due to anticoagulant-mediated aggregation or adherence of RMPs to plastic, which results in a depletion of MPs and thus in an underestimation. Alternatively, specific anticoagulants may affect RMP stability. Regardless of the underlying mechanisms, these data indicate that variation in anticoagulant may very well contribute to the - sometimes considerable - variation in the MP subpopulation sizes in plasma [22,73]. Our results indicate that RMPs may be more abundant in the circulation than previously assessed using citrate [72,74], suggesting that RMPs might play a more important role in circulatory homeostasis than presently believed.

The time between blood collection and MP isolation may affect the number of MPs in the sample, in part depending on the type of anticoagulant used [71,75,76]. We did not observe an increase in PMP nor in RMP number in the first four hours after blood collection using EDTA as an anticoagulant (Figure 2B). Thus, because of the effect of anticoagulant on biological activity of the MP fraction, standardization of the anticoagulant and the time between blood collection and processing is important to compare the results from different laboratories.

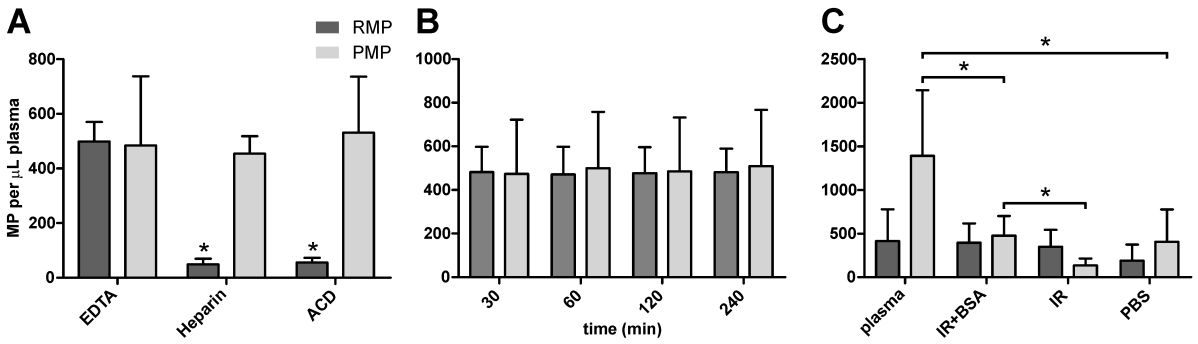

Figure 2. Impact of anticoagulant, wash buffer, and whole blood storage time on RMP and PMP enumeration. PMPs and RMPs from three healthy volunteers were isolated and quantified using α-CD41 and α-CD235a antibodies as described in Figure 1. **(A)** Whole blood was obtained using different anticoagulants, and PMPs and RMPs from whole blood were isolated and quantified. **(B)** PMPs and RMPs from whole blood (EDTA) were isolated and quantified at different time points after blood withdrawal. **(C)** PMPs and RMPs from whole blood (EDTA) were pelleted and either stained directly in plasma, or washed and stained in phosphate-buffered saline (PBS), or calcium-free Ringer (IR) solution with or without BSA. The graphs represent mean values, error bars represent S.D., and **P*<0.05 using repeated measures one-way ANOVA with Tukey's post-test.

Centrifugation

The common centrifugation parameters used for MP isolation vary between 1,500 to 10,000 g for 5 to 20 minutes in the initial centrifugation step to remove cells and platelets, followed by 13,000 to 100,000 g for 30 to 60 minutes to pellet MPs. These differences in centrifugation speed and time greatly affect the outcome of MP enumeration. Centrifugation may induce microparticle aggregation and PS exposure, and thereby also biological activity [68].

In our hands, intact erythrocytes and platelets, and large membranous fragments are effectively removed by centrifugation between 1,200 and 2,000 g for 15 to 20 minutes, whereas the use of an initial centrifugation speed >2,000 g leads to a substantial loss of MPs. We obtained maximum MP counts in our flow cytometry setup (see the Legend to Figure 1), when MPs were pelleted at 20,000 g for 20 to 30 minutes in a commonly used table-top centrifuge. Ultracentrifugation will pellet smaller MPs in the pellet, including the so-called nanovesicles and exosomes [8]. However, the detection limit of most flow cytometers will not allow the analysis of these smaller MPs [9]. Filtration using 0.8 μm porous membranes is occasionally used to remove residual platelets from MP isolates [25]. However, this may not only lead to platelet activation and/or MP fragmentation [77,78], but also leads, in our hands, to a severe loss of MPs (Figure 3).

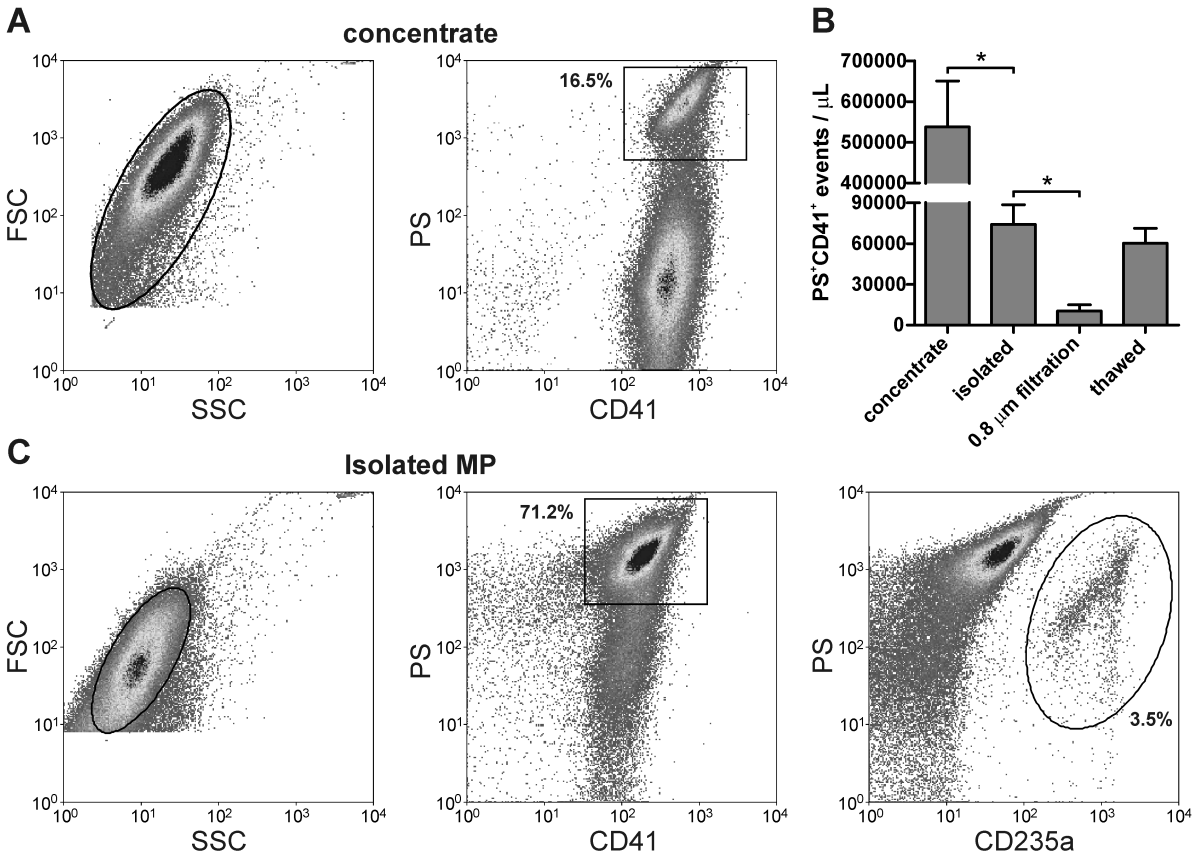

Figure 3. Large-scale PMP isolation from platelet transfusion units. The contents of three 7 day old platelet apheresis ACD plasma products were centrifuged for 15 min at 2000g. Part of each supernatant was used for 0.8 µm filtration. The remaining supernatant was aliquotted (1mL), and MPs were pelleted by 45 min centrifugation at 20.000g, and washed with IR containing BSA. The MPs were then resuspended in 10 µL IR+BSA per aliquot, snap-frozen with liquid N_2, and stored at -80°C. **(A, B)** Platelets and MPs in the unit itself (1:20 dilution), **(B, C)** MPs after isolation, **(B)** after filtration and after thawing were analyzed on a FACSCalibur flow cytometer, according to forward/sideward scatter (FSC and SSC, respectively), for assessment of CD41, CD235a and PS exposure. The graph represents mean values, error bars represent S.D., and *P<0.05 using repeated measures one-way ANOVA with Tukey's post-test.

Washing MPs

The addition of a washing step after MP isolation may affect MP number and morphology [75], but has the advantage that it increases the signal/noise ratio (Figures 3 and 4) Washing enables reliable (calcium-dependent) Annexin V binding to detect PS-positive MPs when calcium-chelating anticoagulants were used in the collection of the blood. Also, washing is a prerequisite for cellular assays, proteomics analysis, and fluorescence and electron microscopy [21,58,68]. The impact of washing on MP recovery depends on the type of MP. Washing led to a significant decrease in the numbers of PMPs, but not of RMPs (Figure 2C). Little attention has been paid to the composition of the buffer used for MP washing. The use of the calcium-free Ringer (IR) solution, often used in experimental work with erythrocytes, did not give superior MP numbers compared to PBS (Figure 2C). However, the addition of

bovine serum albumin (BSA) is beneficial for maintaining MP numbers, probably by preventing MP adhesion to the tubes used or to each other, and/or by stabilizing MP integrity (Figure 2C).

MP storage

At present, the effect of freezing on the quantity and quality of MPs in the final sample is not clear [71,72,75,79,80], and there is no consensus on a uniform freezing and thawing method [81]. We prefer to snap-freeze platelet-poor plasma or concentrated transfusion unit-derived MPs prior to -80°C storage, and to quickly thaw samples in a 37°C water bath before analysis [79,81]. Using this approach, we observe a minimal loss of MPs after thawing (Figure 3 and 4). Occasionally, thawing platelet-poor plasma results in the formation of precipitates that can compromise the analysis (unpublished observations). Although the MPs appear to be intact as observed by electron microscopy (Figure 4), PS exposure is clearly enhanced in the process (Figure 4), indicating freeze/thaw-induced changes in membrane organization and concomitant changes in activity.

Flow cytometry detection

Flow cytometry is a popular method for fast enumeration of MPs and the determination of their cellular origin. Forward and sideward light scatter by MPs, although different from cells, provide a simple way of discerning different MP populations (Figure 1) [9].

After isolation and - optional - washing, cellular origin and putative biological activity of MPs is mostly assessed using fluorochrome-conjugated probes such as antibodies and/or annexin V. Detection may be hampered by the limited number of molecules of interest on the MP surface, due to their small size. Assessment of the binding of isotype control antibodies is essential to exclude aspecific antibody binding to MPs. We advise the use of MPs that do not express the antigen of interest as an additional negative control for antibody binding.

MP enumeration by flow cytometry is usually achieved by addition of a known number of counting beads as an internal standard [67,68]. Hereto, brightly fluorescent polypropylene or latex microspheres with a larger diameter (~10 µm) than MP are typically used, since these can be detected separately from MPs by their size and bright fluorescence in all fluorescence detection channels. Calibrated beads with a size of ~1 µm are often used as an additional external standard to define the upper limit of the size gate used to quantify MPs. This size gate, combined with Annexin V staining, enables proper distinction between MPs from residual platelets and large membrane fragments [68].

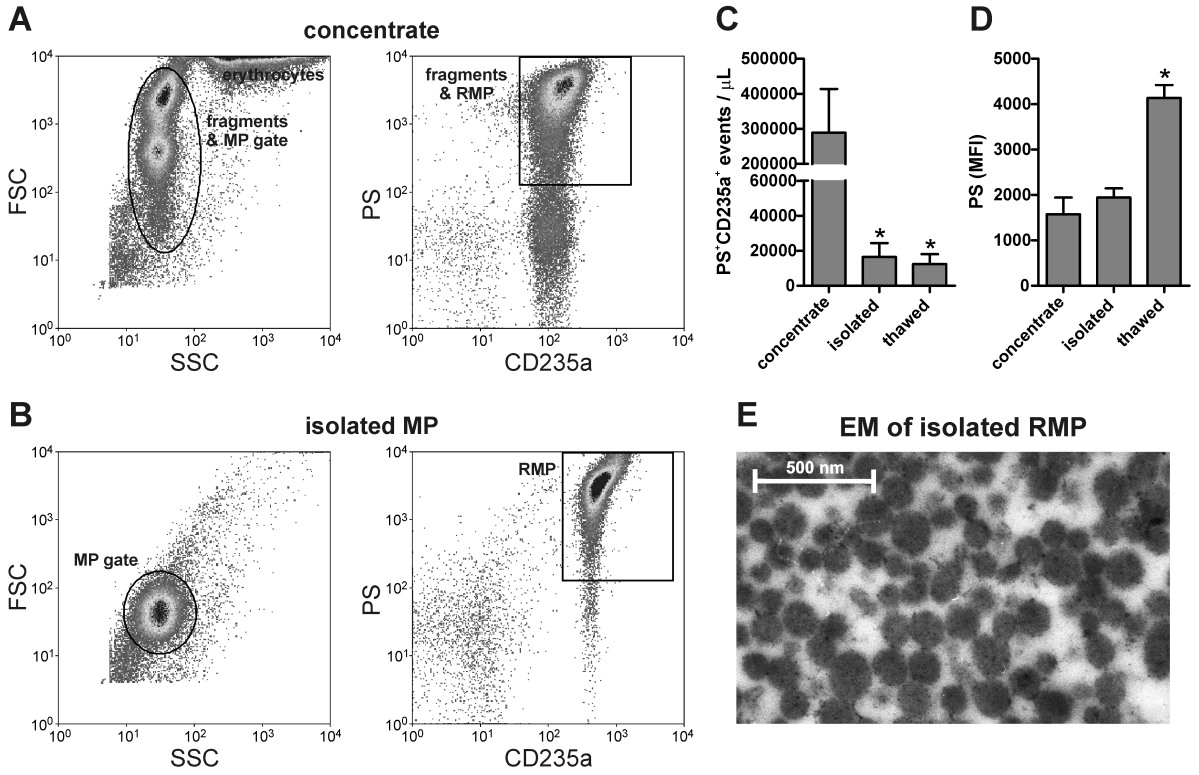

Figure 4. Large-scale RMP isolation from erythrocyte transfusion units. The contents of five 35 day old SAG-M erythrocyte units were centrifuged for 20 min at 1200g. The supernatants were then centrifuged again for 20 min at 1200g, and aliquotted (1 mL). MPs were pelleted by 45 min centrifugation at 20,000g, and washed with IR containing BSA. The MPs were then resuspended in 10 µL IR+BSA per aliquot, snap-frozen with liquid N_2, and stored at -80°C. **(A, C)** Cell fragments (including MPs) in the unit itself (1:20 dilution) and **(B, C)** MPs after isolation and **(B)** after thawing were analyzed on a FACSCalibur flow cytometer, according to forward/sideward scatter (FSC and SSC, respectively), for assessment of CD235a and PS exposure. **(D)** The mean fluorescence intensity (MFI) of the Annexin V staining for PS exposure is also shown. **(E)** Transmission electron microscopy was performed on a fixated MP pellet of a thawed aliquot. The graph represents mean values, error bars represent S.D., and **P*<0.05 using repeated measures one-way ANOVA with Tukey's post-test.

PS exposure is probed using the calcium-dependent binding of fluorochrome-conjugated Annexin V. Although PS exposure is often used to distinguish true MPs from other particles, such as immunocomplexes, PS-negative MP populations have been identified [44,82]. We also found that a considerable part of the PMPs do not bind Annexin V (Figure 1). Circulating RMP could be divided in $PS^{intermediate}$ and PS^{high} populations (Figure 1), possibly reflecting two distinct modes of MP formation by erythrocytes. In contrast, only PS^{high} RMPs are observed in stored erythrocyte units (Figure 4). To distinguish MPs from false-positive protein aggregates, we recommended an additional Triton lysis control [25]. This is particularly important when detecting small MP subpopulations, as small numbers of false-positive events can severely impact the outcome. In this context, filtration of buffers, washing of count beads, and high speed centrifugation of staining solutions is essential to remove small fluorescent particles and protein precipitates that compromise MP analysis [80]. In our

experience, optimizing the forward/sideward scatter settings of the flow cytometer already enables the distinction of PMPs and RMPs (Figure 1). A clear delineation of both populations can thus be obtained by combining cell-specific antigen and PS detection with specific forward/sideward scatter profiles. The detection of a minor population that is positive for both an erythrocyte and a thrombocyte marker (Figure 1), may reflect PMP-RMP adhesion, fusion or “swarm” detection of multiple MPs as a single event [70].

Analysis of MPs by flow cytometry has been driven mainly by our knowledge of the proteins that are present on the plasma membranes of their parent cells. Inventories of the MP proteomes make it possible to overcome this obvious restriction. As a first result, recent proteomic data, especially on RMPs isolated from the blood and transfusion units [20,21,46], have extended the theories on MP generation [83,84]. In a similar fashion, progress is being made with understanding MP formation and pathological function through PMP proteomics [58,85,86]. We foresee that, in the near future, proteomics data will inspire the selection of antibodies for detection of disease-related MP subpopulations. Thus, development of new flow cytometry analysis approaches is dependent on proteomic analysis of MPs, provided they have been isolated using the same, standardized protocols.

Isolation of transfusion unit-derived RMPs and PMPs

Recently, we have developed and optimized a protocol for the large-scale isolation of RMPs and PMPs from transfusion units. Nearly all erythrocyte unit-derived MPs isolated with this protocol are positive for the erythrocyte marker glycophorin, spherical, and have a homogeneous size distribution of around 50-200 nm (Figure 4). Furthermore, the forward/sideward scatter profile matches that of RMPs found in the circulation (Figure 1). Large quantities of clinical grade RMPs can readily be isolated from erythrocyte transfusion units, and used to establish standardized MP measurement protocols and as a microparticulated drug delivery system.

The isolation of MPs from platelet-units using differential centrifugation has proved to be more difficult, since platelets are only 2-3 µm in size [87]. As a consequence, there is substantial overlap in the flow cytometer forward scatter profile of platelets and their MPs, due to the limited size resolution of this technology. The differences in size and shape between platelets and MPs could be used to separate them more efficiently using scanning flow cytometry [88]. Using slightly higher centrifugation speeds, the platelet unit suspension can be depleted of platelets enabling the isolation of MPs. The PMP purity can be monitored by the percentage of PS-positive events and the forward scatter (Figure 3). A convenient

internal standard, as advised above, is provided by the RMPs in the plasma that is used to store the platelets. The forward/sideward scatter profile of the final product overlaps that of platelets found in the circulation, while PS exposure is significantly higher (Figures 1 and 4).

Conclusion & Future Perspectives

The growing recognition of the biological role of microparticles necessitates a standardization of MP isolation and analysis. This is a *sine qua non* to reliably detect and compare MP numbers, origin and biological activity in health and disease. Initiatives to standardize cross-laboratory MP measurements have already been started by the International Society on Thrombosis and Hemostasis and the International Society for Extracellular Vesicles [26,69]. The present comparison of currently used methods for isolation and analysis of MPs, inspired by our recently obtained data, intends to contribute to these initiatives. A simplified overview of our standard protocol for the isolation and analysis of MPs from various sources is provided in Figure 5.

New methods are currently developed to detect even the smallest MPs, enabling reliable semi-quantitative enumeration of MPs in biological fluids [89,90]. These methods employ new flow cytometers equipped with a high-power laser and high-performance photo multiplier tubes and wide angle FSC measurements, in combination with bright fluorochromes [84,91]. Since RMPs and PMPs are easily detectable in plasma compared to other MPs, and can be obtained in large quantities from transfusion products, we propose to use RMPs and/or PMPs to establish standardized MP measurement protocols. Combining these unambiguous protocols with a selective isolation method such as fluorescence-activated sorting or immunoaffinity capture [21,92], and rapidly expanding proteomic approaches [20,21,46,58,85,86], will provide reliable information on the mechanism(s) involved in their generation and on their biological function. They will also enable the meaningful use of RMPs and PMPs as tools in nanomedicine and as biomarkers in a variety of pathological conditions.

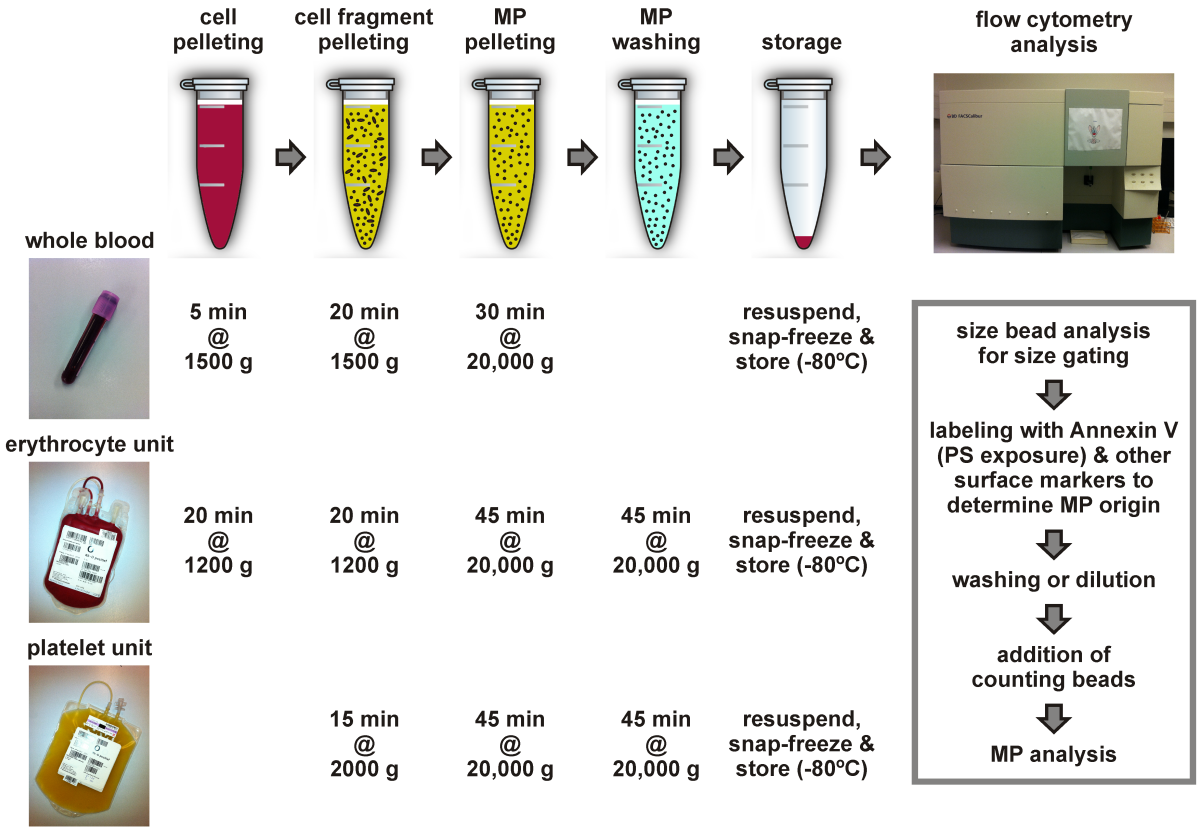

Figure 5. Standard protocol for the isolation of MPs from various sources.

Executive summary

Microparticles (MP)

- There is a need for consensus on microparticle (MP) nomenclature
- Standardized MP isolation and identification protocols are required to understand their biological function
- With standardized protocols, MPs are a promising alternative microparticulated drug delivery system

RMPs and PMPs in health and disease

- Red cell MP (RMP) production is a protective mechanism to prevent untimely erythrocyte removal
- Platelet-derived MPs (PMP) modulate coagulation and immune responses
- RMPs and PMPs are potential biomarkers for various diseases and the quality of blood bank products

MP isolation and flow cytometry

- The use of citrate or heparin as anticoagulant leads to an underestimation of the RMP population size in the circulation
- The optimal protocol for RMP and PMP isolation consists of: 1. Removal of cells by 15 to 20 minutes centrifugation at 1,200 to 2,000 g; 2. MP isolation by 20 to 30 minutes centrifugation at 20,000 g
- Additional washing with a filtered buffer containing bovine serum albumin is required for optimal MP analysis by cellular assays, proteomics, and microscopy
- Proper controls are required to avoid false positive events in flow cytometry analysis
- Probing for PS using flow cytometry reveals the existence of multiple RMP subpopulations
- Erythrocyte transfusion units are an excellent source for RMPs to establish standardized MP analysis protocols and microparticulated drug delivery systems

References

1 Alvarez-Erviti L, Seow Y, Yin H, Betts C, Lakhal S, Wood MJ. Delivery of siRNA to the mouse brain by systemic injection of targeted exosomes. *Nat. Biotechnol.* 29(4), 341-345 (2011).

2 Wang LY, Shi XY, Yang CS, Huang DM. Versatile RBC-derived vesicles as nanoparticle vector of photosensitizers for photodynamic therapy. *Nanoscale.* 5(1), 416-421 (2013).

3 Willekens FL, Werre JM, Kruijt JK *et al*. Liver Kupffer cells rapidly remove red blood cell-derived vesicles from the circulation by scavenger receptors. *Blood* 105(5), 2141-2145 (2005).

4 Sadallah S, Eken C, Schifferli JA. Erythrocyte-derived ectosomes have immunosuppressive properties. *J. Leukoc. Biol.* 84(5), 1316-1325 (2008).

5 Baumgartner JM, Silliman CC, Moore EE, Banerjee A, McCarter MD. Stored red blood cell transfusion induces regulatory T cells. *J. Am. Coll. Surg.* 208(1), 110-119 (2009).

6 Vats N, Wilhelm C, Rautou PE *et al*. Magnetic tagging of cell-derived microparticles: new prospects for imaging and manipulation of these mediators of biological information. *Nanomedicine. (Lond)* 5(5), 727-738 (2010).

7 Wolf P. The nature and significance of platelet products in human plasma. *Br. J. Haematol.* 13(3), 269-288 (1967).

8 Gyorgy B, Szabo TG, Pasztoi M *et al*. Membrane vesicles, current state-of-the-art: emerging role of extracellular vesicles. *Cell Mol. Life Sci.* 68(16), 2667-2688 (2011).

9 van der Pol E, Hoekstra AG, Sturk A, Otto C, van Leeuwen TG, Nieuwland R. Optical and non-optical methods for detection and characterization of microparticles and exosomes. *J. Thromb. Haemost.* 8(12), 2596-2607 (2010).

10 Thery C, Ostrowski M, Segura E. Membrane vesicles as conveyors of immune responses. *Nat. Rev. Immunol.* 9(8), 581-593 (2009).

11 Sullivan R, Saez F. Epididymosomes, prostasomes, and liposomes: their roles in mammalian male reproductive physiology. *Reproduction.* 146(1), R21-R35 (2013).

12 Owens AP, III, Mackman N. Microparticles in hemostasis and thrombosis. *Circ. Res.* 108(10), 1284-1297 (2011).

13 Mause SF, Weber C. Microparticles: protagonists of a novel communication network for intercellular information exchange. *Circ. Res.* 107(9), 1047-1057 (2010).

14 Hind E, Heugh S, Ansa-Addo EA, Antwi-Baffour S, Lange S, Inal J. Red cell PMVs, plasma membrane-derived vesicles calling out for standards. *Biochem. Biophys. Res. Commun.* 399(4), 465-469 (2010).

15 Rank A, Nieuwland R, Toth B *et al*. Microparticles for diagnosis of graft-versus-host disease after allogeneic stem transplantation. *Transplantation* 92(2), 244-250 (2011).

16 Aatonen M, Gronholm M, Siljander PR. Platelet-derived microvesicles: multitalented participants in intercellular communication. *Semin. Thromb. Hemost.* 38(1), 102-113 (2012).

17 Rank A, Nieuwland R, Delker R *et al*. Surveillance of megakaryocytic function by measurement of CD61-exposing microparticles in allogeneic hematopoietic stem cell recipients. *Clin. Transplant.* 25(3), E233-E242 (2011).

18 van Beers EJ, Schaap MC, Berckmans RJ *et al*. Circulating erythrocyte-derived microparticles are associated with coagulation activation in sickle cell disease. *Haematologica* 94(11), 1513-1519 (2009).

19 Willekens FL, Roerdinkholder-Stoelwinder B, Groenen-Dopp YA *et al*. Hemoglobin loss from erythrocytes *in vivo* results from spleen-facilitated vesiculation. *Blood* 101(2), 747-751 (2003).

20 Bosman GJ, Lasonder E, Luten M *et al*. The proteome of red cell membranes and vesicles during storage in blood bank conditions. *Transfusion* 48(5), 827-835 (2008).

21 Bosman GJ, Lasonder E, Groenen-Dopp YA, Willekens FL, Werre JM. The proteome of erythrocyte-derived microparticles from plasma: new clues for erythrocyte aging and vesiculation. *J. Proteomics.* (2012).

22 Willekens FL, Werre JM, Groenen-Dopp YA, Roerdinkholder-Stoelwinder B, de Pauw B, Bosman GJ. Erythrocyte vesiculation: a self-protective mechanism? *Br. J. Haematol.* 141(4), 549-556 (2008).

23 Donadee C, Raat NJ, Kanias T *et al*. Nitric oxide scavenging by red blood cell microparticles and cell-free hemoglobin as a mechanism for the red cell storage lesion. *Circulation* 124(4), 465-476 (2011).

24 Morrell CN. Immunomodulatory mediators in platelet transfusion reactions. *Hematology. Am. Soc. Hematol. Educ. Program.* 2011 470-474 (2011).

25 Gyorgy B, Modos K, Pallinger E *et al*. Detection and isolation of cell-derived microparticles are compromised by protein complexes resulting from shared biophysical parameters. *Blood* 117(4), e39-e48 (2011).

26 Araldi E, Krämer-Albers E, Nolte-'t Hoen E *et al*. Meeting report - International Society for Extracellular Vesicles: first annual meeting, April 17–21, 2012: ISEV-2012. *Journal of Extracellular Vesicles* 1 19995 (2012).

27 Xiong Z, Cavaretta J, Qu L, Stolz DB, Triulzi D, Lee JS. Red blood cell microparticles show altered inflammatory chemokine binding and release ligand upon interaction with platelets. *Transfusion* 51(3), 610-621 (2011).

28 Gao Y, Lv L, Liu S, Ma G, Su Y. Elevated levels of thrombin-generating microparticles in stored red blood cells. *Vox Sang.* (2013).

29 van der Meijden PE, van Schilfgaarde M, van Oerle R, Renne T, ten Cate H, Spronk HM. Platelet- and erythrocyte-derived microparticles trigger thrombin generation via factor XIIa. *J. Thromb. Haemost.* 10(7), 1355-1362 (2012).

30 Sloand EM, Mainwaring L, Keyvanfar K *et al*. Transfer of glycosylphosphatidylinositol-anchored proteins to deficient cells after erythrocyte transfusion in paroxysmal nocturnal hemoglobinuria. *Blood* 104(12), 3782-3788 (2004).

31 Camus SM, Gausseres B, Bonnin P *et al*. Erythrocyte microparticles can induce kidney vaso-occlusions in a murine model of sickle cell disease. *Blood* 120(25), 5050-5058 (2012).

32 Couper KN, Barnes T, Hafalla JC *et al*. Parasite-derived plasma microparticles contribute significantly to malaria infection-induced inflammation through potent macrophage stimulation. *PLoS. Pathog.* 6(1), e1000744 (2010).

33 Rank A, Nieuwland R, Delker R *et al*. Cellular origin of platelet-derived microparticles *in vivo*. *Thromb. Res.* 126(4), e255-e259 (2010).

34 Flaumenhaft R, Dilks JR, Richardson J *et al*. Megakaryocyte-derived microparticles: direct visualization and distinction from platelet-derived microparticles. *Blood* 113(5), 1112-1121 (2009).

35 Sinauridze EI, Kireev DA, Popenko NY *et al*. Platelet microparticle membranes have 50- to 100-fold higher specific procoagulant activity than activated platelets. *Thromb. Haemost.* 97(3), 425-434 (2007).

36 Merten M, Pakala R, Thiagarajan P, Benedict CR. Platelet microparticles promote platelet interaction with subendothelial matrix in a glycoprotein IIb/IIIa-dependent mechanism. *Circulation* 99(19), 2577-2582 (1999).

37 Mause SF, Ritzel E, Liehn EA *et al*. Platelet microparticles enhance the vasoregenerative potential of angiogenic early outgrowth cells after vascular injury. *Circulation* 122(5), 495-506 (2010).

38 Prokopi M, Pula G, Mayr U *et al*. Proteomic analysis reveals presence of platelet microparticles in endothelial progenitor cell cultures. *Blood* 114(3), 723-732 (2009).

39 Rozmyslowicz T, Majka M, Kijowski J *et al*. Platelet- and megakaryocyte-derived microparticles transfer CXCR4 receptor to CXCR4-null cells and make them susceptible to infection by X4-HIV. *AIDS* 17(1), 33-42 (2003).

40 Forlow SB, McEver RP, Nollert MU. Leukocyte-leukocyte interactions mediated by platelet microparticles under flow. *Blood* 95(4), 1317-1323 (2000).

41 Gidlof O, van der Brug M, Ohman J *et al*. Platelets activated during myocardial infarction release functional miRNA, which can be taken up by endothelial cells and regulate ICAM1 expression. *Blood* 121(19), 3908-3926 (2013).

42 Laffont B, Corduan A, Ple H *et al*. Activated platelets can deliver mRNA regulatory Ago2bulletmicroRNA complexes to endothelial cells via microparticles. *Blood* 122(2), 253-261 (2013).

43 Boilard E, Nigrovic PA, Larabee K *et al*. Platelets amplify inflammation in arthritis via collagen-dependent microparticle production. *Science* 327(5965), 580-583 (2010).

44 Cloutier N, Tan S, Boudreau LH *et al*. The exposure of autoantigens by microparticles underlies the formation of potent inflammatory components: the microparticle-associated immune complexes. *EMBO Mol. Med.* 5(2), 235-249 (2013).

45 Cauwenberghs S, Feijge MA, Harper AG, Sage SO, Curvers J, Heemskerk JW. Shedding of procoagulant microparticles from unstimulated platelets by integrin-mediated destabilization of actin cytoskeleton. *FEBS Lett.* 580(22), 5313-5320 (2006).

46 Dinkla S, Novotny VM, Joosten I, Bosman GJ. Storage-induced changes in erythrocyte membrane proteins promote recognition by autoantibodies. *PLoS. One.* 7(8), e42250 (2012).

47 Belizaire RM, Prakash PS, Richter JR *et al*. Microparticles from stored red blood cells activate neutrophils and cause lung injury after hemorrhage and resuscitation. *J. Am. Coll. Surg.* 214(4), 648-655 (2012).

48 Muszynski J, Nateri J, Nicol K, Greathouse K, Hanson L, Hall M. Immunosuppressive effects of red blood cells on monocytes are related to both storage time and storage solution. *Transfusion* 52(4), 794-802 (2012).

49 Vlaar AP, Hofstra JJ, Levi M *et al*. Supernatant of aged erythrocytes causes lung inflammation and coagulopathy in a "two-hit" *in vivo* syngeneic transfusion model. *Anesthesiology* 113(1), 92-103 (2010).

50 Young PP, Uzieblo A, Trulock E, Lublin DM, Goodnough LT. Autoantibody formation after alloimmunization: are blood transfusions a risk factor for autoimmune hemolytic anemia? *Transfusion* 44(1), 67-72 (2004).

51 Burger P, Kostova E, Bloem E *et al*. Potassium leakage primes stored erythrocytes for phosphatidylserine exposure and shedding of pro-coagulant vesicles. *Br. J. Haematol.* 160(3), 377-386 (2013).

52 Flad HD, Brandt E. Platelet-derived chemokines: pathophysiology and therapeutic aspects. *Cell Mol. Life Sci.* 67(14), 2363-2386 (2010).

53 Li N. Platelet-lymphocyte cross-talk. *J. Leukoc. Biol.* 83(5), 1069-1078 (2008).

54 Nomura S, Okamae F, Abe M *et al*. Platelets expressing P-selectin and platelet-derived microparticles in stored platelet concentrates bind to PSGL-1 on filtrated leukocytes. *Clin. Appl. Thromb. Hemost.* 6(4), 213-221 (2000).

55 Refaai MA, Phipps RP, Spinelli SL, Blumberg N. Platelet transfusions: impact on hemostasis, thrombosis, inflammation and clinical outcomes. *Thromb. Res.* 127(4), 287-291 (2011).

56 Vlaar AP, Hofstra JJ, Kulik W *et al*. Supernatant of stored platelets causes lung inflammation and coagulopathy in a novel *in vivo* transfusion model. *Blood* 116(8), 1360-1368 (2010).

57 Sprague DL, Elzey BD, Crist SA, Waldschmidt TJ, Jensen RJ, Ratliff TL. Platelet-mediated modulation of adaptive immunity: unique delivery of CD154 signal by platelet-derived membrane vesicles. *Blood* 111(10), 5028-5036 (2008).

58 Garcia BA, Smalley DM, Cho H, Shabanowitz J, Ley K, Hunt DF. The platelet microparticle proteome. *J. Proteome. Res.* 4(5), 1516-1521 (2005).

59 Rank A, Nieuwland R, Liebhardt S *et al*. Apheresis platelet concentrates contain platelet-derived and endothelial cell-derived microparticles. *Vox Sang.* 100(2), 179-186 (2011).

60 Lee SJ, Park SY, Jung MY, Bae SM, Kim IS. Mechanism for phosphatidylserine-dependent erythrophagocytosis in mouse liver. *Blood* 117(19), 5215-5223 (2011).

61 Setty BN, Betal SG. Microvascular endothelial cells express a phosphatidylserine receptor: a functionally active receptor for phosphatidylserine-positive erythrocytes. *Blood* 111(2), 905-914 (2008).

62 Olsson M, Oldenborg PA. CD47 on experimentally senescent murine RBCs inhibits phagocytosis following Fcgamma receptor-mediated but not scavenger receptor-mediated recognition by macrophages. *Blood* 112(10), 4259-4267 (2008).

63 Burger P, Hilarius-Stokman P, de Korte D, van den Berg TK, van Bruggen R. CD47 functions as a molecular switch for erythrocyte phagocytosis. *Blood* 119(23), 5512-5521 (2012).

64 van der Pol E, Boing AN, Harrison P, Sturk A, Nieuwland R. Classification, functions, and clinical relevance of extracellular vesicles. *Pharmacol. Rev.* 64(3), 676-705 (2012).

65 Rank A, Nieuwland R, Crispin A *et al*. Clearance of platelet microparticles *in vivo*. *Platelets.* 22(2), 111-116 (2011).

66 Dasgupta SK, Le A, Chavakis T, Rumbaut RE, Thiagarajan P. Developmental endothelial locus-1 (Del-1) mediates clearance of platelet microparticles by the endothelium. *Circulation* 125(13), 1664-1672 (2012).

67 Lacroix R, Robert S, Poncelet P, Dignat-George F. Overcoming limitations of microparticle measurement by flow cytometry. *Semin. Thromb. Hemost.* 36(8), 807-818 (2010).

68 Yuana Y, Bertina RM, Osanto S. Pre-analytical and analytical issues in the analysis of blood microparticles. *Thromb. Haemost.* 105(3), 396-408 (2011).

69 Lacroix R, Robert S, Poncelet P, Kasthuri RS, Key NS, Dignat-George F. Standardization of platelet-derived microparticle enumeration by flow cytometry with calibrated beads: results of the International Society on Thrombosis and Haemostasis SSC Collaborative workshop. *J. Thromb. Haemost.* 8(11), 2571-2574 (2010).

70 van der Pol E, van Gemert MJ, Sturk A, Nieuwland R, van Leeuwen TG. Single vs. swarm detection of microparticles and exosomes by flow cytometry. *J. Thromb. Haemost.* 10(5), 919-930 (2012).

71 Jayachandran M, Miller VM, Heit JA, Owen WG. Methodology for isolation, identification and characterization of microvesicles in peripheral blood. *J. Immunol. Methods* 375(1-2), 207-214 (2012).

72 Shah MD, Bergeron AL, Dong JF, Lopez JA. Flow cytometric measurement of microparticles: pitfalls and protocol modifications. *Platelets.* 19(5), 365-372 (2008).

73 Xiong Z, Oriss TB, Cavaretta JP, Rosengart MR, Lee JS. Red cell microparticle enumeration: validation of a flow cytometric approach. *Vox Sang.* 103(1), 42-48 (2012).

74 Berckmans RJ, Nieuwland R, Boing AN, Romijn FP, Hack CE, Sturk A. Cell-derived microparticles circulate in healthy humans and support low grade thrombin generation. *Thromb. Haemost.* 85(4), 639-646 (2001).

75 Ayers L, Kohler M, Harrison P *et al*. Measurement of circulating cell-derived microparticles by flow cytometry: sources of variability within the assay. *Thromb. Res.* 127(4), 370-377 (2011).

76 Connor DE, Exner T, Ma DD, Joseph JE. Detection of the procoagulant activity of microparticle-associated phosphatidylserine using XACT. *Blood Coagul. Fibrinolysis* 20(7), 558-564 (2009).

77 Lawrie AS, Albanyan A, Cardigan RA, Mackie IJ, Harrison P. Microparticle sizing by dynamic light scattering in fresh-frozen plasma. *Vox Sang.* 96(3), 206-212 (2009).

78 Pontiggia L, Steiner B, Ulrichts H, Deckmyn H, Forestier M, Beer JH. Platelet microparticle formation and thrombin generation under high shear are effectively suppressed by a monoclonal antibody against GPIba. *Thromb. Haemost.* 96(6), 774-780 (2006).

79 Trummer A, De Rop C, Tiede A, Ganser A, Eisert R. Recovery and composition of microparticles after snap-freezing depends on thawing temperature. *Blood Coagul. Fibrinolysis* 20(1), 52-56 (2009).

80 Dey-Hazra E, Hertel B, Kirsch T *et al*. Detection of circulating microparticles by flow cytometry: influence of centrifugation, filtration of buffer, and freezing. *Vasc. Health Risk Manag.* 6 1125-1133 (2010).

81 Gelderman MP, Simak J. Flow cytometric analysis of cell membrane microparticles. *Methods Mol. Biol.* 484 79-93 (2008).

82 Connor DE, Exner T, Ma DD, Joseph JE. The majority of circulating platelet-derived microparticles fail to bind annexin V, lack phospholipid-dependent procoagulant activity and demonstrate greater expression of glycoprotein Ib. *Thromb. Haemost.* 103(5), 1044-1052 (2010).

83 Sens P, Gov N. Force balance and membrane shedding at the red-blood-cell surface. *Phys. Rev. Lett.* 98(1), 018102 (2007).

84 Gov N, Cluitmans J, Sens P, Bosman GJCG. Cytoskeletal Control of Red Blood Cell Shape: Theory and Practice of Vesicle Formation. In: *Advances in Planar Lipid Bilayers and Liposomes (Volume 10)*. Lui AL, Iglic A (Ed.), Academic Press, 95-119 (2009).

85 Abdullah NM, Kachman M, Walker A *et al*. Microparticle surface protein are associated with experimental venous thrombosis: a preliminary study. *Clin. Appl. Thromb. Hemost.* 15(2), 201-208 (2009).

86 Dean WL, Lee MJ, Cummins TD, Schultz DJ, Powell DW. Proteomic and functional characterisation of platelet microparticle size classes. *Thromb. Haemost.* 102(4), 711-718 (2009).

87 Thon JN, Italiano JE. Platelets: production, morphology and ultrastructure. *Handb. Exp. Pharmacol.* (210), 3-22 (2012).

88 Konokhova AI, Yurkin MA, Moskalensky AE *et al*. Light-scattering flow cytometry for identification and characterization of blood microparticles. *J. Biomed. Opt.* 17(5), 057006 (2012).

89 van der Vlist EJ, Nolte-'t Hoen EN, Stoorvogel W, Arkesteijn GJ, Wauben MH. Fluorescent labeling of nano-sized vesicles released by cells and subsequent quantitative and qualitative analysis by high-resolution flow cytometry. *Nat. Protoc.* 7(7), 1311-1326 (2012).

90 Hoen EN, van der Vlist EJ, Aalberts M *et al*. Quantitative and qualitative flow cytometric analysis of nanosized cell-derived membrane vesicles. *Nanomedicine.* 8(5), 712-720 (2012).

91 Robert S, Lacroix R, Poncelet P *et al*. High-sensitivity flow cytometry provides access to standardized measurement of small-size microparticles--brief report. *Arterioscler. Thromb. Vasc. Biol.* 32(4), 1054-1058 (2012).

92 Tauro BJ, Greening DW, Mathias RA *et al*. Comparison of ultracentrifugation, density gradient separation, and immunoaffinity capture methods for isolating human colon cancer cell line LIM1863-derived exosomes. *Methods* 56(2), 293-304 (2012).

7

Platelet microparticles inhibit IL-17 production by Tregs through a P-selectin-mediated mechanism

Sip Dinkla[1], Hans J.P.M. Koenen[1], Bram van Cranenbroek[1],

Giel J.C.G.M. Bosman[2] and Irma Joosten[1]

[1]Department of Laboratory Medicine – Laboratory of Medical Immunology,

[2]Department of Biochemistry, Radboud University Medical Centre

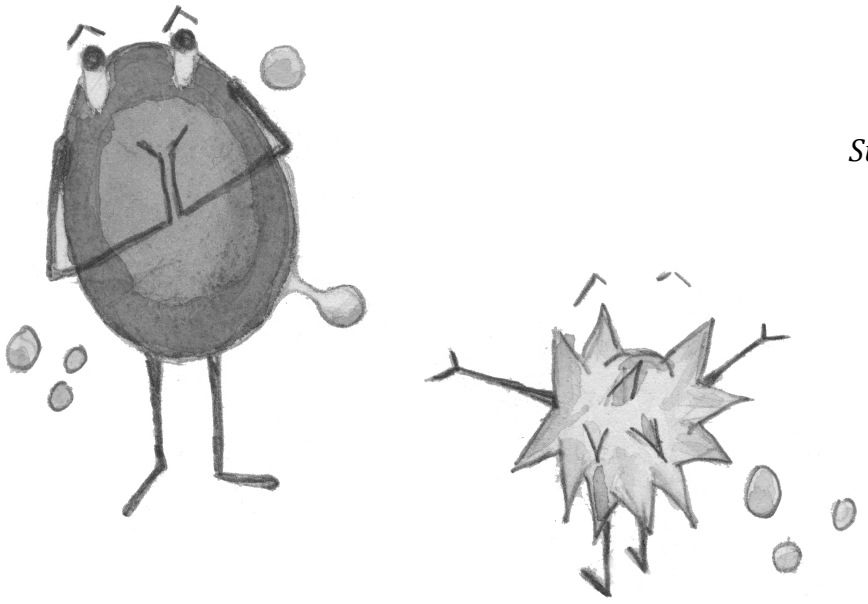

Submitted for publication

Abstract

Self-tolerance and immune homeostasis is orchestrated by $Foxp3^+$ regulatory T cells (Tregs). However, recent insights have revealed that upon stimulation Tregs may exhibit plasticity towards a pro-inflammatory phenotype, producing IL-17 and/or IFN-γ. Here, we report that platelet-derived microparticles (PMPs) have the capacity to prevent the differentiation of peripheral blood-derived Tregs into IL-17 and IFN-γ-producing cells, even in the presence of the pro-inflammatory cytokine IL-1β. The mechanism of action consisted of rapid and selective P-selectin dependent binding of PMPs to a specialized $CCR6^+HLA\text{-}DR^+$ memory-like Treg subset, probably disrupting their eventual differentiation into potentially pathogenic IL-17 producers. Our data also indicate that the inhibitory effect of PMPs on memory-like Treg differentiation may lie in their ability to affect cell proliferation. These findings open up the exciting possibility that PMPs actively regulate the immune response at sites of vascular inflammation, where they are known to accumulate and interact with leukocytes, consolidating the vascular healing process and preventing vascular disease.

Introduction

Forkhead box p3 (Foxp3)$^+$ regulatory T cells (Tregs) play a key role in maintaining dominant self-tolerance and immune homeostasis, and modulate immune responses during infection. The expression of the transcription factor Foxp3 is essential for their suppressive capacity towards effector cells, as is exemplified by the severe systemic autoimmunity observed in humans with impaired Foxp3 function [1].

In recent years, the classical view of helper CD4$^+$ T (T_H) cell subsets belonging to distinct cell lineages, has given way to the idea that these subsets exhibit a certain amount of plasticity, being able to alter their cytokine profile or even switch T_H cell phenotype [2]. We have previously determined that CD4$^+$CD25^{high}Foxp3$^+$ Tregs can differentiate into IL-17 and IFN-γ-producing cells and lose their master regulator Foxp3 when activated, particularly in the presence of the pro-inflammatory cytokine IL-1 [3]. Such functional plasticity of human Tregs has been observed by others as well [4-7]. However, the mechanisms controlling Treg stability are just beginning to be unraveled.

Platelets are small (~2 μm in diameter), circulating, enucleate cells that are derived from megakaryocytes residing in the bone marrow. Once thought to be restricted to their critical role in hemostasis by initiating blood clotting at sites of vascular injury, it is becoming increasingly clear that platelets can modulate immune responses through the expression of immunomodulatory molecules such as CD40L, Toll-like receptors, and various chemokines and cytokines, including IL-1 [8].

Once activated, platelets not only release chemokines and cytokines [8], but also plasma membrane-derived microparticles into the circulation [9]. These platelet-derived microparticles (PMPs) are in the submicron range, and expose molecules specific to the parental cell as well as the lipid phosphatidylserine (PS). Their ability to transfer membrane receptors [10] and microRNA [11] to other cells, mark them as vectors of biological information. Like their parental cells, they are involved in hemostasis, maintenance of vascular health, and immunity [9,12]. An example of their involvement in immune responses, is their potential to induce CD40L-mediated B cell activation [13]. PMPs were also found to accumulate in the joint fluid of patients suffering from inflammatory arthritis, and are suggested to induce a local inflammatory response in the synovium through PMP-bound IL-1-dependent signaling [14].

The notion that PMPs can influence cells of the immune system under inflammatory conditions, combined with the knowledge that such conditions also affect Treg phenotype,

led us to investigate the effect of PMPs on Tregs. Here, we show that PMPs inhibit the differentiation of highly purified peripheral blood $CD4^+CD25^{high}CD127^{low}Foxp3^+$ Tregs into IL-17/IFN-γ-producing cells when stimulated with anti-CD3/CD28 monoclonal antibody (mAb) coated beads and cultured in the presence of IL-2, IL-15 and IL-1β. This PMP interaction with, and the subsequent inhibition of Treg differentiation, appears to be P-selectin-dependent, as PMP blocking with an antagonistic anti-P-selectin mAb before co-culture restored the differentiation capacity of Tregs into 17/IFN-γ-producing cells. Prior to, and during Treg activation and subsequent differentiation, PMPs selectively bound Tregs expressing CCR6 and HLA-DR, believed to represent a memory-like Treg precursor subset for IL-17-producing cells [6,15]. Our data indicate that PMPs affect cell proliferation, providing a possible mechanism by which the memory-like Treg subset is inhibited. These findings open up the exciting possibility that PMPs actively regulate the immune response at sites of vascular injury, where PMPs are known to accumulate [16].

Results

PMPs inhibit $CD25^{high}Foxp3^+$ Treg differentiation into IL-17-producing cells

We reasoned that PMPs, with their arsenal of immune-mediating molecules [9], and their ability to interact with cells of the immune system [13,14], might impact the differentiation of Tregs into IL-17-producing T cells, such as we previously described [3]. As we required large amounts of PMPs for our studies, we used PMPs that were isolated from 7 day stored platelet apheresis products of healthy volunteers, as these products are known to accumulate PMPs during storage [17]. Their purity, size and number was assessed by flow cytometry analysis of the exposure of PS and the platelet-specific marker CD41 (Figure 1A). Over 99 % of all measured events were smaller than 1 μm in diameter, and more than 95 % stained positive for CD41 and PS.

Figure 1. PMPs inhibit Treg differentiation into IL-17-producing cells. Flow cytometry analyses of Tregs that were cultured in the presence of anti-CD3/anti-CD28-coated beads, and human recombinant IL-2, IL-15, and IL-1β, in the presence or absence of PMPs. Intracellular cytokine staining was performed after stimulation with PMA and ionomycin, in the presence of Brefeldin A. (**A**) $CD41^+PS^+$ PMPs <1 μm were purified from platelet apheresis units of healthy volunteers by differential centrifugation and analyzed by flow cytometry for phosphatidylserine (PS) and CD41 exposure as described in methods. Size beads (0.9 μm) were used to set a size exclusion gate, and fluorescent count beads (~10 μm) were added to the PMPs for quantification. The contour plots are representative for three donors. (**B**) Representative experiment showing intracellular IL-17 and IFN-γ staining of the Tregs at day 0. (**C-D**) Representative example of the intracellular IFN-γ, IL-17 and Foxp3 staining of Tregs that were cultured for 7 days with and without 5×10^6 PMPs. (**E**) A representative experiment performed with ascending PMP concentrations from three different healthy volunteers. Surface CCR6, CD27, and intracellular IL-

17, IFN-γ, and Foxp3 staining of the Tregs at day 7 of culture are shown. Error bars represent SD. * $P < 0.05$. (**F**) Overview of experiments showing surface CCR6, CD27, CD62L, and intracellular IL-17, IFN-γ, and Foxp3 staining of Tregs cultured for 7 days with ascending PMP concentrations. Each dot (n = 3-5 PBMC donors) represents the mean of a separate experiment with PMPs from three healthy volunteers tested in parallel. The average mean is presented as bars. * $P < 0.05$.

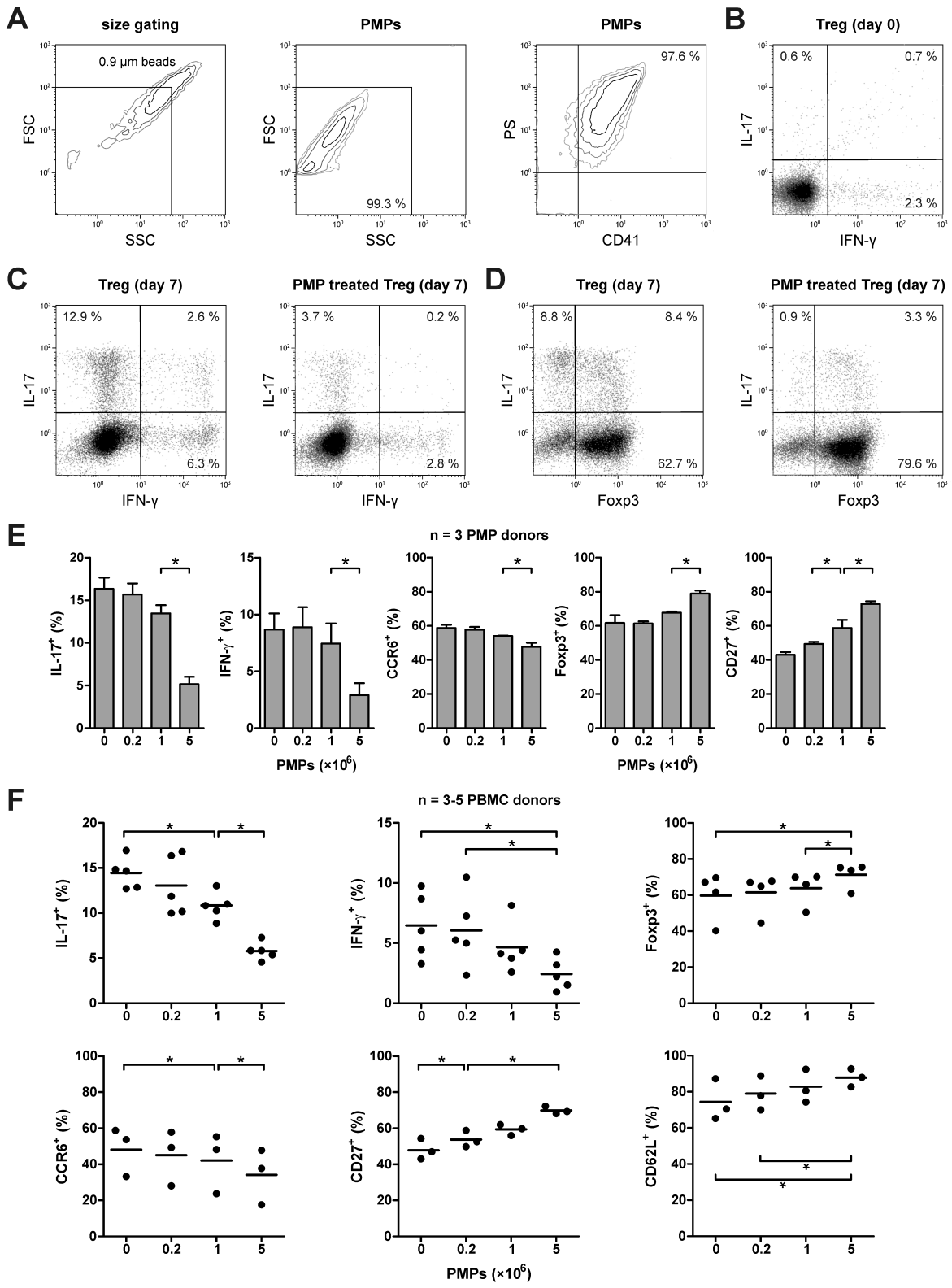

These PMPs were then co-cultured with a highly pure, well-defined, $CD4^+CD25^{high}CD27^+CD127^{low}Foxp3^+$ Treg population isolated from peripheral blood mononuclear cells (PBMCs) by fluorescence-activated cell sorting (Supplemental Figure S1). Typically, anti-CD3/CD28 mAb stimulation of this population in the presence of IL-2/IL-15 and IL1-beta leads to a substantial number of IL-17 producing cells, with concomitant loss of Foxp3 [3].

The addition of PMPs to the freshly isolated Tregs at ratios of 1:8, 1:40, or 1:200 per cell, clearly inhibited the generation of IL-17 and IFN-γ-producing cells in a dose-dependent manner (Figure 1B-C and 1E-F). Similarly, the loss of Foxp3 expression was inhibited. (Figure 1D-F). Interestingly, of the few cells that still managed to acquire IL-17-producing capacity in the presence of PMPs, most did not lose their Foxp3, suggesting a transitory state due to inhibition. Previous studies have revealed that $CD4^+CD25^+CD27^+CD62L^+$ cells constitute a highly suppressive Treg subset [18-20]. In accordance with Foxp3, loss of CD27 and CD62L was also prevented, while the percentage of cells that acquired the T_H17 [21] and memory-associated [22] chemokine receptor CCR6 during culture was inhibited by the PMPs (Figure 1E and 1F).

P-selectin mediates PMP inhibitory effect on Treg differentiation

After establishing that PMPs affect cytokine production by Tregs, the question arose which molecular component(s) of the PMPs were responsible for the observed effect. We first asked ourselves whether the communication between PMPs and Tregs was contact-dependent. A transwell setup was implemented to culture PMPs and Tregs in two separate compartments of a single volume, using identical culture conditions as mentioned before. Intracellular IL-17 expression was assessed on day 7 (Figure 2A), and showed that the Tregs were unaffected by the PMPs in the transwell setup, while the dose-dependent inhibition ($P < 0.05$) of Treg differentiation into IL-17-producing cells was observed in the standard contact-dependent setup as expected.

Figure 2. PMP inhibition of Treg differentiation is P-selectin dependent. Tregs were cultured for 7 days in the presence of anti-CD3/anti-CD28-coated beads, and human recombinant IL-2, IL-15, and IL-1β, in the presence or absence of PMPs (n = 3 PMP donors). Intracellular cytokine staining was performed after stimulation with PMA and ionomycin, in the presence of Brefeldin A. (**A**) The intracellular IL-17 expression in Tregs that were co-cultured with PMPs as a standard mixed culture (control), or separated by a porous membrane (transwell). (**B**) The presence of the platelet-specific marker CD41 was assessed on the $CD4^+$ Tregs after co-culture with ascending PMP concentrations. Each dot represents the mean of a separate experiment with PMPs from three healthy volunteers tested parallel to each other. The average mean is shown. (**C**) Representative contour plots of PMPs stained with anti-CD41-PE and FITC conjugated anti-P-selectin or isotype mAbs. The contour plots are representative for three donors. (**D**) Treg expression of PSGL-1 and CD25 at day 0 of culture. (**E**) Surface staining of CD27, CD41, and intracellular staining of IL-17 on Tregs co-cultured with untreated, isotype, or anti-P-selectin mAb blocked PMPs. (**F**) Surface staining of CD62L, CCR6, and intracellular staining of Foxp3 and IFN-γ

on Tregs co-cultured with untreated, isotype, or anti-P-selectin mAb blocked PMPs. The graphs are representative for two experiments. Mean and SD are shown. * $P < 0.05$. Flow cytometry was employed for the analyses.

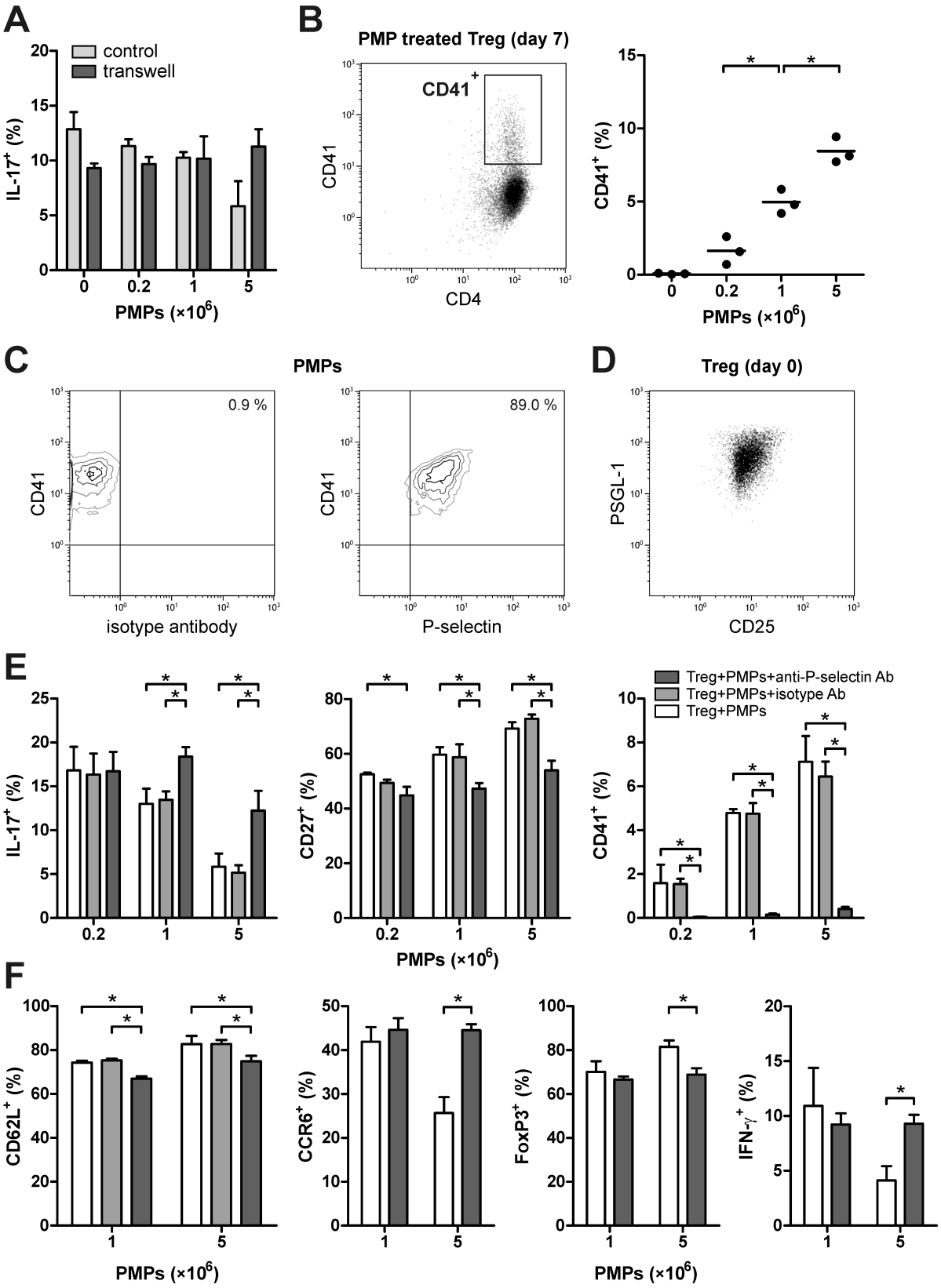

The contact-dependency ruled out the possibility of cytokine scavenging or release by the PMPs significantly affecting Treg differentiation. Therefore, we focused our attention on potential PMP membrane-bound molecules. Since CD40-CD40L co-stimulatory signaling was implicated in PMP-mediated signaling [13], and T cells can sense PS [23], we investigated their involvement. However, blocking of either CD40 in culture or PS on PMPs with an antagonistic anti-CD40 mAb or Annexin V, respectively, did not reduce the inhibitory effect of PMPs on Tregs (Supplemental Figure S2).

As we observed clear staining for the platelet-specific marker CD41 on at least part of the Tregs co-cultured with PMPs (Figure 2B), even after repeated washing steps, we proposed that PMPs firmly bound to these cells and consequently, we hypothesized that adhesion molecules, several of which are present on the PMP membrane [9], might be involved in the interaction. Upon activation, platelets typically expose the adhesion molecule P-selectin, which they can pass onto the PMPs they generate [24]. Like their parental cells, PMPs are able to bind immune cells expressing P-selectin receptor P-selectin glycoprotein ligand-1 (PSGL-1) [25,26]. This led us to investigate whether P-selectin is involved in the observed PMP adhesion to Tregs and/or the inhibition of their differentiation. First, we established that the majority of PMPs (86.3 ± 2.4%) indeed expressed P-selectin (Figure 2C), and that the Tregs express its receptor PSGL-1 at day 0 (Figure 2D), and subsequently performed blocking studies. Prior to co-culture with Tregs, PMPs were incubated with a FITC-conjugated antagonistic anti-P-selectin mAb, an isotype control mAb, or incubated in plain buffer, and subsequently washed. While isotype mAb did not bind to the PMPs (0.4 ± 0.1%), PMPs were effectively blocked with the anti-P-selectin mAb (80.6 ± 4.4%). The anti-P-selectin mAb was still present on the PMPs at day 7 of culture with Tregs (77.4 ± 7.1%). Notably, the blocking of P-selectin not only abrogated ($CD41^+$) PMP adhesion to the Tregs (Figure 2E), it also greatly blunted their inhibitory effect on Treg differentiation into $CCR6^+$ IL-17-producing cells, as shown by CD27 and intracellular IL-17 staining (Figure 2E). Blocking of P-selectin also allowed for loss of Foxp3 and CD62L, and IFN-γ expression by Tregs (Figure 2F), corroborating these results.

PMPs selectively target $CCR6^+HLA\text{-}DR^+$ memory-like and IL-17-producing Tregs

Typically, only a subset of peripheral blood derived Tregs start producing IL-17 upon stimulation [3-7]. Further insight into the features of this subset might guide us in the characterization and regulation of these cells. Sparked by the observation that the PMPs only associated with a subset of the Tregs (Figure 2B), while inhibiting IL-17 production, we argued that we might use this characteristic to pinpoint the IL-17 precursors within the whole Treg population.

To establish the identity of the Treg subset(s) targeted by the PMPs, and to determine whether this interaction occurs before the Treg differentiation progresses, we followed PMP binding to Tregs in time over a 7 day culture (Figure 3). Binding of ($CD41^+$) PMPs to Tregs already occurred within 1 day of culture (Figure 3A). The PMP binding to Tregs increased with enhanced expression of the P-selectin receptor PSGL-1 (Figure 3A), which is in line with the observed requirement of P-selectin in the PMP-Treg interaction. On day 7 a significant reduction in the percentage of $CD41^+$ Tregs was observed (Figure 3A).

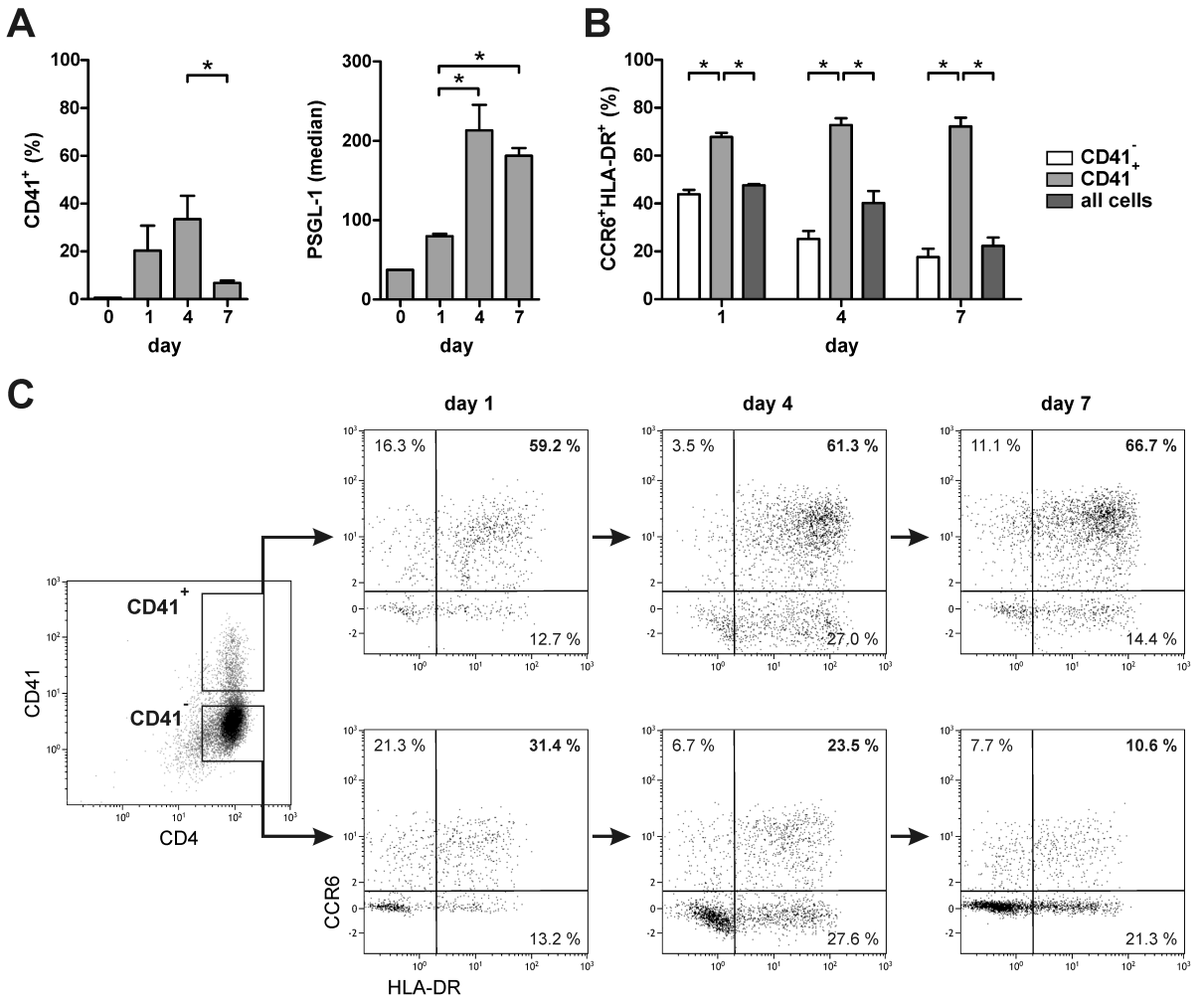

Figure 3. PMPs selectively target $CCR6^+HLA\text{-}DR^+$ Tregs prior to, and during, activation.
Tregs were cultured for 7 days in the presence of anti-CD3/anti-CD28-coated beads, human recombinant IL-2, IL-15, and IL-1β, and 5×10^6 PMPs. Tregs were stained for surface markers and analyzed by flow cytometry at day 0, 1, 4 and 7; (**A**) $CD41^+$ PMP-bound Tregs, and the expression level of PSGL-1 on the Tregs. (**B**) $CCR6^+HLA\text{-}DR^+$ Tregs present in the $CD41^-$ and $CD41^+$ subpopulations. (**C**) Example CCR6/HLA-DR dot plots of $CD41^-$ and $CD41^+$ Tregs. Mean and SD for three PMP donors are shown. * $P < 0.05$.

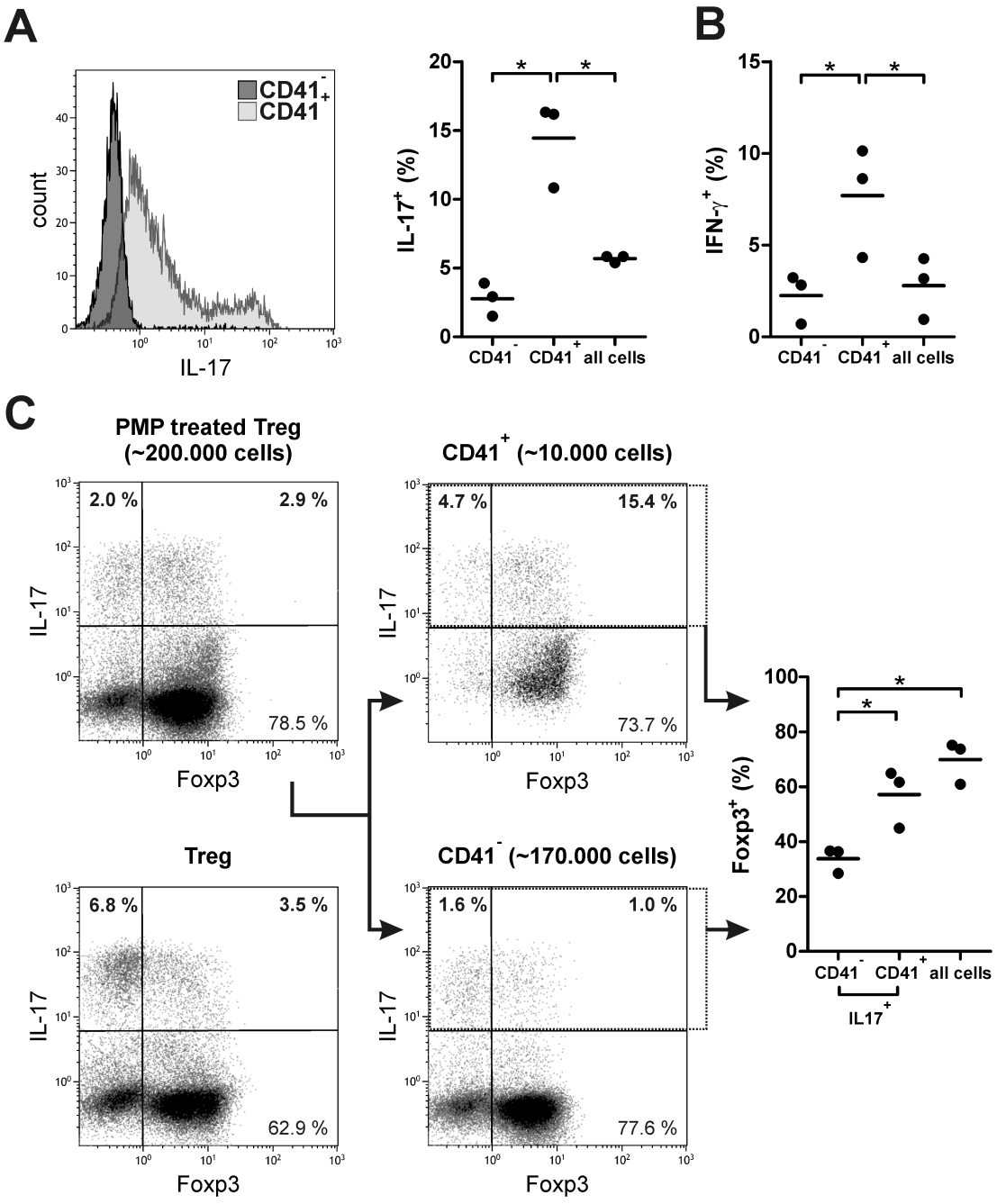

Figure 4. PMPs are bound to Tregs expressing IL-17, IFN-γ, and Foxp3. Tregs were cultured for 7 days in the presence of anti-CD3/anti-CD28-coated beads, human recombinant IL-2, IL-15, and IL-1β, and 5×10^6 PMPs. Intracellular cytokine staining was performed after stimulation with PMA and ionomycin, in the presence of Brefeldin A. Surface and intracellular markers were combined with CD41 staining for flow cytometry analysis of their distribution in the PMP-negative and positive subpopulations; (**A**) IL-17-producing cells, (**B**) IFN-γ-producing cells, and (**C**) IL-17-producing cells that co-express Foxp3. Example IL-17/Foxp3 density plots of all cells, $CD41^-$ and $CD41^+$ Tregs are shown. A density plot of Tregs cultured without PMPs is also shown as reference. Each dot represents the mean of a separate experiment (n = 3) with PMPs from three healthy volunteers tested parallel to each other. The average mean is shown. * $P < 0.05$.

CCR6 positive Tregs constitute a memory-like phenotype [22] that was found to harbor the majority of Tregs with potential IL-17-producing capacity [3,6,15]. Therefore, we assessed CD41 and CCR6 expression on the Tregs in time, combined with HLA-DR which defines a Treg subset with a higher cytokine-producing capacity [27]. Strikingly, a strong binding preference of PMPs was observed for $CCR6^{+}HLA\text{-}DR^{+}$ double-positive, but not for single-positive Tregs, throughout days 1 to 7 of culture (Figure 3B-C). A preference for (memory) $CD45RO^{+}$ and chemokine receptor $CXCR3^{-}$ Tregs was also observed (data not shown).

As PMP co-culture did not fully inhibit IL-17 production, we wanted to check whether the remaining IL-17 producing cells revealed PMP binding at day 7 of culture. Indeed, nearly the entire $CD41^{+}$ Treg pool exhibited enhanced intracellular IL-17 expression and contained approximately 5-fold more potent IL-17 producers, than the $CD41^{-}$ Treg population (Figure 4A). Similar results were obtained for IFN-γ (Figure 4B). Importantly, upon closer examination of the IL-17-producing cells that interacted with the ($CD41^{+}$) PMPs, the majority had retained their FoxP3 expression (Figure 4C), suggesting a state of partial inhibition. In contrast, the majority of IL-17-producing cells that did not have bound PMPs had fully lost their Foxp3 expression, similar to the IL-17-producing cells in the Treg culture without PMPs (Figure 4C). Thus, the PMPs selectively interact with $CCR6^{+}HLA\text{-}DR^{+}$ Tregs throughout co-culture, inhibiting the differentiation of many of these cells into IL-17-producing cells, which was earlier demonstrated by us not to occur before day 6 of culture [3]. Furthermore, of the Tregs with bound PMPs that did acquire IL-17-producing capacity, most were in a $Foxp3^{+}IL\text{-}17^{+}$ transitory state due to the inhibitory effect of the PMPs.

Discussion

In recent years it has become clear that $Foxp3^{+}$ regulatory T cells, known as guardians of dominant self-tolerance and immune homeostasis [1], show plasticity towards IL-17 and IFN-γ production [3-7]. Furthermore, Treg plasticity has been observed towards IFN-γ production in patients with type 1 diabetes [28], and towards IL-17 production in patients with psoriasis [29]. These new insights suggest a pro-inflammatory role for these cells that expands beyond the traditional view of Treg function. We have previously reported that this process is driven by IL-1β and IL-23 [3], and the involvement of other cytokines such as IL-6, IL-21 and TGF-β in T helper 17 (T_H17) cell development have been established as well [30,31]. However, the signaling moieties governing Treg stability are only just beginning to be uncovered.

The immune functions that have recently been ascribed to platelets [8] and their microparticles [9,13,14], their ability to interact with lymphocytes [8,25,26], and the involvement of PMP bound IL-1 in inflammatory arthritis [14], led us to investigate the involvement of PMPs in the differentiation of Tregs into IL-17 and IFN-γ-producing cells.

Our main findings show that PMPs have the capacity to prevent Treg differentiation into IL-17 and IFN-γ-producing cells when activated in the presence of IL-2, IL-15, and the pro-inflammatory cytokine IL-1β. The mechanism of action consisted of rapid and selective P-selectin dependent PMP binding to a $CCR6^{+}HLA\text{-}DR^{+}$ memory-like Treg subset, known to contain the majority of progenitor T_H17-like cells [6,15], disrupting their eventual differentiation into IL-17 producers. The few Tregs with bound PMPs that did acquire IL-17-producing capacity were in a $Foxp3^{+}IL\text{-}17^{+}$ transitory state, likely due to the inhibitory effect of the PMPs.

Leukocytes play a central role in wound repair, and are recruited after coagulation and the resulting vascular inflammation is initiated [32]. PSGL-1 is the high affinity counter receptor for the cell adhesion molecule P-selectin. PSGL-1 is expressed on most leukocytes, and mediates their recruitment to inflamed endothelium by binding P and E-selectin expressed on activated endothelial cells [33]. P-selectin exposure by adherent activated platelets further assists leukocyte recruitment to the inflamed tissue [8]. Moreover, activated platelets release P-selectin positive PMPs [24], which also accumulate at sites of vascular injury [16], and are able to bind PSGL-1 positive leukocytes [25,26].

We show that PMPs can bind peripheral PSGL-1 positive memory-like Tregs through P-selectin-mediated adhesion, possibly participating in their recruitment to sites of vascular injury. Tregs were indeed found to be involved in local tissue repair by restricting the pro-inflammatory response in experimental kidney and lung injury mouse models [34,35]. Vascular infiltration of T_H17 and T_H1 cells is enhanced in patients with systemic vasculitis, and fewer Tregs were observed in the lesions [36,37]. Interestingly, $Foxp3^{+}$ cells were shown to contribute to the IL-17 production in vascular lesions of these patients [38]. Our observations fuel the tantalizing possibility that PMPs might assist in the control, and eventual resolution, of inflammation during tissue repair, by stabilizing Treg phenotype and preventing their differentiation into T_H1 or T_H17-like cells in a pro-inflammatory microenvironment. One could argue that PMPs can easily enter inflamed tissue due to their small size and ability to interact with leukocytes, allowing them to hitchhike to the site of inflammation to exert their regulatory function. P-selectin expression on platelets was found to be upregulated in patients with systemic vasculitis [39]. Also, macrophages are key players in the regulation of tissue inflammation [40], express PSGL-1 which promotes

adherence and functional changes [41], and their pro-inflammatory capacity was also found to be inhibited by PMPs [42]. Finally, loss of P-selectin [43,44] and PSGL-1 [43] has been suggested to promote lupus.

Increased PSGL-1 expression was observed on all Tregs concomitantly with PMP binding upon Treg activation. Nevertheless, the PMPs showed a high preference for $CCR6^{+}HLA\text{-}DR^{+}$ double positive Tregs, suggesting additional requirements need to be met for effective PMP binding. A possible explanation for this differential binding is that only upon T cell activation gycosyltransferases required to modify PSGL-1 to its active binding state are upregulated [45].

PSGL-1 engagement induces downstream signaling events that affect T cell phenotype and function [33]. Deletion of PSGL-1 increased T cell proliferation and exacerbated inflammation in a mouse model [46]. Initial data suggest that PMPs can affect Treg proliferation (data not shown), and might constitute one of the mechanisms for their remarkable ability to hamper Treg differentiation into IL-17-producing cells, as we have previously shown that this transition requires sufficient cell proliferation [3]. Platelets have also been shown to attenuate T cell proliferation, but in contrast to PMPs, promoted T cell differentiation and pro-inflammatory cytokine production *in vitro* [47]. Although PMPs did not significantly alter overall cell death in our study, PSGL-1 cross-linking was found to induce death of activated T cells [48], and might also participate in the observed effect of PMPs on the $CCR6^{+}HLA\text{-}DR^{+}$ Treg subset. Other scenarios could include the involvement of additional signaling pathways next to PSGL-1, for example through the transfer of genetic information from PMPs to their bound Tregs [11], or by initiating Treg-Treg signaling by PMP binding to multiple Tregs [25]. The involvement of other adhesion molecules should also be considered, exemplified by the ability of CD18 to keep Treg differentiation into IL-17-producing cells in check [49].

In contrast to what the name implies, most PMPs in the circulation were found not to originate from platelets, but are instead produced by megakaryocytes in the bone marrow [50,51]. These megakaryocyte-derived microparticles (MKMPs) are abundant in healthy individuals [9,12], while platelet-derived microparticles, identified by the expression of platelet activation markers P-selectin and/or CD63, are only observed during (cardiovascular) disease [24,52]. This implies that while MKMPs have a more systemic function, PMPs may act locally at sites of platelet activation, and each have their own distinct role in homeostasis. We used platelet apheresis units as a source for our PMPs, since they are known to generate relatively large quantities of PMPs in a controlled and sterile environment [53]. The majority of the isolated PMPs were P-selectin positive, and thus

originated from activated platelets in the concentrates. Our findings also add to the understanding of PMPs in platelet transfusion medicine, of which little is known thus far [54]. We have identified a novel function of PMPs to selectively bind a specialized subset of T_H17-like progenitor cells in the Treg compartment, and inhibit their differentiation into potentially pathogenic effector cells. The direct involvement of the cell adhesion molecule P-selectin and its counter receptor PSGL-1 in this process, suggests a role for PMPs in vascular healing by participating in the regulation of the required inflammatory response.

Methods

PMP isolation, storage and anti-P-selectin mAb blocking

Single donor platelet-rich plasma (PRP) was collected from three healthy volunteers by apheresis upon written informed consent according to the Declaration of Helsinki for scientific use. Using a component collection system (MCS+, Haemonetics, Braintree, MA) in combination with Acid Citrate Dextrose Solution A, 300×10^9 leukoreduced ($<1\times10^6$ leukocytes/unit) platelets were collected in 300 mL of plasma, and stored in a lateral shaking device at 22 ± 2°C for 7 days.

At day 7 of storage PMPs were isolated from the PRP product under sterile conditions using a differential centrifugation method previously described [55]: The PRP was centrifuged at 2000g for 15 min to remove platelets and cell debris. The supernatant was aliquotted (1 mL), centrifuged for 45 min at 20.000g to pellet PMPs, and washed with 0.22 µm filtered calcium-free Ringer's solution (125 mM NaCl, 5 mM KCl, 1 mM $MgSO_4$, 32 mM HEPES, 5 mM glucose, 0.2% bovine serum albumin, pH 7.4). The PMPs were then resuspended in 10 µL calcium-free Ringer's solution, snap-frozen with liquid N_2, and stored at -80°C until use. The microparticle purity and quantity was assessed by flow cytometry on a FACSCalibur system (BD Biosciences, Franklin Lakes NJ, USA) as previously described [56], using sulfate latex microspheres (0.9 µm; Invitrogen, Carlsbad CA, USA), washed Flow-Count Fluorospheres (Beckman Coulter, Brea CA, USA), and combined Annexin V-FLUOS (Roche, Basel, Switzerland) and anti-CD41-PE mAb (P2; Beckman Coulter) labeling.

P-selectin blocking was performed by incubating PMPs for 30 min at room temperature in 1 mL calcium-free Ringer's solution containing anti-P-selectin-FITC mAb (10 µg/mL, AK-4; eBioscience, Uithoorn, The Netherlands), known to block P-selectin [57]. PMPs were pelleted by centrifugation and all but 10 µL of supernatant was removed. PMPs incubated with FITC-labeled isotype mAb or plain calcium-free Ringer's solution served as a negative control. PMPs were then washed with calcium-free Ringer's solution. Antibody binding was checked by flow cytometry directly after blocking, and on PMPs recovered from day 7 culture

medium of co-cultures with Tregs. PS blocking of PMPs with human recombinant Annexin V (100 µg/mL; kindly provided by Dr. W.L. van Heerde) was performed in a similar fashion, with the addition of 2.5 mM calcium during blocking and throughout culture to enable effective Annexin V binding.

Cell isolation and culture of cells

PBMCs were isolated by density gradient centrifugation (Lymphoprep; Nycomed-Pharma AS, Oslo, Norway) of buffy coats obtained from healthy donors upon written informed consent according to the Declaration of Helsinki with regard to scientific use. $CD4^+$ T cells were purified from PBMCs by magnetic bead sorting using CD4 MicroBeads (Miltenyi Biotec, Leiden, The Netherlands) according to the manufacturer's instructions. Purified $CD4^+$ T cells were labeled with CD4-FITC (MT310; DAKO, Glostrup, Denmark) and CD25-PE (MA251; BD Biosciences, Erembodegem, Belgium), after which $CD4^+CD25^{high}$ cells (Tregs) were isolated by high-purity flow cytometry cell sorting using an Aria cell sorter (Beckman Coulter). A rerun was performed to analyze the cell purity of the sorted cells; sorted cells were always >99% pure.

Cells were cultured in culture medium (RPMI-1640 with glutamax supplemented with 0.02 mM pyruvate, 100 U/mL penicillin, 100 µg/mL streptomycin [all from Gibco, Paisley, United Kingdom], and 10% human pooled serum) at 37°C, 95% humidity, and 5% CO2, in 96-well round-bottom plates (Greiner, Frickenhausen, Germany). Anti-CD3/anti-CD28-coated beads (1:10; Invitrogen, Breda, The Netherlands), and recombinant human cytokines IL-2 (25 U/mL; Cetus, Amsterdam, The Netherlands), IL-15 (10 ng/mL), and IL-1β (50 ng/mL) (Biosource, Etten-Leur, The Netherlands) were added at the start of the cultures, in the presence or absence of an ascending number of PMPs. CD40 blocking on Tregs was performed by the addition of an antagonistic anti-CD40 mAb kindly provided by Dr. M. de Boer (1 µg/mL; Tanox Pharma B.V., Amsterdam, The Netherlands) at least 1 hour before the addition of PMPs. ThinCerts™ cell culture inserts (0.4 µm; Greiner Bio-one, Wemmel, Belgium) for 24-well flat-bottom plates were used for the transwell assay, with the cells and the PMPs placed in the upper and the lower compartments, respectively.

Flow cytometry and antibodies

Cells were phenotypically characterized using the FC500 and the Gallios^{TM} Flow Cytometers (Beckman Coulter, Miami, FL, USA). The following conjugated mAb antibodies were used: CD4(MT310)-FITC, CD27(M-T271)-FITC (DAKO), CD25(M-A251)-PE, CCR6(11A9)-PE (BD Biosciences), PSGL-1(FLEG)-APC, CD25(BC96)-PeCy7, CD127(eBioRDR5)-PeCy7 (eBioscience), CD4(SFCI12T4D11)-ECD or PeCy7, CD41(P2)-FITC or PE, CD62L(DREG56)-ECD, HLA-DR(Immu-357)-ECD (Beckman Coulter). Prior to flow

cytometry analyses, all conjugates were titrated and individually tested for sensitivity, resolution and compensation of spectral overlap. Isotype-matched antibodies were used to define marker settings.
Intracellular analysis of Foxp3(PCH101)-FITC, IL-17A(EBIO64DEC17)-AlexaFluor647, and IFN-γ(4S.B3)-PeCy7 (eBioscience) was performed after fixation and permeabilization using Fix/Perm reagent (eBioscience). Before intracellular cytokine measurements, the cells were stimulated for 4 hours with PMA (12.5 ng/mL) plus ionomycin (500 ng/mL) in the presence of Brefeldin A (5 µg/mL; Sigma-Aldrich, Zwijndrecht, The Netherlands). All flow cytometry data were analyzed using Kaluza® software (Beckman Coulter). The "logicle" scale was applied in certain cases to better visualize negative populations.

Statistics
Paired t tests, repeated measures one-way (+Tukey's post-test) or two-way (+Bonferroni post-test) ANOVAs were used for statistical analysis. The reported (two-sided) *p* values of <0.05 were considered significant and are indicated with an asterisk (*). Data in the text is presented as mean ± SD.

Acknowledgements

We thank Gaby Derksen and Rob Woestenenk from the Department of Laboratory Medicine for performing the flow cytometry cell sorting.

References

1 Sakaguchi S, Miyara M, Costantino CM, Hafler DA. FOXP3+ regulatory T cells in the human immune system. *Nat. Rev. Immunol.* 10(7), 490-500 (2010).

2 O'Shea JJ, Paul WE. Mechanisms underlying lineage commitment and plasticity of helper CD4+ T cells. *Science* 327(5969), 1098-1102 (2010).

3 Koenen HJ, Smeets RL, Vink PM, van Rijssen E, Boots AM, Joosten I. Human CD25highFoxp3pos regulatory T cells differentiate into IL-17-producing cells. *Blood* 112(6), 2340-2352 (2008).

4 Beriou G, Costantino CM, Ashley CW *et al*. IL-17-producing human peripheral regulatory T cells retain suppressive function. *Blood* 113(18), 4240-4249 (2009).

5 Voo KS, Wang YH, Santori FR *et al*. Identification of IL-17-producing FOXP3+ regulatory T cells in humans. *Proc. Natl. Acad. Sci. U. S. A* 106(12), 4793-4798 (2009).

6 Ayyoub M, Deknuydt F, Raimbaud I *et al*. Human memory FOXP3+ Tregs secrete IL-17 ex vivo and constitutively express the T(H)17 lineage-specific transcription factor RORgamma t. *Proc. Natl. Acad. Sci. U. S. A* 106(21), 8635-8640 (2009).

7 Miyara M, Yoshioka Y, Kitoh A *et al*. Functional delineation and differentiation dynamics of human CD4+ T cells expressing the FoxP3 transcription factor. *Immunity.* 30(6), 899-911 (2009).

8 Semple JW, Italiano JE, Jr., Freedman J. Platelets and the immune continuum. *Nat. Rev. Immunol.* 11(4), 264-274 (2011).

9 Aatonen M, Gronholm M, Siljander PR. Platelet-derived microvesicles: multitalented participants in intercellular communication. *Semin. Thromb. Hemost.* 38(1), 102-113 (2012).

10 Rozmyslowicz T, Majka M, Kijowski J *et al*. Platelet- and megakaryocyte-derived microparticles transfer CXCR4 receptor to CXCR4-null cells and make them susceptible to infection by X4-HIV. *AIDS* 17(1), 33-42 (2003).

11 Laffont B, Corduan A, Ple H *et al*. Activated platelets can deliver mRNA regulatory Ago2*microRNA complexes to endothelial cells via microparticles. *Blood* 122(2), 253-261 (2013).

12 Owens AP, III, Mackman N. Microparticles in hemostasis and thrombosis. *Circ. Res.* 108(10), 1284-1297 (2011).

13 Sprague DL, Elzey BD, Crist SA, Waldschmidt TJ, Jensen RJ, Ratliff TL. Platelet-mediated modulation of adaptive immunity: unique delivery of CD154 signal by platelet-derived membrane vesicles. *Blood* 111(10), 5028-5036 (2008).

14 Boilard E, Nigrovic PA, Larabee K *et al*. Platelets amplify inflammation in arthritis via collagen-dependent microparticle production. *Science* 327(5965), 580-583 (2010).

15 Duhen T, Duhen R, Lanzavecchia A, Sallusto F, Campbell DJ. Functionally distinct subsets of human FOXP3+ Treg cells that phenotypically mirror effector Th cells. *Blood* 119(19), 4430-4440 (2012).

16 Merten M, Pakala R, Thiagarajan P, Benedict CR. Platelet microparticles promote platelet interaction with subendothelial matrix in a glycoprotein IIb/IIIa-dependent mechanism. *Circulation* 99(19), 2577-2582 (1999).

17 Cauwenberghs S, Feijge MA, Harper AG, Sage SO, Curvers J, Heemskerk JW. Shedding of procoagulant microparticles from unstimulated platelets by integrin-mediated destabilization of actin cytoskeleton. *FEBS Lett.* 580(22), 5313-5320 (2006).

18 Godfrey WR, Ge YG, Spoden DJ *et al*. In vitro-expanded human CD4(+)CD25(+) T-regulatory cells can markedly inhibit allogeneic dendritic cell-stimulated MLR cultures. *Blood* 104(2), 453-461 (2004).

19 Hoffmann P, Eder R, Kunz-Schughart LA, Andreesen R, Edinger M. Large-scale in vitro expansion of polyclonal human CD4(+)CD25high regulatory T cells. *Blood* 104(3), 895-903 (2004).

20 Koenen HJ, Fasse E, Joosten I. CD27/CFSE-based ex vivo selection of highly suppressive alloantigen-specific human regulatory T cells. *J. Immunol.* 174(12), 7573-7583 (2005).

21 Singh SP, Zhang HH, Foley JF, Hedrick MN, Farber JM. Human T cells that are able to produce IL-17 express the chemokine receptor CCR6. *J. Immunol.* 180(1), 214-221 (2008).

22 Kleinewietfeld M, Puentes F, Borsellino G, Battistini L, Rotzschke O, Falk K. CCR6 expression defines regulatory effector/memory-like cells within the CD25(+)CD4+ T-cell subset. *Blood* 105(7), 2877-2886 (2005).

23 Freeman GJ, Casasnovas JM, Umetsu DT, DeKruyff RH. TIM genes: a family of cell surface phosphatidylserine receptors that regulate innate and adaptive immunity. *Immunol. Rev.* 235(1), 172-189 (2010).

24 van der Zee PM, Biro E, Ko Y *et al*. P-selectin- and CD63-exposing platelet microparticles reflect platelet activation in peripheral arterial disease and myocardial infarction. *Clin. Chem.* 52(4), 657-664 (2006).

25 Forlow SB, McEver RP, Nollert MU. Leukocyte-leukocyte interactions mediated by platelet microparticles under flow. *Blood* 95(4), 1317-1323 (2000).

26 Nomura S, Okamae F, Abe M *et al*. Platelets expressing P-selectin and platelet-derived microparticles in stored platelet concentrates bind to PSGL-1 on filtrated leukocytes. *Clin. Appl. Thromb. Hemost.* 6(4), 213-221 (2000).

27 Baecher-Allan C, Wolf E, Hafler DA. MHC class II expression identifies functionally distinct human regulatory T cells. *J. Immunol.* 176(8), 4622-4631 (2006).

28 McClymont SA, Putnam AL, Lee MR *et al*. Plasticity of human regulatory T cells in healthy subjects and patients with type 1 diabetes. *J. Immunol.* 186(7), 3918-3926 (2011).

29 Bovenschen HJ, van de Kerkhof PC, van Erp PE, Woestenenk R, Joosten I, Koenen HJ. Foxp3+ regulatory T cells of psoriasis patients easily differentiate into IL-17A-producing cells and are found in lesional skin. *J. Invest Dermatol.* 131(9), 1853-1860 (2011).

30 Annunziato F, Cosmi L, Liotta F, Maggi E, Romagnani S. Defining the human T helper 17 cell phenotype. *Trends Immunol.* 33(10), 505-512 (2012).

31 Weaver CT, Hatton RD. Interplay between the TH17 and TReg cell lineages: a (co-)evolutionary perspective. *Nat. Rev. Immunol.* 9(12), 883-889 (2009).

32 Eming SA, Krieg T, Davidson JM. Inflammation in wound repair: molecular and cellular mechanisms. *J. Invest Dermatol.* 127(3), 514-525 (2007).

33 Carlow DA, Gossens K, Naus S, Veerman KM, Seo W, Ziltener HJ. PSGL-1 function in immunity and steady state homeostasis. *Immunol. Rev.* 230(1), 75-96 (2009).

34 D'Alessio FR, Tsushima K, Aggarwal NR *et al*. CD4+CD25+Foxp3+ Tregs resolve experimental lung injury in mice and are present in humans with acute lung injury. *J. Clin. Invest* 119(10), 2898-2913 (2009).

35 Gandolfo MT, Jang HR, Bagnasco SM *et al*. Foxp3+ regulatory T cells participate in repair of ischemic acute kidney injury. *Kidney Int.* 76(7), 717-729 (2009).

36 Samson M, Audia S, Fraszczak J *et al*. Th1 and Th17 lymphocytes expressing CD161 are implicated in giant cell arteritis and polymyalgia rheumatica pathogenesis. *Arthritis Rheum.* 64(11), 3788-3798 (2012).

37 Terrier B, Geri G, Chaara W *et al*. Interleukin-21 modulates Th1 and Th17 responses in giant cell arteritis. *Arthritis Rheum.* 64(6), 2001-2011 (2012).

38 Espigol-Frigole G, Corbera-Bellalta M, Planas-Rigol E *et al*. Increased IL-17A expression in temporal artery lesions is a predictor of sustained response to glucocorticoid treatment in patients with giant-cell arteritis. *Ann. Rheum. Dis.* 72(9), 1481-1487 (2013).

39 Maugeri N, Baldini M, Rovere-Querini P, Maseri A, Sabbadini MG, Manfredi AA. Leukocyte and platelet activation in patients with giant cell arteritis and polymyalgia rheumatica: a clue to thromboembolic risks? *Autoimmunity* 42(4), 386-388 (2009).

40 Murray PJ, Wynn TA. Protective and pathogenic functions of macrophage subsets. *Nat. Rev. Immunol.* 11(11), 723-737 (2011).

41 Fox R, Nhan TQ, Law GL, Morris DR, Liles WC, Schwartz SM. PSGL-1 and mTOR regulate translation of ROCK-1 and physiological functions of macrophages. *EMBO J.* 26(2), 505-515 (2007).

42 Sadallah S, Eken C, Martin PJ, Schifferli JA. Microparticles (ectosomes) shed by stored human platelets downregulate macrophages and modify the development of dendritic cells. *J. Immunol.* 186(11), 6543-6552 (2011).

43 He X, Schoeb TR, Panoskaltsis-Mortari A *et al*. Deficiency of P-selectin or P-selectin glycoprotein ligand-1 leads to accelerated development of glomerulonephritis and increased expression of CC chemokine ligand 2 in lupus-prone mice. *J. Immunol.* 177(12), 8748-8756 (2006).

44 Morris DL, Graham RR, Erwig LP *et al*. Variation in the upstream region of P-Selectin (SELP) is a risk factor for SLE. *Genes Immun.* 10(5), 404-413 (2009).

45 Ley K, Kansas GS. Selectins in T-cell recruitment to non-lymphoid tissues and sites of inflammation. *Nat. Rev. Immunol.* 4(5), 325-335 (2004).

46 Matsumoto M, Miyasaka M, Hirata T. P-selectin glycoprotein ligand-1 negatively regulates T-cell immune responses. *J. Immunol.* 183(11), 7204-7211 (2009).

47 Gerdes N, Zhu L, Ersoy M *et al*. Platelets regulate CD4(+) T-cell differentiation via multiple chemokines in humans. *Thromb. Haemost.* 106(2), 353-362 (2011).

48 Chen SC, Huang CC, Chien CL *et al*. Cross-linking of P-selectin glycoprotein ligand-1 induces death of activated T cells. *Blood* 104(10), 3233-3242 (2004).

49 Singh K, Gatzka M, Peters T *et al*. Reduced CD18 levels drive regulatory T cell conversion into Th17 cells in the CD18hypo PL/J mouse model of psoriasis. *J. Immunol.* 190(6), 2544-2553 (2013).

50 Rank A, Nieuwland R, Delker R *et al*. Cellular origin of platelet-derived microparticles in vivo. *Thromb. Res.* 126(4), e255-e259 (2010).

51 Flaumenhaft R, Dilks JR, Richardson J *et al*. Megakaryocyte-derived microparticles: direct visualization and distinction from platelet-derived microparticles. *Blood* 113(5), 1112-1121 (2009).

52 Mobarrez F, He S, Broijersen A *et al*. Atorvastatin reduces thrombin generation and expression of tissue factor, P-selectin and GPIIIa on platelet-derived microparticles in patients with peripheral arterial occlusive disease. *Thromb. Haemost.* 106(2), 344-352 (2011).

53 Cauwenberghs S, Feijge MA, Harper AG, Sage SO, Curvers J, Heemskerk JW. Shedding of procoagulant microparticles from unstimulated platelets by integrin-mediated destabilization of actin cytoskeleton. *FEBS Lett.* 580(22), 5313-5320 (2006).

54 Morrell CN. Immunomodulatory mediators in platelet transfusion reactions. *Hematology. Am. Soc. Hematol. Educ. Program.* 2011 470-474 (2011).

55 Dinkla S, Brock R, Joosten I, Bosman GJ. Gateway to understanding microparticles: standardized isolation and identification of plasma membrane-derived vesicles. *Nanomedicine. (Lond)* 8(10), 1657-1668 (2013).

56 Dinkla S, Wessels K, Verdurmen WP *et al*. Functional consequences of sphingomyelinase-induced changes in erythrocyte membrane structure. *Cell Death. Dis.* 3 e410 (2012).

57 Li JM, Podolsky RS, Rohrer MJ *et al*. Adhesion of activated platelets to venous endothelial cells is mediated via GPIIb/IIIa. *J. Surg. Res.* 61(2), 543-548 (1996).

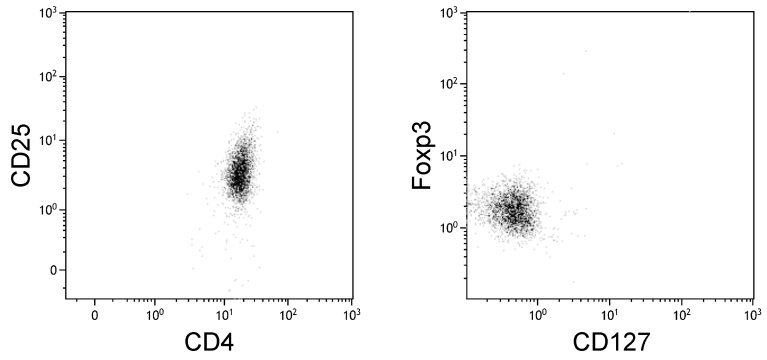

Figure S1. CD4$^+$CD25^{high}CD27$^+$CD127^{low}Foxp3$^+$ Tregs cell sorting. After CD4$^+$ T cell isolation from PBMCs by magnetic bead sorting, CD4$^+$CD25^{high} T cells were purified by fluorescence-activated cell sorting. The sorted cells were checked for surface CD25, CD27, CD127, and intracellular FoxP3 expression. Flow cytometry was employed for the analyses.

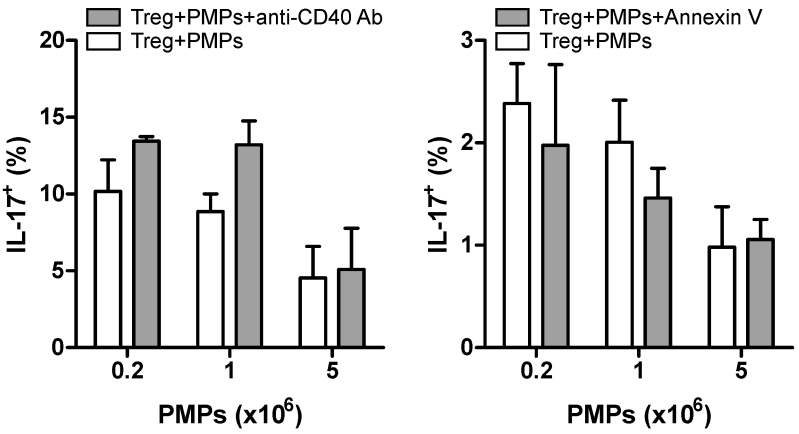

Figure S2. CD40 and PS blocking does not affect PMP inhibition of Treg differentiation. Left: Intracellular staining of IL-17 on Tregs co-cultured with PMPs in the presence of anti-CD40 antagonistic mAb. Right: Intracellular staining of IL-17 on Tregs co-cultured with untreated and Annexin V blocked PMPs. Tregs were cultured for 7 days in the presence of anti-CD3/anti-CD28-coated beads, and human recombinant IL-2, IL-15, and IL-1β, in the presence of PMPs (n = 3 PMP donors). Intracellular cytokine staining was performed after stimulation with PMA and ionomycin, in the presence of Brefeldin A. Flow cytometry was employed for the analyses. Mean and SD are shown.

8

Summary and General Discussion

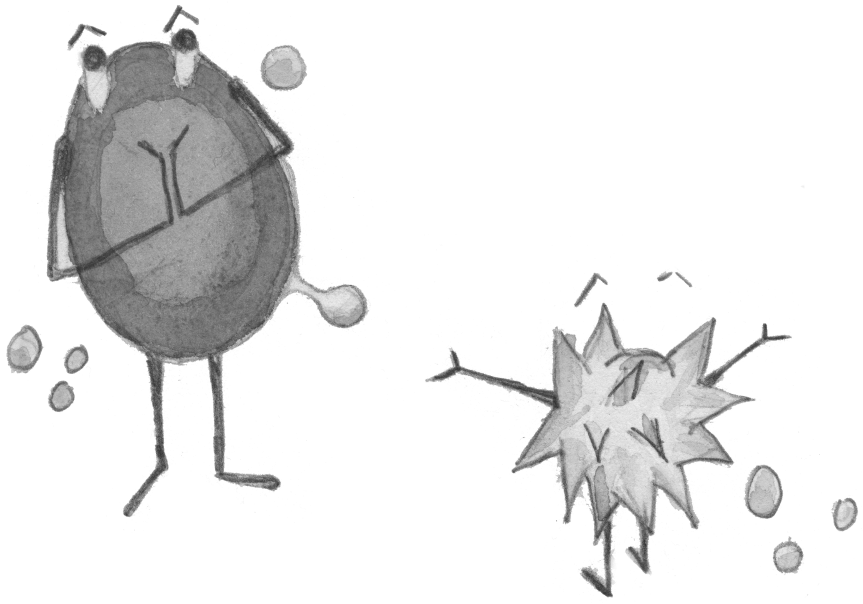

Summary and General Discussion

Erythrocytes are unique in their ability to transport oxygen to, and remove CO_2 from the peripheral tissues. Another unique feature of the erythrocyte is its extensive deformability, which is required to efficiently pass through the narrow capillaries of the microvasculature and the fenestrae in the spleen [1]. Their lack of intracellular organelles prevents erythrocytes from undergoing apoptosis in the manner of nucleated cells. However, erythrocytes have a well-defined life span of about 120 days [2], resulting in the removal of 2.5 million old erythrocytes from the circulation per second.

Although the exact mechanisms governing physiological erythrocyte removal remain elusive, significant progress has been made by the identification of a few key regulatory components. Binding of physiological autoantibodies to antigens that are formed as the result of oxidative damage, is assumed to be the essential trigger leading to erythrocyte phagocytosis by the reticulo-endothelial system [3]. Phosphatidylserine (PS) externalization to the outer plasma membrane leaflet plays a central role in the apoptosis of nucleated cells, as it leads to recognition and subsequent phagocytosis of these cells by macrophages. Research fueled by this knowledge has led to the consensus that PS exposure is a co-factor in the removal of damaged erythrocytes as well [4].

Erythrocyte vesiculation has been suggested to play an integral part in erythrocyte survival, by enabling the erythrocyte to get rid of damaged cell components [5]. Although much progress has been made in recent years in our ability to characterize the resulting extracellular microparticles, we are only just beginning to understand their function in the homeostasis of the human body.

The majority of this thesis focusses on erythrocyte plasma membrane changes that occur during storage and systemic inflammation, in the context of erythrocyte removal. In the last part of this thesis, the attention shifts towards the characterization of extracellular microparticles in transfusion products, and the role of these microparticles in immune homeostasis. An overview of the current knowledge regarding these topics is provided in **Chapter 1**.

Erythrocyte storage

Erythrocyte transfusions save the lives of millions of patients coping with severe blood loss after trauma, inadequate erythrocyte production or enhanced erythrocyte clearance [6].

However, erythrocyte transfusions can also have serious side effects, such as acute lung injury, severe organ damage due to iron deposition, vasoconstriction, and alloantibody and autoantibody formation [7]. Especially a frequent transfusion regime causes severe side effects, as is often the case for patients suffering from a myelodysplastic syndrome, aplastic anemia or a hemoglobinopathy. The structural and biochemical changes that occur during erythrocyte storage are thought to be responsible for these side effects [8].

A prominent side effect that arises often after repeated transfusions, is the generation of anti-erythrocyte autoantibodies [9]. A plausible explanation for this side effect is the formation of aberrant antigens during erythrocyte storage. In order to identify these antigens, we screened erythrocytes for pathologic antigen formation during storage (**Chapter 2**). We observed an increase in pathologic anti-erythrocyte autoantibody binding with storage time, demonstrating that non-physiological autoantigens are formed during storage. Immunochemical and mass spectrometric analysis revealed several candidate antigens on the erythrocytes, which differed from those on erythrocyte concentrate-derived microparticles. The latter suggests that storage microparticles have immunological activity that is different from stored erythrocytes.

In the Netherlands, erythrocyte concentrates must be used for transfusion within 35 days after their collection, in order to meet the quality standards of a maximum of 0.8% hemolysis in the concentrate and 75% erythrocyte survival during the first 24 hours after transfusion [10,11]. Erythrocyte survival after transfusion is seldom measured due to practical limitations, but a large variation in erythrocyte survival is observed after transfusion [12], which is likely related to both the blood donor and the recipient patient. The commonly used parameters for erythrocyte concentrate quality, such as hemolysis and ATP concentration, are poor predictors of erythrocyte survival after transfusion [13-15].

In **Chapter 3**, we investigated whether PS exposure might be a parameter for donor-dependent variation in erythrocyte product quality. PS exposure was found to vary between donors, both on freshly isolated and stored erythrocytes, and increased with time in most concentrates. The initial PS exposure was predictive for erythrocyte PS exposure upon stress *in vitro*, and was associated with hemolysis and microparticle concentration. These data reveal that the fraction of PS-exposing erythrocytes is a sensitive parameter of cell integrity in erythrocyte concentrates. Given its functional relationship with erythrocyte removal, PS exposure may be an indicator for erythrocyte survival after transfusion as well.

During the 1940's and 1950's, several erythrocyte survival studies were performed in volunteers *in vivo* [16]. The wealth of biochemical data on erythrocyte changes during

storage that have been revealed since that time [8], including the work described in **Chapters 2** and **3**, calls for erythrocyte quality trials *in vivo* aimed at assessing the impact of these changes on erythrocyte survival. These trials can, for example, clarify whether erythrocyte HbA_{1c} concentration [17], PS exposure, and/or vesiculation during storage may affect and/or predict erythrocyte survival after transfusion. If so, they can be used as a biomarker to select superior erythrocyte units, or even donors, for patients who require repeated transfusions over an extended period of time. Unfortunately, erythrocyte clearance characteristics in mice are different from those in humans [18], ruling out the use of mouse models for the reliable evaluation of erythrocyte survival parameters. The use of radioactive isotopes (e.g. chromium-51), and the recent biotinylation approach to label erythrocytes for erythrocyte survival trials, raise concerns regarding their potentially harmful side effects [19,20]. Instead, we propose to transfuse erythrocyte concentrates mismatched for minor blood group antigens, in order to enable identification and/or isolation of the transfused erythrocytes [12].

The plethora of data available on the changes observed in the erythrocyte during storage [8] sparked the discussion that longer storage time increases the risk of side effects for the recipient. Controversy remains over whether or not erythrocyte storage time affects clinical outcome in the total patient population [21-23]. In order to resolve this controversy, two large clinical trials are currently underway, the US-based initiative Red Cell Storage Duration Study (RECESS), and the complementary UK and Canadian co-initiative Age of Blood Evaluation (ABLE) [22]. Meanwhile, we support the recent shift in research focus towards (the regulation of) intracellular changes during erythrocyte storage, made possible by new techniques such as proteomics and metabolomics [24], as this will propel our understanding of the erythrocyte storage lesion to the next level. Also, the use of novel *ex vivo* erythropoiesis techniques in combination with siRNA protein knockdown [25], lentiviral expression of proteins tagged with (fluorescent) reporter proteins, or lentiviral knockdown [26] will certainly contribute to our understanding of erythrocyte homeostasis in health and disease.

Erythrocyte membrane lipid remodeling in the critically ill

Erythrocyte transfusions are associated with increased morbidity and mortality in critically ill patients [27]. The systemic inflammation that is typically observed in these patients is likely to affect the function and survival of the transfused erythrocytes, and this effect may very well become more pronounced with storage. This notion is fueled by the observation that erythrocyte shape, deformability, and aggregability were altered in septic patients [28,29].

Interestingly, incubation of erythrocytes from healthy volunteers with plasma of septic patients was found to induce PS exposure and hydrolysis of membrane sphingomyelin (SM), generating ceramide [30]. Ceramide formation is known to alter plasma membrane function and integrity [31]. Sphingomyelinase (SMase) is secreted into the circulation during inflammation, and is the primary catalyst for SM hydrolysis [32].

We studied the functional consequences of SMase on erythrocyte function in detail (**Chapter 4**). We found that erythrocytes are very sensitive to SMase-induced ceramide formation. Ceramide build-up in the plasma membrane led to loss of discoid shape, followed by PS exposure, and subsequent loss of cell integrity. During this process, enhanced microparticle formation and reduced deformability were observed. Erythrocytes aged both *in vivo* and *in vitro* were far more sensitive to SMase-induced changes than younger erythrocytes.

In **Chapter 5**, we describe the analysis of the plasma membrane lipid content of freshly isolated erythrocytes from healthy volunteers after incubation with the plasma of patients with septic shock. While ceramide could not be detected, we found markedly increased levels of lysophosphatidylcholine (LPC), which is produced by phospholipase A2. Although secretory phospholipase A2 IIA was greatly enhanced in the plasma of septic patients, its concentration did not correlate with the LPC levels. Enhanced LPC levels were not detected when erythrocytes were incubated with the plasma of healthy volunteers, in whom sepsis was simulated by infusion of a low dose of lipopolysaccharide. Thus, the experimentally-induced acute endotoxemia model does not fully mimic sepsis at the erythrocyte level. Interestingly, erythrocyte PS exposure increased in these subjects after lipopolysaccharide infusion.

These data show that the lipid constituents of the erythrocyte membrane are altered during systemic inflammation, which may affect erythrocyte survival in these patients. Stored erythrocytes have an enhanced sensitivity for the SMase-induced changes, as described in **Chapter 4**. The increase of this sensitivity with storage time indicates that the age of erythrocyte concentrates may very well affect transfusion outcome in patients with systemic inflammation. This issue may be clarified by the aforementioned clinical studies [22]. Although lipid metabolism is significantly altered during systemic inflammation [33], lipid alterations in the erythrocyte have not received much attention so far [34]. The work described in **Chapter 5** paves the way for a more detailed investigation of the effects of lysophospholipids on the (stored) erythrocyte and the identity of the lipase(s) responsible for their formation. It will be informative to determine the fate of transfused erythrocytes, including removal rate, PS exposure and LPC content, in patients with systemic inflammation using the noninvasive minor antigen method referred to in the previous section.

The resulting data could then be correlated to other parameters of lipid metabolism, such as phospholipase activity in the plasma.

Extracellular microparticles: harmful or helpful?

During its time in the circulation, the erythrocyte loses membrane surface due to continuous vesiculation [5,35,36]. The resulting vesicles, often termed red cell microparticles (RMPs), are thought to result from an innate process that is intended to remove damaged/aged membrane patches, which postpones the recognition and elimination of functional erythrocytes [5,37-39]. Therefore, it comes as no surprise that erythrocytes shed similar microparticles during blood bank storage [37].

In the last decade, it has become clear that extracellular microparticles play an active role in homeostasis and pathogenesis, the latter including atherosclerosis, autoimmune disorders, and infection [40-42]. This has triggered investigations into the nature and function of microparticles of different origin, including RMPs. In **Chapter 6**, our current understanding of the potential involvement of RMPs in disease and transfusion side-effects is highlighted. RMPs are procoagulant [43,44], and impair vasodilation through NO scavenging [45]. Also, RMPs are involved in the procoagulant state and vaso-occlusions in patients with sickle cell disease [46,47]. Recent data show that RMPs from malaria-infected erythrocytes contribute to inflammation through potent macrophage stimulation [48], and these RMPs have even been suggested to be a means of cellular communication within the parasite population [49].

Until now, RMPs were only incidentally recognized as potential mediators of transfusion-related side-effects. As a result, only a few studies have been performed to assess the implications of the RMP transfusion burden for the recipient. RMPs contain high levels of bound immunoglobulins and complement factors [37], which implies that they have immunomodulatory properties. In **Chapter 2**, we observed that pathologic anti-erythrocyte autoantibodies recognize RMPs from erythrocyte concentrates, suggesting that RMPs expose pathologic autoantigens as well. As RMPs were rapidly removed by cells of the immune system in a rat model [36], a sudden peak in circulating allogeneic RMPs after transfusion is likely to affect immune homeostasis. Indeed, RMPs from erythrocyte concentrates were shown to have a pro-inflammatory effect on monocytes, and to boost subsequent T cell responses *in vitro* [50]. We therefore propose future investigations on RMPs as a potential trigger of erythrocyte transfusion-induced anti-erythrocyte autoantibody formation [9].

In contrast to erythrocytes and RMPs, platelets are increasingly recognized to initiate and accelerate immune responses [51,52]. As reviewed in **Chapter 6**, platelet-derived microparticles (PMPs) possess pro-inflammatory properties of their own, illustrated by the observation that glycoprotein VI-mediated PMP generation causes PMPs to accumulate in the joint fluid of patients suffering from inflammatory arthritis (but not osteoarthritis), inducing an inflammatory response through interleukin-1 signaling [53]. Therefore, PMPs are now implicated to play a role in the inflammatory side-effects often observed after platelet transfusion [54]. Recent work has revealed that most 'PMPs' in the circulation do not originate from platelets at all, but are produced by megakaryocytes instead [55,56]. However, true PMPs, expressing the platelet activation marker P-selectin, are abundantly present in platelet concentrates [57,58], and may have inflammatory functions that are different than those of the megakaryocyte-derived microparticles found in the circulation.

In **Chapter 7**, we present a novel regulatory function of PMPs in regulatory T cell (Treg) plasticity. Forkhead box p3 (Foxp3)-positive Tregs are essential for maintaining dominant self-tolerance and immune homeostasis [59]. However, recent insights have revealed that, upon stimulation, Tregs exhibit plasticity towards a pro-inflammatory phenotype, producing IL-17 and/or IFN-γ [60-64]. The signaling moieties governing Treg stability are only just beginning to be uncovered. We show that PMPs possess the capacity to inhibit cytokine IL-1β-driven differentiation of peripheral blood-derived Tregs into IL-17 and IFN-γ-producing cells. This inhibitory effect was caused by rapid and selective binding of PMPs to a specialized $CCR6^{+}HLA\text{-}DR^{+}$ memory-like Treg subset, which is known to host progenitors of potentially pathogenic IL-17 producers [63,65]. Binding of, and inhibition by PMPs, was P-selectin-dependent, since pre-treatment of PMPs with a P-selectin-blocking antibody inhibited their effect. Our data indicate that PMPs affect cell proliferation, providing a possible mechanism by which the memory-like Treg subset is affected.

Leukocyte recruitment is an essential part of vascular healing [66], involving P-selectin-mediated interaction with the vascular endothelium [67] and the adherence of activated platelets [68]. Vascular infiltration of T_H17 and T_H1 cells is enhanced in patients with systemic vasculitis and $Foxp3^{+}$ Tregs were not observed in the lesions [69,70]. Interestingly, $Foxp3^{+}$ cells contribute to the IL-17 production in vascular lesions of these patients [71]. P-selectin-expressing PMPs that are released by activated platelets, also accumulate at sites of vascular injury [72]. Thus, our findings open up the possibility that PMPs might assist in the control, and eventual resolution, of inflammation during tissue repair, by stabilizing the Treg phenotype in a pro-inflammatory microenvironment. Also, macrophages play a central role in the regulation of tissue inflammation [73], and their function was also found to be

regulated by PMPs [74]. Finally, as we used platelet apheresis units as a source for P-selectin-expressing PMPs, our findings add to the understanding of the effects of PMPs in platelet transfusion medicine.

Conclusion

In this thesis we provide new insights into the erythrocyte storage-induced biochemical changes of the erythrocyte plasma membrane that may contribute to unwanted side effects as well as reduced erythrocyte survival after transfusion. Also, our data indicate that erythrocyte membrane lipid remodeling is linked to reduced erythrocyte survival in patients with systemic inflammation, which might explain the increased morbidity and mortality observed in critically ill patients after transfusion. Future erythrocyte survival studies *in vivo* may help to identify the physiological and pathological significance of the observed changes.

We have also identified a novel activity of PMPs, namely the binding to a specialized subset of Tregs, and the inhibition of their differentiation into pro-inflammatory cytokine-producing cells. The involvement of the cell adhesion molecule P-selectin suggests a role for PMPs in vascular healing by participating in the regulation of the inflammatory response. *In vivo* studies focusing on PMPs in vascular healing and inflammation may shed more light on the physiological relevance of the immune-regulating properties of PMPs.

References

1 Mohandas N, Gallagher PG. Red cell membrane: past, present, and future. *Blood* 112(10), 3939-3948 (2008).

2 Dornhorst AC. The interpretation of red cell survival curves. *Blood* 6(12), 1284-1292 (1951).

3 Kay M. Immunoregulation of cellular life span. *Ann. N. Y. Acad. Sci.* 1057 85-111 (2005).

4 Brown GC, Neher JJ. Eaten alive! Cell death by primary phagocytosis: 'phagoptosis'. *Trends Biochem. Sci.* 37(8), 325-332 (2012).

5 Willekens FL, Werre JM, Groenen-Dopp YA, Roerdinkholder-Stoelwinder B, de Pauw B, Bosman GJ. Erythrocyte vesiculation: a self-protective mechanism? *Br. J. Haematol.* 141(4), 549-556 (2008).

6 World Health Organization. Blood safety and availability - Fact sheet N°279. http://www.who.int/mediacentre/factsheets/fs279/en/; 2013 Jul. Report No.: Fact sheet N°279.

7 Perrotta PL, Snyder EL. Non-infectious complications of transfusion therapy. *Blood Rev.* 15(2), 69-83 (2001).

8 Bosman GJ, Werre JM, Willekens FL, Novotny VM. Erythrocyte ageing in vivo and in vitro: structural aspects and implications for transfusion. *Transfus. Med.* 18(6), 335-347 (2008).

9 Young PP, Uzieblo A, Trulock E, Lublin DM, Goodnough LT. Autoantibody formation after alloimmunization: are blood transfusions a risk factor for autoimmune hemolytic anemia? *Transfusion* 44(1), 67-72 (2004).

10 Dumont LJ, AuBuchon JP. Evaluation of proposed FDA criteria for the evaluation of radiolabeled red cell recovery trials. *Transfusion* 48(6), 1053-1060 (2008).

11 European Directorate for the Quality of Medicines & HealthCare. Guide to the Preparation, Use, and Quality Assurance of Blood Components. 17 ed. Council of Europe publishing; 2013.

12 Luten M, Roerdinkholder-Stoelwinder B, Schaap NP, de Grip WJ, Bos HJ, Bosman GJ. Survival of red blood cells after transfusion: a comparison between red cells concentrates of different storage periods. *Transfusion* 48(7), 1478-1485 (2008).

13 Hess JR, Greenwalt TG. Storage of red blood cells: new approaches. *Transfus. Med. Rev.* 16(4), 283-295 (2002).

14 Hogman CF, Meryman HT. Storage parameters affecting red blood cell survival and function after transfusion. *Transfus. Med. Rev.* 13(4), 275-296 (1999).

15 Tinmouth A, Chin-Yee I. The clinical consequences of the red cell storage lesion. *Transfus. Med. Rev.* 15(2), 91-107 (2001).

16 The Transfusion of Red Cells. In: *Mollison's Blood Transfusion in Clinical Medicine (Volume Eleventh Edition)*. Klein HG, Anstee DJ (Ed.), Blackwell Science Ltd, Oxford, UK, 352-405 (2007).

17 Cohen RM, Franco RS, Khera PK *et al*. Red cell life span heterogeneity in hematologically normal people is sufficient to alter HbA1c. *Blood* 112(10), 4284-4291 (2008).

18 Khandelwal S, Saxena RK. Assessment of survival of aging erythrocyte in circulation and attendant changes in size and CD147 expression by a novel two step biotinylation method. *Exp. Gerontol.* 41(9), 855-861 (2006).

19 Franco RS. Measurement of red cell lifespan and aging. *Transfus. Med. Hemother.* 39(5), 302-307 (2012).

20 Cordle DG, Strauss RG, Lankford G, Mock DM. Antibodies provoked by the transfusion of biotin-labeled red cells. *Transfusion* 39(10), 1065-1069 (1999).

21 Lee JS, Gladwin MT. Bad blood: the risks of red cell storage. *Nat. Med.* 16(4), 381-382 (2010).

22 Edelstein SB. Blood product storage: does age really matter? *Semin. Cardiothorac. Vasc. Anesth.* 16(3), 160-165 (2012).

23 van de Watering L. Pitfalls in the current published observational literature on the effects of red blood cell storage. *Transfusion* 51(8), 1847-1854 (2011).

24 Hess JR. Red cell storage. *J. Proteomics.* 73(3), 368-373 (2010).

25 Satchwell TJ, Bell AJ, Pellegrin S *et al*. Critical band 3 multiprotein complex interactions establish early during human erythropoiesis. *Blood* 118(1), 182-191 (2011).

26 Lee YT, de Vasconcellos JF, Yuan J *et al*. LIN28B-mediated expression of fetal hemoglobin and production of fetal-like erythrocytes from adult human erythroblasts ex vivo. *Blood* 122(6), 1034-1041 (2013).

27 Napolitano LM, Kurek S, Luchette FA *et al*. Clinical practice guideline: red blood cell transfusion in adult trauma and critical care. *Crit Care Med.* 37(12), 3124-3157 (2009).

28 Piagnerelli M, Boudjeltia KZ, Brohee D *et al*. Alterations of red blood cell shape and sialic acid membrane content in septic patients. *Crit Care Med.* 31(8), 2156-2162 (2003).

29 Reggiori G, Occhipinti G, De Gasperi A, Vincent JL, Piagnerelli M. Early alterations of red blood cell rheology in critically ill patients. *Crit Care Med.* 37(12), 3041-3046 (2009).

30 Kempe DS, Akel A, Lang PA *et al*. Suicidal erythrocyte death in sepsis. *J. Mol. Med. (Berl)* 85(3), 273-281 (2007).

31 Lopez-Montero I, Monroy F, Velez M, Devaux PF. Ceramide: from lateral segregation to mechanical stress. *Biochim. Biophys. Acta* 1798(7), 1348-1356 (2010).

32 Jenkins RW, Canals D, Hannun YA. Roles and regulation of secretory and lysosomal acid sphingomyelinase. *Cell Signal.* 21(6), 836-846 (2009).

33 Khovidhunkit W, Kim MS, Memon RA *et al*. Effects of infection and inflammation on lipid and lipoprotein metabolism: mechanisms and consequences to the host. *J. Lipid Res.* 45(7), 1169-1196 (2004).

34 Piagnerelli M, Cotton F, van Nuffelen M, Vincent JL, Gulbis B. Modifications in erythrocyte membrane protein content are not responsible for the alterations in rheology seen in sepsis. *Shock* 37(1), 17-21 (2012).

35 Willekens FL, Roerdinkholder-Stoelwinder B, Groenen-Dopp YA *et al*. Hemoglobin loss from erythrocytes in vivo results from spleen-facilitated vesiculation. *Blood* 101(2), 747-751 (2003).

36 Willekens FL, Werre JM, Kruijt JK *et al*. Liver Kupffer cells rapidly remove red blood cell-derived vesicles from the circulation by scavenger receptors. *Blood* 105(5), 2141-2145 (2005).

37 Bosman GJ, Lasonder E, Luten M *et al*. The proteome of red cell membranes and vesicles during storage in blood bank conditions. *Transfusion* 48(5), 827-835 (2008).

38 Bosman GJ, Lasonder E, Groenen-Dopp YA, Willekens FL, Werre JM. The proteome of erythrocyte-derived microparticles from plasma: new clues for erythrocyte aging and vesiculation. *J. Proteomics.* (2012).

39 Ferru E, Giger K, Pantaleo A *et al*. Regulation of membrane-cytoskeletal interactions by tyrosine phosphorylation of erythrocyte band 3. *Blood* 117(22), 5998-6006 (2011).

40 Thery C, Ostrowski M, Segura E. Membrane vesicles as conveyors of immune responses. *Nat. Rev. Immunol.* 9(8), 581-593 (2009).

41 Mause SF, Weber C. Microparticles: protagonists of a novel communication network for intercellular information exchange. *Circ. Res.* 107(9), 1047-1057 (2010).

42 EL Andaloussi S, Mager I, Breakefield XO, Wood MJ. Extracellular vesicles: biology and emerging therapeutic opportunities. *Nat. Rev. Drug Discov.* 12(5), 347-357 (2013).

43 Gao Y, Lv L, Liu S, Ma G, Su Y. Elevated levels of thrombin-generating microparticles in stored red blood cells. *Vox Sang.* 105(1), 11-17 (2013).

44 van der Meijden PE, van Schilfgaarde M, van Oerle R, Renne T, ten Cate H, Spronk HM. Platelet- and erythrocyte-derived microparticles trigger thrombin generation via factor XIIa. *J. Thromb. Haemost.* 10(7), 1355-1362 (2012).

45 Donadee C, Raat NJ, Kanias T *et al*. Nitric oxide scavenging by red blood cell microparticles and cell-free hemoglobin as a mechanism for the red cell storage lesion. *Circulation* 124(4), 465-476 (2011).

46 van Beers EJ, Schaap MC, Berckmans RJ *et al*. Circulating erythrocyte-derived microparticles are associated with coagulation activation in sickle cell disease. *Haematologica* 94(11), 1513-1519 (2009).

47 Camus SM, Gausseres B, Bonnin P *et al*. Erythrocyte microparticles can induce kidney vaso-occlusions in a murine model of sickle cell disease. *Blood* 120(25), 5050-5058 (2012).

48 Couper KN, Barnes T, Hafalla JC *et al*. Parasite-derived plasma microparticles contribute significantly to malaria infection-induced inflammation through potent macrophage stimulation. *PLoS. Pathog.* 6(1), e1000744 (2010).

49 Mantel PY, Hoang AN, Goldowitz I *et al*. Malaria-infected erythrocyte-derived microvesicles mediate cellular communication within the parasite population and with the host immune system. *Cell Host. Microbe* 13(5), 521-534 (2013).

50 Danesh A, Inglis HC, Jackman RP *et al*. Exosomes from RBC units bind to monocytes and induce pro-inflammatory cytokines, boosting T cell responses in vitro. *Blood* (2013).

51 Flad HD, Brandt E. Platelet-derived chemokines: pathophysiology and therapeutic aspects. *Cell Mol. Life Sci.* 67(14), 2363-2386 (2010).

52 Li N. Platelet-lymphocyte cross-talk. *J. Leukoc. Biol.* 83(5), 1069-1078 (2008).

53 Boilard E, Nigrovic PA, Larabee K *et al*. Platelets amplify inflammation in arthritis via collagen-dependent microparticle production. *Science* 327(5965), 580-583 (2010).

54 Morrell CN. Immunomodulatory mediators in platelet transfusion reactions. *Hematology. Am. Soc. Hematol. Educ. Program.* 2011 470-474 (2011).

55 Rank A, Nieuwland R, Delker R *et al*. Cellular origin of platelet-derived microparticles in vivo. *Thromb. Res.* 126(4), e255-e259 (2010).

56 Flaumenhaft R, Dilks JR, Richardson J *et al*. Megakaryocyte-derived microparticles: direct visualization and distinction from platelet-derived microparticles. *Blood* 113(5), 1112-1121 (2009).

57 Nomura S, Okamae F, Abe M *et al*. Platelets expressing P-selectin and platelet-derived microparticles in stored platelet concentrates bind to PSGL-1 on filtrated leukocytes. *Clin. Appl. Thromb. Hemost.* 6(4), 213-221 (2000).

58 Rank A, Nieuwland R, Liebhardt S *et al*. Apheresis platelet concentrates contain platelet-derived and endothelial cell-derived microparticles. *Vox Sang.* 100(2), 179-186 (2011).

59 Sakaguchi S, Miyara M, Costantino CM, Hafler DA. FOXP3+ regulatory T cells in the human immune system. *Nat. Rev. Immunol.* 10(7), 490-500 (2010).

60 Koenen HJ, Smeets RL, Vink PM, van Rijssen E, Boots AM, Joosten I. Human CD25highFoxp3pos regulatory T cells differentiate into IL-17-producing cells. *Blood* 112(6), 2340-2352 (2008).

61 Beriou G, Costantino CM, Ashley CW *et al*. IL-17-producing human peripheral regulatory T cells retain suppressive function. *Blood* 113(18), 4240-4249 (2009).

62 Voo KS, Wang YH, Santori FR *et al*. Identification of IL-17-producing FOXP3+ regulatory T cells in humans. *Proc. Natl. Acad. Sci. U. S. A* 106(12), 4793-4798 (2009).

63 Ayyoub M, Deknuydt F, Raimbaud I *et al*. Human memory FOXP3+ Tregs secrete IL-17 ex vivo and constitutively express the T(H)17 lineage-specific transcription factor RORgamma t. *Proc. Natl. Acad. Sci. U. S. A* 106(21), 8635-8640 (2009).

64 Miyara M, Yoshioka Y, Kitoh A *et al*. Functional delineation and differentiation dynamics of human CD4+ T cells expressing the FoxP3 transcription factor. *Immunity.* 30(6), 899-911 (2009).

65 Duhen T, Duhen R, Lanzavecchia A, Sallusto F, Campbell DJ. Functionally distinct subsets of human FOXP3+ Treg cells that phenotypically mirror effector Th cells. *Blood* 119(19), 4430-4440 (2012).

66 Eming SA, Krieg T, Davidson JM. Inflammation in wound repair: molecular and cellular mechanisms. *J. Invest Dermatol.* 127(3), 514-525 (2007).

67 Carlow DA, Gossens K, Naus S, Veerman KM, Seo W, Ziltener HJ. PSGL-1 function in immunity and steady state homeostasis. *Immunol. Rev.* 230(1), 75-96 (2009).

68 Semple JW, Italiano JE, Jr., Freedman J. Platelets and the immune continuum. *Nat. Rev. Immunol.* 11(4), 264-274 (2011).

69 Samson M, Audia S, Fraszczak J *et al*. Th1 and Th17 lymphocytes expressing CD161 are implicated in giant cell arteritis and polymyalgia rheumatica pathogenesis. *Arthritis Rheum.* 64(11), 3788-3798 (2012).

70 Terrier B, Geri G, Chaara W *et al*. Interleukin-21 modulates Th1 and Th17 responses in giant cell arteritis. *Arthritis Rheum.* 64(6), 2001-2011 (2012).

71 Espigol-Frigole G, Corbera-Bellalta M, Planas-Rigol E *et al*. Increased IL-17A expression in temporal artery lesions is a predictor of sustained response to glucocorticoid treatment in patients with giant-cell arteritis. *Ann. Rheum. Dis.* (2012).

72 Merten M, Pakala R, Thiagarajan P, Benedict CR. Platelet microparticles promote platelet interaction with subendothelial matrix in a glycoprotein IIb/IIIa-dependent mechanism. *Circulation* 99(19), 2577-2582 (1999).

73 Murray PJ, Wynn TA. Protective and pathogenic functions of macrophage subsets. *Nat. Rev. Immunol.* 11(11), 723-737 (2011).

74 Sadallah S, Eken C, Martin PJ, Schifferli JA. Microparticles (ectosomes) shed by stored human platelets downregulate macrophages and modify the development of dendritic cells. *J. Immunol.* 186(11), 6543-6552 (2011).

Nederlandse Samenvatting

Rode bloedcellen zijn verantwoordelijk voor het transport van zuurstof naar en de verwijdering van CO_2 uit de organen in het lichaam. Om tot bij alle cellen te kunnen komen, moeten rode bloedcellen zeer vervormbaar zijn, zodat ze zelfs de kleinste haarvaatjes en het filtreersysteem in de milt kunnen passeren. In tegenstelling tot de meeste andere cellen bezitten rode bloedcellen geen intracellulaire organellen. Deze organellen voeren voor de cel essentiële functies uit, waaronder de gecontroleerde dood van de cel wanneer deze te oud en/of beschadigd is. Ondanks de afwezigheid van deze organellen hebben rode bloedcellen toch een goed gedefinieerde levensduur van ongeveer 120 dagen. Elke seconde worden er 2.5 miljoen oude bloedcellen uit onze bloedstroom verwijderd. Voor deze gereguleerde verwijdering is een belangrijke rol weggelegd voor het celmembraan, dat is opgebouwd uit eiwitten en vetten.

Alhoewel de exacte mechanismen die verantwoordelijk zijn voor de verwijdering van rode bloedcellen niet bekend zijn, kennen we wel enkele belangrijke schakels. Gespecialiseerde eiwitten van het immuunsysteem, autoantistoffen genaamd, herkennen specifieke patronen (antigenen) in beschadigde eiwitten op het celmembraan van oude rode bloedcellen. De binding van deze autoantilichamen leidt tot de herkenning en verwijdering van deze rode bloedcellen door fagocyten, in opruimen gespecialiseerde cellen. Het verschijnen van het vet fosfatidylserine, dat zich normaliter aan de binnenzijde van het celmembraan bevindt, aan de buitenzijde van de cel helpt hierbij.

Cellen kunnen delen van hun celmembraan afsnoeren en vervolgens afstoten in de vorm van vesikels, ook wel extracellulaire micropartikels genoemd. Alhoewel er de afgelopen jaren veel vooruitgang is geboekt met betrekking tot de identificatie en karakterisatie van deze micropartikels, weten we nog maar weinig over hun functie. Er wordt verondersteld dat rode bloedcellen hun levensduur vergroten door beschadigde delen van hun celmembraan te verwijderen via dergelijke micropartikels.

Het grootste deel van dit proefschrift gaat over veranderingen die plaats vinden in het celmembraan van rode bloedcellen gedurende hun opslag in de bloedbank of in het lichaam tijdens gegeneraliseerde ontstekingsprocessen en die betrokken zijn bij hun uiteindelijke verwijdering uit het bloed. In de laatste twee hoofdstukken van dit proefschrift wordt er aandacht besteed aan de karakterisatie van micropartikels in bloedzakken en hun rol bij het moduleren van ons immuunsysteem. In **Hoofdstuk 1** van dit proefschrift wordt een overzicht gegeven van de huidige stand van zaken betreffende deze onderwerpen.

Ieder jaar redden bloedtransfusies de levens van miljoenen mensen. Helaas kunnen bloedtransfusies soms ook ernstige bijwerken hebben, zoals acute longschade,

orgaanschade door ijzerstapeling, vernauwing van de bloedvaten en de vorming van schadelijke (auto)antistoffen. Deze bijwerkingen worden hoogstwaarschijnlijk veroorzaakt door veranderingen die plaats vinden in de rode bloedcellen terwijl ze bewaard worden in de bloedbank.

De vorming van schadelijke autoantistoffen die gericht zijn tegen rode bloedcellen is een bekende bijwerking van herhaalde bloedtransfusies. In sommige gevallen leiden deze antilichamen tot het verlies van rode bloedcellen, met bloedarmoede tot gevolg. Een plausibele verklaring voor dit fenomeen is het onstaan van abnormale antigenen op rode bloedcellen tijdens hun opslag in bloedzakken. In **Hoofdstuk 2** hebben we de mogelijke vorming van dergelijke antigenen onderzocht. We zagen een toename in binding van schadelijke autoantistoffen gericht tegen rode bloedcellen naarmate rode bloedcellen langer bewaard werden. Dit toont aan dat er abnormale antigenen gevormd worden op rode bloedcellen tijdens hun opslag. Ook hebben we enkele membraaneiwitten kunnen aanwijzen waaruit de abnormale antigenen waarschijnlijk ontstaan. Een vergelijkbare aanpak liet zien dat rode bloedcel-micropartikels uit bloedzakken ook abnormale antigenen hebben, maar dit bleken niet helemaal dezelfde te zijn als die in de rode bloedcellen.

In Nederland moeten rode bloedcel bloedzakken binnen 35 dagen na afname gebruikt worden om te kunnen voldoen aan de kwaliteitsnormen. Deze normen bestaan uit een maximaal verlies van 0.8% van de rode bloedcellen (hemolyse) gedurende hun opslag en een minimaal overlevingspercentage van 75% van de rode bloedcellen in de eerste 24 uur na transfusie. Hoewel het bekend is dat er een grote variatie is in dit overlevingspercentage, die waarschijnlijk afhangt van zowel de bloeddonor als de ontvanger, wordt dit vanwege praktische beperkingen maar zelden gemeten. Andere conventionele kwaliteitsparameters voor rode bloedceleenheden zijn helaas geen goede graadmeters voor rode bloedceloverleving na transfusie.

In **Hoofdstuk 3** hebben we onderzocht of de aanwezigheid van fosfatidylserine aan de buitenkant van de rode bloedcel gebruikt kan worden als een graadmeter voor bloeddonorafhankelijke variatie in de kwaliteit van bloedzakken. De mate van aanwezigheid van fosfatidylserine aan de buitenkant van de rode bloedcel varieerde van donor tot donor én nam toe met de bewaartijd van rode bloedceleenheden. Ook bleek het percentage rode bloedcellen met fosfatidylserine aan hun buitenkant in vers afgenomen bloed een goede voorspeller te zijn voor de toename in het percentage positieve rode bloedcellen na blootstelling aan experimentele stress die vergelijkbaar is met de stress die rode bloedcellen ondergaan in de bloedvaten. Ook kwam het percentage fosfatidylserine-positieve rode bloedcellen overeen met de mate van hemolyse en de hoeveelheid micropartikels in bloedzakken. Deze bevindingen laten zien dat het percentage rode bloedcellen met

fosfatidylserine aan hun buitenkant een bruikbare graadmeter is voor de kwaliteit van rode bloedcellen in bloedzakken.

Transfusies van rode bloedcellen zijn geassocieerd met een verhoogde morbiditeit en mortaliteit bij ernstig zieke patiënten. De gegeneraliseerde ontsteking die doorgaans wordt waargenomen bij deze patiënten heeft naar alle waarschijnlijkheid een nadelig effect op de functie en levensduur van de getransfuseerde rode bloedcellen. Ook is het goed mogelijk dat de mate van dit effect toeneemt met de bewaartijd van de rode bloedcelzak. Deze notie wordt gevoed door eerdere waarnemingen dat onder andere de vorm en vervormbaarheid van rode bloedcellen veranderen in patiënten die een gegeneraliseerde ontsteking hebben ten gevolge van sepsis (bloedvergiftiging). Een eerdere studie liet zien dat, wanneer rode bloedcellen van gezonde vrijwilligers in contact kwamen met het bloedplasma van patiënten met sepsis, het aantal fosfatidylserine-positieve rode bloedcellen toenam. Ook werd sfingomyeline, een ander vet in het celmembraan, afgebroken tot ceramide. Van ceramide is bekend dat het een sterke invloed heeft op de functie en de integriteit van het celmembraan en daarmee op de rode bloedcel in zijn geheel. Ceramide wordt vooral gevormd door het enzym sfingomyelinase en dit enzym komt vrij in de bloedstroom tijdens gegeneraliseerde ontsteking.

In **Hoofdstuk 4** hebben we in detail onderzocht wat de gevolgen zijn van een behandeling van rode bloedcellen met sfingomyelinase. Rode bloedcellen bleken hiervoor zeer gevoelig te zijn. Behandeling met sfingomyelinase leidde tot een verlies van de kenmerkende discusvorm van de rode bloedcel, direct gevolgd door het verschijnen van fosfatidylserine aan de buitenkant van de cel en uiteindelijk celdood. Gedurende dit proces nam de vervormbaarheid van de cel af en ging hij meer micropartikels vormen. Oude rode bloedcellen van gezonde vrijwilligers en uit bloedzakken bleken veel gevoeliger voor de behandeling met sfingomyelinase dan jongere rode bloedcellen. Dit laatste zou gevolgen kunnen hebben voor de levensduur van bewaarde rode bloedcellen na transfusie in patiënten met gegeneraliseerde ontsteking.

In **Hoofdstuk 5** identificeerden we de vetten in het celmembraan van rode bloedcellen van gezonde vrijwilligers nadat deze waren blootgesteld aan het bloedplasma van patiënten met sepsis. We vonden geen ceramide, maar wel een duidelijke toename van het vet lysofosfatidylcholine. Dit wordt doorgaans geproduceerd door enzymen van de fosfolipase A2 familie. Alhoewel gesecreteerd fosfolipase A2 type IIA sterk verhoogd was in het bloedplasma van patiënten met sepsis, bleek er geen verband te zijn tussen de hoeveelheid van dit enzym en de hoeveelheid lysofosfatidylcholine die werd aangetroffen in de onderzochte celmembranen. Vervolgens kregen gezonde vrijwilligers een lage dosis van de bacteriële bouwsteen lipopolysaccharide toegediend, waarmee een milde, experimentele sepsis werd geïnduceerd. Daarna werden rode bloedcellen blootgesteld aan het

bloedplasma van deze vrijwilligers en werden de vetten in het celmembraan geanalyseerd. Een toename in lysofosfatidylcholine werd niet gevonden in deze rode bloedcellen. Dit toont aan dat het gebruikte experimentele model sepsis niet volledig nabootst, althans niet wat de rode bloedcel betreft. In deze vrijwilligers nam de mate van fosfatidylserine aan de buitenkant van rode bloedcellen wél toe. Deze gegevens laten zien dat de vetten in rode bloedcelmembranen veranderen tijdens gegeneraliseerde ontsteking. Dit kan gevolgen hebben voor de functie en levensduur van rode bloedcellen.

Rode bloedcellen verliezen delen van hun membraan als micropartikels, die teruggevonden kunnen worden in het bloed. De rode bloedcel vormt deze micropartikels waarschijnlijk om beschadigde eiwitten en vetten uit het celmembraan te verwijderen en daarmee vroegtijdige herkenning en verwijdering te voorkómen. Micropartikels worden ook gevormd door rode bloedcellen in bloedzakken gedurende hun opslag in de bloedbank. De afgelopen jaren is het duidelijk geworden dat micropartikels afkomstig van verschillende soorten cellen een rol spelen in de fysiologie en pathologie van het menselijk lichaam. In **Hoofdstuk 6** wordt een overzicht gegeven van de huidige kennis over de mogelijke betrokkenheid van micropartikels afkomstig van rode bloedcellen bij allerlei ziekteprocessen en de schadelijke bijwerkingen van transfusies.

Bloedplaatjes zijn de kleinste cellen in ons bloed en onmisbaar voor de bloedstolling, dat bloedverlies stopt na beschadiging van een bloedvat. Bloedplaatjes zijn ook betrokken bij de activatie en ondersteuning van ons immuunsysteem. Het immuunsysteem beschermt ons tegen ziekteverwekkers zoals bacteriën en virussen en zorgt er ook voor dat onze weefsels goed functioneren. Bloedplaatjes worden net zoals rode bloedcellen verzameld en opgeslagen voor transfusie. Gedurende hun verblijf in de bloedstroom en opslag in bloedzakken produceren ook de bloedplaatjes micropartikels. Het is gebleken dat deze door plaatjes gevormde micropartikels (PMPs) net als plaatjes zelf de werking van ons immuunsysteem kunnen beïnvloeden. Ook dat wordt besproken in **Hoofdstuk 6**.

In **Hoofdstuk 7** beschrijven we onze ontdekking van een beschermend effect van PMPs op de stabiliteit van de regulatoire T cellen van het immuunsysteem. Regulatoire T cellen voorkomen dat het immuunsysteem zich tegen ons eigen lichaam keert en zorgen ervoor dat het immuunsysteem tot rust komt nadat het een infectie overwonnen heeft. Echter, in uitzonderlijke situaties kunnen regulatoire T cellen van aard veranderen en stoffen gaan produceren die het immuunsysteem juist activeren, zoals interleukine-17 en interferon-γ. In deze studie hebben we een model gebruikt waarin regulatoire T cellen hun beschermende functie deels verliezen en interleukine-17 en/of interferon-γ gaan produceren. Dit functieverlies kon worden geremd door toevoeging van PMPs. We hebben ook aangetoond dat de PMPs bij voorkeur binden aan een specifieke groep regulatoire T cellen waarvan bekend is dat die na stimulatie interleukine-17 produceren. Ook hebben we laten zien dat

deze interactie tussen PMPs en regulatoire T cellen tot stand komt via het membraaneiwit P-selectine, dat aanwezig is op de PMPs. Deze bevindingen tonen aan dat PMPs mogelijk assisteren bij de controlerende rol van het immuunsysteem.

Dit proefschrift biedt nieuwe inzichten in de biochemische veranderingen die plaatsvinden in het celmembraan van rode bloedcellen tijdens hun opslag en die bijdragen aan hun verminderde overleving na en de schadelijke bijwerkingen van transfusies. Verder maakt ons onderzoek zeer waarschijnlijk dat veranderingen in de vetten van het celmembraan kunnen leiden tot verminderde overleving van rode bloedcellen in patiënten met een gegeneraliseerde ontsteking. Ook beschrijven we een nieuwe functie van bloedplaatjes in het immuunsysteem, namelijk het reguleren van de activiteit van regulatoire T cellen door middel van micropartikels.

Curriculum Vitae

Sip Dinkla werd geboren op 4 april 1984 te Eindhoven. Aldaar behaalde hij in 2001 zijn HAVO-diploma aan het van Maerlant Lyceum. Datzelfde jaar begon hij aan de opleiding Toegepaste Natuurwetenschappen aan de Fontys Hogeschool in Eindhoven. Tijdens deze studie liep hij achtereenvolgens stage bij Pamgene International te ’s Hertogenbosch en bij het Nijmegen Centre for Molecular Life Sciences. Gedurende laatstgenoemde stage deed hij onderzoek naar de oligomerisatie en het transport van aquaporine-2 onder begeleiding van Dr. Erik-Jan Kamsteeg. In 2005 verhuisde hij naar Nijmegen om daar de masteropleiding Biomedische Wetenschappen te volgen aan de Radboud Universiteit. In het eerste jaar van deze opleiding onderzocht hij tijdens een onderzoeksstage in de groep van Dr. Frank Wagener de rol die heem oxygenase speelt in prostaglandine E_2-gedreven migratie van dendritische cellen. In het tweede jaar liep hij stage bij Organon te Oss om onder begeleiding van Dr. Roger Sutmuller endogene liganden van de Toll-like receptor familie nader te bestuderen. Na het voltooien van zijn masteropleiding in 2008 is hij direct begonnen aan zijn promotieonderzoek naar de rol die veroudering van rode bloedcellen speelt in de immunologische bijwerkingen van bloedtransfusies, onder supervisie van Prof. dr. Irma Joosten, Dr. Giel Bosman, Prof. dr. Roland Brock en Dr. Věra Novotný. De resultaten van zijn promotietraject staan beschreven in verschillende wetenschappelijke publicaties en in dit proefschrift. Momenteel is Sip werkzaam als postdoc bij St. George’s University of London onder begeleiding van Dr. Ingrid Dumitriu en Prof. Dr. Juan Carlos Kaski. Zijn huidige onderzoek richt zich op de functie van regulatoire lymfocyten in atherosclerose.

List of Publications

Dinkla S, Koenen HJ, van Cranenbroek B, Wallbrecher R, Bosman GJ, Joosten I. Platelet-derived microparticles inhibit IL-17 production by regulatory T cells through P-selectin. Submitted.

Dinkla S*, van Eijk LT*, Fuchs B, Schiller J, Joosten I, Brock R, Pickkers P, Bosman GJ. Inflammation-associated changes in lipid composition and organization of the erythrocyte membrane. Submitted.

Dinkla S, Peppelman M, van Der Raadt J, Atsma F, Novotny VM, van Kraaij MG, Joosten I, Bosman GJ. Phosphatidylserine exposure on stored red blood cells as a parameter for donor-dependent variation in product quality. *Blood Transfus.* 12(2), 204-209 (2014).

Dinkla S, Brock R, Joosten I, Bosman GJ. Gateway to understanding microparticles: standardized isolation and identification of plasma membrane-derived vesicles. *Nanomedicine. (Lond)* 8(10), 1657-1668 (2013).

Dinkla S*, Wessels K*, Verdurmen WP, Tomelleri C, Cluitmans JC, Fransen J, Fuchs B, Schiller J, Joosten I, Brock R, Bosman GJ. Functional consequences of sphingomyelinase-induced changes in erythrocyte membrane structure. *Cell Death. Dis.* 3 e410 (2012).

Cluitmans JC, Hardeman MR, Dinkla S, Brock R, Bosman GJ. Red blood cell deformability during storage: towards functional proteomics and metabolomics in the Blood Bank. *Blood Transfus.* 10 Suppl 2 s12-s18 (2012).

Dinkla S, Novotny VM, Joosten I, Bosman GJ. Storage-induced changes in erythrocyte membrane proteins promote recognition by autoantibodies. *PLoS. One.* 7(8), e42250 (2012).

Chung YD, Sinzinger MD, Bovee-Geurts P, Krause M, Dinkla S, Joosten I, Koopman WJ, Adjobo-Hermans MJ, Brock R. Analyzing the homeostasis of signaling proteins by a combination of Western blot and fluorescence correlation spectroscopy. *Biophys. J.* 101(11), 2807-2815 (2011).

* Both authors contributed equally to this work

Dankwoord

Met lichte verbazing en toegegeven ook een gemengd gevoel van opluchting en voldoening realiseer ik mij dat de tijd daar is om mijn dank te betuigen aan allen die mij direct dan wel indirect hebben geholpen met het tot stand komen van dit proefschrift. Het geluk wil dat de vele samenwerkingsverbanden die (meestal spontaan) zijn ontstaan gedurende mijn promotieonderzoek stuk voor stuk erg prettig waren, zowel op professioneel als persoonlijk vlak. Graag wil ik een bijzondere dankbetuiging richten aan de volgende personen:

Irma, hartelijk dank voor je scherpe blik op ons werk, het aansturen op de noodzakelijke koerswijzigingen tijdens het onderzoek, het leren denken in figuren en verhalen, het enthousiasmeren dan wel kalmeren na het zien van nieuwe resultaten en het adequaat handelen wanneer er een probleem opgelost moest worden. Van onze talloze vergaderingen blijft mij de rust waarmee je dacht en handelde het meest bij.
Giel, van alle mensen ben ik jou als directe begeleider de meeste dank verschuldigd. Ik kon op ieder moment bij je binnen lopen, wetende dat ik op je hulp kon rekenen. Ik heb genoten van onze vele discussies, de mooie verhalen en de ruimte die je gaf om mijn eigen interpretatie van ons onderzoek vorm te geven. Je aanstekelijke enthousiasme en je oog voor de mens achter de wetenschapper heb ik altijd gewaardeerd. Dank je voor de ontelbare uren die je in mijn ontwikkeling hebt gestoken.
Roland, hartelijk dank voor de extra aandacht en energie die je gaandeweg aan mijn onderzoek en de erytrocytengroep in zijn geheel gaf. Je directe betrokkenheid in de vorm van vele goede ideeën, je mooie en creatieve taalgebruik dat ik ontving in de vorm van manuscriptcorrecties en het opzetten van samenwerkingsverbanden stel ik bijzonder op prijs.
Věra, dank je voor je enthousiasme tijdens onze discussies, je hulp met het interpreteren van de serologische data van de (potentiële) AIHA patiënten, het nodige papierwerk en de goed getimede schouderklopjes.

Graag wil ik alle mensen van Medische Immunologie bedanken voor de goede tijd die ik er gehad heb. Jorieke, Diana en Elena (en stiekem ook Kjeld), dank je voor jullie hulp, optimisme en gezelligheid/leedvermaak in en buiten onze promokamer. Xuehui, Claire, Clive and Vivian, it was a pleasure to get to know you. Esther v R, Esther F, Marina en Bram wil ik bedanken voor de hulp en de goede sfeer in het kweeklab. Bram, dank je voor de prachtige PMP-Treg co-culture experimenten. Hans, hartelijk dank voor het beantwoorden van de vele vragen die ik had over Tregs. Alle mensen van de bloedgroep serologie en in het bijzonder Wim, Hetty, Gani, Tom en Richard wil ik bedanken voor hun expertise en het verzamelen van de vele patiëntensera en transfusieproducten voor mijn onderzoek. Gaby en Rob, hartelijk dank voor de vele celsorteringen die jullie voor mij gedaan hebben.

Bij Biochemistry of Integrated Systems heb ik mij de afgelopen jaren altijd welkom gevoeld. Alokta, Ivo, Jenny, Joris, Judith, Marco, Merel, Michael, Petra, Rike, Theo, Wim, Wouter and Yi-Da, thank you for all your help and for making me feel at home in the lab. Carlo a.k.a. Mr. Montana, Judith and Giel, it was a pleasure to study those funny-looking little red cells (and even smaller microparticles) together as a team. Ik heb het geluk gehad een aantal uitstekende studenten te mogen begeleiden tijdens mijn promotie. Katharina, Malou, Jori en Luc, dank je voor jullie uitstekende werk en motivatie.

Peter en Lucas, onze samenwerking met betrekking tot de erytrocytenfunctie tijdens sepsis heb ik als uitermate prettig ervaren, waarvoor dank. Jürgen und Beate, vielen Dank für die schnelle und detaillierte Lipidanalyse von den vielen Proben, die wir nach Leipzig geschickt haben. Marian en Femke, het was fijn met jullie samen te hebben gewerkt aan fosfatidylserine als kwaliteitsparameter voor bewaarde rode bloedcellen.

Tijdige ontspanning is essentieel voor de promovendus. Ik wil de Radballers bedanken voor de enerverende basketbalsessies op de dinsdagavond en de feestelijke gelegenheden buiten het veld. Joris a.k.a. JJ, Floortje, Jonathan a.k.a. Chocka, Eric d M, Loek a.k.a. Skywalker, Elles, Martijn a.k.a. Martini, Bianca, Eric vd M a.k.a. Schredder, Philipp a.k.a. Flippie, Robert Jan a.k.a. RJ, Sietze, Pim(metje), Naima, Bar(ddd)t, Anneke en niet te vergeten Joke, het was alsof ik per toeval bij een dozijn oude middelbareschoolvrienden in een team terecht kwam. Over middelbareschoolvrienden gesproken: mannen, bedankt!

Etienne, Alwin, Rick, Joris, Marc en Tom, dank je voor de vriendschap, de goede gesprekken en de (ernstige) buikpijn van het lachen. Joris en Franzi, Eric en Inge, dank je voor jullie hulp. Anchel and Ganesh, I definitely made the right decision moving in with you guys. Ganesh, I truely enjoy your warm friendship and your great story-telling. Anchel Gonzalez Barriga, somos como dos manos en una barriga. Through you I got to know a bunch of wonderful people, habibis (you know who you are), thank you for your friendship and the great time we have had (and will have) together.

Nuria, bonica, le estoy muy agradecido a la Dama Fortuna por hacer que nuestros caminos se cruzaran. Espero que nuestra pequeña aventura en Inglaterra sea la primera de muchas.

Lieve ouders, het behoeft geen uitleg dat ik zonder jullie nooit aan het schrijven van dit proefschrift was toegekomen. Ik wil jullie danken voor jullie onvoorwaardelijke steun, de vele goede adviezen (die ik slechts mondjesmaat opvolgde), het subtiele zetje in de rug en bovenal een liberale opvoeding. Kasper, gezond verstand, goede humor, geweldige broer.